Manufacturing Lentiviral Vectors for Gene Therapies: Optimisation of Cellular Factories

A thesis submitted to The University of Manchester for the degree of

Doctor of Philosophy

in the Faculty of Science and Engineering

2021

Emily L. Powell

Department of Chemical Engineering and Analytical Sciences

Table of Contents

Word count excluding references: 39,876

List of Figures

List of Tables

Abstract

The use of Lentiviral Vectors (LVV) as tools for gene delivery has gained momentum in recent years due to successes in clinical trials for rare diseases. Production of high-titre LVVs is a limiting factor in their wider application in diseases with large patient populations, such as cancer. LVVs are commonly produced by the transient transfection of HEK293T cells, however this process is costly and inefficient. An alternative stable, scalable manufacturing system for LVV production is necessary.

Before the development of a stable cell line can be achieved, it is vital to gain an understanding of how individual vector components interact with HEK293T cells at a molecular level. HIV-1 GagPol is the major viral structural protein constituting approximately 70% of a bona fide virion. It is not known how synthetic GagPol, utilised during LVV production at GSK, interacts with HEK293T cells. Given that HIV-1 utilises several host cell systems for its own propagation, it is hypothesised that synthetic GagPol may have similar effects, potentially stressing the capacity of a HEK293T cell to carry out typical homeostatic functions. This could be detrimental to HEK293T cells in terms of causing cellular stress due to the burden of ectopic protein production, and may also impact negatively on GagPol production.

This thesis therefore aimed to develop an understanding of the interactions between synthetic GagPol and HEK293T cellular physiology in order to define approaches to identify and intervene in molecular bottlenecks associated with LVV production. To do this, plasmid constructs encoding GagPol and fluorescently-tagged GagPol were generated and used in HEK293T transient transfections, where a maximum GagPol production titre of over 1250 ng p24/mL was achieved. HEK293T cellular physiology was examined during high-level GagPol production. Activation of the unfolded protein response (UPR) and endoplasmic reticulum (ER) stress pathway, in addition to the induction of apoptosis and autophagy were observed. The effects of chemical inhibitors of cellular stresses were examined, with chemical inhibitors of apoptosis leading to a modest increase in GagPol production, in addition to increased cell viability. These investigations with chemical inhibitors of cellular stress illuminate the potential for genetic targets of manipulation within HEK293T cells that could enable increased GagPol production which would, in turn, be beneficial for LVV production.

Declaration

No portion of the work referred to in the thesis has been submitted in support of an application for another degree or qualification of this or any other university or other institute of learning.

Copyright Statement

i. The author of this thesis (including any appendices and/or schedules to this thesis) owns certain copyright or related rights in it (the “Copyright”) and s/he has given the University of Manchester certain rights to use such Copyright, including for administrative purposes.

ii. Copies of this thesis, either in full or in extracts and whether in hard or electronic copy, may be made only in accordance with the Copyright, Designs and Patents Act 1988 (as amended) and regulations issued under it or, where appropriate, in accordance with licensing agreements which the University has from time to time. This page must form part of any such copies made.

iii. The ownership of certain Copyright, patents, designs, trademarks and other intellectual property (the “Intellectual Property”) and any reproductions of copyright works in the thesis, for example graphs and tables (“Reproductions”), which may be described in this thesis, may not be owned by the author and may be owned by third parties. Such Intellectual Property and Reproductions cannot and must not be made available for use without the prior written permission of the owner(s) of the relevant Intellectual Property and/or Reproductions.

iv. Further information on the conditions under which disclosure, publication and commercialisation of this thesis, the Copyright and any Intellectual Property and/or Reproductions described in it may take place is available in the University IP Policy (see http://documents.manchester.ac.uk/DocuInfo.aspx?DocID=2442 0), in any relevant Thesis restriction declarations deposited in the University Library, the University Library’s regulations (see http://www.library.manchester.ac.uk/about/regulations/) and in the University’s policy on Presentation of Theses.

Acknowledgements

This page of my thesis has naturally been the last one for me to write, but it is by far the easiest.

Alan, I cannot thank you enough for your support and guidance as a mentor to me during my PhD. Lessons learned over the last few years will stick with me for life, not least of which is the value of hard work. Conrad and Chris, thank you for being such supportive supervisors whilst at GSK, your intellectual input has been invaluable and I am very grateful.

Thank you to all members of the Dickson lab, past and present, for all of the help and encouragement. It has been a pleasure to work with you each day. Thanks also to the Vector Development team at GSK for being so helpful and kind during my time in Stevenage.

I could not have completed my PhD without my family. Mum, Dad, Laura, and Tom, thank you for always supporting me in everything I do. I am incredibly lucky to have a family like you. Thanks Buddy and Charlie even though you can't read, good boys. Laura, you have helped me in more ways than you know and I love having you as my dearest sister and best friend. I love you all very much.

Ashleigh and Serena, thank you for being the best friends I could ever wish for. I couldn't have done this without your encouragement and reminders that I am good enough. Thank you to everyone else along the way, Adelaide, Aisha, Alastair, Baz, Ellie, Ibrahim, Izzy, Lauren, Mark, the Proper Mancs, and Tom.

Thank you to BBSRC and GSK for funding this PhD project.

Abbreviations

3-MA	3-Methyladenine
AAV	Adeno-Associated Virus
ABCE1	ATP-Binding Cassette Sub-Family E Member 1
ADA	Adenosine Deaminase
AEP	Amphotropic Envelope Protein
AIDS	Acquired Immune Deficiency Syndrome
AIF	Apoptosis Inducing Factor
ALG	Apoptosis-Linked Gene
ALIX	Apoptosis-Linked Gene (ALG) Interacting Protein X
ALL	Acute Lymphoblastic Leukaemia
AMP	Adenosine Monophosphate
AMPK	AMP-Activated Protein Kinase
ANOVA	Analysis Of Variance
AP	Clathrin-Associated Adaptor Protein
ASCGT	American Society For Cell And Gene Therapy
ATF6	Activating Transcription Factor 6
ATG	Autophagy Related Genes
ATP	Adenosine Triphosphate
AU	Arbitrary Units
AV	Adenovirus
BAC	Bacterial Artificial Chromosome
BAX	Bcl-2 Associated X, Apoptosis Regulator
BCL-2	B-Cell Lymphoma-2
BDS	Bright Detail Similarity R3
BF	Bright Field
BH	Bcl-2 Homologous
BH3	Bcl-2 Homology 3
BHK	Baby Hamster Kidney
BHQ	2,5-Di-T-Butyl-1,4-Benzohydroquinone
BID	BH3-Intercting Domain Death Agonist
BiP	Immunoglobulin Heavy Chain-Binding Protein
BP	Base Pairs
BR	Biological Repeat
BSA	Bovine Serum Albumin
C/EBP	CCAAT-Enhancer-Binding Protein
CaM	Calmodulin
CAR-T	Chimeric Antigen Receptor T-Cell Therapy
CCM	Central Carbon Metabolism

CDKL3	Cyclin-Dependent Kinase-Like 3 Protein
CDKN	Cyclin-Dependent Kinase Inhibitors
CDKN2A	Cyclin-Dependent Kinase Inhibitor 2A
cDNA	Complementary DNA
CHO	Chinese Hamster Ovary
CHOK	Choline Kinase
CHOP	CCAAT-Enhancer-Binding Protein Homologous Protein
CMV	Cytomegalovirus
CMV-IE	Cytomegalovirus-Immediate Early Promoter
COX15	Cytochrome-C Oxidase Subunit 15
cPPT	Central Polypurine
CPSF6	Cleavage And Polyadenylation Specific Factor 6
CRISPR	Clustered Regularly Interspaced Short Palindromic Repeats
Ct	Cycle Threshold
CypA	Cyclophilin A
DAPI	4′,6-Diamidino-2-Phenylindole
DDIT3	DNA-Inducible Transcript 3
ddPCR	Droplet Digital Polymerase Chain Reaction
DEPC	Diethyl Pyrocarbonate
DLG1	Discs Large Homolog 1
DMEM	Dulbecco’s Modified Eagle Medium
DMSO	Dimethyl Sulfoxide
DNA	Deoxyribonucleic Acid
E. coli	Escherichia Coli
EDTA	Ethylenediaminetetraacetic Acid
EF1a	Elongation Factor 1A Promoter
eGFP	Enhanced Green Fluorescent Protein
EIF3	Eukaryotic Initiation Factor 3
ELISA	Enzyme-Linked Immunosorbent Assay
ER	Endoplasmic Reticulum
ERK-2	Extracellular Signal-Regulated Kinase 2
ESCRT	Endosomal Sorting Complex Required For Transport
FBS	Fetal Bovine Serum
FDA	Food And Drug Administration
FITC	Fluorescein Isothiocyanate
FSC	Forward Scatter
G	Glycoprotein G
GADD34	Growth Arrest And DNA Damage-Inducible Protein
GAPDH	Glyceraldehyde 3-Phosphate Dehydrogenase
gDNA	Genomic DNA
GFP	Green Fluorescent Protein

GMP	Good Manufacturing Practices
GOI	Gene Of Interest
GRP	Gastrin-Releasing Peptide
GRV	Gamma-Retroviral
HARS2	Histidyl-tRNA Synthetase Homolog Ho3
HEK	Human Embryonic Kidney
HIF1	Hypoxia-Inducible Factor
HIV-1	Human Immunodeficiency Virus 1
Hsp70	Heat Shock Protein Family 70
HSPA5	Heat Shock Protein Family (Hsp70) Member 5
HSV	Herpes Simplex Virus
IAP	Inhibitor Of Apoptosis
ICAM-1	Intracellular Adhesion Molecule A
ICER	Inducible cAMP Early Repressor
IMP1	Insulin-Like Growth Factor II mRNA-Binding Protein 1
IQGAP1	IQ Motif-Containing GTPase Activating Protein
IRE1	Inositol-Requiring Enzyme 1
ISX	ImageStreamX
KCl	Potassium Chloride
KIF4	Kinesin Superfamily Protein 4
LAMP-1	Lysosomal Associated Membrane Protein 1
LC3	Microtubule-Associated Protein Light Chain 3
LDL	Low-Density Lipoprotein
LTR	Long Terminal Repeats
LV	Lentivirus
LVV	Lentiviral Vector
MA	Matrix
mAb	Monoclonal Antibody
MAP4K3	Mitogen-Activated Protein Kinase Kinase Kinase Kinase 3
MAPK	Mitogen-Activated Protein Kinase
MBG	Minor Groove Binder
MCL	Myeloid-Cell Leukemia 1
MEM	Minimal Essential Medium
MLV	Murine Leukemia Virus
MMLV	Moloney Murine Leukaemia Virus
MOI	Multiplicity Of Infection
MP	Microtubule-Associated Proteins
mRNA	Messenger RNA
mTOR	Mammalian Target Of Rapamycin
MVB	Multivesicular Body
NaCl	Sodium Chloride

NC	Nucleocapsid
Nedd4	Neural Precursor Cell Expressed Developmentally Down-Regulated Protein 4
NTP	Nucleoside Triphosphate
NUP153	Nucleoporin 153
NUP358	Nucleoporin 358
OD	Optical Density
ORF	Open Reading Frame
PACSIN2	Protein Kinase C And Casein Kinase Substrate In Neurons 2
PBS	Phosphate Buffered Saline
PC	Pyruvate Carboxylate
PCR	Polymerase Chain Reaction
PDIA2	Protein Disulphide Isomerase Family A Member 2
PDK	Pyruvate Dehydrogenase Kinase
PE	Phosphatidylethanolamine
PEI	Polyethylenimine
PERK	Protein Kinase R (PKR)-Like Endoplasmic Reticulum Kinase
PERT	Product Enhanced Reverse Transcriptase Assay
PET	Polyethylene Terephthalate
PFA	Paaformaldehyde
PI	Propidium Iodide
PI(4,5)P2	Phosphatidylinositol-4,5-Bisphosphate
PI(3)P	Phosphatidylinositol-3-Phosphate
PIN1	Peptidyl-Propyl Cis-Trans Isomerase Nima-Interacting 1
Pit-2	Sodium-Dependent Phosphate Transporter
PKR	Protein Kinase R
PM	Plasma Membrane
polyA	Polyadenylation Signal
PR	Protease
Pr160GagPol	HIV-1 Gagpol Precursor
Pr55Gag	HIV-1 Gag Precursor
PS	Phosphatidylserine
qPCR	Quantitative Polymerase Chain Reaction
qRT-PCR	Real-Time Quantitative Reverse Transcription PCR
RCV	Replication-Competent Virus
RER	Rough Endoplasmic Reticulum
RMCE	Recombinase Mediated Cassette Exchange
RNA	Ribonucleic Acid
RNAi	RNA Interference
ROS	Reactive Oxygen Species
RPM	Revolutions per minute

RRE	Rev-Response Element
RT	Reverse Transcriptase
rTetR	Reverse Tetracycline Repressor
rtTA	Reverse Tetracycline Transactivator
RV	Retrovirus
RVB-2	RuvB-Like 2
SCID	Severe Combined Immunodeficiency
SD	Standard Deviation
SEM	Standard Error of the Mean
SFFV	Spleen Focus Forming Virus
SIN	Self-Inactivating Vector
SLC	Solute Carrier
SM	Sec1/Munc18
SMA	Spinal Muscular Atrophy
SMAC	Second Mitochondria-Derived Activator Of Caspases
SNARE	Soluble N-Ethylmaleimide-Sensitive Factor Receptor
SOC	Super Optimal Broth
SOCS1	Suppressor Of Cytokine Signalling Protein 1
SP	Spacer Peptide
SQSTM1	Sequestosome 1
SRC	Proto-Oncogene Tyrosine-Protein Kinase Src
SSC	Side Scatter
STAU1	Staufen Double-Stranded RNA Binding Protein 1
SU	Gp120
SV40	Simian Virus 40
SYNGP	Synthetic Gagpol
TAE	Tris-Acetate-EDTA
tDNA	Transfer DNA
Tet	Tetracycline
TetO	Tet Opertor Sequence
TetR	Tetracycline Repressor
TM	Transmembrane
TMB	3,3′,5,5′-Tetramethylbenzidine
TNF	Tumor Necrosis Factor
TNFR	Tumor Necrosis Factor Receptor
TR	Technical Repeat
TRE	Tetracycline-Response Element
TRIM5a	Tripartite Motif-Containing Protein 5
TRIS	Tris(Hydroxymethyl)Aminomethane
Tsg101	Tumour-Susceptibility Gene 101
tTa	Tetracycline Transactivator

TU	Transducing Units
ULK1	Unc-51-Like Kinase 1
UPR	Unfolded Protein Response
V-ATPase	Vacuolar-Type ATPase
VAN	Virion-Associated Nuclear Shuttling Protein
VLP	Virus-Like Particles
VPS	Vacuolar Protein Sorting
vRNA	Viral RNA
VSV-G	Vesicular Stomatitis Virus G
WPRE	Woodchuck Hepatitis Virus Post-Transcriptional Regulatory Element
WT	Wild-Type
XBP1	X-Box Binding Protein
XIAP	X-Linked Inhibitor Of Apoptosis Protein
ZFN	Zinc Finger Nucleases

1. Introduction

1.1. General Introduction

Gene therapies have been propelled to the forefront of medical research in recent decades. The treatment of genetic disease by use of gene-modifying technologies to replace, repair, or correct genes in the body existed only in concept until the 1990s. As of May 2021, 1,745 gene therapies are in development, ranging from pre-clinical studies through to pre-registration (ASCGT 2021). These trials cover a broad spectrum of genetic diseases, many of which have no other cures, or require chronic treatment.

In the 1990s, the first fully-regulated gene therapy trial approved by the US Food and Drug Administration (FDA) took place, involving the use of a retroviral vector for the treatment of severe combined immunodeficiency (SCID) due to a lack of adenosine deaminase (ADA) enzyme (Bordignon et al., 1995). This trial saw significant expression of ADA in genetically-modified cells with no adverse effects for the patients. Despite clear clinical benefit, regular infusions of genetically modified cells were required due to use of a transient system for gene expression.

Recent successes in cell and gene therapy have enabled the development and approval of several products in the last five years with two *in vivo* gene therapies (Luxturna and Zolgensma) and three cell therapies (Kymriah, Tescartus, Yescarta) presenting highly visible exemplars of what can be possible (Yip and Webster, 2018). These therapies are unquestionably life-changing for patients, in addition to having a much broader impact for development of the foundations for treatments of other conditions.

Whilst presenting a truly exciting frontier for treatment, gene therapy products come with a shocking price-tag. Kymriah, a chimeric antigen receptor T-cell (CAR-T) therapy for the treatment of B-cell acute lymphoblastic leukaemia (ALL) in paediatrics and young adults, costs $475,000 per dose (Galluzzi and Martin, 2017). Even more striking is the cost of Zolgensma, a single-dose gene therapy treatment for patients with spinal muscular atrophy (SMA). This medicine, dubbed the most expensive medicine in the world, costs £1.79 million per dose (Dean et al., 2021).

This raises the question, how can a drug cost so much? The high cost of gene therapies is one of many significant challenges faced in gene therapy manufacture.

Rare diseases remain one of the top therapeutic targets for gene therapies. Current gene therapy vector production is sufficient to enable treatment of rare diseases as these come with small patient populations. Before gene therapies can be employed to treat disease with larger patient populations, such as cancer, it is essential that a more economically viable production platform is developed to enable large-scale GMP-grade vector manufacturing.

1.2. Vectors in Gene Therapy

Delivery of genetic material to a cell is achieved using a vector delivery system (Figure 1.1). The approaches to this can be broadly categorised as viral or non-viral. The non-viral vector space includes various methods for physical gene delivery (microinjection and electroporation), and methods for chemical gene delivery (such as polymer-based and lipid-based vectors) (Gantenbein et al., 2020). Although these approaches are generally safer than viral gene delivery, there are various limitations, with low transfection efficiency being a key issue with currently available technologies (Schalk et al., 2006). Low plasmid DNA production yields must also be increased before non-viral methods are considered as commercially-viable.

Due to their high level of efficiency at delivering nucleic acids to various cell types, viral vectors are attractive tools for therapeutic gene delivery for a range of applications, including cell and gene therapies and vaccine development. Next-generation platforms for the development of vaccines against COVID-19 include viral vector systems, which have been shown to have long-term stability, enable high-level endogenous antigen production, and are capable of inducing a strong cellular and humoral immune response as a result (Le et al., 2020; van Riel and Wit, 2020).

The use of viral vectors for gene delivery has dominated clinical trials recently, with 89% of gene therapies currently in development using a viral delivery method (ASCGT 2021). Viral vectors offer a plethora of advantages over non-viral methods,

which include highly efficient gene transduction processes, specific delivery of genetic information to target cells, and an ability to robustly induce an immune response.

Despite these benefits, challenges with viral vector use do exist, include cytotoxicity, immunogenicity, and insertional mutagenesis (Bushman 2020). Insertional mutagenesis, caused by ectopic integration of viral DNA, is a major concern as it has the potential to activate oncogenes or disrupt tumour suppression genes. This could cause malignant cell transformation and in turn lead to cancer. It must be noted that the first fatality during clinical trials for gene therapy was related to complications through use of a recombinant Adenoviral vector, which caused a severe immune reaction and subsequent death (Sibbald 2001).

Viral vector platforms currently available include Adenoviruses, Adeno-associated viruses (AAV), Retroviruses (RV), and Lentiviruses (LV), whose properties are summarised in Table 1.1.

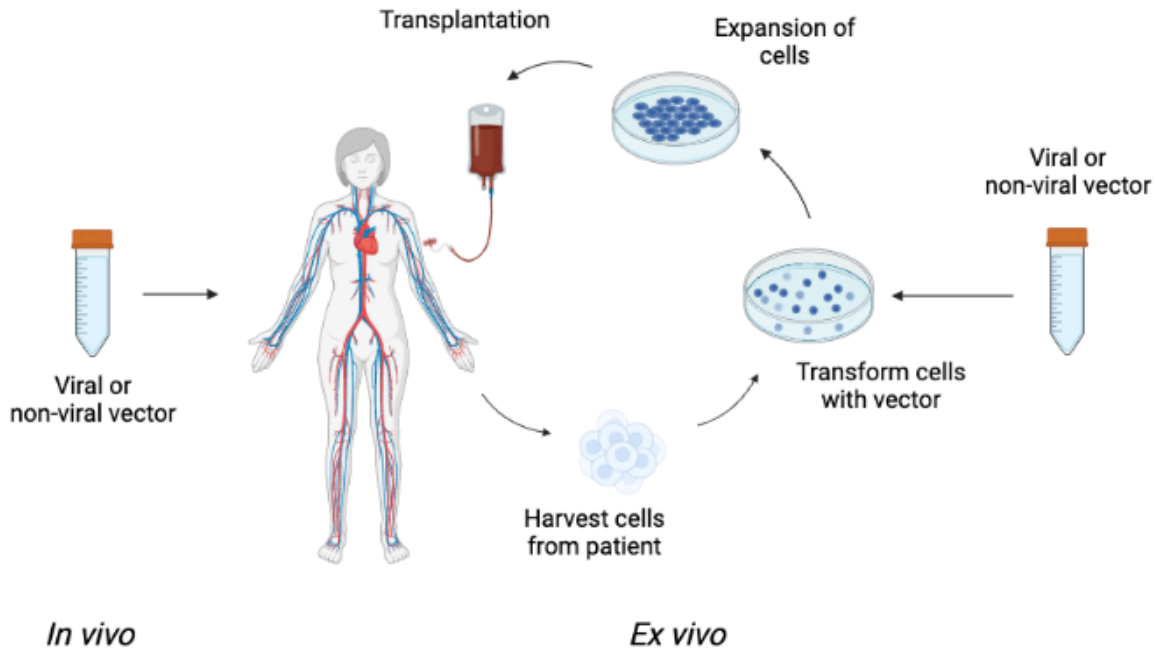

Figure 1.1 Schematic diagram of *In vivo* and *Ex vivo* gene therapy. Therapeutic genetic information is packaged in a vector and is directly administered into a patient in *In vivo* gene therapy, either locally to the target organ, or intravenously through use of an IV. Common targets for *In vivo* gene therapy include the eye, liver, brain, and skeletal muscle (Keeler et al., 2017). Delivery of therapeutic genetic information can be carried out using physical, chemical, or viral methods, as described in Section 1.2. In *Ex vivo* gene therapy, patients' cells must first be extracted. Vector carrying the therapeutic genetic information is used to modify these cells. Cells then undergo selection and expansion, and are finally infused back into the patient (Bulcha et al., 2021). Hematopoietic stem cells (HSCs) are a common target for *ex vivo* gene therapy to treat immunological diseases, blood diseases, and various genetic diseases (Tajer et al., 2019). Created in BioRender.

Table 1.1 Properties of most popular viral vectors used for gene therapy

	Retrovirus	Lentivirus	Adeno-associated virus	Adenovirus
Coat	Enveloped	Enveloped	Non-Enveloped	Non-Enveloped
Packaging capacity (kb)	8kb	8kb	Approx. 4.5kb	7.5kb
Diameter of vector	Approx. 80-100nm	Approx. 80-100nm	Approx. 25nm	Approx. 90-100nm
Tropism	Dividing cells	Broad (dividing and non-dividing cells)	Broad (not Hematopoietic stem cells)	Broad
Inflammatory potential	Reduced	Reduced	Reduced	High
Host genome interaction	Integrating	Integrating	Integrating/Non-Integrating	Integrating/Non-Integrating
Efficiency of transduction	Moderate	Moderate	Moderate	High
Transgene expression	Long-lasting (stable)	Long-lasting (stable)	Potentially long-lasting	Depends on immunogenicity

1.2.1 Lentiviral vectors

Lentiviruses (LV) are a genus within the *Retroviridae* family. These enveloped viruses are approximately 80-120nm in diameter, and comprise two copies of positive-sense single-stranded RNA (Segura et al., 2006) (Figure 1.2). LV RNA is positive-sense, meaning viral mRNA can be directly translated into viral proteins by ribosomes within the host cell.

The replication cycle of the LV HIV-1 can be broadly categorised into early phase and late phase (Freed 2015). The early phase involves binding and entry into the host cell, and the integration of viral DNA into the genome of the host cell. The late phase encompasses all stages from expression of viral genes to the release of virions (Figure 1.3). This includes the transcription of viral genes, nuclear export of viral RNA into the cytoplasm, translation of viral RNA for the production of the viral envelope glycoprotein (Env), Gag and GagPol polyprotein precursors, and other viral proteins, following which Gag, GagPol and Env are trafficked via different pathways to the plasma membrane for assembly. The assembling Gag lattice encapsidates viral RNA and new virions bud off from the cell. Like all other viruses, LVs are proficient at exploiting the host synthetic systems for the production of replicant virus copies, and this presents a major advantage for their use in gene therapy.

Lentiviral vectors (LVV) are effective tools for gene delivery into mammalian cells and their use has gained momentum over recent years (Elegheert et al., 2018). These vectors have many advantages over other viral vectors, including increased patient safety, ability to infect both dividing and non-dividing cells, large transgene capacity and integration into the host genome of target cells, with long-term stable expression of transgenes (Biffi et al., 2011; Lewinski et al., 2006). In addition, LVVs have a lower rate of insertional mutagenesis compared to other RV vectors, and have been shown to preferentially integrate near active transcriptional loci (Ustek et al., 2012; Roth et al., 2011). Due to these advantages, the development of LVVs has been a key focus of research for gene therapy applications.

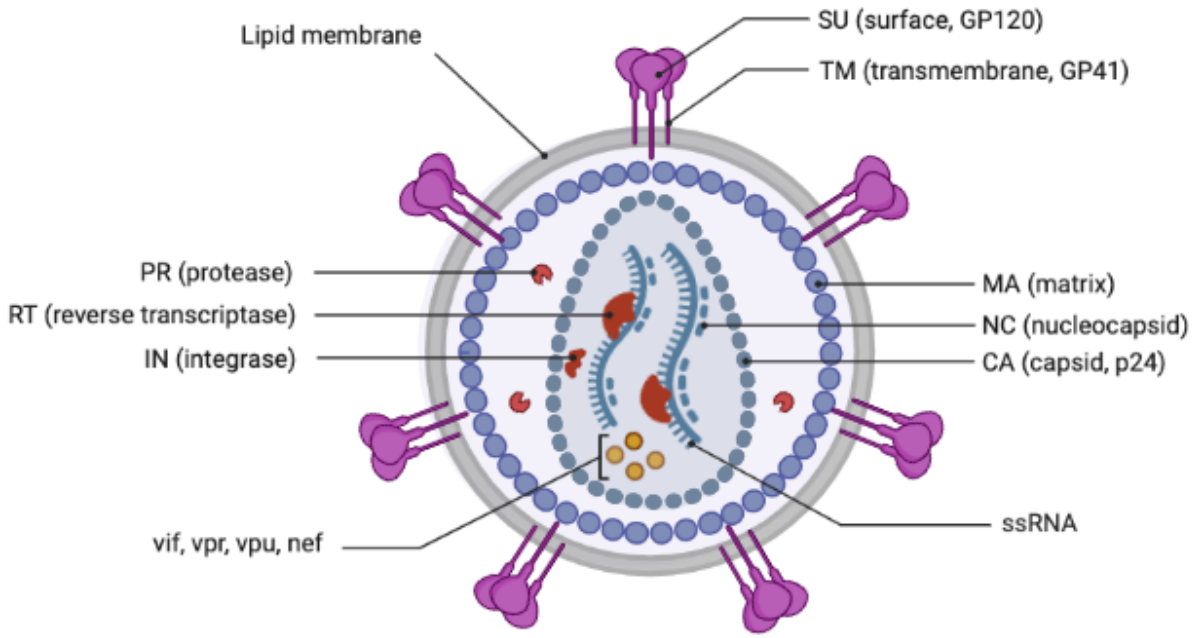

Figure 1.2 HIV-1 Lentivirus structure. HIV-1 is composed of two single-stranded copies of positive-sense RNA, enclosed by a viral core consisting of Matrix (MA), Capsid (CA), Nucleocapsid (NC). The HIV-1 genome contains enzymes essential for replication (Protease (PR), Reverse transcriptase (RT), and Integrase (IN)). Upon maturation, the viral surface glycoprotein gp160 is cleaved, forming gp120 (SU) and gp41 transmembrane protein (TM). Other accessory genes (vif, vpu, vpr, and nef) and regulatory genes (tat and rev) are included in the HIV-1 genome. (Pluta and Kacprzak 2009). Created in BioRender.

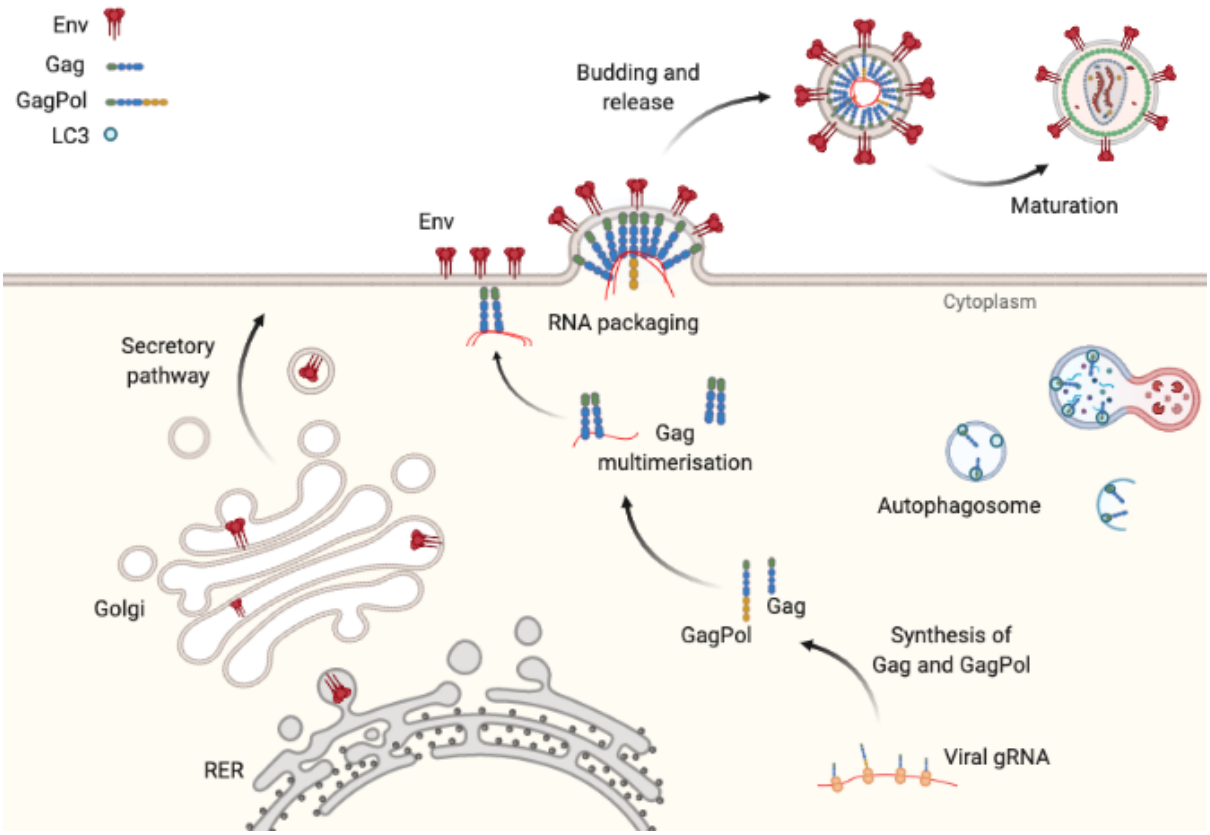

Figure 1.3 Late events in HIV-1 replication. Gag and GagPol polyprotein precursors are synthesised in the cytosol and are targeted to the plasma membrane (PM). Gag multimerises and recruits viral genomic RNA, and traffics to the PM by a pathway that is still unknown. The Matrix (MA) domain of Gag interacts with phosphatidylinositol-4,5-bisphosphate (PI[4,5]P2) on the inner leaflet of the PM (Murphy and Saad 2020; Floderer et al., 2018). Gag has been shown to specifically target lipid raft microdomains on the PM (Freed 2015). Gag has also been observed to co-localise with LC3 on autophagosomal membranes, including the isolation membrane (Killian 2012). The viral Env glycoprotein is synthesised in the rough endoplasmic reticulum (RER) and traffics via the Golgi/secretory pathway to the PM (Checkley et al., 2012). Endosomal sorting complex required for transport I (ESCRT-I) is recruited along with vacuolar sorting protein 4 (VPS4) and ESCRT-associated factor ALG2-interacting protein X (ALIX), which drives particle release by membrane scissions (Sette et al., 2010). Finally, maturation triggered by cleavage of Gag and GagPol by virally-encoded protease (PR) occurs, forming the conical capsid core. Created in BioRender.

1.2.2 Development of Lentiviral Vectors

LVVs were initially developed based on an understanding of the genome of HIV-1 virus, which consists of nine genes, flanked by long terminal repeats (LTR). There are three open-reading frames (ORF) coding for viral structural proteins and enzymes essential for replication of the 9.7kb HIV-1 genome (Petropoulos et al., 1997). Several different generations of LVV have been developed through the years, with each generation having modifications for increased safety (Figure 1.4).

First generation LVV expression systems split the HIV-1 genome across three separate plasmids; a packaging plasmid, an envelope plasmid, and a transfer plasmid. The packaging plasmid contains the *Gag* gene (encoding Matrix (MA), Capsid (CA), Nucleocapsid (NC) and p6), and the *Pol* gene (encoding Protease (PR), Reverse transcriptase (RT), and Integrase (IN)). *Tat* and *Rev* are expressed from a viral promoter (Briggs and Kräusslich, 2011).

The envelope plasmid typically contains the Vesicular Stomatitis Virus G (VSV-G) protein, replacing the HIV-1 gp120 envelope protein (Ikeda et al., 2003). Pseudotyping with VSV-G allows LVVs to transduce a broad range of cell types due to its ability to recognise the low-density lipoprotein (LDL) ubiquitously expressed receptor (DePolo et al., 2000).

The transfer plasmid encodes two long terminal repeats (LTR) which facilitate integration of the gene of interest (GOI) into the host genome. The LTRs can be divided into three regions (U3, R, and U5). Viral transcription is driven by enhancer and promoter sequences contained in U3. A 5' capping sequence and polyadenylation (polyA) signal sequence is encoded in R. The U5 region contains a unique regulatory sequence that aids transcription. This plasmid also contains a Psi packaging signal (Ψ), a 150-250 base highly-structures sequence that facilitates selective packaging of vRNA and efficient viral replication (Ding et al., 2020), and the Rev-Response Element (RRE). The RRE is present on all unspliced and partially spliced viral mRNAs and acts as a framework with which multiple Rev molecules are able to assemble (Rev is an RNA-binding protein that shuttles RNA between the nucleus and cytoplasm) (Fernandes et al., 2012). The Rev-RRE complex is then

able to mediate the export of mRNAs from the nucleus to the cytoplasm for translation into proteins.

The packaging plasmid also contains a central polypurine tract (cPPT) upstream of the transgene expression cassette, which has been shown to increase the efficiency of transduction and also increase expression of the transgene (Barry et al., 2001; Follenzi et al., 2000). It does this by initiating the synthesis of a downstream plus strand of viral cDNA, creating a 'flap' which enables increase nuclear import.

The woodchuck hepatitis virus post-transcriptional regulatory element (WPRE) present in the packaging plasmid is able to increase transgene expression (Zufferey et al., 1999). This element is inserted at the 3' end of the transfer vector, and increases the amount of mRNA in cells by promoting nuclear export of transcripts by increasing the efficiency of transcript polyadenylation (Higashimoto et al., 2007).

In second generation LVVs, accessory genes that are not necessary for LVV production are deleted from the packaging plasmid, including *Nef*, *Vif*, *Vpr*, and *Vpu* (Kim et al., 1998; Zufferey et al., 1997). Interestingly, some of these accessory genes have been associated with disease. HIV-1 *Vpr* has been shown to trigger cell cycle arrest and apoptosis, which is thought to cause T-cell dysfunction in patients with Acquired Immune Deficiency Syndrome (AIDS). As a result of the removal of these accessory genes, second generation LVVs are much safer than first generation LVVs, as they contain a considerably smaller portion of the HIV-1 genome.

Third generation LVVs further split the viral genome. *Gag* and *Pol* are encoded on a plasmid separate to the accessory protein *Rev*, improving the safety of the virus. This physical separation of viral genes reduces the risk of generating replication-competent viruses (RCV) by recombination events more unlikely, and it would mean multiple recombination events are required to generate a virus that is able to replicate (Kim et al., 1998; Dull et al., 1998). It must be noted here that prior to use in patients, all cell-based therapeutics that have been modified by LVVs must be tested to ensure they are not RCV.

The *Tat* gene, used to drive gene expression from the LTRs, is also removed from the packaging construct in third generation LVVs. This is possible when a constitutively active promoter sequence, often the CMV promoter, is put in place of the U3 region of the 5' LTR. Further safety modifications include deletions in the U3 region of the 3' LTR, including transcription-factor binding sites and the TATA box. This deletion is transferred to the 5' LTR following reverse transcription, and as a result, leads to transcriptional inactivation of the LTR. These self-inactivating (SIN) vectors maintain high levels of expression without a significant decrease in vector titre (Zufferey et al., 1998).

Usually, the expression of *Gag*, *Pol*, and *Env* genes in HIV-1 is reliant on the presence of Rev and the RRE due to sequences of RNA instability in the coding regions for these genes. A codon-optimised synthetic GagPol (SYNGP) sequence has been developed to enable Rev-independent production of LVVs, whilst not significantly affecting vector titre (Kotsopoulou et al., 2000). In SYNGP, the majority of codons has been altered to suit the favourable codon usage of human cells (by eliminating AU-rich sequences), in addition to retaining the primary amino acid sequence. This synthetic sequence does not contain any extensive regions of homology with WT HIV-1 GagPol, meaning the possibility for recombination events with Gag sequences in the genome of the transfer vector is non-existent. This Rev-independence allows the RRE to be removed from the packaging plasmid. This is a key example of how LVVs are continuing to develop past third generation LVVs.

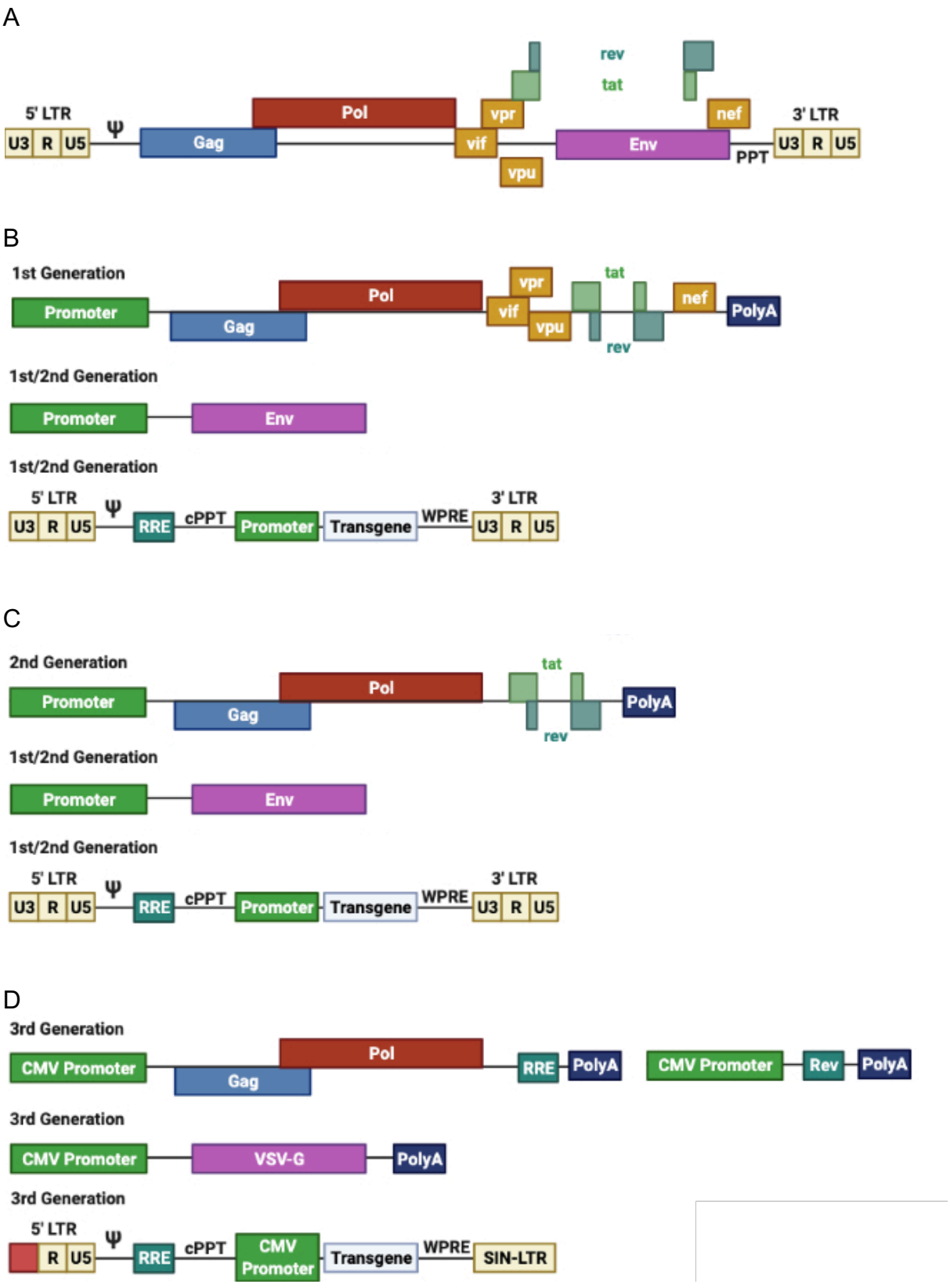

Figure 1.4 First, Second and Third generation Lentiviral Vectors. (A) Genome of HIV-1 with 9 genes encoding 15 viral proteins. (B) First generation LVVs consist of three plasmids. The packaging plasmid contains *Gag, Pol*, *Tat*, *Rev,* and a

polyadenylation (poly(A)) signal. The envelope plasmid contains VSV-G (Briggs and Krausslich, 2011; Ikeda et al., 2003). The transfer plasmid encodes two long terminal repeats (LTR), a packaging signal (Ψ), the rev-response element (RRE), a central polypurine tract (cPPT), the gene of interest (GOI), and the woodchuck hepatitis virus post-transcriptional regulatory element (WPRE). (C) Accessory genes *Nef*, *Vif*, *Vpr*, and *Vpu* are deleted from the packaging plasmid in second generation LVVs (Kim et al., 1998; Zufferey et al., 1997). (D) Third generation LVVs split the viral genome over at least four plasmids, with *Gag* and *Pol* being encoded on a plasmid separate to the accessory protein *Rev*. *Tat* is also removed. A constitutively active promoter sequence is put in place of the U3 region of the 5' LTR. Third generation LVVs are self-inactivating (SIN) due to deletions in the U3 region of the 3' LTR (Zufferey et al., 1998). Created in BioRender

1.3. Production of Lentiviral Vectors in HEK293T cells

HEK293T cells are the 'gold standard' cell for producing LVVs for a plethora of reasons. The Human Embryonic Kidney (HEK) 293 cell line is epithelial in origin and adherent in nature. It was initially generated in 1973 in the Netherlands in the Alex van der Eb lab. These cells were produced by transfection with sheared adenovirus 5 DNA, which resulted in some of the adenoviral genome being incorporated into human chromosome 19 of the HEK cell genome. One of Alex van der Eb's post docs, Frank Graham, had the original idea of naming these cells 'HEK293' due to it being his 293rd experiment. HEK293T cells are a derivative of HEK293 cells that stably express a mutant form of the Simian Virus 40 (SV40) large T antigen, which can bind to the SV40 enhancer of expression, in turn increasing protein production. HEK293T cells are highly transfectable and have increased cell growth profiles compared to HEK293 cells. From a practical view, HEK293T cells are easy to grow and maintain, and can be adherent or suspension-adapted.

Although there is no defined standard process for vector manufacturing, generic LVV production processes are generally split into upstream and downstream workflows. Upstream manufacturing has a focus on mass-producing LVVs, and involves the development and large-scale production of plasmids, cell expansion, and transfection for LVV production (Perry and Rayat, 2021). Downstream manufacturing involves harvesting and purification of the LVV, followed by various steps for the clarification, concentration, purification, and characterisation of the LVV (Valkama et al., 2020). Optimisation of these steps is key to ensure that vector recovery is maximised. There is much to be learned from the manufacturing processes of other therapeutics; for example, the production of monoclonal antibodies (mAbs) in CHO cells is well-established, with current production of mAbs occurring continuously at large-scale, as discussed in Section 1.3.1 (Tihanyi et al., 2021). Various obstacles including vector cytotoxicity must first be overcome before LVVs can be continuously produced at large-scale.

Two strategies exist for the production of LVVs in HEK293T cells, through the use of either transient gene expression or stable gene expression. Transient production of

LVVs involves the temporary expression of viral genes following introduction of plasmid DNA into HEK293T cells. Stable expression involves the stable integration of DNA into the HEK293T host cell genome following selection and amplification of transfected cells. In the case of LVVs, a stable packaging cell line provides all necessary packaging components (Gag, Pol, and Env) needed to package the gene of interest. Following stable transfection of packaging cells with a therapeutic transgene, producer cells are generated. Transient and stable production of LVVs will be discussed in detail in Sections 1.3.1 and 1.3.2 respectively, however a broad summary of these processes can be found in Figure 1.5.

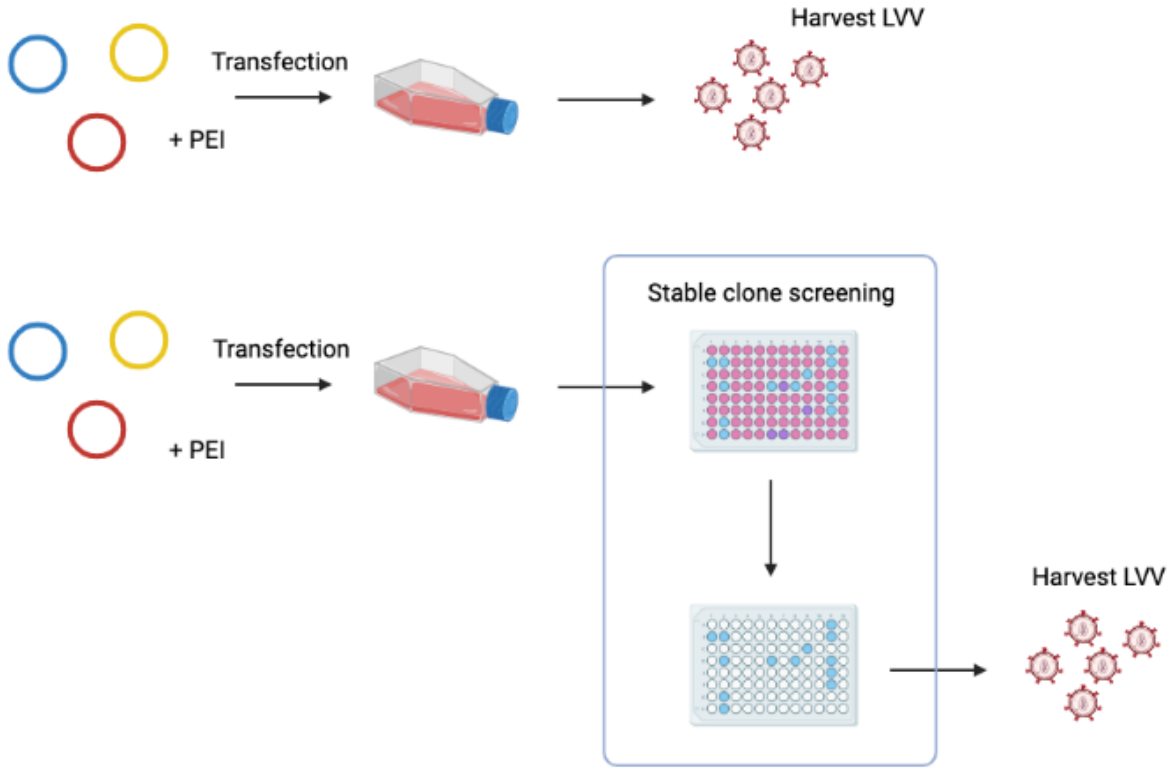

Figure 1.5 Schematic diagram of transient and stable gene expression processes. Top: Transient LVV production involves the introduction of plasmid DNA into HEK293T cells with subsequent harvest approximately 48 hours post-transfection. Expression of plasmid DNA is transient. Bottom: Stable LVV production involves introduction of plasmid DNA into HEK293T cells using a transfection agent, for example polyethylenimine (PEI). Plasmid DNA contains a selection marker, often based on antibiotic resistance. Following transfection, the appropriate selection marker is added to culture medium, generating a stable cell pool enriched in producer cells. Single cells will then be separated to produce a clonal cell line, which are expanded and screened to analyse productivity and cell growth. Created in BioRender.

1.3.1 Transient production of Lentiviral Vectors

Current standard production of clinical-grade LVVs by delivery of packaging, envelope, and transfer plasmids is based on the transient transfection of adherent HEK293T cells, resulting in the temporary expression of viral genes following transfection. This approach is useful for when small quantities of LVV need be generated in a short length of time, which can be used in pre-clinical analyses for example (Merten et al., 2014).

Transient production of LVVs can be performed using various physical or chemical methods. Physical gene delivery methods include electroporation. Electroporation has reported high transfection efficiency and yields when used at small scale, however this process is rather complex as various buffers are required, in addition to high cell concentrations (Gutierres-Granados et al., 2018). Several methods for chemical gene delivery exist such as the use of polymer-based and lipid-based vectors (Gantenbein et al., 2020). A popular method is Calcium Phosphate transfection which gives a high transfection efficiency, however this method remains incompatible with serum-free medium (Batard et al., 2001). Polyethylenimine (PEI) is another popular chemical agent used to enable efficient transient gene expression (Carpentier et al., 2007).

Vector titres of approximately 10^7 TU/mL are achieved using transient transfection, with this increasing to 10^9 TU/mL following concentration of vector by ultracentrifugation (vector titres are most commonly expressed as transducing unit (TU), whereby a TU represents the number of viral particles in a solution that are functionally capable of transducing a target cell and expressing a transgene). Ultracentrifugation is a necessary step in LVV preparation as it allows for production of highly concentrated viral vector stocks, which in turn permits high multiplicities of infection (MOI) to be achieved in a transduction which is important for clinical applications to ensure therapeutic benefit to the patient (Reiser 2000; Sena-Esteves et al., 2004). Considering that LVV titres of over 1-5 x 10^9 TU/mL are required for some clinical applications, it is vital that titres are vastly improved in order to treat more patients and lower the cost of production (Biffi et al., 2013; Aiuti et al., 2013; Humbert et al., 2016; Alton et al., 2017).

Use of adherent cells means that there is limited scale-out capacity for LVV generation due to space constraints. A cell factory of 10 layers (equivalent of 170 T150 flasks) would enable a harvest of 50 L of vector stock per transfection batch. Following purification, 6 x 10^{11} TU can be obtained from such a multilayer cell factory (Merten et al., 2011).

There is a current focus in shifting LVV production from adherent cells to suspension cells, in order to overcome the requirement for expensive reagents, labour-intensive production, and the need for large surface-areas involved with the scale-out of adherent cells. This is discussed in detail in Section 1.4.1.1. Suspension cells are easy to maintain, do not need mechanical or enzymatic dissociation, are animal serum-free, and have proven scalability (Lesch et al., 2011). In 2006, suspension HEK293E cells, a derivative of the HEK293 cell line that expresses the Epstein-Barr Virus (EBV) nuclear antigen 1 (EBNA1) which allows episomal replication of oriP-harbouring plasmids (Backliwal et al., 2008; Rajendra et al., 2012), were used by Segura et al. (2006). These cells produced good yields of LVVs, and these authors illustrated the potential to scale up providing data for use in a 3L bioreactor (Segura et al., 2006). A similar approach was taken by Kamen et al. using HEK293SF-3F6 cells, a cell line originally developed for AAV production but adapted for LVV production (Kamen et al., 2007). HEK293SF-3F6 cells are HEK293-derived cells that were adapted in a step-wise manner to serum-free culture. Here, titres of up to 8 x 10^7 TU/mL and a total 3.5 x 10^{11} transducing units were achieved. Given the potential advantages of a suspension format, enhancing the production capacity of suspension cells is currently a key focus of development in the LVV space.

There are many other challenges with transient LVV production systems, with a key issue being that the expression of viral genes following introduction of DNA into HEK23T cell is only temporary. Transient transfection also requires large amounts of plasmid DNA. For example, 2.5 µg per 10^6 HEK293T cells was reported to be required by Marceau et al. to reach high a transfection efficiency, which equates to 750 mg of plasmid DNA for transfection in a 200L bioreactor (Marceau et al., 2013). Sourcing clinical-grade DNA plasmids is expensive and involves long lead-times which can directly impact the patient (Praeres and Monteiro 2014). Batch-to-batch variability can often be difficult to control when using transient production.

It is clear that an alternative manufacturing model is required to enable high LVV titres. Achieving high-titre production of LVV would enable this field of research to move from treating rare diseases to other conditions which have much larger patient populations, such as cancer. A way to accomplish this would be to develop a stable producer cell line. Historically, the development of stable cell lines has allowed rapid and efficient production of other therapeutics such as mAbs in Chinese Hamster Ovary (CHO) cell lines (Tihanyi et al., 2021). It would be wise to utilise existing knowledge learned from over 40 years of development of CHO cell platforms and apply this to HEK manufacturing platforms for production of LVVs at large scale. This will be discussed in detail in the following Sections.

1.3.2 Stable production of Lentiviral Vectors

The development of a high-yield stable cell line remains a key target for gene therapy manufacturers. One way to achieve this involves the development of a packaging cell line stably expressing packaging and envelope genes (Gag, Pol, and Env), which would then become the producer cell line once the transfer vector is provided, enabling production of a completely packaged LVV. This approach would enable multiple vector batches to be harvested from a single culture, in turn reducing batch-to-batch variability (LaGory et al., 2015). In addition, the cost of large-scale LVV production would be reduced, the whole process would be less labour-intensive, costs would decrease as additional transfection reagents and plasmids are not required, and overall the upstream process would be simplified (Tandon et al., 2018). Several groups have attempted to create stable cell lines (summarised in Table 1.2).

The generation of stable cell lines can be time-consuming with development taking several months from initial cloning until cell banking and it can be a very costly and monotonous process from a practical point of view at the beginning of the drug development campaign. A further difficulty with stable cell line generation is the cytotoxicity associated with the continuous expression of certain toxic vector components; cytotoxicity to host cells has been observed with the expression of GagPol (Figure 1.7) (Kräusslich 1992), Rev (Miyazaki et al. 1995), and VSV-G (Burns et al. 1993). Currently, there are two methods that enable stable LVV

production (constitutive and inducible), which will be discussed in Sections 1.3.2.1 and 1.3.2.2.

1.3.2.1 Constitutive cell lines

Constitutive packaging cell lines involve the continuous expression of vector components. These cell lines can be difficult to produce, as they require the development of non-toxic alternatives to the components expressed from some vector components, mainly VSV-G and certain domains within GagPol such as Protease (PR) (Korant et al., 1998; Nie et al., 2002; Rumlova et al., 2014).

The first constitutive packaging cell line ('STAR' cells), developed by Ikeda *et al.* in 2003, attempted to introduce several novel aspects; (i) the use of HEK293T, HeLa, and HT1080 as starting cells (ii) the use of three envelope proteins in place of VSV-G, including a protein derived from the Feline Endogenous GRV RD114 non-toxic envelope with an additional protease cleavage site, a derivative of the Gibbon Ape Leukaemia Virus envelope protein, and the MLV-4070A Amphotropic envelope; and (iii) introducing the packaging genes (Gag and Pol) by transduction with a MLV-integrating vector, rather than traditional stable transfection (Cosset et al., 1995; Marandin et al., 1998; Demaison et al., 2002). This cell line enabled continuous LVV production with titres of approximately 1 x 10^7 TU/mL following 3 months of culture (Ikeda et al., 2003). Despite this promising result, STAR producers were not put forward for clinical application due to the risk of recombination between the MLV genome and LVV particles during transduction, which poses considerable risk as these vectors were not self-inactivating (Ikeda et al., 2003).

Further attempts at creating a constitutive packaging cell line include the development of WinPac cells (Sanber et al., 2015). This cell line was developed using a modular approach whereby Recombinase Mediated Cassette Exchange (RMCE) was used for targeted delivery/exchange of viral components during transduction (Coroadinha et al., 2006). In this system, the non-toxic envelope RD114-PR, *rev*, and the vector genome were sequentially transfected, and antibiotic selection was used to screen producer clones. Titres of approximately 1 x 10^8 TU/mL were achieved (following ultracentrifugation), which is considerably lower than

desired for a stable cell line, when considering transient systems are capable of similar titres.

1.3.2.2 Inducible cell lines

Inducible packaging cell lines mitigate the cytotoxic effects of continuous expression of toxic vector components. The expression of vector components can be transcriptionally controlled using regulatory systems such as the Tet-On and Tet-Off gene expression systems (Figure 1.6). Here, the presence of the antibiotic tetracycline (or a derivate such as doxycycline) is able to reversibly turn the expression of certain genes on or off. These systems are able to tightly control gene expression, with examples of inducible cell lines given in Table 1.2.

The Tet-Off inducible expression system was developed by Hermann Bujard and Manfred Gossen in 1992, and involves inhibition of gene expression in the presence of tetracycline, where gene expression is under the control of a tetracycline-response element (TRE) (Gossen and Bujard, 1992). A benefit of using the Tet-Off system is that tetracycline does not need to be present during vector production, which is advantageous for downstream processing. A drawback of this is that a complete medium exchange is required to remove tetracycline entirely, as well as needing extended culture periods in order for expression to peak, both of which are problematic for large-scale vector production.

The Tet-On inducible expression systems was developed in 1995 (Gossen et al., 1995). An issue with the Tet-On system is that it requires tetracycline addition to the growth medium and this needs to be removed from harvested supernatant and therefore adds further steps to downstream purification processes.

GlaxoSmithKline (GSK) recently developed a novel inducible system allowing the rapid generation of a LVV producer cell line using a single large DNA construct, a bacterial artificial chromosome (BAC) (Vink et al., 2020). In this system, all vector components are encoded on a single construct, each with their own separate transcription units. To avoid the generation of replication-competent LVV, each component is flanked by its own promoter and polyadenylation signal. This construct

contains a CMV promoter with two TetO sequences, enabling inducible transcription, and therefore avoiding cytotoxicity from certain vector components. Transcription is activated by the presence of doxycycline, typical of a Tet-On system. This platform enables a high degree of flexibility in terms of allowing further development of individual vector components. A single cloning step would be sufficient to replace each component if, for example, an improved GagPol or Rev was developed, or the pseudotype needed alteration. Depending on the transgene, these constructs are approximately 45kb in size, which is advantageous as this means gene synthesis technologies could comfortably generate these constructs. Functional titres achieved in this system achieved over 10^7 TU/mL unconcentrated, which is similar to the titres obtained with routine transient transfection of HEK293T cells (Segura et al., 2013; McCarron et al., 2016; Milani et al., 2017).

Table 1.2 Examples of Constitutive and Inducible stable cell lines for Lentiviral Vector production.

Name	Parental cell line	Mode of expression	Pseudotype	SIN	Information	Titre	Reference
PS5.8 PS46.2	HEK293T	Inducible, Tet-On	VSV-G	Yes	Sequential transfection of vector components	< 10^6 TU/mL	Stewart et al., 2009
HEK293SF-PacLV	HEK293SF	Inducible, Cumate switch, Tet-On	VSV-G	Yes	3 plasmid transfection with GagPol, rev, VSV-G followed by transfection with transfer vector	3.4 x 10^7 TU/mL	Broussau et al., 2008
No name	PVG3 (HEK293T)	Inducible, Tet-Off	VSV-G	Yes	tTa is constitutively expressed, VSV-G is under inducible expression, GagPol, tat, and rev are stably transfected	1 x 10^{10} Infectious units/mL (concentrated)	Hu et al., 2015
SODK1 cSCG	HEK293T.tTA	Inducible, Tet-Off	VSV-G	Yes	Introduction of transfer vector by transduction, followed by co-transfection of GagPol, tat, rev, and VSV-G	2 x 10^6 Infection units/mL	Xu et al., 2001
STAR	HEK293T	Constitutive	MLV 4070A, GaLV, RD114-PR	No	Transduction of GagPol followed by transfection of RD114 env and rev	1 x10^7 infection units/mL	Ikeda et al., 2003
WinPac	HEK293FT	Constitutive	RD114-PR	Yes	GagPol constitutively expressed in 293T by Cre recombinase-mediated cassette exchange, followed by serial transfection of rev, env, and vector genome	1 x 10^8 TU/mL (concentrated)	Sanber et al., 2015
LentiPro26-A59	HEK293T	Constitutive	VSV-G	Yes	Producer cell line with less active viral PR	1 x 10^6 TU/mL/day	Tomas et al., 2018

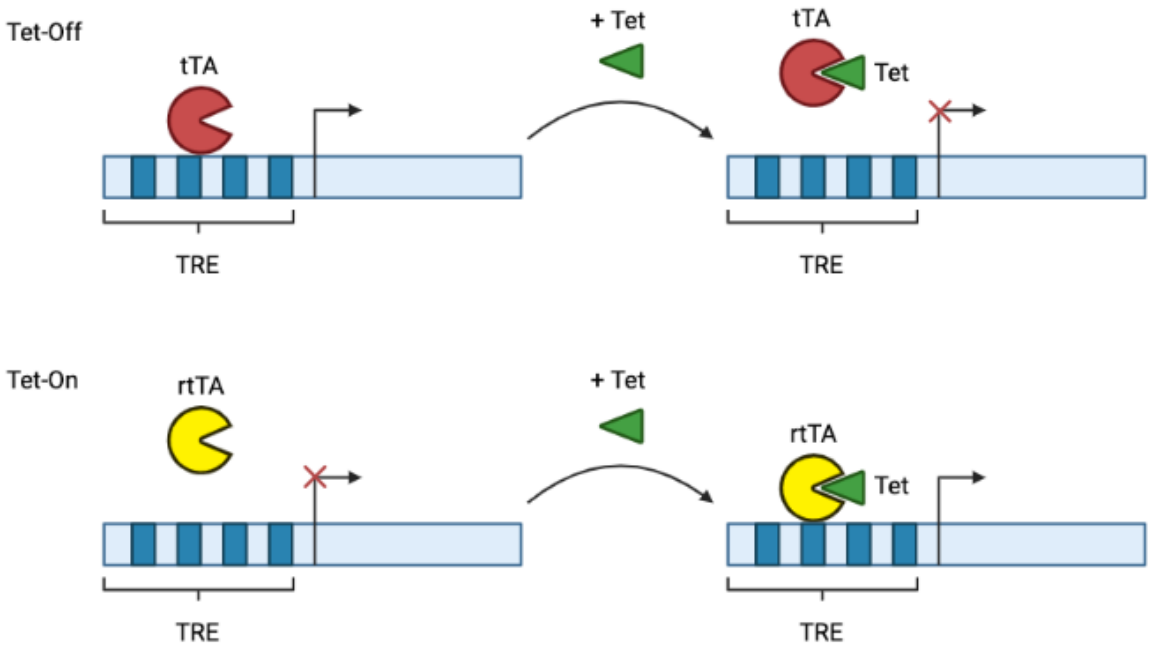

Figure 1.6 Tetracycline-inducible expression systems. In the Tetracycline (Tet)-Off system, fusion of the tetracycline repressor (TetR) in *E. coli* to the activation domain of HSV VP16 results in the formation of the tetracycline transactivator (tTa) protein (Kim et al., 1995). The Tet-responsive element (TRE) often consists of several repeats of *TetO* operator sequences upstream of a promoter (e.g. the CMV promoter). The expression of TRE-controlled genes can be suppressed in the presence of tetracycline in a Tet-Off system. Tetracycline binds to tTa which in turn cannot bind to the TRE sequence, so transcription cannot occur. In the Tet-On system, gene expression is activated by the addition of tetracycline. Reverse-TetR (rTetR) in Tet-On systems has only 4 amino acids different to the TetR in Tet-Off systems, and was identified through random mutation and phenotype screening (Urlinger et al., 2000). Fusion of rTetR to the activation domain of HSV VP16 leads to the formation of the reverse tetracycline transactivator (rtTA) protein. There is a conformational change to rtTA upon binding to tetracycline, which subsequently promotes TetO binding, in turn driving the expression of the downstream gene. Created in BioRender.

1.4. Improving Lentiviral Vector production

A clear objective for large-scale LVV production is to make the process more economically viable. To do this, each stage of the manufacturing process must be examined to identify strategies for improvement. A more economically viable production platform would involve increasing vector titres in any given system, and therefore lowering the cost of vector production. Approaches for improving culture performance and protein expression can be broadly categorised as optimising the bioprocessing conditions for LVV production, optimising the vector, and optimising the cell factory via targeted cell engineering, all of which will be discussed in detail.

1.4.1 Optimising HEK293T bioprocessing conditions

1.4.1.1 Adherent vs. Suspension

LVV titres can be increased through packaging cell expansion and improving cell culture conditions (Soldi et al., 2020). High quantities of cells are required to produce high titres of LVVs and there are several strategies for packaging cell expansion in different culture vessels. As discussed previously, adherent cells are typically used to produce vector by transient transfection. Corning CellSTACKS provide up to 40 layers for cell attachment, and Corning HYPERflasks and HYPERstacks offer multi-layer attachment surfaces with the advantage of using gas-permeable plastic (Segura et al., 2013; Spier et al., 1985; Merten et al., 2011 Kutner et al., 2009). Despite the common use of adherent culture vessels during development stages, they have limited scale-up potential, and require scaling-out to increase the surface area for attachment. Handling such large cell factories increases the risk of contamination when pooling batches for downstream processing.

Microcarriers offer another potential option to allow packaging cell expansion. These are small spheres approximately 150-200 microns in diameter to which adherent cells can attach (Barrett et al., 2009). Microcarriers are able to reduce labour intensity and process complexity when compared with multi-layer cell culture vessels. Drawbacks to the use of microcarriers include cell clumping and

detachment from surfaces, in addition to the occurrence of microenvironments within the centre of the microcarriers which may impact on nutrient transfer, oxygen transfer, and release of CO_2 and other toxic metabolites (Li et al., 2015).

Fixed bed bioreactors are a common alternative to flask-based adherent cell culture, providing efficient scale-up for LVV production (Wang et al., 2015). An example of this is the iCELLis™ marketed by Pall Life Sciences. In this system, many hundreds (sometimes thousands) of roller bottles are replaced with a fixed-bed bioreactor, with the surface area increased by use of microfiber microcarriers. In the iCELLis™ system, polyethylene terephthalate (PET) fibres are used. The process of LVV production becomes more economically viable when considering (i) the minimised need for space to accommodate bulky cell factories, (ii) the reduced man power needed to operate the fixed-bed bioreactor system, and (iii) the overall decreased waste as the risk of contamination is drastically reduced, meaning lower risk of having to scrap big batches (Lennaertz et al., 2013). Advantages of this system include recording pH, O_2, and CO_2 levels, coupled with replenishment of cell culture medium and removal of toxic metabolites. In a transient system, the iCELLis™ Nano has been shown to obtain LVV titres of 1.3×10^{10} TU from a 2.67 m^2 surface, and the iCELLis™ 500+ has achieved 1.12×10^{12} TU from a 333 m^2 surface (Valkama et al., 2018; Lennaertz et al., 2013).

Moving from adherent to suspension cell culture enables scale-up of LVV production and offers various advantages where (i) cell growth is no longer limited by surface area as with adherent culture, (ii) manual handling is minimised in that cell passaging is easier and cells do not require enzymatic dissociation, (iii) perfusion culture is possible, therefore waste productions can be removed, nutrients can be maintained as necessary, and vector can be continually harvested, (iv) cultures can be automated, (v) addition of transfection reagents is much simpler, and (vi) suspension cells do not require serum in media, meaning a lower risk of contamination, simpler downstream processing, and an extra reduction in cost (Bauler et al., 2019). Stable LVV producer cells that are suspension-adapted are therefore key in the future of LVV production at large scales (Segura et al., 2007).

Several successful strategies for adapting adherent cells to suspension culture have been described, with several in detail in Table 1.2, with stirred tank bioreactors providing a straight-forward scale-up approach. HEK293T cells can be grown in an Ambr bioreactor up to a scale of 10,000L, with Allegro™ single-use system (Pall Life Sciences) achieving titres of 1.1 x 10^{10} TU/L (Sena-Esteves et al., 2018). Rocking bioreactors offer an alternative approach for producer cell expansion, whereby suspension cells are rocked on a platform in single-use inflatable bag at scales of up to 200L. An advantage of this system is that this environment favours a decreased risk of shear damage to cells because of a lack of impellers. GMP-compliant stable producer systems have been able to produce LVV at clinical scale using rocking bioreactors (Sorrentino et al., 2012).

1.4.1.2 Cell culture media supplementation

Medium supplements aid mammalian cells in producing proteins by improving cell growth and viability (Ritacco et al., 2018; Perez-Rodriguez et al., 2020). Supplementation of medium has been shown to increase recombinant protein productivity in CHO cells (Reinhart et al., 2015; Blondeel et al., 2016). Developments in this area enabled improved product titres through optimisation of culture media. Fed-batch CHO cell cultures often have basal mediums containing essential nutrients that cells require for proliferation and protein production, with feeds that tend to be much more concentrated in order to maximise volumetric productivity and recombinant protein product titre (Huang et al., 2010; Martens et al., 2017; Fan et al., 2018). Culture composition has been shown to influence not only protein productivity and cell growth, but also gene expression, the quality of the product, and certain metabolic profiles including lactate and ammonia (Pan et al., 2017). During LVV production, medium formulation has been shown to have a direct correlation with producer cell expansion, cell viability, and vector stability (Ballas et al., 2005).

As discussed previously, the removal of animal serum is a focus of development in LVV production. To remove serum in culture, it must be gradually removed for cells to become adapted to low concentrations (Caron et al., 2018). Despite serum assisting cell growth and vector stability, it poses issues for downstream processing as removal of serum contaminants is difficult. There is also the risk of serum

shortage in the event of bovine-related disease outbreaks. Supplementing medium with albumin may act as a substitute for animal serum as this has shown to aid vector stabilisation during downstream processing (Mekkaoui et al., 2018). The continued development of serum-free media has led to LV titres that are comparable with serum-containing media. This has been clearly shown, for example, with the commercially available chemically-defined GMP-grade FreeStyle 293 medium (Do Minh et al., 2020).

Optimised cell culture medium has been demonstrated to support efficient and high-yielding protein production (Cervera et al., 2011; Liste-Calleja et al., 2014). The addition of supplements to cell culture medium has been shown to improve LVV titre, such as sodium butyrate (Jaalouk et al., 2006). This has been linked to improved production of recombinant proteins by inhibiting histone deacetylate, which enabled improved transcription factor function (Davie 2003; Steliou et al., 2012). As a result, RNA copies are increased from viral LTRs, and ultimately LVV titres are improved. A combination of decitabine and sodium butyrate has been shown to promote the expression of transgenes, improve specific productivity, and inhibit apoptosis in CHO cells (Li et al., 2022). Further examples include the addition of Cholesterol, which is known to be involved with lipid raft formation on cell surfaces, in turn facilitating budding of virions (Campbell et al., 2001; Pipik et al., 2002; Kamiyama et al., 2009). Other supplements benefitting suspension culture include non-ionic surfactants such as Pluronic, which enhances cell yields and reduces clumping (Tharmalingam et al., 2008).

1.4.2 Optimisation of the vector

Optimisation of vector plasmids is an important consideration when aiming to enhance LVV production, from both a safety aspect but also to improve vector titres, as discussed in Section 1.3.2. Improving packaging and transfer plasmids has been shown to give increased LVV production (Maruggi et al., 2009; Cesana et al., 2014). Promoter choice is an important consideration, with the following characteristics being important (i) use of strong promoters (the CMV promoter is often used in LVV production as it is strong and provides robust gene expression, as is the Elongation factor 1a (EF1a) promoter, and the Spleen focus-forming virus (SFFV) promoter), (ii)

use of promoters that are induced by external stimuli including small molecules (antibiotics including tetracycline and doxycycline), temperature variations, or other endogenous molecules (such as pro-inflammatory cytokines), and ideally which exhibit no leakage, and (iii) potential use of synthetic promoters that are stronger and smaller in size by determining the minimal promoter length that is capable of achieving good gene expression levels (Suzuki et al., 2018; Li et al., 2010; Merten et al., 2016).

Manufacturing and characterisation of plasmid DNA is also key in improving LVV production. As plasmid DNA is the starting material for gene therapies, it is important that it is high-quality in order to meet the requirements for clinical trials as discussed in Section 1.3.2. The term 'high-quality' in terms of plasmid manufacturing denotes a high percentage of supercoiled plasmid (>80%), with low endotoxin contamination levels due to endotoxin presence causing decreased transfection efficiency and protein expression (Merten et al., 2016).

Optimising packaging plasmid ratios during transfection and quantities of plasmid per cell can have a positive influence on transfection and therefore vector titre (Bauler et al., 2020). Adjusting the ratio of transfer, envelope, and packaging plasmid is important for obtaining optimum LVV titres. It is also key in keeping costs low, as for example, transfection with too much packaging plasmid could result in production of empty viral particles, which is disadvantageous.

It is also possible to improve transfection efficiency by reducing extraneous vector sequences which are not necessary for LVV production. For example, eliminating the HIV-1 viral accessory genes Nef, Vif, Vpr, and Vpu creates a reduced vector length and in turn superior vector titres. Deletion of these genes is demonstrated in Figure 1.4 (Zufferey et al., 1997; Naldini et. Al., 1996; Kim et al., 1998). It has been shown that it is possible to substantially reduce HIV-1 sequences in LVV without compromising the efficiency of transduction. Sertkaya et al. showed that LV genomes can be decreased in length by deletion of regions in Gag and Env that are not essential for vector production, in addition to repositioning the RRE (Sertkaya et al., 2021). By doing this, the potential for RCV formation is reduced, and transgene capacity is increased.

1.4.3 Optimising HEK293T cells via targeted cell engineering

The most important characteristic of a HEK293T cell is arguably its human origin, given that the biologics these cells produce are for human use. These cells produce protein with human post-translational modifications, which is an advantage over other non-human cell lines such as CHO cells (Dumont et al., 2016). However, at present, HEK293 (and cell lines derived from HEK293) cell growth and productivity is inferior to that of CHO cells.

For example (i) maximum growth capacity of CHO cell is 1-2 x 10^7 cells/mL, whereas for HEK293 cells it is only 3-5 x 10^6 cells/mL (Chin et al., 2019) (ii) doubling time of CHO cells is 14-17 h in comparison to approximately 33 h for HEK293 cells and (iii) recombinant protein product yields for CHO cells are about 4 g/L compared to a maximum of 600 mg/L for HEK293 antibody production (Frenzel et al., 2013). Studies have shown that modifying genes implicated in key cellular processes such as apoptosis, cell proliferation, glycosylation, metabolism, protein folding, and secretion are able to vastly improve CHO cell performance (Kim et al., 2012; Lai et al., 2013; Fischer et al., 2015; Kuriakose et al., 2016; Orellana et al., 2017;). Similar cell engineering approaches in HEK293 cells are limited in comparison and must be expanded upon, given that the use of HEK293 cells in gene therapy vector production is increasing due to successful clinical trials. The paradigms developed over the past 20 years for enhancements of CHO cell factory system performance serve as exemplars upon which to build future directions to enhance LVV production in HEK cell factory systems.

The quantity of recombinant protein that a HEK293T cell can produce is ultimately limited by the cell's biology, even if bioprocessing conditions and vector sequences have been optimised. Genetic engineering strategies that target bottlenecks in cell proliferation, carbon metabolism, secretion, and protein folding have the potential to improve LVV titres, and will be discussed in more detail below.

The objective of genetically engineering cell proliferation is to enhance maximum cell density and culture longevity, whilst maintaining protein production per cell, thus

enhancing LVV titres. This can be accomplished by modifying the cell growth rate. Recombinant protein expression can be enhanced by increasing cell growth, particularly by over-expressing genes involved in the G1/S transition such as eukaryotic initiation factor 3 complexes EIF3I and EIF3C, cytochrome-C oxidase subunit 15 (COX15), and cyclin-dependent kinase-like 3 protein (CDKL3) (Jaluria et al., 2007; Roobol et al., 2020). Cells are commonly larger in size and more active metabolically during transition between phases G0/G1 and G2/M and slowing the growth rate by over-expressing cyclin-dependent kinase inhibitors (CDKN) 1A, 1B, and 2C at these points has the potential to improve recombinant protein production by approximately 6-fold in HEK293 cells (Backliwal et al., 2008; Wemer et al., 2007). Looking specifically at recombinant IgG expression, coupling these strategies with optimised vector design and treatment with valproic acid has achieved 27-fold increase in a transient expression system (40 mg/L up to 1.1 g/L) (Backliwal et al., 2008). Despite clear benefits of modifying cell growth, it must be done very carefully as vital cellular resources may be directed towards cell proliferation and away from LVV production.

Apoptosis is a genetically-regulated form of programmed cell death, defined by membrane blebbing, shrinkage of cells, chromatin condensation and DNA fragmentation (Kerr et al. 1972). Generating a cell that is resistant to apoptosis would enable increased viable cell numbers, improved culture longevity, and support higher LVV titres (Tey et al., 2000; Mastrangelo et al.; 2000 Kim and Lee 2002; Figueroa et al., 2007). Apoptosis is tightly controlled by a number of anti-apoptotic and pro-apoptotic genes which are activated by stimuli such as DNA damage, deprivation of nutrients, insufficient oxygen levels and high osmolarity (Elmore 2007). Up-regulation of anti-apoptotic genes also has the ability to delay apoptosis as exhibited with the anti-apoptotic B-cell lymphoma 2 (BCL2) gene (Formas-Oliveira et al., 2020; Sandhu et al., 2009), and over-expression of X-linked inhibitor of apoptosis (XIAP) (Sauerwald et al., 2002; Sandhu et al., 2009, Sauerwald et al., 2002). Alternatively, down-regulation of pro-apoptotic genes has been shown to delay the onset of apoptosis in HEK293 cells as exhibited with the double knock-out of BAX and BAK which resulted in volumetric production of a recombinant protein to increase by 53% (Arena et al., 2019), and the quadruple knock-out of AIF1, and Caspases 3, 6, and 7 which has led to an 8-fold increase in viable cell numbers (Zhang et al., 2017).

The effect of autophagy on ectopic protein production is not yet fully defined in both CHO and HEK cells (Baek et al., 2016). Autophagy, a pathway for programmed cell death, is a highly-conserved homeostatic mechanism characterised by delivery of cytosolic components in a double-membraned vesicle to the lysosome for subsequent degradation and recycling (Ohsumi et al., 2001). This pathway is induced through a number of stimuli including but not limited to nutrient starvation, hyperosmolality, and the presence of misfolded proteins (Musiwaro et al., 2013). Autophagy has also been shown to function in both a pro-viral and anti-viral manner (Choi et al., 2018). This is of particular interest when looking at LV production, given that LVs are designed based on HIV-1. HIV-1 has previously been demonstrated to utilise autophagic organelles as sites of packaging in macrophages, with Gag-derived proteins co-localising with microtubule-associated protein light chain 3 (LC3) on autophagosomal membranes (Kyei et al., 2009). HIV-1 is able to hijack the earlier stages of autophagy in order to improve viral yields, whilst also preventing its own degradation by inhibiting the later stages of autophagy (Kyei et al., 2009). Because of this, autophagy is a very interesting target for cell engineering when producing LVVs. Engineering the autophagy pathway has been shown to have a positive impact on monoclonal antibody production (Braasch et al., 2021), and CHO cell survival (Lee et al., 2013). The inhibition of autophagy through use of chemicals such as 3-Methyladenine (3-MA) has also been shown to result in an increase the specific protein productivity of a recombinant CHO cell line, however the mechanism linking autophagy and protein production has not yet been established (Jardon et al., 2012; Braasch et al., 2021).

Subversion of the normal protein synthetic processes of cells e.g. unnaturally high production quantities of recombinant or non-natural protein places strain on the protein folding machinery of producer cell lines. When misfolded proteins accumulate in the endoplasmic reticulum (ER), the unfolded protein response (UPR) may be triggered, which in turn initiates apoptosis (Nakatsukasa et al., 2008; Ron et al., 2007). This can be prevented through strategies to engineer protein folding. For example, X-box binding protein 1 (XBP1) is a key target for engineering because of its role in inducing UPR-related genes (He et al., 2010). The over-expression of XBP1, along with protein disulphide isomerase family A member 2 (PDIA2) and chaperone heat shock protein family (Hsp70) member 5 (HSPA5), has been

demonstrated to improve GRV production in HEK293 cells by 92% (Formas-Oliveira et al., 2020; Tigges et al., 2006).

A common limitation with high-producing cell lines lies with inefficient secretory systems and vesicle trafficking. Several genes have been engineered in order to enhance the secretory capacity of mammalian cells. Tetraspanin CD9 plays a role in various cellular processes such as exosome biogenesis, and a 26% increase in AAV production was reported upon its over-expression in HEK293FT cells (Oka et al., 2010; Schiller et al., 2018). In CHO cells, over-expression of Sec1/Munc18 (SM) protein-coding genes and soluble N-ethylmaleimide-sensitive factor receptor (SNARE) protein-coding genes has been shown to improve recombinant protein expression (Peng et al., 2009).

Optimising central carbon metabolism (CCM) is a key aim in metabolic engineering in HEK293 cells, with a specific focus on the accumulation of certain by-products. For example, HEK293 cells consume high quantities of glutamine for energy production, leading to by-products lactate and ammonia (Newland et al., 1990; Goochee et al., 1991, Grammatikos et al., 1998; Gawlitzek et al., 1998; Rajendra et al., 2011; Rodrigues et al., 2016). This can cause premature cell death, low protein titres, and may also have a negative impact on protein glycosylation (Karengera et al., 2017). Recent studies with HEK293 cells attempted to optimise CCM by over-expressing pyruvate carboxylate (PC) and knocking-down pyruvate dehydrogenase kinase (PDK) and its activator, hypoxia inducible factor 1 (HIF1) (Karangera et al., 2017 Elias et al., 2003; Vallee et al., 2014, Henry et al., 2011, Rodrigues et al., 2016). Because of this, the link between the tricarboxylic acid cycle and glycolysis can be restored, leading to up to 30-fold increase in the specific productivity of infectious viral particles. Optimising bioprocessing conditions such as maintaining glucose concentration during culture and substituting glutamine with other substrates (glutamate, alpha-ketoglutarate, pyruvate) has enhanced over-expression of PC even further (Karengera et al., 2017).

Novel target molecules that influence LVV production can be identified by employing techniques such as; transcriptomic analyses, proteomic analyses, metabolomic analyses, RNA interference screens, random mutagenesis, and other whole genome

analytical tools (Martínez-Molina et al., 2020). Once identified, these targets can be specifically modified by gene editing systems such as CRISPR-Cas9, Zinc Finger Nucleases (ZFNs), and RNA interference (RNAi).

1.5. GagPol as a potential target for HEK293T cell engineering

A single HIV-1 infected CD4+ T-cell is able to generate approximately 5 x 10^4 virions per day (Chen et al., 2007). This virus is remarkably efficient at propagating itself, with events late in the HIV-1 life cycle being particularly efficient. The 'late events' mentioned here can be categorised broadly into four different stages. These include the assembly of Gag and GagPol polyprotein precursors, budding of the immature capsid from an infected cell, release of the immature viral particle, and finally, cleavage of Gag and GagPol precursor proteins by PR leading to maturation of the virus (Lingappa et l., 2014). The fact that HIV-1-infected CD4+ T-cells are able to produce 5 x 10^4 virions per day shows why it is important to gain an understanding of how, at the molecular and cellular level, the late events of the HIV-1 viral life cycle are as efficient as they are. This could aid in gaining an understanding of why there is such a disparity in HIV-1 production compared with LVV production.

Gag and GagPol play key roles in the late-stages of the HIV-1 virus life-cycle, including virus assembly and release (Figure 1.7). From the perspective of LVV production, there is very little known about how Gag and GagPol (from SYNGP, Kotsopoulou et al., 2000) interact with HEK293T cells. Understanding this in greater depth would allow identification of areas where LVV titres can be improved by targeted cell engineering, as the converse option of re-introducing HIV-1 genes to make LVV production more efficient is not attractive due to vector safety concerns, which have been discussed in detail in Section 1.2.2.

The Gag and Pol polyproteins are encoded by overlapping ORFs, which means that several proteins are translated from the same sequence, meaning genetic storage capacity is maximised (Figure 1.7). The 55kDa protein Gag possesses its own start

and stop codons, whereas the synthesis of the 160 kDa GagPol precursor occurs from a -1 frameshift event, the site of which is at the 3' end of the nucleocapsid coding region (Kobayashi et al., 2010). This frameshifting event occurs at a frequency of approximately 5-10% during translation (Jacks et al., 1988). This 20:1 ratio of Gag/GagPol is key for formation of infectious virus particles, is important for RNA stability, and ensures that more structural Gag protein is synthesised relative to the enzymatic Pol protein (Shehu-Xhilaga et al., 2001).

Gag and GagPol precursor polyproteins are cleaved by its own viral protease during assembly and release of the virus (Hunter et al., 1994; Swanstrom et al., 1997; Garnier et al., 1998; Freed et al., 1998). This forms the mature structural proteins matrix (MA), capsid (CA), nucleocapsid (NC), and p6 domain, with the spacer peptides SPI and SPII, and the enzymatic proteins protease (PR), reverse transcriptase (RT), and integrase (IN). The domains of GagPol each have unique functions which will be discussed below.

At the N-terminus of Gag, the 17 kDa MA protein is structurally responsible for targeting Gag to lipid raft-rich domains within the plasma membrane during particle assembly (Ono and Freed 2005). A myristoyl moiety within MA interacts with phosphatidyl-inositol-4,5-bisphosphate [PI(4,5)P2] on the inner leaflet of the plasma membrane (Hermida-Matsumoto et al., 2000; Ono et al., 2004). Recent studies have shown that the binding of tRNA to MA helps to prevent the non-specific binding of Gag to other cellular membranes (Gaines et al., 2018; Thornhill et al., 2019). However, Gag has also been reported localise at late-endosomal membranes and autophagosomal membranes, providing evidence for vesicular movement towards the plasma membrane for assembly (Pelchen-Matthews et a., 2003; Kyei et al., 2009).

A

B

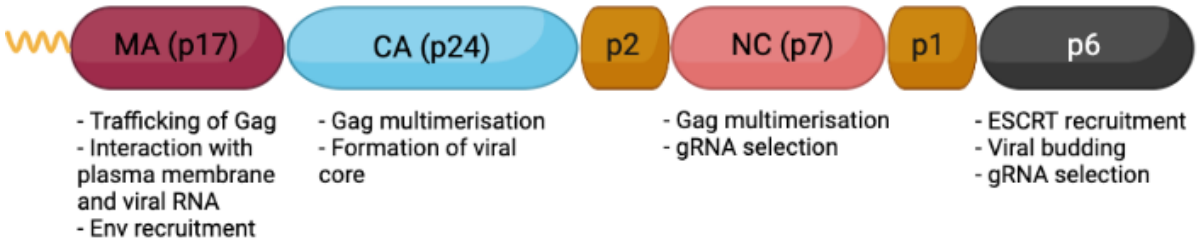

Figure 1.7 Schematic representation of HIV-1 Gag (Pr55Gag) and GagPol (Pr160GagPol) precursor and the role of each domain. (A) Functional domains of HIV-1 Pr160 GagPol. MA: Matrix, CA: Capsid, p2: Spacer peptide 1, NC: Nucleocapsid, p1: Spacer peptide 2, PR: Protease, RT: Reverse transcriptase, IN: Integrase. (B) A description of the roles of the functional domains of HIV-1 Pr55 Gag. Pr55Gag has an N-terminal myristoylated Glycine 2, and a highly-basic region on the surface of MA. MA is responsible for various roles in the viral life-cycle including trafficking and interaction of Gag to the plasma membrane, Interaction of Gag with vRNA, in addition to the recruitment of Env. CA is responsible for driving the multimerisation of GagPol, leading to viral core formation. NC interacts with gRNA and tRNA, the latter of which is a primer for reverse transcription. Spacer peptides p1 and p1 regulate viral maturation. p6 is involved in the recruitment of the Endosomal Sorting Complex Required for Transport (ESCRT) host cell machinery that aids budding of the viral particle (Bussienne et al., 2021). Created in BioRender.

The 24 kDa CA protein is the most abundant of the viral proteins. It forms a protective shell around the genomic RNA; 1,000-1,500 molecules of CA form a conical capsid core made from 12 pentameric rings and over 100 hexameric rings (Zhao et al., 2013). There are approximately 1,500 - 3,000 p24 molecules per virion (Vogt and Simon, 1999; Summers et al., 1992). CA has been shown to interact with cyclophilin A (CypA), cleavage and polyadenylation specific factor 6 (CPSF6), and peptidyl-propyl cis-trans isomerase NIMA-interacting 1 (PIN1) (Braaten and Luban, 2001; Dochi et al., 2014). It has also been shown to interact with nucleoporin 358 (NUP358) and nucleoporin 153 (NUP153) which mediates trafficking of CA across the nuclear envelope (Dharan et al., 2016).

The 7 kDa NC protein is a nucleic acid chaperone that has essential roles in mediating reverse transcription and in specific gRNA interactions, whilst also promoting viral assembly through contributing to Gag multimerization (Cimarelli et al., 2000; Ott et al., 2009; El Meshri et al., 2015; Levin et al., 2010; Ott et al., 2005). This domain has two zinc finger motifs (CCHC) that are able to bind specifically with Psi (Dannull et al., 1994; Webb et al., 2013). NC interacts with several host factors in order to promote assembly and budding of virions, including staufen double-stranded RNA binding protein 1 (STAU1), ATP-binding cassette sub-family E member 1 (ABCE1), apoptosis-linked gene (ALG) interacting protein X (ALIX), and the endosomal sorting complex required for transport (ESCRT)-II subunit EAP30 (Chatel-Chaix et al., 2004; Mouland et al., 2000; Klein et al., 2010; Sette et al., 2012; Ghoujal et al., 2012). The spacer peptides, SPI and SPII, that flank the NC domain, are essential for virus assembly (Kräusslich et al., 1995).

At the C-terminus of Gag is the 6 kDa p6 domain, which is responsible for binding to gRNA (Dubois et al., 2018). This domain has a role in recruiting ESCRT machinery, which helps to regulate budding of viral particles. p6 has been reported to play a key role in modulating the activation of PR, and hence modulating virus maturation (Yu et al., 2015). Recent studies have shown that extensive mutations to the central region of p6 do not abolish virus replication or infectivity in vivo (Leiherer et al., 2020).

One of the three viral enzymes, PR, is embedded within Pol is responsible for the processing of Gag and GagPol polyprotein precursor proteins (Huang and Chen,

2014). The mature 22 kDa is an aspartic protease, comprising of two 99-amino acid identical subunits which can only function when in dimer form (Navia et al., 1989; Wlodawer et al., 1989). The auto-processing of PR, whereby PR is able to catalyse and cleave other PR precursors, is necessary for maturation of the virus, however the mechanism in which PR becomes activated remains largely unknown.

The reverse transcription of viral RNA into DNA is performed by RT, which exists as a heterodimer comprised of two subunits, p66 (66 kDa) and p51 (51 kDa) (Davis et al., 2008). RT has two enzymatic functions, first being a DNA polymerase that can copy an RNA/DNA template, and second an RNAse H that is able to cleave RNA when it is in a DNA/RNA complex (Sarafianos et al., 2010). This activity allows RT to convert viral RNA into linear dsDNA in the cytoplasm. The viral dsDNA is then integrated into the host genome following translocation into the nucleus, creating a provirus DNA copy.

At the C-terminus of Pol is the 32 kDa viral enzyme IN, which is responsible for the integration or viral dsDNA into the host genome (Schröder et al., 2002). Following this, viral DNA is maintained and replicated alongside host cell DNA following integration into a host chromosome. There are certain regions within the genome where viral DNA is preferentially integrated, which tend to be in active gene-rich regions (Ciuffi et al., 2008). It is thought that the favoured integration at transcriptionally active regions aids in promoting the expression of viral genes following integration.

Despite the structure and function of each domain of GagPol being relatively well-defined, interactions with and impact on the host cell are still not fully known. Some of the key known interactions between domains of HIV-1 Gag and HIV-1-infected cells are summarised in Table 1.3.

Table 1.3 Interactions between cellular proteins and structural domains of Gag

Domain of Gag	Host cell protein that interacts with Gag	Interaction/role with Gag	Reference
MA	Actin	Component of cytoskeleton that is involved in correct localisation and activation of RT	Bukrinskaya et al., 2007
	Clathrin-associated adaptor protein 1 (AP-1)	Transports Gag to budding sites and facilitates interaction of Gag with other host cell proteins	Camus et at., 2007
	Clathrin-associated adaptor protein 3 (AP-3)	Trafficking of Gag to MVBs and involved in assembly	Dong et al., 2005
	Adenomatous polyposis coli protein (APC)	Multimerisation of Gag at PM, incorporation of vRNA	Miyakawa et al., 2017
	Calmodulin (CaM)	A multi-functional calcium-binding messenger enabling MA myristate exposure following binding	Ghanam et al., 2010 Samal et al., 2011, Taylor et al., 2012
	Eukaryotic elongation factor 1-alpha (eEF1a)	A translation elongation factor involved in tRNA incorporation into virions, viral uncoating, RT interactions	Cimarelli et al., 1999 Li et al., 2015
	Histidyl-tRNA synthetase homolog HO3 (HARS2)	An aminoacyl-tRNA synthetase that increases infectivity	Lama et al., 1998
	Intracellular adhesion molecule A (ICAM-1)	Immunoglobulin that enhances formation of syncytia, promotes entry into cells	Beausejour et al., 2004 Jalaguier et al., 2015
	Kinesin superfamily protein (KIF4)	A microtubule-stimulated ATPase that regulates trafficking and stability of Gag	Martinez et al., 2008 Sabo et al., 2013 Tang et al., 1999
	RuvB-like 2 (RVB-2)	Involved in controlling expression of viral proteins (Env and Gag)	Le Sage et al., 2015 Mu et al., 2015
	Suppressor of cytokine signalling protein 1 (SOCS1)	Facilitates Gag trafficking to PM, increases stability via network of microtubules, potential role in enhancing ubiquitination of Gag	Nishi et al., 2009 Ryo et al., 2008
	Virion-associated nuclear shuttling protein (VAN)	A nuclear/cytoplasm shuttling protein that aids in facilitating import into nucleus and retention of pre-integration complex	Bishop et al., 2008

CA	Clathrin-associated adaptor protein 2 (AP-2)	Involved in regulation of virus assembly/release	Batonick et al., 2005
	Cyclophilin A and B (CypA and CypB respectively)	Aids in protecting virions from TRIM5a (a restriction factor)	Kim et al., 2019 DeBoet et al., 2016
	Filamin A	Trafficking of Gag to PM	Cooper et al., 2011
	Lysyl-tRNA synthetase (LysRS)	tRNA packaging into virions	Javanbakht et al., 2003 Na Nakorn et al., 2011
	Microtubule-associated proteins (MAP1A and MAP1S)	Aids tethering of viral CA to microtubules	Fernandes et al., 2015
	Mitogen-activated protein kinase (MAPK)/Extracellular signal-regulated kinase 2 (ERK-2)	A serine-threonine kinase that aids incorporation of Gag into viral particle	Gupta et al., 2011
	Tripartite motif-containing protein 5 (TRIM5a)	Restriction factor that actively degrades Gag polyproteins	Luban et al., 2012 Sakuma et al., 2007
NC	ATP-binding cassette sub-family E member 1 (ABCE1)	ATPase essential for CA assembly	Smirnova et al., 2008 Wilk et al., 1999
	Apoptosis-linked gene 2-interacting protein X (ALIX)	An adaptor protein involved in recruitment of ESCRT proteins for budding and release of virus particles	Strack et al., 2003 Usami et al., 2007 Sette et al., 2016 Sette et al., 2012
	Discs large homolog 1 (DLG1)	Scaffold and anchor protein at PM involved in modulating cellular distribution of Gag	Perugi et al., 2009
	Eukaryotic elongation factor 1-alpha (eEF1a)	tRNA incorporation into virions, viral uncoating, RT interactions	Cimarelli et al., 1999 Li et al., 2015

	Insulin-like growth factor II mRNA-binding protein 1 (IMP1)	RNA binding factor that blocks virus particle formation	Zhou et al., 2008
	IQ motif-containing GTPase activating protein (IQGAP1)	Scaffold protein that prevents Gag accumulation at PM, hence inhibits budding and release of virus	Sabo et al., 2020
	Neural precursor cell expressed developmentally down-regulated protein 4 (Nedd4-1 and Nedd4-2)	E3 ubiquitin ligase that ubiquitinates Gag and subsequently leads to ESCRT complex recruitment	Weiss et al., 2010
	Nucleolin	An RNA-binding protein that enhances assembly and release of virions	Gao et al., 2014 Bacharach et al., 2000
	Soluble N-ethylmaleimide-sensitive factor attachment protein receptor (SNARE)	Usually mediates vesicle function, also interrupts trafficking pathways within the cell required for transport of Gag to PM	Joshi et al., 2011
	Suppressor of cytokine signalling protein 1 (SOCS1)	Facilitates Gag trafficking to PM, increases stability via network of microtubules, potential role in enhancing ubiquitination of Gag	Nishi et al., 2009 Ryo et al., 2008
	dsRNA-binding Staufen homolog 1 (Staufen-1)	Involved in Gag multimerisation and Gag trafficking to PM, also has role during cellular stress	Ghoujal et al., 2012 Rao et al., 2018
	Tumour-susceptibility gene 101 (Tsg101)	A member of the vacuolar protein sorting (VSP) family and a component of the ESCRT I complex involved in ESCRT complex recruitment and viral release	Garrus et al., 2001 VerPlank et al., 2001 Dussupt et al., 2011 El Meshri et al., 2018

P6	Apoptosis-linked gene 2-interacting protein X (ALIX)	Involved in recruitment of ESCRT proteins for budding and release of virus particles	Bendjennat et al., 2016 Sette et al., 2016
	IQ motif-containing GTPase activating protein (IQGAP1)	Scaffold protein that prevents Gag accumulation at PM, hence inhibits budding and release of virus	Sabo et al., 2020
	Neural precursor cell expressed developmentally down-regulated protein 4 (Nedd4-1 and Nedd4-2)	E3 ubiquitin ligase that ubiquitinates Gag and subsequently leads to ESCRT complex recruitment	Weiss et al., 2010
	Protein kinase C and casein kinase substrate in neurons 2 (PACSIN2)	Potential role in connecting actin to Gag but not defined	Popov et al., 2014
	Tumour-susceptibility gene 101 (Tsg101)	A member of the vacuolar protein sorting (VSP) family and a component of the ESCRT I complex involved in ESCRT complex recruitment and viral release	El Meshri et al., 2018 Dussupt et al., 2011 VerPlank et al., 2001 Garrus et al., 2001

1.6. Aims and Objectives

Given that the GagPol utilised by GSK (SYNGP) in LVV production is based on HIV-1 GagPol, which itself hijacks several host cellular systems for packaging budding and release of virus, it is logical to hypothesise that the expression of SYNGP may potentially stress the capacity of HEK293T cells to carry out “normal” cell maintenance functions, which in turn impacts on the maximum recombinant LVV productivity. This project therefore aims to understand and elucidate interactions between synthetic GagPol and HEK293T cellular physiology in order to define approaches to identify, and subsequently intervene in, molecular bottlenecks in LVV production.

In order to address this aim, the following specific objectives were outlined and developed within the context of this project:

1. Develop an appropriate GagPol over-expression cassette in addition to a fluorescently-tagged GagPol construct to allow for the detection and tracking of GagPol in live and fixed HEK293T cells

2. Perform transient over-expression of HEK293T cells with GagPol and GagPol-EGFP expression cassettes, characterising the output of transductions through various titration assays including p24 ELISA, PERT assay, and ddPCR copy number assay

3. Assess the impact of GagPol over-expression on HEK293T host cell physiology and function, with a specific focus on cell viability and key cellular stresses including apoptosis, autophagy, ER stress, and UPR activation

4. Determine the effects of cellular stress inhibitors on (i) HEK293T cell viability and (ii) the production of GagPol following transductions at various MOIs, in order to identify and define potential genetic targets for improvement of LVV production

2. Materials and Methods

2.1. Materials

2.1.1 General chemicals and reagents

A full list of chemicals, reagents and enzymes can be found in Appendix Section 8.1

2.1.2 Equipment and Software

A full list of equipment and software used can be found in Appendix Section 8.2.

2.1.3 Preparation of solutions

All reagents were prepared by dissolving in double distilled H_2O and stored at room temperature, unless otherwise stated.

2.2 Methods

2.2.1 Generation and purification of plasmids

2.2.1.1 PCR amplification of DNA fragments

For each DNA fragment to be amplified, 25 µL Q5 Hot Start High-Fidelity DNA Polymerase, 2.5 µL 10 µM forward primer, 2.5 µL 10 µM reverse primer, 19 µL nuclease-free water, and 1 µL template DNA or 1 µL water were prepared in a 0.2 mL tube. Amplicons were produced by PCR using the conditions in Table 2.1. Details of primers are given in Appendix Section 8.3.

Table 2.1. PCR conditions used to generate DNA fragments.

Temperature (ºC)	Duration	Number of cycles
95	2 minutes	1
95	30 seconds	30
See Appendix Table 8.3 and 8.4	30 seconds	
72	1 minute per kb	1
4	∞	1

2.2.1.2 Agarose gel electrophoresis

1.5% [w/v] agarose powder was added to 1X TAE buffer (40 mM TRIS acetate, 5mM EDTA pH 8.0) and heated until the agarose was dissolved completely. 0.1 µL SafeView™ nucleic acid stain per 1mL gel was added once cooled to approximately 50°C. This was poured into a casting mould with a comb in place and left to set. The gel was placed in an electrophoresis tank filled with 1X TAE buffer). 5 µL 100bp or 1kb DNA ladder was loaded as a molecular weight marker. 6X Gel Loading Buffer was added to each sample to give a 1X final concentration. 30 µL sample with loading buffer was loaded into each well. Electrophoresis was performed at 90 V until the loading dye had migrated a suitable distance. DNA bands were visualised with a BioRad ChemiDoc UV-gel imaging system.

2.2.1.3 Fragment extraction and purification

DNA Fragments were extracted from the gel and purified using a QiaQuik Gel Extraction Kit following the protocol provided by the manufacturer. In brief, this involved binding of DNA to a silica membrane in a high-salt buffer, followed by eluting DNA into water. DNA samples were purified to remove impurities (such as primers, nucleotides, agarose and enzymes).

2.2.1.4 Determining DNA concentration and purity

The concentration and purity of purified DNA fragments were analysed using a NanoDrop™ spectrophotometer. The spectrophotometer was blanked using 1 µL water to measure the background absorbance. 1 µL purified DNA was pipetted onto the NanoDrop™ pedestal. DNA concentration was determined by measuring at an absorbance of 260nm (A260). To evaluate DNA purity, the ratio of absorbance at 260nm and 280nm was measured. DNA was considered of good quality when the A260/A280 ratio was between 1.8-2.0. Measurements were taken in triplicate for each sample.

2.2.1.5 Gibson assembly reaction

Purified DNA fragments were assembled in a Gibson Assembly reaction using a Gibson Assembly ® cloning kit. A reaction mixture was prepared on ice and consisted of 10 µL 2X Gibson Assembly® MasterMix, 0.5 pmol of each DNA fragment to be assembled, and nuclease-free water added to a final volume of 20 µL. The mixture was incubated in a thermocycler at 50°C for 15 minutes. DNA was stored at -20°C until transformation.

2.2.1.6 Transformation of competent E. coli

Selection plates were made with Luria Bertani (LB) broth (1% [w/v] tryptone, 0.5% [w/v] yeast extract, 0.5% [w/v] NaCl) supplemented with 1.5% [w/v] agar and 100

μg/mL ampicillin. 10 mL of this mixture was poured into a 100 mm dish in aseptic conditions and left to set. Plates were stored at 4°C for no longer than 2 weeks.
A vial containing 0.2 mL 10-ß Competent *E. coli* cells as thawed on ice. 100 ng plasmid DNA was pipetted into the tube and mixed gently by tapping the vial. The transformation mixture was placed on ice for 2 minutes, heat-shocked at 42°C for 30 seconds, and returned to ice for 2 minutes. 950 µL pre-warmed SOC medium was added. 100 µL of the mixture was spread onto pre-warmed agar selection plates. Selection plates were incubated at 37°C overnight.

2.2.1.7 Preparation of plasmid DNA

Individual colonies were picked from agar plates containing transformed *E. coli* using sterile pipette tips. These were streaked onto individual fresh selection plates containing 100 μg/mL ampicillin for antibiotic selection, as described in Section 2.2.1.6. Plates were incubated overnight at 37°C. Plates were stored at 4°C for a maximum of two weeks until DNA extraction. Individual colonies were picked from each plate and added to a sterile 50 mL falcon tube containing 6 mL Luria Bertani (LB) broth (Section 2.2.1.6), and incubated overnight at 37°C on a shaker at 220 RPM. DNA was extracted using a Plasmid Mini or Maxi Kit following manufacturer's instructions. DNA was resuspended in nuclease-free water. Concentration and purity of plasmid DNA was determined as in Section 2.2.1.4. DNA was stored at 4°C.

2.2.1.8 Restriction enzyme digestion of plasmid DNA

Restriction digestion analysis was used to confirm production of the correct plasmid. 1 µg plasmid DNA (concentration determined as in Section 2.2.1.4) was incubated with 10 Units of the appropriate restriction enzyme(s), 2 µL 10X restriction enzyme buffer, and 16 µL RNAse-free water. This was mixed gently and incubated at 37°C for 1 hour, followed by thermal inactivation at 65°C for 20 minutes. The fragment sizes of DNA were confirmed by agarose gel electrophoresis as in Section 2.2.1.2.

2.2.1.9 Sequencing of DNA

Fragment sequences within plasmids were sequenced using primers in Appendix Table 8.4. DNA fragments for plasmids pQCXIX (Clontech), pG3-SYNGP (GSK), B2modT-v2 (GSK), pQCXIX-SYNGP, and pQCXIX-SYNGP-EGFP were sequenced in-house at GSK by GeneWiz Sanger Sequencing. DNA fragments for plasmids pQCXIP-EGFP-F, SLC20A2, pMD2.G, pBS-CMV-GagPol were sequenced by Eurofins Genomics Sanger Sequencing TubeSeq service.

2.2.2 Mammalian cell culture

2.2.2.1 Revival of cells

Cryovials containing 1 mL HEK293T or 1 mL Amphopack-293 cells were removed from liquid nitrogen storage and rapidly thawed in a 37ºC water bath. Cells were immediately transferred to a 15 mL Falcon tube containing 5 mL pre-warmed culture medium (DMEM + 10% [v/v] FBS). An additional 10 mL pre-warmed medium was added. Cells were pelleted by centrifugation at 900 g for 5 minutes. The supernatant was discarded and the cell pellet was resuspended in 10 mL fresh pre-warmed medium. Resuspended HEK293T cells were transferred to a T75 flask. Resuspended Amphopack-293 cells were transferred to a collagen-I-coated 100 mm tissue culture dish for recovery. Cells were placed in a static incubator and grown at 37ºC and 5% CO_2 for 3-4 days.

2.2.2.2 Cell maintenance

Cell passaging was performed once cells approached >70% confluence, approximately every 2-3 days. Medium was discarded and cells were washed with 5 mL PBS to prevent shrivelling due to osmosis. PBS was discarded and 3 mL Accutase solution was added to each flask. The flask was incubated at 37ºC and 5% CO_2 for 5 minutes. Once cells began to detach, Accutase solution was diluted with 8 mL pre-warmed medium. Cells were resuspended by aspirating up and down using a stripette. Cells were counted (Section 2.2.2.3) and the resultant cells were harvested into a sterile 15 mL falcon tube and centrifuged at 900 g for 5 minutes. The cell pellet

was resuspended in 10 mL fresh medium, and split (1:10) into new T75 flasks each containing 9 mL fresh medium. Cells were incubated at 37ºC and 5% CO_2.

2.2.2.3 Cell counting

10 µL cell sample mixed with 10 µL 0.5 % [w/v] Trypan Blue in PBS was placed on a haemocytometer slide. A light microscope was used to count viable cells. Bright and colourless cells were determined as viable. Blue cells were determined as dead due to their uptake of trypan blue. Percentage viability was determined as below:

$$\%\, Viability = \frac{Number\ of\ live\ cells}{Number\ of\ live + dead\ cells}\ x100$$

2.2.2.4 Cryopreservation of cells

Cells were bulked up into T75 flasks prior to liquid nitrogen storage. Following 3-4 days of growth, medium was discarded. As above for maintenance culture, the cell sheets were washed with 5 mL PBS. 3 mL Accutase solution was applied to cells, and flasks were incubated at room temperature for 5 minutes, followed by the addition of 8 mL pre-warmed medium Cells were resuspended and counted as in Section 2.2.2.3. Cells were centrifuged at 900 g for 10 minutes. Supernatant was discarded and cells were resuspended at a density of $1x10^6$ cells/mL in freezing medium (DMEM + 10% [v/v] FBS + 10% [v/v] DMSO).

1 mL resuspended cells were added to each labelled cryovial, and transferred to a Mr Frosty freezing container for freezing at -80ºC overnight. Cryovials were transferred to liquid nitrogen for long-term storage the next day.

2.2.2.5 Intracellular cell sampling

Protein extracts from HEK293T cells were extracted by harvesting 2 x 10^7 cells by centrifugation at 900 g for 5 minutes. 5 mL PBS was added to the cell pellet to wash, centrifuged at 900 g for 5 minutes, and the supernatant was removed. This washing step was repeated. For analysis by p24 ELISA, cells were resuspended in chilled 1X

Cell Extraction Buffer PTR. Cells were incubated on ice for 20 minutes, and centrifuged at 900 g for 20 minutes at 4ºC. Pellets were discarded and supernatant transferred into a new clean tube and either assayed immediately or stored at -80ºC.

2.2.2.6 Sampling of culture medium

Cell culture supernatant was collected and centrifuged at 2,000 g for 10 minutes to remove any potential debris from samples. For analysis by p24 ELISA, samples were diluted in Sample Diluent NS and assayed. Undiluted samples were stored at -20ºC. Freeze-thaw cycles were avoided.

2.2.2.7 Supplementing cell culture medium

Apoptosis inhibitors were added to HEK293T cell culture medium in specified experiments. Inhibitor final concentrations were 50μM for Caspase-8, Capase-9 and Pan-Caspase inhibitor made in DMSO based on data presented by Sauerwald et al. (2003). To induce apoptosis as a positive control, HEK293T cells were incubated with 5 μg/mL Actinomycin D for 4 hours (Kleef et al., 2000).

ER stress was induced in HEK293T cells by addition of 10μg/mL Tunicamycin to transduction medium (Section 2.5) (Lin et al., 2007).

To inhibit autophagy, several inhibitors were added to transduction medium (Section 2.5) with final concentrations based on those utilised in previous publications. Inhibitors and concentrations were 50nM Wortmannin (Lin et al., 2014), 25μM Spautin-1 (Daussy et al., 2020), 50nM Bafilomycin A1 (Musiwaro et al., 2013), or 50μM Chloroquine (Mauthe et al., 2018).

To inhibit HIV-1 Protease, 1.5μM Saquinavir was added to transduction medium (Section 2.5) (Sparacio et al., 2001).

2.2.3 Vector preparation

2.2.3.1 Transfection in Amphopack293

Recombinant MMLV-based GRV vector particles pseudotyped with amphotropic envelope protein were produced by transfection of Amphopack-293 cells using the Xfect™ Transfection Reagent. A 100 mm plate was seeded with 5 x 10^6 cells in 10 mL DMEM + 10% [v/v] FBS, and incubated at 37ºC and 5 % CO_2 24 hours prior to transfection. At this stage, cells were >70% confluent. 15 µg retroviral plasmid DNA was diluted with Xfect™ Reaction Buffer to a final volume of 600 µL, and mixed by vortexing for 5 seconds. Xfect™ polymer was thoroughly vortexed. 4.5 µL Xfect™ polymer was added to retroviral buffer-diluted retroviral plasmid DNA and mixed by vortexing for 10 seconds. The DNA-Xfect™ mixture was incubated for 10 minutes at room temperature. Then the mixture was added dropwise to the medium in the cell culture plate, the plate was swirled gently to mix, and incubated at 37ºC and 5 % CO_2 overnight. The medium from the plate was then discarded and replaced with 10 mL DMEM + 10% [v/v] FBS, and incubated for a further 48 hours. Retroviral supernatants were harvested and stored at -80ºC.

2.2.3.2 Transfection in HEK293T

VSV-G-pseudotyped GRV vector was produced by transfection of HEK293T cells. A 6-well plate was seeded with 3 x 10^5 HEK293T cells per well in 2 mL DMEM + 10% [v/v] FBS and incubated overnight at 37ºC in 5% CO_2. Medium was replaced with the same volume of fresh DMEM + 10% [v/v] FBS and incubation was continued for 2 hours prior to transfection.

Transfections were performed at different scales. The general process is described below for 6-well plate transfections and for transfection at larger scale, quantities of reagents are given in Table 2.2. For 6-well plate transfections with 2 mL volume culture medium for each well, plasmids were diluted in 200 µL OptiMEM to give concentrations as in Table 2.2. 5.33 µL PEI, a stable cationic polymer, was added to diluted plasmid, vortexed, and incubated for 30 minutes at room temperature. This

mixture was then added to cells in a dropwise manner, and the plate was swirled gently to ensure even distribution of the transfection mixture.

Cells were incubated at 37ºC and 5% CO_2. After 16 hours, medium was removed and replaced with 2 mL fresh DMEM + 10% [v/v] FBS, with further incubation at 37ºC and 5% CO_2. After 28-32 hours, cell culture supernatant was transferred to an appropriate tube, and was filtered through a 0.22 µm low-protein binding membrane using a 10 mL syringe. Aliquots were separated in 2 mL tubes and stored at -80ºC.

Table 2.2. Reagents for transfection of adherent HEK293T cells:

		6-well plate	10 cm dish
Area		10 cm^2	60 cm^2
Seeded cells		8 x 10^5	5 x 10^6
DMEM + 10% [v/v] FBS		2 mL	10 mL
DMEM after transfection		1.3 mL	8 mL
Accutase		1 mL	2.5 mL
PBS		1 mL	2.5 mL
Plasmid 1 (pBS-CMV-GagPol (GagPol))		1.37 µg	8.35 µg
Plasmid 2 (pMD2.G (VSV-G))		1.37 µg	8.35 µg
Plasmid 3 (pQCXIX-SYNGP, pQCXIX-SYNGP-EGFP, or pQCXIP-EGFP-F) (Transfer vector)		1.37 µg	8.35 µg
PEI	OptiMEM	200 µL	1 mL
	PEI*	5.33 µL	32.5 µL

*DNA (µg):PEI (µL) ratio 1:1.3

2.2.4 Titration of vector preparations

2.2.4.1 GFP titration to determine vector titre in Transducing Units

A 6-well plate was seeded with 3 x 10^5 HEK293T cells per well in a final volume of 2 mL DMEM + 10% [v/v] FBS, and incubated overnight at 37ºC and 5% CO_2. Vector was thawed at room temperature and dilutions of 10^{-1}, 10^{-2}, and 10^{-3} of viral supernatant (from Section 2.2.3) were made in 500µL DMEM + 10% [v/v] FBS. Polybrene, a cationic polymer used to improve transduction efficiency, was diluted in DMEM + 10% [v/v] FBS to achieve a final concentration of 10 µg/mL. Cells were counted (Section 2.2.2.3) in one well of the 6-well plate. Medium from the other wells

was discarded, and 500 µL polybrene in DMEM + 10% [v/v] FBS was added to each well. 500 µL viral supernatant dilution was added to each well, with 500 µL DMEM + 10% [v/v] FBS being added to the negative control well. Plates were incubated at 37ºC and 5% CO_2. An additional 1mL DMEM + 10% [v/v] FBS was added to each well after 2 hours. After 72 hours, medium was discarded and replaced with 1 mL Accutase solution to dissociate cells. Cells were pipetted up and down after 5 minutes incubation. 150 µL cell suspension was added to 1 mL PBS, and pipetted thoroughly to prevent clumping of cells. Cells were immediately analysed by flow cytometry to determine % GFP-positive cells (Section 2.2.6.1). Titres were calculated from a dilution factor where the % of GFP-positive cells was between 3-30%. The following calculation was used to determine the transducing units (TU) per mL:

$$Titre\ \left(\frac{TU}{mL}\right) = \frac{cells\ per\ well\ at\ transduction\ \times\ \%GFP\ positive\ cells\ \times\ D.F.}{vol\ (ml)\ of\ neat\ vector\ in\ transduction}$$

D.F.: Dilution Factor of viral vector stock used during transduction.

2.2.4.2 HIV-1 p24 ELISA

A HIV-1 p24 SimpleStep ELISA® kit was used to quantitatively measure HIV-1 p24 protein in cell lysates and cell culture medium, collected as specified in Sections 2.2.2.5 and 2.2.2.6, respectively.

All reagents and materials were equilibrated to room temperature prior to performing the p24 ELISA. 50 µL sample or standard from the HIV-1 p24 SimpleStep ELISA® Kit was added to each well in duplicate. 50 µL p24 Antibody Cocktail was added to each well. The plate was sealed and incubated for 1 hour at room temperature, on a plate shaker at 400 RPM. Each well was washed three times with 350 µL 1X Wash Buffer PT, ensuring all liquid was removed from wells. The plate was blotted against paper towels to remove excess liquid. 100 µL TMB Development Solution was added to each well, and plates were incubated for 10 minutes in the dark on a plate shaker at 400 RPM. 100 µL Stop Solution was added to each well, and mixed for 1 minute on a plate shaker at 400 RPM. The OD was then recorded at 450 nm. The range of detection was 4.69 pg/mL – 300 pg/mL. p24 concentration was then

determined using known values of the standard reagent provided in the p24 ELISA kit.

2.2.4.3 Product Enhanced Reverse Transcriptase assay by qPCR

VLP output was assessed using a SYBR-Green PERT assay to quantify the activity of the reverse transcriptase (RT) enzyme. Aliquots of 2 mU/µL HIV-1 RT standards were prepared by diluting 1 µL RT in 2000 µL DMEM + 10% [v/v] FBS. A 2X PERT lysis buffer was prepared as in Table 2.3. A PERT assay mix was prepared with 0.1 µL of 100 µM PERT_F primer, 0.1 µL of 100 µM PERT_R primer, 0.1 µL MS2 RNA, and 4.7 µL water per well.

Unconcentrated vector samples (Section 2.2.3) were diluted 1:100 with DMEM + 10% [v/v] FBS. 5 µL diluted vector or 5 µL diluted HIV-1 RT standard was added to 5 µL 2X Lysis buffer containing 0.5 µL RNase inhibitor, and incubated for 10 minutes at room temperature. 40 µL nuclease-free water was added to diluted vector or diluted HIV-1 RT. For each sample, a PCR mix was prepared containing 10 µL PowerUp SYBR-Green MasterMix and 5 µL PERT mix (0.1 µL 100 µM PERT_F primer (5'-TCCTGCTCAACTTCCTGTCGAG-3'), 0.1 µL 100 µM PERT_R primer (CACAGGTCAAACCTCCTAGGAATG), 0.1 µL MS2 RNA, 4.7 µL water). 5 µL diluted sample was added to 15 µL PCR mix. qPCR was performed using the programme in Table 2.4.

Table 2.3. Reagents for 2X PERT Lysis Buffer

Reagent	Conc. of stock	Conc. required	Dilution needed (1 in x)	Volume (mL) for 50mL
Triton x-100	10% (v/v)	0.25%	40	1.25
Tris-HCl	1M	0.1M	10	5
KCl	1M	50mM	20	2.5
Glycerol	diluted to 50%	40%	1.25	40
Water	-	-	-	1.25

Table 2.4. qPCR conditions used during PERT assay.

Stage	Temperature (ºC)	Duration	Number of cycles
Incubation	42	20 minutes	1
RT Inactivation/ Hot-start DNA Pol activation	92	2 minutes	1
Denaturation	95	5 seconds	40
Annealing	55	15 seconds	
Elongation	72	30 seconds	
Melt curve using 0.15ºC rate in fast mode			

2.2.4.4. Copy number assay

A DNeasy Blood & Tissue Kit was used to purify DNA from HEK293T cells. All reagents were prepared prior to genomic DNA isolation, according to manufacturer's protocol. Cells were counted as in Section 2.2.2.3. $1x10^6$ cells were centrifuged at 6000 g for 5 minutes. The pellet was resuspended in 200 µL PBS, and 20 µL Proteinase K (600 mAU/mL) was added. 200 µL Buffer AL was added and mixed immediately and thoroughly by vortexing. The mixture was incubated at 56ºC for 10 minutes. 200 µL 96% [v/v] ethanol was added and mixed thoroughly by vortexing. A DNeasy mini spin column was placed in a 2 mL collection tube. The mixture was transferred to the column and centrifuged at 6,000 g for 1 minute, discarding flow-through. The DNeasy spin column was transferred to a new 2 mL collection tube. 500 µL Buffer AW2 was added and centrifuged at 20,000 g for 3 minutes, discarding flow-through. The DNeasy spin column was transferred into a clean 1.5 mL microcentrifuge tube. 200 µL Buffer AE was pipetted directly onto the DNeasy membrane and incubated for 2 minutes at room temperature. DNA concentration was then determined using a NanoDrop™ as in Section 2.2.1.4.

Mixtures of primers and probes (Table 2.5) were prepared to final concentrations of 900 nM and 250 nM, respectively. A 20X primer/probe stock mixture for GagPol or RNaseP (Target Chr.14:20811565, assumed 3 copies per HEK293T cell by NGS, as determined by the supplier, Thermo Fisher Scientific Cat. No. 4403328) was prepared by adding 36 µL forward primer, 36 µL reverse primer, 10 µL probe, and 118 µL nuclease-free water to a 1.5 mL safe-lock tube, and stored at -20ºC or used

immediately. For each sample, 11 µL 2X SuperMix, 1.1 µL 20X GagPol primer/probe mix, 1.1 µL 20X reference primer/probe mix, and 8.8 µL gDNA diluted to 10 ng/µL were added to a well in a 96-well plate. Samples were prepared in duplicate. The 96-well plate was sealed, centrifuged at 400 g for 2 minutes, and placed inside an automated droplet generator. Droplet generation was performed by following provided in the instruction manual. The final PCR plate was sealed and placed inside a PCR thermal cycler using the conditions in Table 2.6.

Table 2.5. Primer and probe sequence used to determine GagPol copy number by ddPCR

Primer name	Primer sequence (5'-3')	Probe (5'-FAM-x-MBG/BHQ1-3')
SynGP-Pol1_F	AAGACTGAGCTGCAGGCC	CCTCGCTTTGCAGGACTCGGGC
SynGP-Pol1_R	GCATACTGAGAGTCTGTCACGA	

Table 2.6. PCR conditions for ddPCR

Temperature (ºC)	Duration	Number of cycles
95	10 minutes	1
94	30 seconds	45
57	1 minute	
98	10 minutes	1
12	∞	1

2.2.5 Transduction

HEK293T cells were seeded in a 96-well plate and incubated at 37ºC and 5% CO_2, 16-20 hours prior to transduction. Aliquots of titrated retroviral stock (Section 2.2.4.1) were thawed rapidly at 37ºC and mixed gently. Retroviral stock was diluted with DMEM supplemented with 10% [v/v] FBS to obtain the desired Multiplicity of Infection (MOI). MOI refers to the number of virions added per cell during transduction. The number of Transducing Units (TU) in a solution represents the number of functional viral particles present that are able to transduce a HEK293T cell and express the transgene. The number of TU's was calculated using the equation was used:

$$Total\ transducing\ units\ needed\ (TU) = Desired\ MOI\ \times\ Total\ number\ of\ cells\ per\ well$$

Polybrene was diluted in DMEM + 10% [v/v] FBS to a final concentration of 10 µg/mL. Polybrene and diluted retroviral stock was added to wells. The volume of medium in target cell culture wells was adjusted to accommodate the addition of retroviral stock and polybrene, with a total volume of 200µL in one well. Cells were incubated overnight at 37ºC and 5% CO_2. Transduction medium was discarded and replaced with pre-warmed medium. Cells were incubated at 37ºC and 5% CO_2 for a further 48 hours. Cells and supernatant were harvested for analys3is as in Sections 2.2.2.5 and 2.2.2.6, respectively.

2.2.6 Cellular analysis

2.2.6.1 Flow cytometry

2.2.6.1.1 Apoptosis detection

1 x 10^5 cells were collected by centrifugation at 900g for 5 minutes. Cells were resuspended in 500 µL 1X Binding Buffer. 5 µL Annexin V and 5 µL Propidium Iodide (PI) (50 µg/mL) was added to each sample and incubated in the dark for 5 minutes at room temperature. A Sony SH800S cell sorter was used to record 5000 events per sample, with each sample taken in triplicate. Debris and cell doublets were excluded using forward scatter (FSC) and side scatter (SSC) parameters. FSC is proportional to the diameter of a cell, and SSC provides information about the granularity (and therefore internal complexity) of a cell. Untransduced HEK293T cells were used as a negative control with >99% of this population determined as negative to set the fluorescence gate. Annexin V binding was analysed by flow cytometry using the FITC signal detector, and PI with the phycoerythrin signal detector (Excitation 488nm, Emission 530nm). Data was analysed using FlowJo V9.

2.2.6.2 Imaging flow cytometry

2.2.6.2.1 Sample preparation

$1x10^6$ HEK293T cells were washed in ice-cold PBS supplemented with 1% [v/v] FBS. Cells were collected by centrifugation at 900 g for 5 minutes at 4ºC. Cells were fixed in 500 μL 1% [v/v] PFA on ice for 20 minutes. Cells were again collected by centrifugation at 900 g for 5 minutes and the supernatant was discarded. Cells were resuspended in 500 μL PBS supplemented with 3% [v/v] Bovine Serum Albumin (BSA), and left for 30 minutes at 4ºC. Antibody solutions were made up in PBS supplemented with 1% [v/v] BSA and containing the desired antibody diluted as specified (Appendix Table 8.1). As antibodies were conjugated with fluorophores, handling at this stage was undertaken in reduced light conditions. Cells were pelleted by centrifugation at 900 g for 5 minutes and resuspended in 250 μL antibody solution, and incubated in the dark for 4 hours at 4ºC. Cells were pelleted by centrifugation at 900 g for 5 minutes and washed three times with 500 μL PBS. A nuclear stain was applied by adding 250 μL PBS with DAPI (0.1 μg/mL) to each sample, and incubated in the dark for 5 minutes at 4ºC. Cells were washed with 500 μL PBS and pelleted by centrifugation at 900 g for 5 minutes. Cells were resuspended in 500 μL ice-cold PBS supplemented with 10% (w/v) FBS, and 0.5% (w/v) sodium azide. Cells were kept in the dark at 4ºC until analysis.

2.2.6.2.2. Image acquisition

Images were acquired using the Amnis ImageStreamX imaging flow cytometer and the INSPIRE® software. An aliquot of a positive control was loaded to establish the appropriate instrument laser sensitivity. Positive control samples were then singly-stained, and were then loaded to produce a compensation matrix. 5,000 events for each sample were then acquired at 60X magnification.

2.2.6.2.3 Image analysis

Data analysis was performed with IDEAS® v.6.0 analysis software using compensated image files. Analysis was performed following published protocols (Rajan et al., 2015; Pugsley et al., 2017). A compensation matrix was applied to correct for spectral overlap. Debris and cell doublets were excluded using forward scatter and side scatter parameters.

The built-in 'Spot Count Wizard' was used to generate a new spot count mask to calculate the number of LC3-positive puncta in a single cell.

The 'Bright Detail Similarity (BDS) R3 Wizard' was used to compute the intensity and location of bright spots from different fluorescent probes within a single cell. BDS R3 represents the log-transformed Pearson's correlation coefficient of bright spots 3 pixels in radius or less, from an input of images from two fluorescent channels. Bright spots were analysed depending on their spatial location, thereby computing the co-localisation of two fluorescent probes, LC3-AF647 and LAMP-1-PE. The correlation coefficient spanned from 0 (uncorrelated, different spatial location), to 1 (perfect correlation, same spatial location), assuming no negative values. The correlation coefficient was log-transformed to enable increased dynamic range. A bivariate plot of Spot Count vs. BDS R3 was generated to assess autophagic flux (Rajan et al., 2015; Pugsley et al., 2017).

2.2.7 mRNA analysis

2.2.7.1 RNA extraction

Adherent cell sheets were washed with PBS at 24 hours and 48 hours post-transduction and transferred to a 15mL falcon tube. 5 mL Trizol™ was added to approximately 8 x 10^6 cells, counted in Section 2.2.2.3, and pipetted until homogenous. This was incubated at room temperature for 5 minutes. All the following steps were performed at 4°C.

Chloroform was added to each Trizol extract (0.2 mL for every 1 mL Trizol™ used). Tubes was shaken for 15 seconds, incubated for a further 5 minutes, and centrifuged at 12,000 g for 15 minutes at 4ºC. If the mixture was cloudy, centrifugation was repeated. The upper aqueous phase containing RNA was transferred to a 2 mL Eppendorf tube.

In the subsequent processing, isopropanol was added to Trizol extracts (0.5 mL isopropanol to 1 mL Trizol). That mixture was incubated for 10 minutes and then centrifuged at 1500 g for 15 minutes at 4ºC. The supernatant was removed and discarded. The RNA pellet was washed with 1mL 70% [v/v] ethanol and centrifuged at 1500 g for 10 minutes at 4ºC. Again, the supernatant was removed and discarded. The pellet was air-dried for approximately 10 minutes. The pellet was then dissolved in 50 μL DEPC-treated RNase-free water. If the pellet was difficult to dissolve, this step was performed at 55-60ºC. RNA was analysed for concentration and purity using a NanoDrop™ (Section 2.7.2).

2.2.7.2 DNase treatment

10 μg RNA (Section 2.2.7.1) was mixed with 3 μL DNase I enzyme, 6 μL DNase I buffer, and nuclease-free water up to a volume of 100 μL. This was incubated for 45 minutes at 37ºC, then 10 minutes at 75ºC.

2.2.7.3 Determining RNA concentration and purity

The concentration and purity of RNA was analysed using a NanoDrop™ spectrophotometer. The absorbance ratio at 260nm and 280nm was assessed with a ratio of 2 being acknowledged as ‘pure’ RNA.

2.2.7.4 cDNA synthesis

cDNA was synthesised using a cDNA synthesis kit. All solutions were thoroughly vortexed before use. For each reaction, a mix was prepared on ice in a 0.2 mL PCR tube with the following components; 5 μg RNA, 1 μL Oligo dT, 1μL 10mM dNTP mix,

4 μL 5X RT Buffer, 1 μL RiboSafe RNase Inhibitor, 1 μL Reverse Transcriptase (200 U/μL), and DEPC-treated water up to 20 μL total volume. This was mixed gently by pipetting. Samples were incubated at 42ºC for 45 minutes, then 85ºC for 5 minutes. Samples were stored at -20ºC.

2.2.7.5 qRT-PCR

qRT-PCR mixes were prepared containing 2.5 μL cDNA (stock of 1μL cDNA diluted in 15μL RNAse-free H_2O), 1.25 μL forward primer, 1.25 μL reverse primer, and 5 μL PowerUp™ SYBR™ Green Master Mix (Primers in Appendix Table 8.5). Samples were prepared in duplicate. 10 μL total volume of qRT-PCR mix was pipetted into one well in a 96-well plate. qPCR was performed using the programme in Table 2.7.

Table 2.7. qRT-PCR conditions

Temperature (ºC)	Time	Cycles
42	20 minutes	1
95	2 minutes	1
95	5 seconds	40
55	15 seconds	
72	30 seconds	

This was followed by melting curve analysis using 0.15ºC in fast mode.

The quantity of target, normalised to the endogenous reference gene GAPDH, was given by the following equation:

$2^{-\Delta\Delta Ct}$

Where $\Delta\Delta Ct = \Delta Ct_{\text{Sample}} - \Delta Ct_{\text{Reference control}}$

2.2.8 Statistics

Data presented is represented as the Mean +/- Standard Deviation (SD), or +/- Standard Error of the Mean (SEM) as stated. These were calculated as below:

$$Standard\ deviation\ (SD) = \sqrt{\frac{\Sigma(x - mean)^2}{N}}$$

Where:

x = Observed value

N = Number of values in data set

$$Standard\ Error\ of\ the\ Mean\ (SEM) = \frac{SD}{\sqrt{n}}$$

Where:

SD = Standard deviation

N = Number of observations

ANOVA (One- and Two-Way) was performed where described, using GraphPad Prism 7 7.0e Software to determine statistical significance. Data with *p* values under 0.05 were considered to be statistically significant.

For imaging flow cytometry, differences in cell populations were evaluated using a Mann-Whitney test, a non-parametric test which allows comparison of groups without assuming a normal distribution.

3 Production and characterisation of GagPol and GagPol-EGFP vectors

3.1 Introduction

A key aim for standardisation of LVV manufacture is to generate a high-titre stable cell line as discussed in Section 1.3.2. As described, various methods exist to improve vector titres, including optimisation of bioprocessing conditions, improving the packaging and transfer plasmids, and the use of targeted cell engineering. Targeted cell engineering is of particular interest given that it has shown to be successful in improving titres in HEK293T cells for the production of biotherapeutics including monoclonal antibodies, LVVs, and AVs (reviewed in Abaandou et al., 2021).

The growth and production properties of HEK293T cells are not well-characterised when compared with other cell factories. Prior to defining targets for HEK293T cell engineering to improve LVV production, it is vital to gain an understanding of how individual vector components interact with the cell. For example, and directly relevant to the objectives of this thesis, it is not known how the viral structural protein used in LVV production, synthetic GagPol (SYNGP), interacts with HEK293T cells, and how its production may affect key cellular homeostatic mechanisms. By gaining an insight into how GagPol production affects HEK293T cells, this information has the potential to illuminate novel targets for targeted cell engineering to improve LVV production. The work presented in this Chapter aimed to generate a system where HEK293T cells were producing only GagPol. Cells were then transduced at high MOIs to determine the production limit of GagPol in HEK293T cells.

The key objectives of this Chapter are to:

1. Develop an appropriate GagPol over-expression cassette, in addition to a fluorescently-tagged GagPol construct to allow for the detection and tracking of GagPol in both live and fixed HEK293T cells
2. Perform transient over-expression of HEK293T cells with GagPol and GagPol-EGFP expression cassettes, following which the output of transductions will be characterised through various titration assays including p24 ELISA, PERT assay, and ddPCR copy number assay

3.2 Generating GagPol and GagPol-EGFP constructs

This Chapter first aimed to generate a plasmid construct enabling high-titre retroviral expression of GagPol. pQCXIX, a self-inactivating (SIN) retroviral vector was used as a backbone to enable high vector titres and high-level GagPol gene expression. This plasmid contains deletions in the 3' long terminal repeat (LTR), allowing production of replication-incompetent infectious particles following reverse transcription of the expression cassette. This plasmid is optimised for the production of high titres due to containing the strong and constitutively-active cytomegalovirus-immediate early (CMV-IE) promoter present in the 5' LTR.

A codon-optimised synthetic GagPol sequence, SYNGP (from pG3-SYNGP, GSK, Section 2.2.1.1), was inserted into a cloning site within pQCXIX, generating the plasmid pQCXIX-SYNGP (Figure 3.1 A) (Kotsopoulou et al., 2000). The SYNGP sequence is a completely codon-optimised sequence of the HIV-1 *gag-pol* gene, which enables Rev-independent high-level expression of GagPol while exploiting the favoured codon usage of human cells (Kotsopoulou et al., 2000). This sequence also enabled production of vectors that lack all HIV-1 accessory proteins, meaning increased safety as a result.

pQCXIX-SYNGP was generated by a Gibson assembly reaction following production of three fragments by PCR (Figure 3.1 B). This approach ensured that fragments did not contain more than one LTR, which could potentially anneal to each other during PCR and lead to production of the incorrect recombinant plasmid. Restriction digestion with the restriction enzyme *VspI* confirmed the production of the correct recombinant plasmid (Figure 3.2).

A

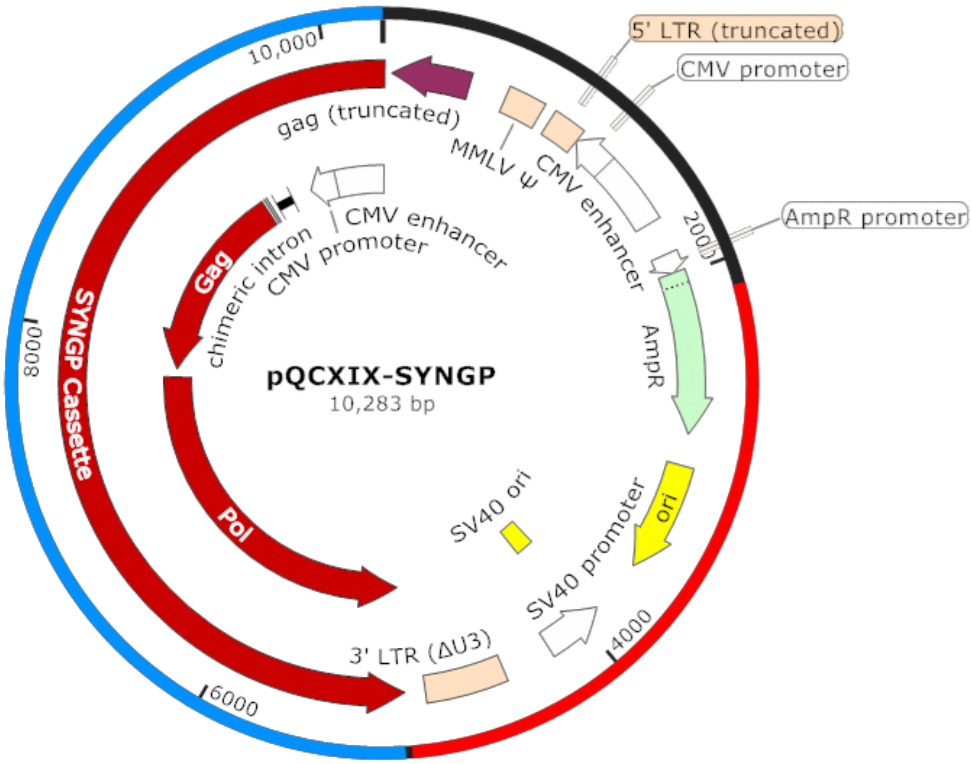

B

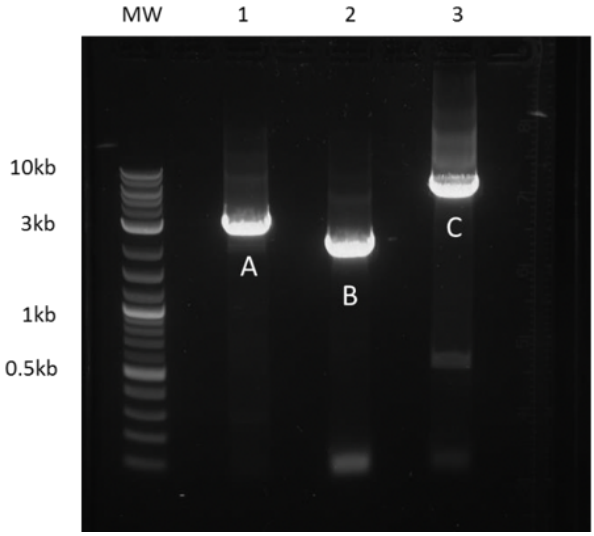

Figure 3.1 *In silico* design and production of pQCXIX-SYNGP for retroviral expression of GagPol. (A) Plasmid map of pQCXIX-SYNGP, 10283bp (Section 2.2.1). Red fragment: Fragment A (2942bp), Black fragment: Fragment B (2127bp), Blue fragment: Fragment C (5308bp). CMV promoter: Cytomegalovirus (CMV) immediate early promoter. CMV: CMV immediate early enhancer. Gag (truncated); the packaging cis-acting sequence lacking the start codon. MMLV Ψ: packaging signal of Moloney murine leukaemia virus (MMLV). 5' LTR (truncated): truncated LTR of MMLV. AmpR: sequence conferring resistance to ampicillin, carbenicillin, and

related antibiotics. Ori: high copy-number ColE1/pMB1/pBR322/pUC origin of replication. SV40 promoter: Similan Virus 40 early enhancer and promoter. 3' LTR Δ (U3): Self-inactivating 3' LTR from MMLV. (B) Agarose gel electrophoresis of PCR-amplified products. Fragments were generated by PCR (Section 2.2.1.1) and the size of these fragments was confirmed by agarose gel electrophoresis (Section 2.2.1.2). Fragments were extracted and purified (Section 2.2.1.3) ready for Gibson Assembly Reaction (Section 2.2.1.5). MW: 2-log molecular weight marker, Lane 1: Fragment A (2942bp), Lane 2: Fragment B(2127bp), Lane 3: Fragment C (5308bp).

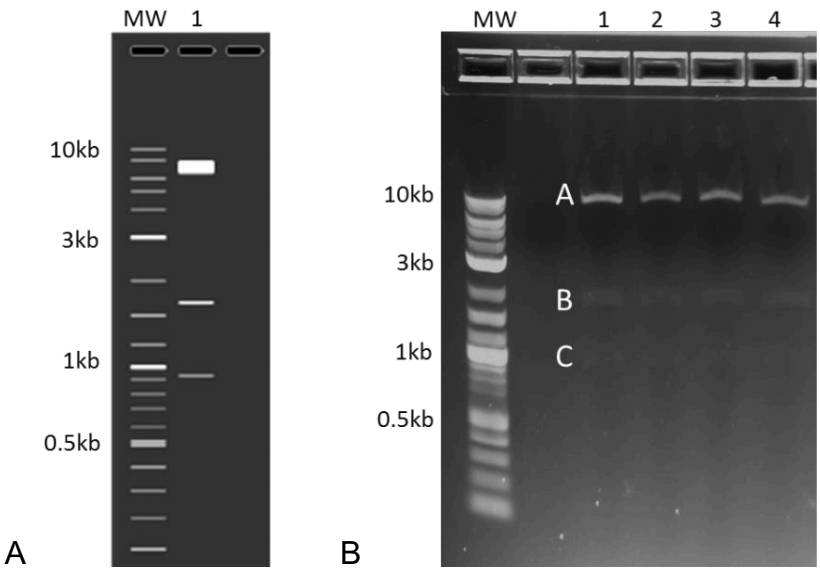

Figure 3.2 Restriction digestion of pQCXIX-SYNGP by restriction enzyme *VspI*. (A) The restriction enzyme *VspI* was pre-determined *in silico* as suitable for confirming production of the correct plasmid through analysis of restriction sites in SnapGene. MW: 2-log molecular weight marker. Lane 1: Expected fragments following restriction digestion with VspI. (B) Agarose gel electrophoresis with products from *VspI* restriction digestion (Section 2.2.1.8). Lanes 1-4: Fragments produced using *VspI* following maxipreps (Section 2.2.1.7) of 4 selected colonies. Fragment A: 7690bp, Fragment B: 1675bp, Fragment C: 928bp.

In order to allow detection of GagPol cellular localisation through use of various methods including flow cytometry in live and fixed cell samples, it was necessary to develop a fluorescently-tagged GagPol construct. Enhanced Green Fluorescent Protein (EGFP) was utilised as the fluorescent tag in this project. This variant of GFP has two mutations at positions F64L and S65T, and is reported to be much brighter than GFP (Heim and Tsien, 1996, Brejc et al., 1997).

Inserting a fluorescent tag in the appropriate position within GagPol was important to ensure that the functionality of GagPol was not affected. For example, inserting a fluorescent tag at the N-terminus would affect the targeting of GagPol to the inner leaflet of the plasma membrane due to specific interactions between phosphatidylinositol-(4,5)-bisphosphate [PI(4,5)P2] and the myristoylated matrix domain of Gag (Ono et al., 2004; Chukkapalli et al., 2008). Along with other basic residues, this myristoyl group enables membrane anchoring and subsequent assembly of GagPol proteins on the inner leaflet of the plasma membrane (Bouamr et al., 2003). Insertion of a fluorescent tag between the p6 domain of Gag and the PR domain of Pol would interfere with the Gag:GagPol (20:1) splicing ratio, generated from a -1 ribosomal frameshift event (Atkins et al., 1990; Gesteland et al., 1992). Disturbing this ratio would be detrimental to replication and assembly of the virus. Alternatively, inserting a fluorescent tag at the C-terminus of Gag would impact on maturation of the VLP, as the p6 domain is crucial for maturation and PR activation (Yu et al., 2015).

Gag is remarkably tolerant to the insertion of proteins between MA and CA (Hubner et al., 2006). A previously described approach of fluorescently tagging GagPol has previously been described by Hubner *et al.,* which enabled physiologically accurate localisation and oligomerisation of fluorescently-tagged GagPol in trafficking studies (Hubner et al., 2007). Here, an interdomain eGFP-fusion protein was inserted in between the Matrix (MA) and the Capsid (CA) domain within Gag, flanked either side by a functional protease cleavage sequence (Figure 3.3). This sequence, SQNYPIVQ, is similar to the PR cleavage site between the MA and CA domain of GagPol. Following assembly, EGFP will be cleaved from the Gag precursor protein due to the linker region being accessible to PR, meaning fluorescence will be diffuse

throughout the cell. This approach ensures that folding and function of Gag is not disturbed.

Using the rationale behind this approach, a fluorescently-tagged GagPol construct, pQCXIX-SYNGP-EGFP, was designed *in silico* on SnapGene (Figure 3.4 A). A three-fragment Gibson assembly reaction was used to generate two fragments from the previously generated pQCXIX-SYNGP plasmid as a template, and one fragment from Bt-mod-V2 (GSK) plasmid containing the EGFP sequence (Figure 3.4 B). Fragments were generated by PCR and were assembled by Gibson assembly reaction, following which restriction digestion with *VspI* confirmed production of the correct recombinant plasmid, as the expected sized fragments were generated (Figure 3.2).

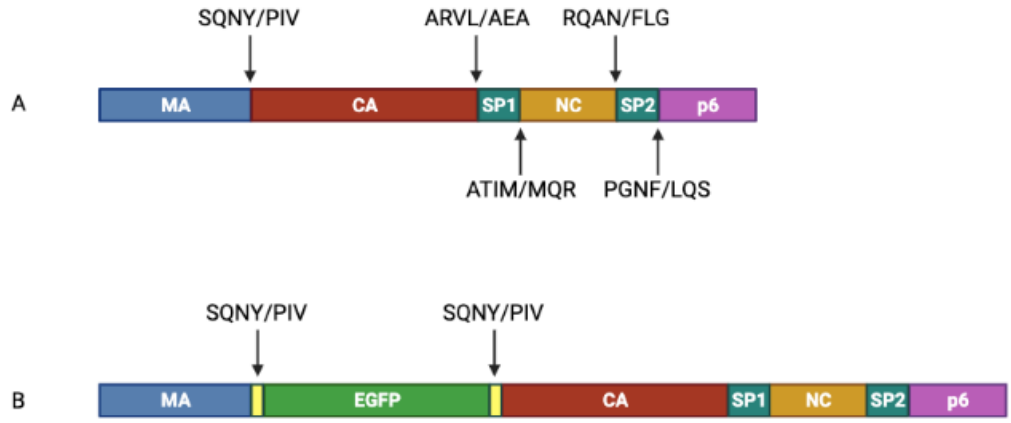

Figure 3.3 Structure of HIV-1 Gag polyprotein precursor and EGFP tag. (A) Structure of Gag precursor and internal structural proteins (MA: Matrix, CA: Capsid, SPI: Spacer peptide, NC: Nucleocapsid, SP2: Spacer peptide, p6). (B) Design of fluorescently-tagged GagPol within Gag. The fluorescent protein, EGFP, was inserted between MA and CA of Gag, flanked either side by a functional protease cleavage site, SQNYPIVQ, specific to HIV-1 PR. Black arrows indicate residues that encompass cleavage sites. The forward slash represents scissile bond position (Mammano et al., 2010). Created in BioRender.

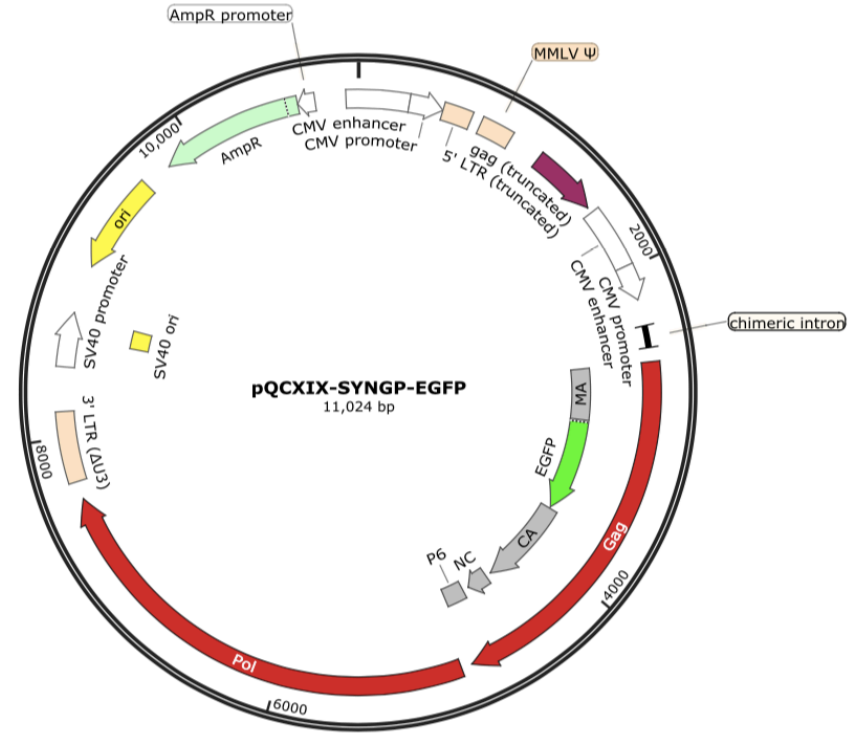

A

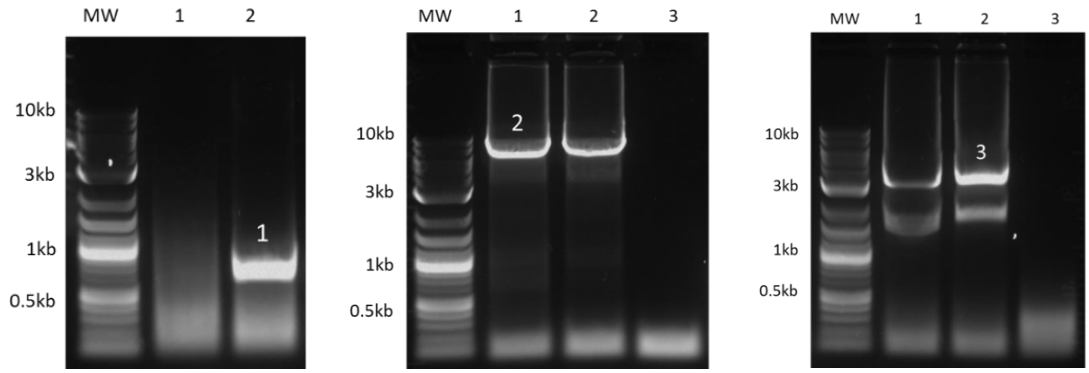

B

Figure 3.4 *In silico* design and production of pQCXIX-SYNGP-EGFP for the expression of fluorescently-tagged GagPol. (A) *In silico* design of pQCXIX-SYNGP-EGFP in Snapgene. SQNYPIVQ protease cleavage sites were inserted at the 3' and 5' of EGFP. Components are described in Figure 3.1. (B) Agarose gel electrophoresis of PCR-amplified products for plasmid generation. Fragments were generated by PCR (Section 2.2.1.1) and the size of each fragment was confirmed by agarose gel electrophoresis (Section 2.2.1.2). Fragment 1: 773bp (T_m 60°C), Fragment 2: 6865bp (T_m 65°C), Fragment 3: 3504bp (T_m 55°C), MW: 2-log molecular weight marker.

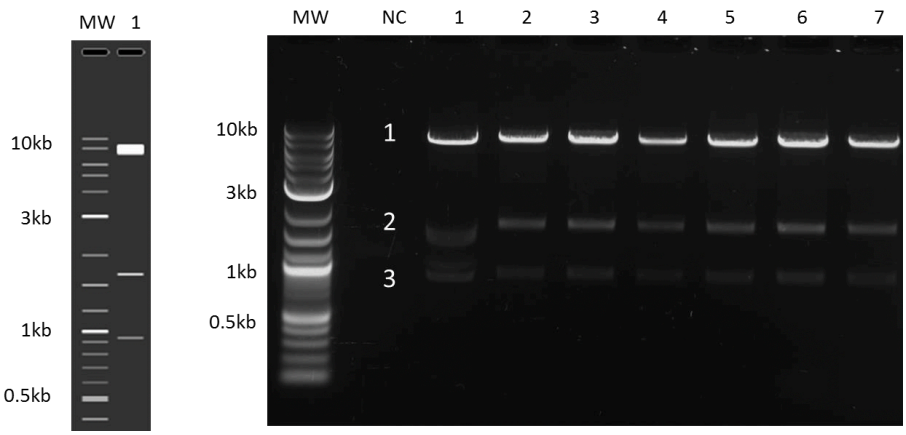

Figure 3.5 Restriction digestion of pQCXIX-SYNGP-EGFP by restriction enzyme *VspI*. Left: The restriction enzyme *VspI* was determined suitable for confirming production of correct recombinant plasmid by analysing restriction sites in Snapgene. MW: 2-log molecular weight marker. Lane 1: Expected fragments following *VspI* restriction digestion. Right: Agarose gel electrophoresis (Section 2.2.1.2) of digested plasmid following restriction digestion (Section 2.2.1.8). NC: No-template control. Lanes 1-7: Fragments produced during restriction digestion with *VspI* from maxipreps (Section 2.2.1.7) of 7 colonies. Fragment 1: 8421bp, Fragment 2: 1675bp, Fragment 3: 928bp.

3.3 Vector production in Amphopack293 and HEK293T cells

Following the production of plasmids expressing GagPol and GagPol-EGFP, a further objective in this Chapter was to develop a vector production system that was able to facilitate high-level expression of GagPol in HEK293T cells (Figure 3.6). Two vector production methods were utilised.

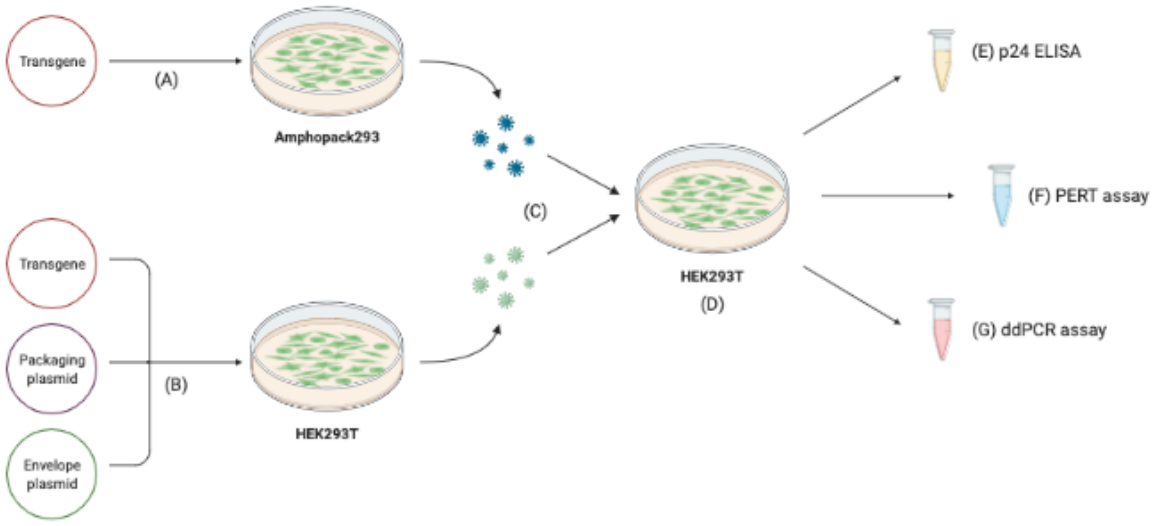

Figure 3.6 Workflow diagram of two vector production systems and subsequent characterisation of vector products. (A) Transfection of Amphopack293 packaging cells to produce AEP-pseudotyped vector (Section 2.2.3.1). (B) Three-plasmid transfection of HEK293T cells to produce VSV-G-pseudotyped vector (Section 2.2.3.2). (C) Vector is harvested and titred following transfections (Section 2.2.4.1). (D) Vector is used to transduce HEK293T cells at a known MOI (Section 2.2.2.5). The output of transductions is determined by (E) p24 ELISA (Section 2.2.4.2), (F) PERT assay (Section 2.2.4.2), and (G) a ddPCR copy number assay (Section 2.2.4.4). Created in BioRender.

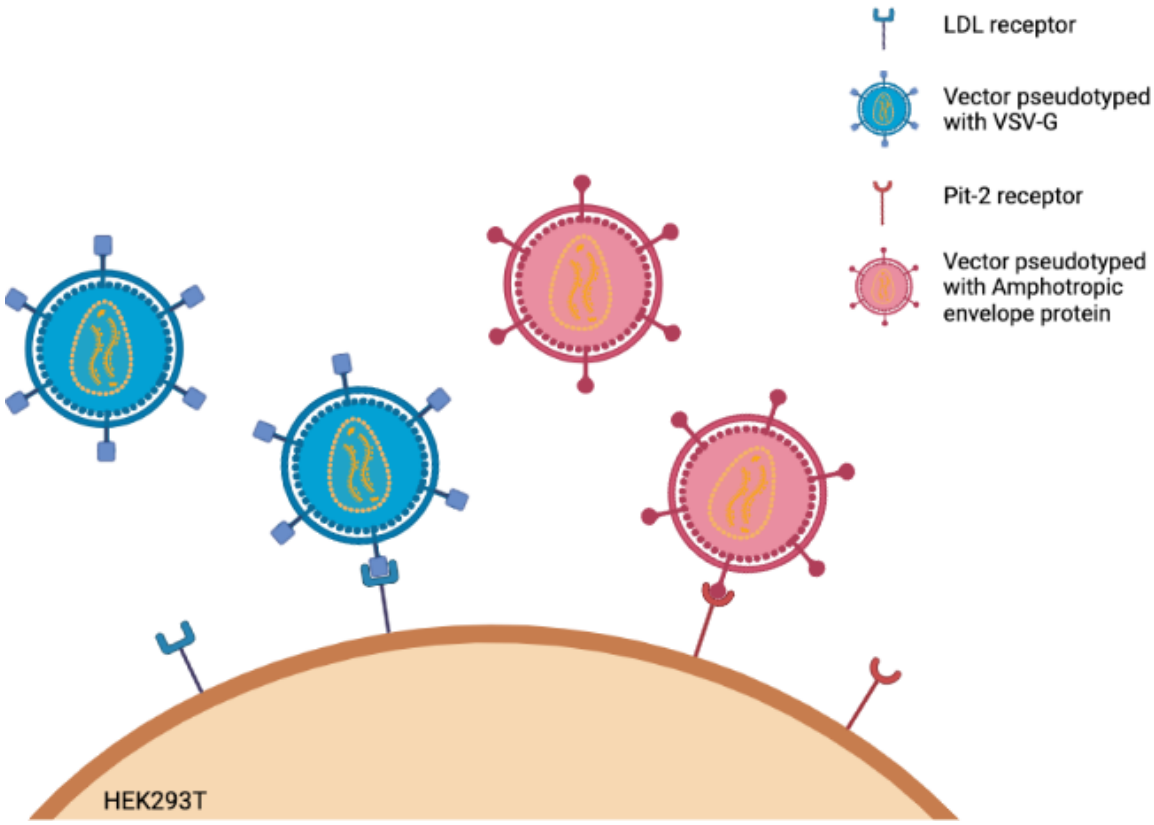

Figure 3.7 Schematic diagram of rationale behind vector production in either HEK293T cells or Amphopack293 cells. Vector produced by 3-plasmid transfection in HEK293T cells were pseudotyped with Vesicular Stomatitis Virus G (VSV-G) (Blue on diagram). The major entry port for VSV-G on HEK293T cells is the LDL-receptor. Vector produced by transfection with a single plasmid in Amphopack293 cells were pseudotyped with Amphotropic Envelope Protein (AEP), which enabled cell entry into HEK293T cells via Pit-2 (Red on diagram). The tropism of these vectors is determined by the interactions between the viral envelope protein on the vector and the viral receptor on the HEK293T host cell. As these vectors have different receptors on the HEK293T cell, they therefore will not have the same entry method. This could influence transduction outputs. Created in BioRender.

3.3.1 Production of vector by transfection of Amphopack293 cells

The first vector production method utilised the Amphopack293 commercially available packaging cell line. This is a HEK-derived cell line designed specifically for rapid and high-titre production of replication-incompetent MMLV-based retroviral particles following transfection. The Amphopack293 cell line stably expresses the viral *gag*, *pol*, and *4070A env* genes that were introduced using puromycin and bleomycin resistance genes. Vector generated from transfection of Amphopack293 is able to infect a broad range of mammalian cells due to being pseudotyped with the 4070A Amphotropic MLV envelope.

It is important to note that this cell line expresses the Amphotropic Envelope Protein (AEP), from the Murine Leukemia Virus (MuLV), which recognises the amphotropic receptor Ram-1, also referred to as Pit-2, which is present on HEK293T cell surfaces (Miller and Miller, 1994; Ragheb et al., 1995) (Figure 3.7). Pit-2 is a sodium-dependent phosphate transporter; many other RVs also use cell surface transporter proteins as routes of entry into various cell types (Kavanaugh et al., 1994; Uckert et al., 1998; Salaun et al., 2002; Feldman et al., 2004).

To produce vector in Amphopack293 cells, a single plasmid transfection with either GagPol or GagPol-EGFP vector was performed. Following transfection, vector was titrated by transducing HEK293T cells with serial dilutions of each vector, as described in Section 2.2.4.1. The titre of each vector was assessed by flow cytometry 2 days after transduction by detecting the percentage of GFP-expressing HEK293T cells (Figure 3.8). Titre was expressed as transducing units (TU) per millilitre of harvested supernatant. A TU is the number of viral particles in a solution with are functionally capable of transducing one cell and expressing a transgene.

Following GFP titration 2 days post-transduction, GagPol-EGFP vector produced in Amphopack293 cells achieved titres of 1.18×10^8 TU/mL.

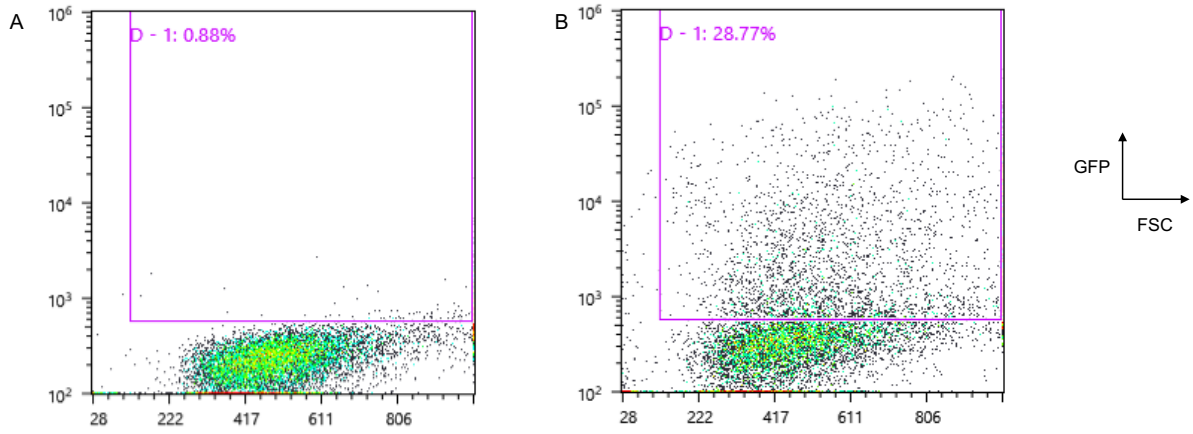

Figure 3.8 Titration of GagPol-EGFP vector produced in Amphopack293 cells by flow cytometry. HEK293T cells were transduced with serial dilutions of GagPol-EGFP vector (Section 2.2.4.1) produced by transfection in Amphopack293 cells (Section 2.2.3.1). GFP expression was determined by flow cytometry 48 hours post-transduction (Section 2.2.6.1). (A) Untransduced cells, (B) 0.1μL GagPol-EGFP vector. Images are example populations, the percentage of GFP-expressing cells is given as a percentage in the gate (Section 2.2.6.2). GFP: Green Fluorescent Protein. FSC: Forward Scatter.

3.3.2 Production of vector by transfection of HEK293T cells

A second approach to package GagPol and GagPol-EGFP utilised a three-plasmid transfection of HEK293T cells (pQCXIX-SYNGP-EGFP, pMD2.G, pBS-CMV-GagPol). This three-plasmid transfection with a packaging plasmid (pBS-CMV-GagPol), envelope plasmid (pMD2.G) and plasmid containing the genome of interest (pQCXIX-SYNGP-EGFP) mirrors the production of vector in Amphopack, which already stably express packaging and envelope genes.

The key difference between vector production in HEK293T cells and Amphopack293 cells is the vector pseudotype. Pseudotyping is the introduction of different viral envelope proteins on the surface of an enveloped virus, with the purpose of broadening the host cell range (tropism) that the viral vector can infect. Vector produced in HEK293T was pseudotyped with VSV-G (encoded by plasmid pMD2.G), the receptor of which is LDL-R, which leads a broad cell tropism (Finkelshtein et al., 2013; Cronin et al., 2005). The VSV genome encodes a transmembrane glycoprotein (G) in addition to four other structural proteins (Albertini et al., 2012). G has a crucial role in the early steps of viral infection, including being responsible for attachment of the virus to a specific receptor. Following entry into the cell by clathrin-mediated endocytosis, G is able to trigger fusion between the endosomal and viral membranes (Cureton et al., 2009; Johannsdottir et al., 2009). This allows subsequent infection steps to occur as the genome is released into the cytosol.

Following transfection, HEK293T cells were transduced with serial dilutions of vector. The titre of each vector was determined by flow cytometry 2 days post-transduction by detecting the percentage of GFP-expressing HEK293T cells (Figure 3.9). GagPol-EGFP vector produced in HEK293T cells achieved titres of 2.28×10^8 TU/mL, which is comparable to titres reported in literature (Vink et al., 2020).

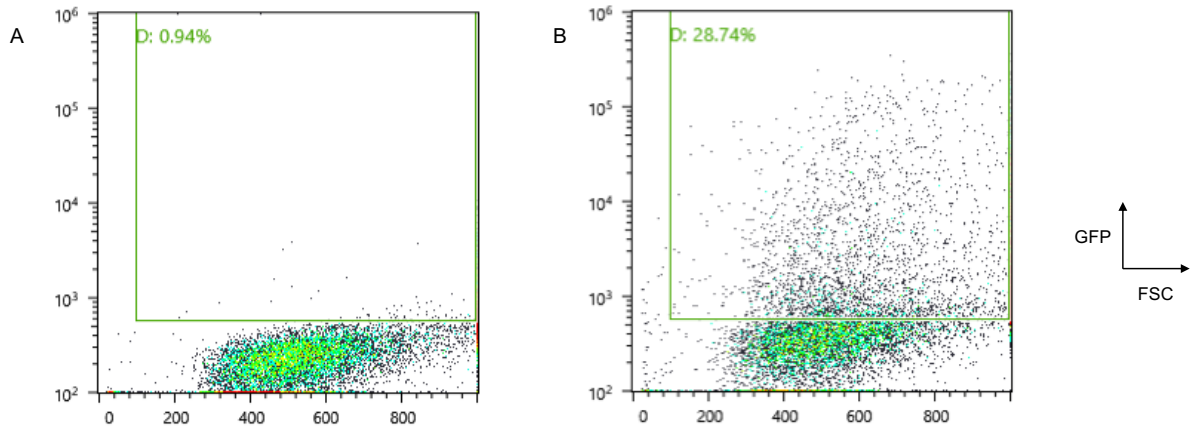

Figure 3.9 Titration of GagPol-EGFP vector produced in HEK293T cells by flow cytometry. HEK293T cells were transduced with serial dilutions of GagPol-EGFP vector (Section 2.2.4.1) produced by transfection in HEK293T cells (Section 2.2.3.2). GFP expression was determined by flow cytometry 48 hours post-transduction (Section 2.2.6.1). (A) Untransduced cells, (B) 0.1μL GagPol-EGFP vector. Images are example populations, the percentage of GFP-expressing cells is given as a percentage in the gate (Section 2.2.6.2). GFP: Green Fluorescent Protein. FSC: Forward Scatter.

3.4 Characterising VLP output following HEK293T transductions at a range of MOIs

HEK293T cells were transduced with known titres of vector produced in Sections 3.3.1 and 3.3.2 to determine which vector production method enabled high-level expression of GagPol (summarised in Figure 3.6). This comparison involved assessing physical titre, functional titre, and copy numbers achieved following transduction at defined MOIs.

3.4.1 Amphotropic Envelope Protein-pseudotyped vector

To assess the physical titre of vectors, a Product Enhanced Reverse Transcriptase (PERT) assay was performed (Vermeire et al., 2012). This assay, used routinely to determine RV titre, quantifies the activity of Reverse Transcriptase (RT) using SYBR Green-based qPCR. In a PERT assay, an exogenous RNA template – in this case, RNA from the bacteriophage MS2 – was added to viral supernatant. The amount of MS2 RNA converted to cDNA by RT was used to estimate retroviral RT activity following treatment with a mild detergent to release vector from cells.

The PERT assay was performed on viral supernatant 48 hours post-transduction with GagPol and GagPol-EGFP-containing vector produced in Amphopack293 cells at a range of MOIs (Figure 3.10). GagPol vector produced a maximum of 3683.23 nU RT/mL at an MOI of 12.5. GagPol-EGFP vector produced a maximum of 3480.35 nU RT/mL, also at an MOI of 12.5. Although there is a modest increase in nU RT/mL with GagPol vector compared to GagPol-EGFP vector, this was not significantly higher at any time point or MOI (One-way ANOVA, Figure 3.10). The number of RT units did not increase despite transducing cells with MOIs of 12.5 and above.

To further compare vector titres, a p24 ELISA was performed (Figure 3.11). This method quantifies the physical titre of a sample, given by the concentration of p24 viral proteins. It is estimated that there are approximately 2000 molecules of p24 per physical LV particle, and approximately 1 x 10^4 physical particles of LV for 1pg of the

p24 antigen (Summers et al., 1992; Vogt et al., 1999). This roughly equates to 100 TU per 1pg of p24.

The maximum physical titre of GagPol vector in cell culture extracts was found to be 1.11 x 10^3 ng p24/mL at MOI 15 and in cell culture supernatant was 8.67 x 10^2 ng p24/mL at MOI 12.5. The maximum physical titre of GagPol-EGFP vector in cell culture extracts was found to be 1.0 x 10^3 ng p24/mL at MOI 12.5 and in cell culture supernatant was 8.8 x 10^2 ng p24/mL at MOI 15. Despite increasing the MOI up to an MOI of 25, no additional p24 was produced. Again, there was no difference between tagged and untagged GagPol in both cell culture extracts and cell culture supernatants at all time points and MOIs (One-way ANOVA, Figure 3.11).

A Droplet Digital PCR (ddPCR) assay was used to quantify the vector copy number 48 hours after transduction (Figure 3.12). ddPCR involves the use of water-oil emulsion droplets which partitions a PCR reaction into 20,000 droplets. PCR reactions are carried out in each nanolitre-sized droplet independently, and then are analysed depending on whether droplets are PCR-positive or PCR-negative. ddPCR was performed using a primer and probe set targeted to a sequence in GagPol to determine the copy number of GagPol per cell. Cells transduced with either GagPol or GagPol-EGFP vectors had a maximum copy number of 8.9 and 8.5 respectively, both at an MOI of 15. For all MOIs, the difference in copies/cell in transductions with GagPol and GagPol-EGFP vector was not statistically significant at 48 hours post-transduction (One-way ANOVA, Figure 3.12). Copy number did not increase at higher MOI's despite increasing the MOI used during transductions. As it stands, there is no published data for AEP-pseudotyped vectors to compare this with.

Considering all parameters analysed here (nU RT/mL by PERT assay, ng p24/mL by p24 ELISA, copy number by ddPCR), it is encouraging that there is a trend where a maximum is being observed at approximately MOI 10-15. This indicates that there is some form of molecular bottleneck during the production of GagPol which must be elucidated further.

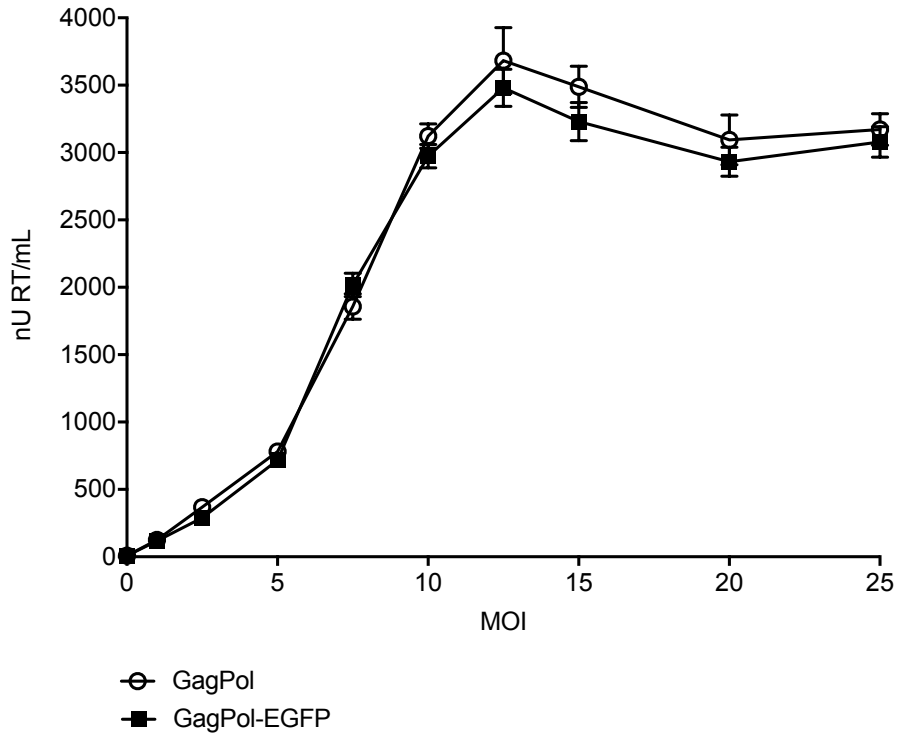

Figure 3.10 Product Enhanced Reverse Transcriptase (PERT) assay to determine titre of vector produced in Amphopack293 cells. GagPol and GagPol-EGFP vector was produced by transfection of Amphopack293 cells (2.2.3.1). Vector was used to transduce HEK293T cells at a range of MOIs (Section 2.2.5). Cell culture supernatant was collected 48 hours post-transduction (Section 2.2.2.6). Vector titre was assessed using a PERT assay (2.2.4.3). Values are mean +/- SEM of 3 biological repeats with 3 technical repeats each. Statistical analysis was carried out using one-way ANOVA.

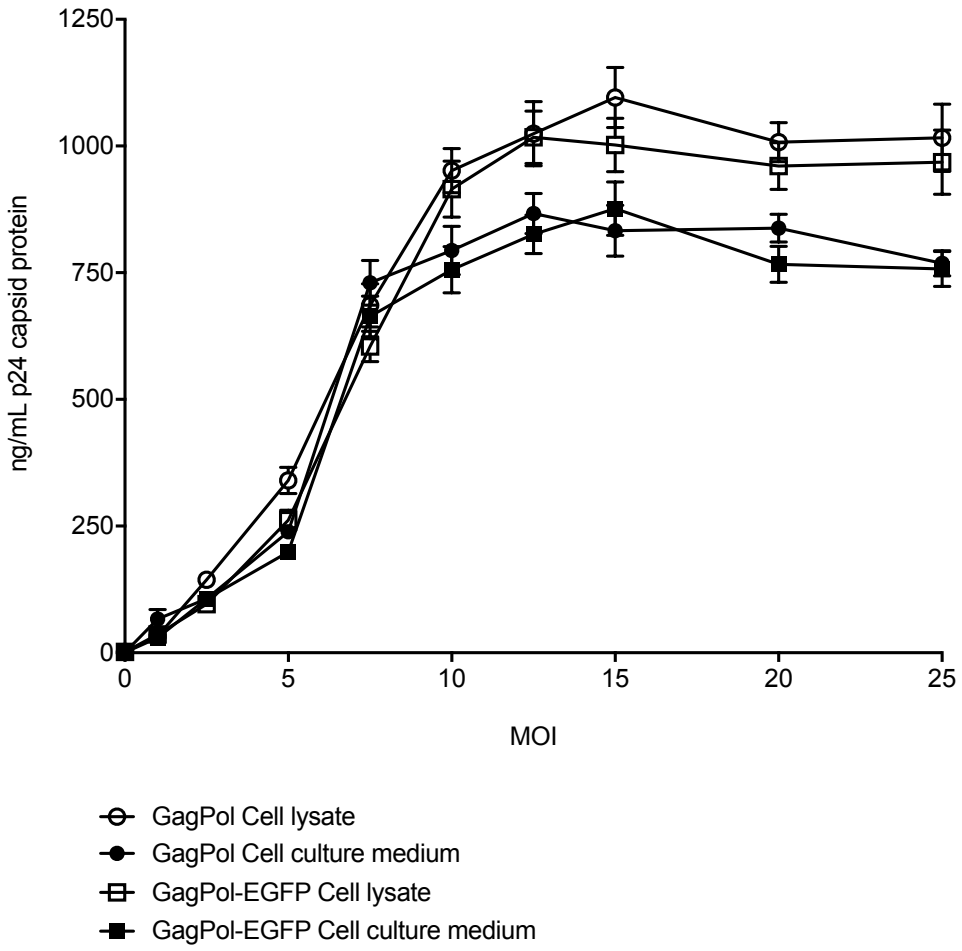

Figure 3.11 Titration of GagPol and GagPol-EGFP vector by p24 ELISA. Vector was generated by transfection of Amphopack293 cells (Section 2.2.3.1) and used to transduce HEK293T cells at a range of MOIs (Section 2.2.5). Cell lysate and cell culture medium samples were collected 48 hours post-transduction (Sections 2.2.2.5 and 2.2.2.6 respectively). p24 in cell lysate and cell culture medium was assessed by p24 ELISA (Section 2.2.4.2). Values are mean +/- SEM of 3 biological repeats with 3 technical repeats each. Statistical analysis was carried out using one-way ANOVA.

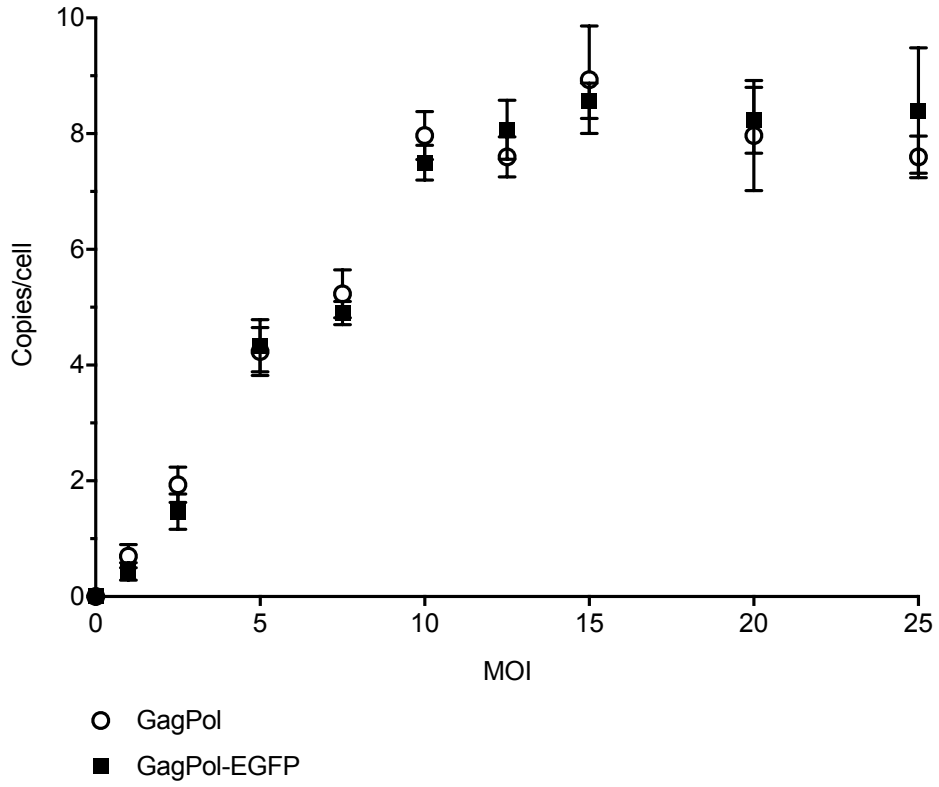

Figure 3.12 Quantification of vector copy number by ddPCR 48 hours post-transduction with vector generated in Amphopack293 cells. Vector produced in Amphopack293 cells (Section 2.2.3.1) was used to transduced HEK293T cells at a range of MOIs (Section 2.2.5). A copy number assay was performed on HEK293T cells 48 hours post-transduction (Section 2.2.4.4). Values are mean +/- SEM of 3 biological repeats with 3 technical repeats each. Statistical analysis was carried out using one-way ANOVA.

3.4.2 VSV-G-pseudotyped vector

The data presented in Section 3.4.1 showed no significant difference in VLP output with regards to p24 antigen, RT units, and in copies of GagPol per cell when comparing GagPol and GagPol-EGFP vector produced by transfection of Amphopack293 cells. As such, Section 3.4.2 will present a characterisation of VLP output following transduction with GagPol-EGFP produced by transfection of HEK293T cells.

Following transductions with GagPol-EGFP vector, VLP output was assessed by PERT assay, p24 ELISA, and by ddPCR. Samples were taken at 24 hours and 48 hours post-transduction to determine the timeframe of maximum vector production by PERT assay. Maximum GagPol-EGFP production occurred at 48 hours post-transduction with a maximum of 4204.07 nU RT/mL produced when transducing cells at an MOI of 75 (Figure 3.13).

Output of HEK293T transductions with GagPol-EGFP vector at various MOIs was further characterised by p24 ELISA. Similar to PERT data, MOI 75 resulted in the maximum p24 antigen produced in both cell lysate samples and cell culture medium samples, producing 1440 ng p24/mL and 1330 ng p24/mL respectively (Figure 3.14). It appears from this that the biosynthetic capacity of HEK293T cells is saturated when transducing cells with MOIs greater than 75. The shape of the cell culture supernatant curve follows the cell lysate curve fairly similarly, suggesting that the release of VLP's into cell culture supernatant from HEK293T cells is not a bottleneck in vector production. This suggests that the bottleneck causing a limit in GagPol production may therefore happening before secretion.

A ddPCR assay was performed to determine vector copy number in HEK293T cells. The number of copies per cell of GagPol continued to increase past an MOI of 175 with VSV-G-pseudotyped vector (Figure 3.15 A). Copies per cell was then plotted against p24 antigen produced to interrogate this data further (Figure 3.15 B). There appeared to be a limit in p24 production past 25 copies per cell, despite copy number continuing to increase when using up to an MOI of 175. This non-linear

relationship between p24 produced and the transcript level confirms that the biosynthetic pathway of GagPol has a post-translational bottleneck.

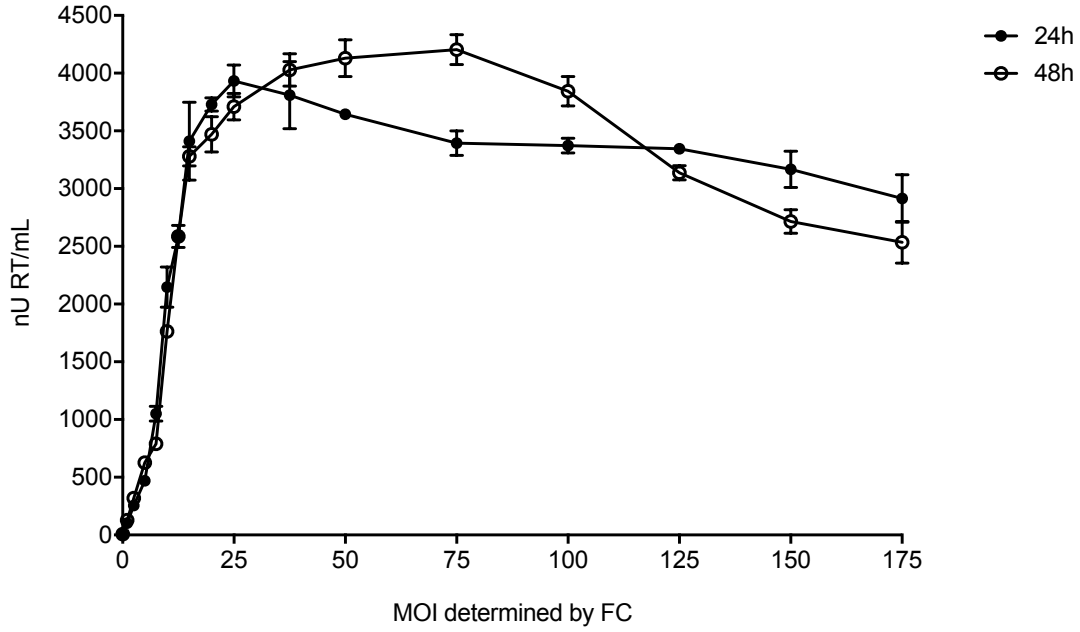

Figure 3.13 Product Enhanced Reverse Transcriptase (PERT) assay to determine titre of GagPol-EGFP vector produced in HEK293T cells. GagPol-EGFP vector was produced by transfection of HEK293T cells (2.2.3.2). Vector was used to transduce HEK293T cells at a range of MOIs (Section 2.2.5). Cell culture supernatant was collected 24 hours and 48 hours post-transduction (Section 2.2.2.6). Vector titre was assessed using a PERT assay (2.2.4.3). Values are mean +/- SEM of 3 biological repeats with 3 technical repeats each. Statistical analysis was carried out using one-way ANOVA.

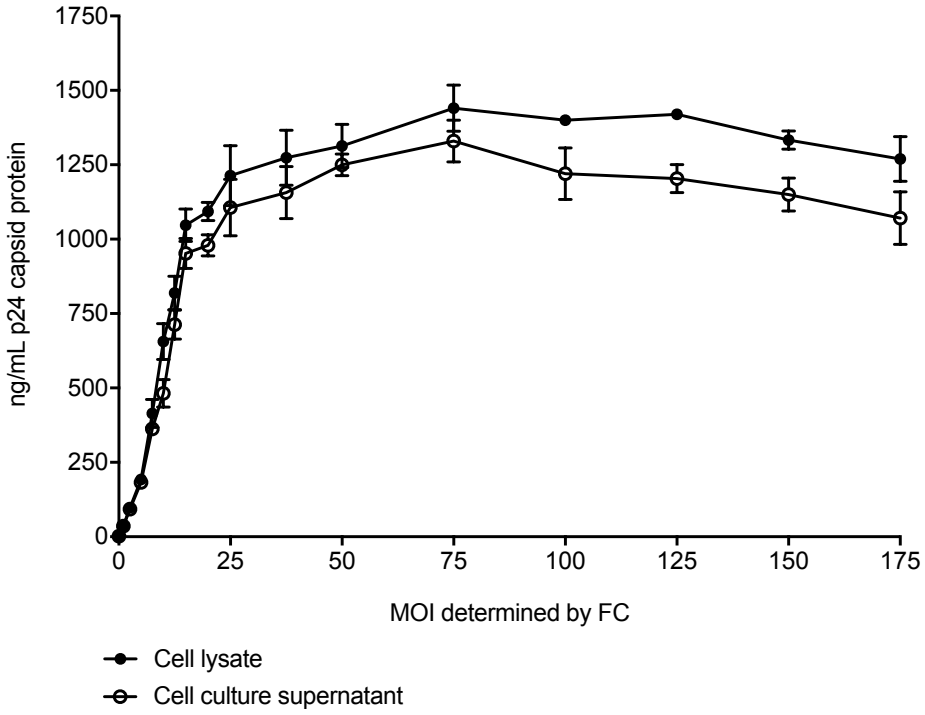

Figure 3.14 Titration of GagPol-EGFP vector by p24 ELISA. GagPol-EGFP vector was produced by transfection of HEK293T cells (Section 2.2.3.2) and used to transduce HEK293T cells at a range of MOIs (Section 2.2.5). Cell lysate and cell culture medium samples were collected at 48 hours post-transduction (Sections 2.2.2.5 and 2.2.2.6 respectively). p24 in cell lysate and cell culture medium was assessed by p24 ELISA (Section 2.2.4.2). Values are mean +/- SEM of 3 biological repeats with 3 technical repeats each. Statistical analysis was carried out using one-way ANOVA.

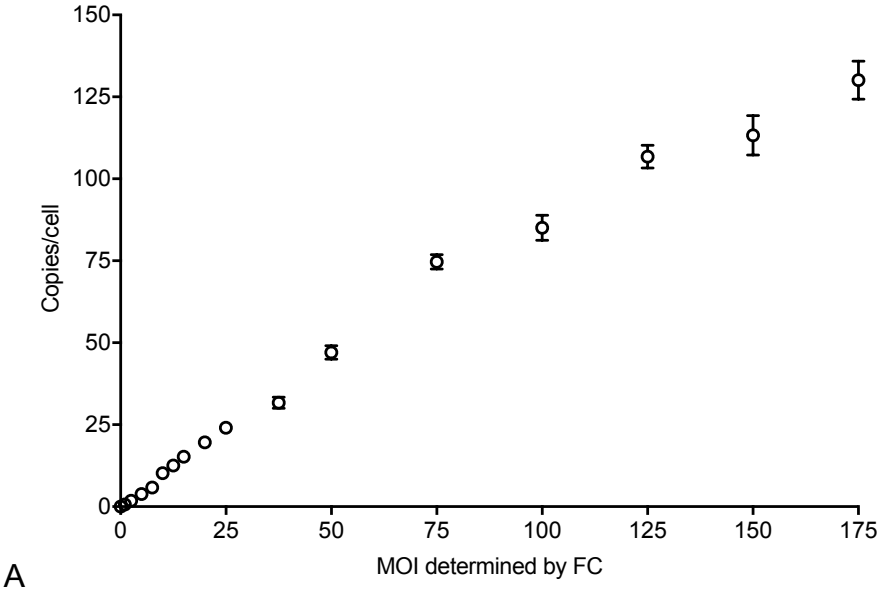

A

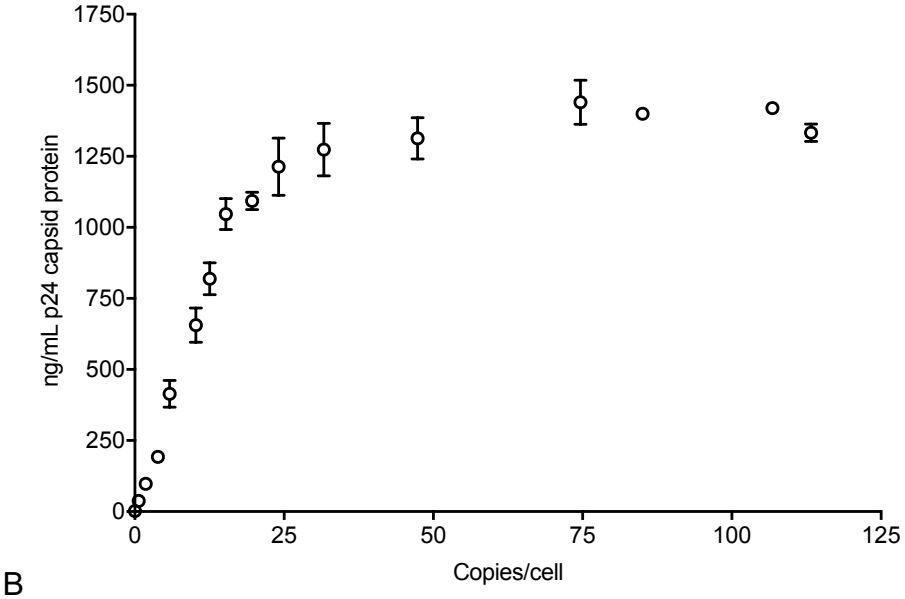

B

Figure 3.15 Quantification of vector copy number by ddPCR with GagPol-EGFP vector generated in HEK293T cells. GagPol-EGFP vector produced in HEK293T cells (Section 2.2.3.1) was used to transduce HEK293T cells at a range of MOIs (Section 2.2.5). A ddPCR copy number assay was performed on transduced HEK293T cells 48 hours post-transduction (Section 2.2.4.4). (A) GagPol copy number vs. MOI (B) GagPol copy number vs. p24 concentration. Values are mean +/- SEM of 3 biological repeats with 3 technical repeats each.

3.5 Concluding remarks

This Chapter achieved the broad objective of generating a system where HEK293T cells produce the viral structural protein GagPol.

A construct enabling expression of GagPol was produced in addition to generating a suitable fluorescently-tagged construct. Work conducted in Section 3.3.1 demonstrated that there was no significant difference in titres achieved between GagPol and GagPol-EGFP vector, confirmed by p24 ELISA and PERT assay, as well as no significant difference in vector copy numbers achieved.

Vector produced in HEK293T cells consistently led to higher physical titres and vector copy numbers when compared with vector produced in Amphopack293 cells, which can be explained in part by the entry mechanism for each vector. To demonstrate this, transductions with an AEP-pseudotyped vector at MOI 25 achieved approximately 3000 nU RT/mL 48 hours post transfection with GagPol-EGFP vector (Figure 3.10), whereas transductions with VSV-G-pseudotyped vector at MOI 25 achieved approximately 3600 nU RT/mL (Figure 3.13). Similarly, with transductions with AEP-pseudotyped GagPol-EGFP vector at MOI 25, p24 in cell lysate achieved a titre of just over 1000 ng p24/mL (Figure 3.11), whereas transductions with VSV-G-pseudotyped GagPol-EGFP vector at MOI 25 achieved over 1250 ng p24/mL (Figure 3.14). This represents approximately a modest 25% increase in VLP-output using a VSV-G pseudotyped vector. As such, vector production by three-plasmid transfection of HEK293T was utilised throughout the remainder of this project (Section 2.2.2.3).

A potential explanation for these higher titres with VSV-G-pseudotyped vector may lie with the number of appropriate receptors on HEK293T cell surfaces. Vector produced in HEK293T cells is pseudotyped with VSV-G, compared with vector produced in Amphopack293 cells which is pseudotyped with AEP (Method of production in Section 2.2.2.3). These envelope proteins utilise different cell surface receptors as ports of entry (Figure 3.7). There may be fewer receptors on HEK293T cell surfaces for AEP-pseudotyped vector compared to VSV-G-pseudotyped vector.

This could mean that in a transduction with AEP-pseudotyped vector, fewer RV particles will be able to enter the HEK293T cell due to fewer entry receptors, and therefore will lead to fewer integration events. The exact numbers of each cell surface receptor are not known. This would be an interesting aspect to look into for future work and would illuminate areas of optimisation for improved transduction and therefore gene delivery.

VSV-G-pseudotyped vector copy number did not saturate, whereas AEP-pseudotyped vector did not get past more than 10 copies per cell, further indicating that the delivery mechanism is key for maximum GagPol production. Pre-transfecting HEK293T cells with a Pit-2 expression plasmid prior to transduction is a potential strategy by which AEP-pseudotyped vector titres could be increased. This strategy would mean more Pit-2 receptor would be present on the cell surface with which AEP-pseudotyped vector would be able to bind to and enter cells. However, as VSV-G is a commonly used envelope protein during LVV production, it would be of more value to ensure there are sufficient receptors for VSV-G on HEK293T cell surfaces.

Production of vector in HEK293T cells has been shown to be superior to vector produced in Amphopack293 cells in terms of vector integration and physical titre (Section 3.4.2). Titres of approximately 1350 ng p24/mL were achieved in cell lysate samples following transduction of HEK293T cells with GagPol-EGFP which is comparable to titres achieved in industry (in-house observations, GSK) (Vink et al., 2020). From a bioprocessing perspective, there is potentially a lot more capacity for GagPol production in HEK293T cells. The following Chapter will investigate how HEK293T cells respond to the over-expression of GagPol, with a particular focus on various types of cellular stresses as a result of the disruption of key cellular homeostatic mechanisms, which may aid in illuminating a potential explanation for the observed limit in GagPol production.

As it is not currently known exactly how GagPol traffics to the plasma membrane (Figure 1.3), it is vital to clarify what types of cellular stresses occur during GagPol over-expression, which will in turn highlight pathways involved in the synthesis of this viral protein.

4 Effect of GagPol production on HEK293T cells

4.1 Introduction

Work conducted in Chapter 3 provided the tools with which to study the response of HEK293T cells to the production of GagPol. As it has not yet been elucidated exactly how GagPol is trafficked to the plasma membrane (Figure 1.3), it is important to establish which mechanisms are involved with the trafficking of GagPol that could cause cellular stress. The aim of Chapter 4 is therefore to determine how GagPol production affects HEK293T cells, and whether the production of this protein disrupts key cellular homeostatic mechanisms.

This Chapter therefore aimed to generate information about the impact of GagPol over-expression on HEK293T host cell physiology and function, with a specific focus on cell viability and key cellular processes that may be disrupted in response to high-level expression of GagPol, including apoptosis, autophagy, ER stress, and activation of the UPR.

4.2 Cell viability

The consequence of transduction of HEK293T cells with VSV-G-pseudotyped GagPol-EGFP vector was investigated at various MOIs (Section 2.2.3). The viability of control HEK293T cells remained above 90% in the absence of transduction. This was also true for mock transductions (without DNA) where the transduction reagent polybrene was present at 10 μg/mL. Generally, as MOI during transduction increased, p24 protein production was also seen to increase in both cell lysates (which encompasses the assembling virus-like particles still inside the cell) and cell culture supernatant (virus-like particles that have budded from the cell) (Figure 3.14), HEK293T cell viability decreased (Figure 4.1). 66.9% of HEK293T cells were viable 48 hours post-transduction with an MOI of 25. When the MOI was increased to 75, only 34.1% of cells were viable at that same time point. This further decreased when an MOI of 150 was used during transduction, with only 14.3% of cells being viable at this time point. All cells were dead after 96 hours when transducing cells at an MOI of 150.

The largest drop in HEK293T cell viability was observed between 24-48 hours when over 1330 ng p24/mL GagPol-EGFP vector was being produced (Figure 3.14). When transductions at higher MOIs were performed, there was no further increase in p24 protein production in cell lysate, however there was a decrease in cell viability. This may represent a kind of biosynthetic bottleneck whereby the HEK293T cells are at capacity for viral protein production, to the point that production of more protein is toxic to cells. As discussed in Section 3.4.2, p24 production detected in both cell lysate and cell culture medium follows a similar trend, which indicates that release of GagPol from the cell may not be a bottleneck here, as this could indicate that cell viability is decreasing due to events happening before secretion. It cannot be firmly stated that the release of virus particles is not a bottleneck, but it can be deduced that when reaching a certain p24 production titre ‘ceiling’, cell function is damaged.

A potential explanation for the decrease in cell viability observed is that GagPol-EGFP expression is toxic to cells. There are various potential ways that the overexpression of GagPol-EGFP can be harmful to cells. Specific biological

pathways may be overloaded and as a result resources for protein production and transport in the cell may become exhausted (pathway of GagPol production and trafficking to PM remains unknown, Figure 1.3). This remainder of this Chapter will look in more detail at how GagPol production stresses HEK293T cells.

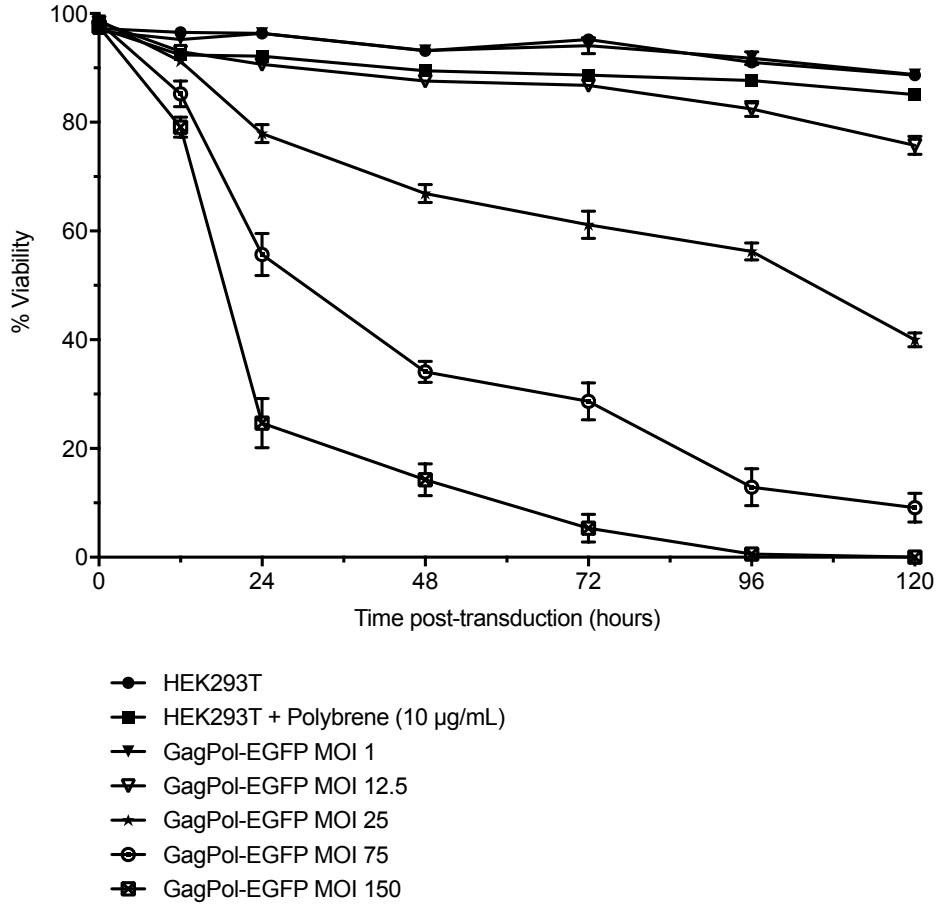

Figure 4.1 HEK293T cell viability following transductions with vector containing GagPol-EGFP. HEK293T cells were transduced at a range of MOIs (Section 2.2.5). Cell viabilities were measured at several time points (Section 2.2.2.3). Values are mean +/- SEM of 3 biological repeats with 3 technical repeats each. Statistical analysis was carried out using one-way ANOVA.

An additional investigation was undertaken to examine whether the decrease in viability occurred because of the over-expression of any intracellular protein (EGFP in this instance), or whether due to toxicity of GagPol-EGFP over-expression specifically. For this, vector encoding EGFP was produced by a three-plasmid transfection of HEK293T cells with a transfer plasmid for the retroviral expression of EGFP (pQCXIP-EGFP-F). Following transfection, HEK293T cells were transduced with serial dilutions of vector. The titre of each vector was determined by flow cytometry 2 days post-transduction by detecting the percentage of GFP-expressing HEK293T cells (Figure 4.2).

The viability of HEK293T cells following transduction with EGFP at various MOIs was recorded (Figure 4.3). HEK293T cells remained more viable at all time points throughout transduction with EGFP compared with GagPol-EGFP. At MOI 25 and above, the percentage of viable HEK293T cells was significantly higher when transduced with EGFP. Interestingly, HEK293T cells remained over 68% viable at 72 hours when EGFP was overexpressed at an MOI of 150, which suggests that over-expression of GagPol-EGFP is more toxic to cells than the over-expression of EGFP (Figure 4.2 C).

It is clear that the transduction process with higher MOIs is damaging to cells, however, transduction with GagPol-EGFP is more damaging than with EGFP. EGFP was used as a comparison in this investigation to ensure the fluorescent tag within GagPol did not cause additional decrease in cell viability. There may be several explanations for this, such as GagPol-EGFP being a more complex protein to produce when compared with EGFP, and therefore placing a higher burden on HEK293T cellular machinery. The greater decrease in viability could also be a result of GagPol being translated in a different way to EGFP which may cause HEK293T cells more stress. This fluorescent tag could also generate a structural or potential functional difference in viral particle formation which may be toxic to HEK293T cells, however this tagging approach has previously been reported to not affect the function, structure, or localisation of GagPol in HEK293T cells (Hubner et al., 2007).

It must also be considered that EGFP and GagPol-EGFP may localise to different compartments of HEK293T cells, which could influence the difference in cell

viabilities at higher MOIs during transduction (Figure 1.3 for potential locations of GagPol). GagPol has been shown to target the inner leaflet of the plasma membrane due to a highly-basic region in the N-terminus of the MA domain of Gag (Figures 1.3 and 1.7, discussed in Section 1.5), and so EGFP in GagPol-EGFP will also be trafficked to the plasma membrane where viral PR cleaves it. EGFP itself (without GagPol) is relatively small (27 kDa) and has been reported to localise in both the nucleus and in a diffuse manner in the cytoplasm (Belardinelli and Jackson 2017). The fact that GagPol over-expression leads to a greater decrease in cell viability compared with EGFP over-expression indicates that the location that these proteins are targeted to may have some influence on cell viability.

An additional experiment here to consider for future work would be to over-express a protein that also targets the inner leaflet of the plasma membrane, to allow for a more balanced comparison to GagPol, in addition to expressing just GagPol without the fluorescent tag. For example, there are many cytoskeletal, transport, and signalling proteins that must be localised to the plasma membrane for them to perform their usual functions (Heo et al., 2013).

Flow cytometry was performed to compare EGFP expression at several MOIs with both GagPol-EGFP and EGFP vector (Figure 4.4). The percentage of EGFP-expressing cells was consistently higher when using EGFP vector compared to GagPol-EGFP vector above an MOI of 12.5. This could indicate that the transfection process itself is easier for HEK293T cells to carry out, meaning it is easier for the cell to survive.

Together, these observations indicate that the over-expression of GagPol-EGFP in HEK293T cells causes cells to die at a higher extent to the over-expression of EGFP. The toxicity and decrease in cell viability, potentially caused by protein over-expression, may be dependent on the specific characteristics of GagPol, which may place a burden the machinery that produces it.

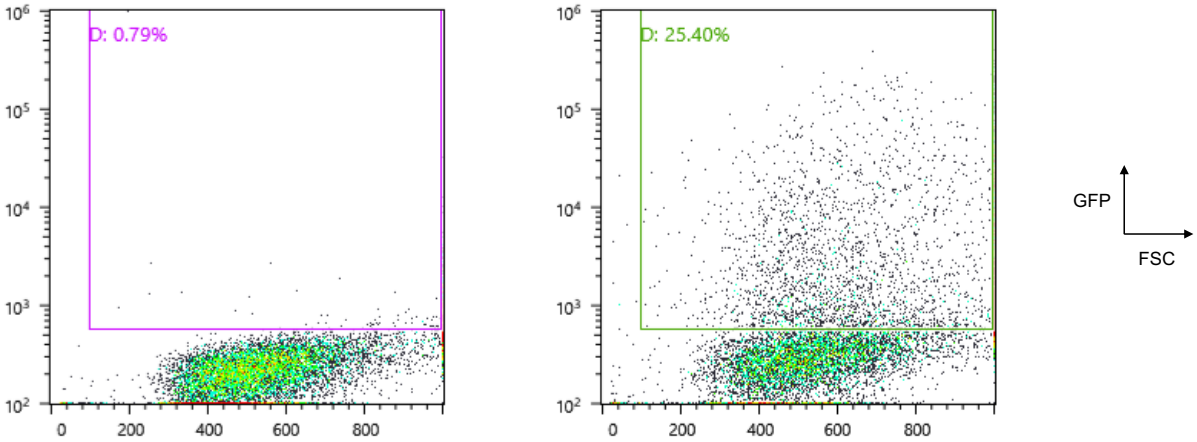

Figure 4.2 Titration Titration of EGFP vector produced in HEK293T cells by flow cytometry. HEK293T cells were transduced with serial dilutions of EGFP vector (Section 2.2.4.1) produced by transfection in HEK293T cells (Section 2.2.3.2). GFP expression was determined by flow cytometry 48 hours post-transduction (Section 2.2.6.1). (A) Untransduced cells, (B) 0.1μL EGFP vector. Images are example populations, the percentage of GFP-expressing cells is given as a percentage in the gate (Section 2.2.6.2). GFP: Green Fluorescent Protein. FSC: Forward Scatter.

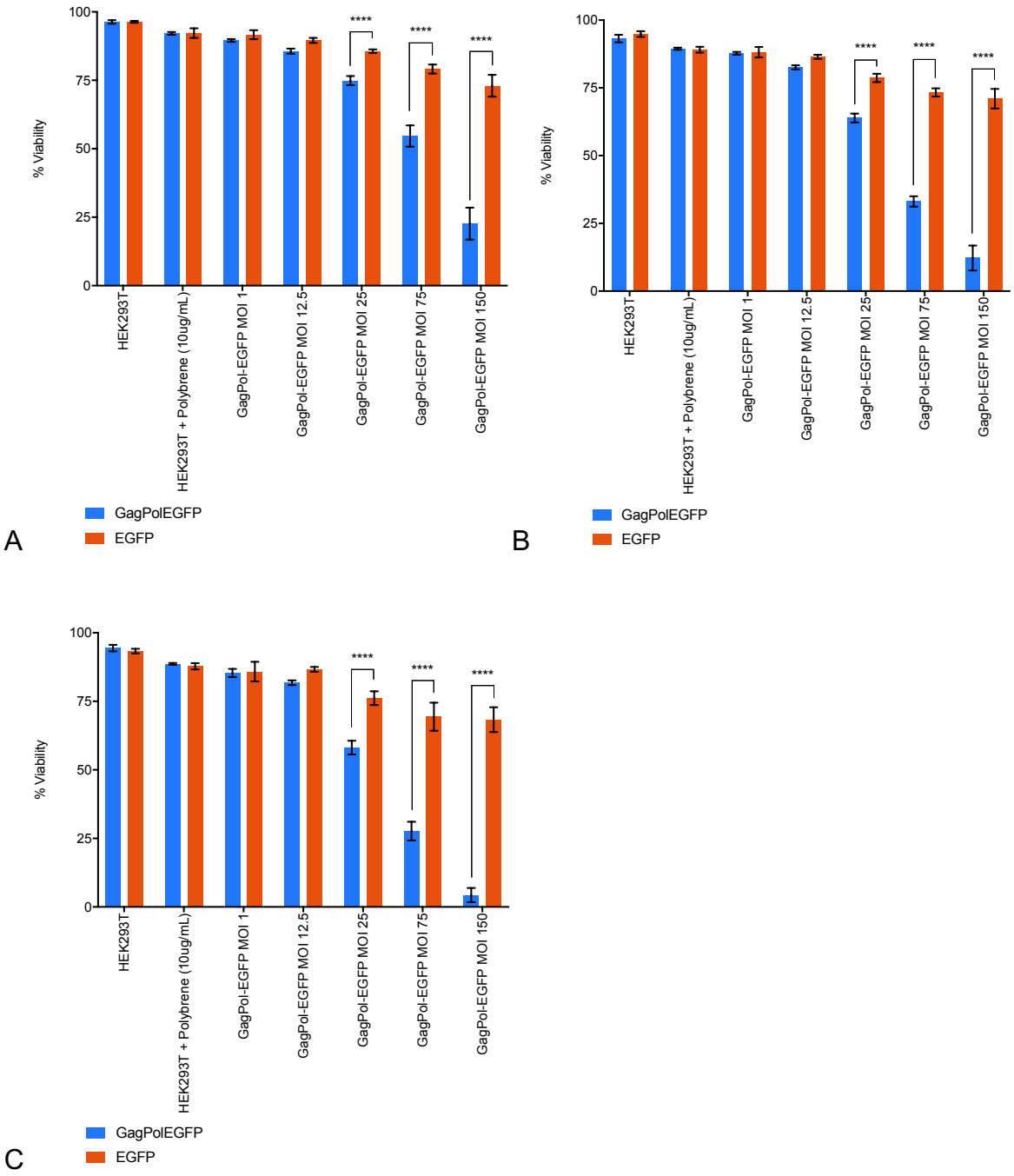

Figure 4.3 HEK293T cell viability following transduction with vector containing EGFP and GagPol-EGFP. HEK293T cells were transduced at a range of MOIs with vector encoding EGFP or GagPol-EGFP (Section 2.2.5). Cell viabilities were measured at several time points (Section 2.2.2.3). Values are mean +/- SEM of 3 biological repeats with 3 technical repeats each. Statistical analysis was carried out using one-way ANOVA. **** = $p<0.0001$.

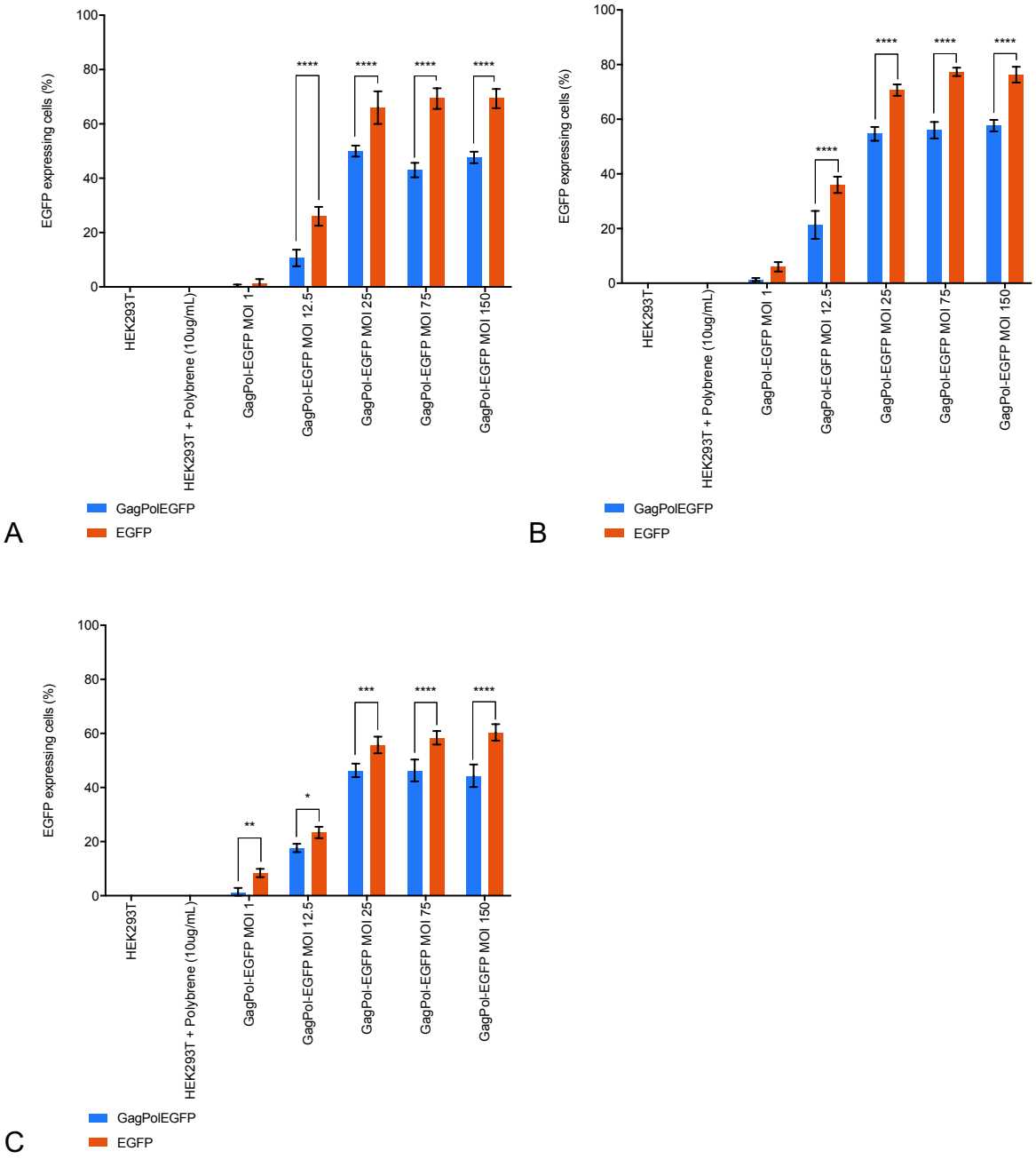

Figure 4.4 Determining GFP expression in HEK293T cells following transduction with vector containing EGFP and GagPol-EGFP. HEK293T cells were transduced at a range of MOIs with vector encoding EGFP or GagPol-EGFP (Section 2.2.5). The percentage of EGFP-expressing cells at several time points was determined by flow cytometry (2.2.6.2). Values are mean +/- SEM of 3 biological repeats with 3 technical repeats each. Statistical analysis was carried out using one-way ANOVA. *= p<0.05, **= p<0.01, ***= p<0.001, **** = p<0.0001.

4.3 Endoplasmic Reticulum Stress and the Unfolded Protein Response

Following observations of a decrease in HEK293T cell viability in response to GagPol-EGFP overexpression (Figure 4.1), various cellular stress assays were performed to investigate how HEK293T cells were becoming stressed and dying. Of particular interest was endoplasmic reticulum (ER) stress and the unfolded protein response (UPR). Upon accumulation of unfolded proteins in the ER, the UPR is triggered, resulting in several responses to reduce cellular stress. This includes an increase in the ER's protein-folding ability, reduced protein influx to the ER, and increased decomposition of unfolded proteins (Wang and Kaufman, 2016; Hollien et al., 2006). If a cell is unable to re-establish "normal" ER function, damaged cells will be eliminated by apoptosis or autophagy (Bernales et al., 2006; Kamimoto et al., 2006; Yorimitsu et al., 2006; Kouroku et al., 2007).

Recognising the activation of cellular pathways such as ER stress and the UPR in response to the production of viral proteins is key in terms of identifying targets for the optimisation of LVV production. For example, it is widely known that HIV-1 Env and VSV-G both utilise endomembrane systems for production and trafficking to the plasma membrane (Figure 1.3), specifically the Golgi apparatus and secretory vesicles (Blot et al., 2003; Groppelli et al., 2014; Sevier et al., 2017). As it is not yet understood how GagPol traffics to the plasma membrane, it is important to consider how its production might influence the UPR pathway and ER stress, as it may induce a wider response to stress in terms of macromolecular synthesis.

Upon viral infection, the cellular machinery used for translation is hijacked and used to produce high amounts of viral proteins, and as a result ER homeostasis is inevitably disturbed, leading to ER stress (Zhang and Wang et al., 2012). For gene therapy to be successful, it is vital that the transduced cell not only survives, but also achieves a sustained level of gene expression. As such, future work must be carried out to investigate precisely how LVV interact with UPR machinery.

4.3.1 XBP1 Splicing

As part of the UPR, GRP78 (also referred to as BIP), the primary sensor of ER stress, is released from IRE1, which activates various ER stress sensors. IRE1a oligomerises and *trans*-autophosphorylates, leading to the cleavage of a 26 base-pair intron from unspliced X-box binding protein 1 (XBP1) mRNA (Figure 4.5) (Yoshida et al., 2001). The transcription factor, XBP1, is a major regulator of ER stress and the UPR. A frame shift in the coding sequence of XBP1 occurs due to intron removal, which leads to the translation of 376 amino acids to produce a 40 kDa XBP1 isoform, rather than the unspliced XBP1 from translation of 261 amino acids to produce a 33 kDa isoform (Yoshida et al., 2001). The ratio of unspliced XBP1 to spliced XBP1 correlates with the level of proteins that are expressed to enable the ER to adapt to its environment (Hirota et al., 2006).

Monitoring the level of XBP1 mRNA splicing can be achieved by various methods including PCR and qRT-PCR. Primers were designed to enable individual detection of each splice variant (Figure 4.5). These primers were validated by use of HEK293T cells treated with Tunicamycin at 10 μg/mL. Tunicamycin is able to specifically trigger ER stress by blocking essential enzymes involved in the production of asparagine-linked carbohydrates, in addition to inhibiting protein glycosylation (Pahl, 1999; Wu et al., 2018). As such, Tunicamycin was found to act as a potent stimulator of XBP1 splicing for HEK283T cells in this investigation.

Unspliced and spliced XBP1 mRNA expression was assessed in HEK293T cells transduced with several MOIs of GagPol-EGFP vector (Figure 4.6) and EGFP vector (Figure 4.7). PCR products were analysed by agarose gel electrophoresis. There was a clear increase in spliced XBP1 mRNA levels in HEK293T cells treated with 10 μg/mL Tunicamycin at both 24 hours and 48 hours, shown by a strong band at the size expected for a transcript generated from the splicing reaction (120 base pairs; Figure 4.6). Strong bands were also seen at 24 hours with GagPol-EGFP MOI 25, 75, and 150 (Figure 4.7).

To quantify XBP1 mRNA splicing, qRT-PCR was performed with primers to detect unspliced XBP1 mRNA and spliced XBP1 mRNA. Initially, cell samples from 24

hours and 48 hours post-transduction were assessed (included in Figure 4.8). At 24 hours post-transduction, there was a slight increase in spliced XBP1 mRNA, however by 48 hours there was not much of a response. XBP1 splicing is a rapid process, and spliced XBP1 is degraded quite quickly, which might explain the lack of spliced XBP1 at 48 hours. To further interrogate XBP1 splicing, samples were taken at earlier time points post-transduction.

There was a clear stimulation of spliced XBP1 with GagPol production, detected by qRT-PCR (Figure 4.8 B). The positive control of Tunicamycin at 6 hours post-transduction gave a 6.2-fold increase in relative mRNA expression levels of spliced XBP1, a significantly higher increase than spliced XBP1 mRNA in basal HEK293T cells (Two-way ANOVA, Figure 4.8B, $p<0.0001$). At an MOI of 75 with GagPol-EGFP, samples taken 6 hours post-transduction had a 3.9-fold increase in relative mRNA expression of spliced XBP1 compared with basal HEK293T cells (Two-way ANOVA, Figure 4.8B, $p<0.0001$). Interestingly, the production of GagPol-EGFP at this level stimulated a similar response to that of a potent inducer of XBP1 splicing. However, it is not clear whether this 3.9-fold increase in spliced XBP1 expression during GagPol expression would be enough to have a biological action within the HEK293T cell, such as having an effect on protein synthesis and cell growth.

As spliced XBP1 mRNA increased, there was a general decrease in unspliced XBP1 mRNA (Figure 4.8). A particularly clear example of this was seen when HEK293T cells were transduced with an MOI of 75 and 150 at all time points between 3-24 hours post-transduction, where unspliced XBP1 mRNA was significantly lower than that of basal HEK293T cells (Two-way ANOVA, Figure 4.8A, $p<0.01$). This mirrors the effect seen when Tunicamycin is present in cell culture medium, with unspliced XBP1 mRNA decreasing significantly compared with basal HEK293T cells at all time points, with the largest decrease of 0.4-fold at 24 hours post-transduction (Two-way ANOVA, Figure 4.8A, $p<0.0001$).

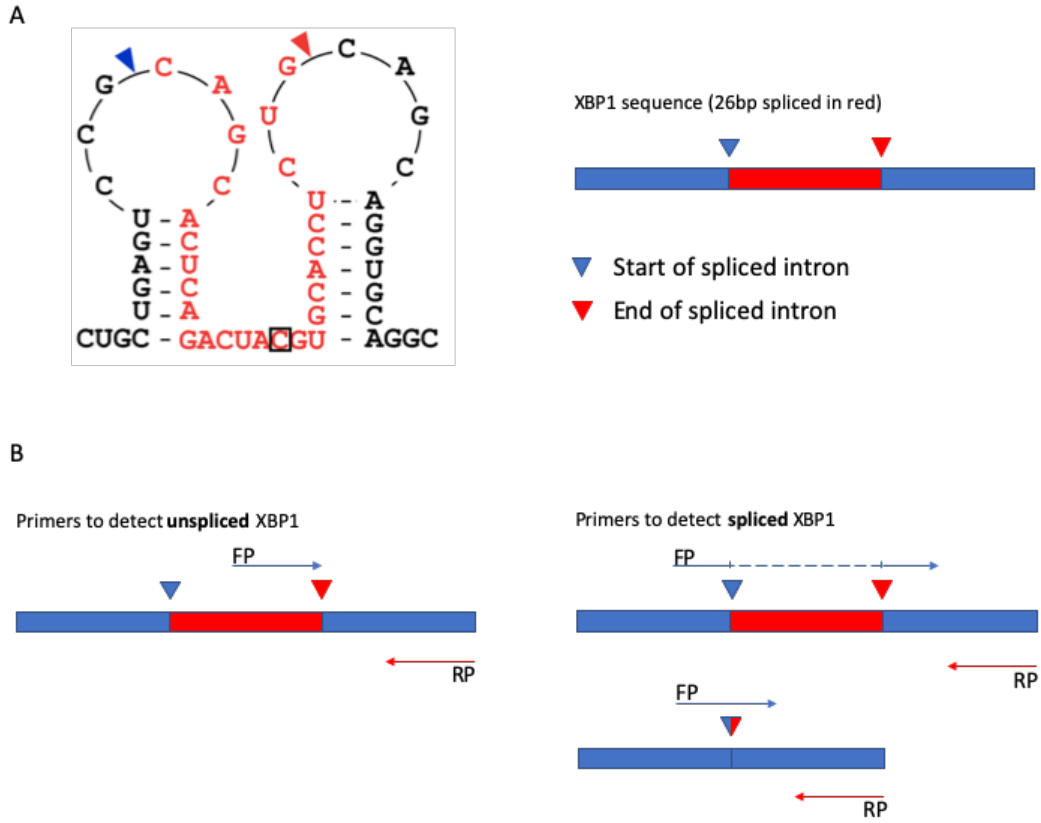

Figure 4.5 Rationale for detection of spliced and unspliced XBP1. (A) The 26bp XBP1 consensus sequence and structure in humans. The red text indicates the region of XBP1 that is spliced out. The blue arrow represents the start of the spliced region and the red arrow represents the end of the spliced region. The black box represents the different sequence in mice where C is U. This was adapted from Yoon et al. 2019. (B) Primer design to detect spliced and unspliced XBP1. To detect unspliced XBP1, the forward primer starts in the middle of the spliced sequence. To detect unspliced XBP1, the forward primer binds to bases at either side of the spliced sequence. Both primer pairs have the same reverse primer.

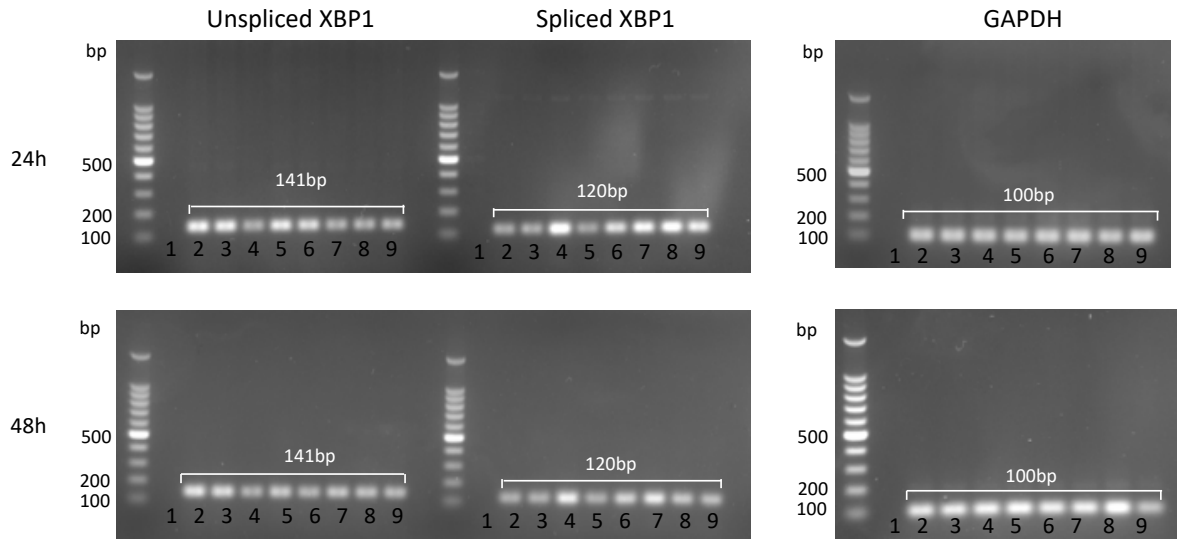

Figure 4.6 Assessment of spliced and unspliced XBP1 mRNA with GagPol-EGFP vector. HEK293T cells were transduced with GagPol-EGFP vector at a range of MOIs (Section 2.2.5). Cell samples were collected at 24 hours and 48 hours post-transduction (Section 2.2.2.5), RNA was extracted (Section 2.2.7.1) and cDNA was synthesised (Section 2.2.7.4). Spliced and unspliced mRNA expression was assessed by PCR (Section 2.2.1.1), and analysed by agarose gel electrophoresis (Section 2.2.1.2). DNA Ladder: 100bp DNA ladder. 1: No template control, 2: Untransduced HEK293T, 3: Empty transduction (Polybrene 10 µg/mL), 4: Positive control cells treated with Tunicamycin 10 µg/mL, 5: GagPol-EGFP MOI 1, 6: GagPol-EGFP MOI 12.5, 7: GagPol-EGFP MOI 25, 8: GagPol-EGFP MOI 75, 9: GagPol-EGFP MOI 150. Product sizes: Unspliced XBP1 141bp, Spliced XBP1 120bp, GAPDH 100bp.

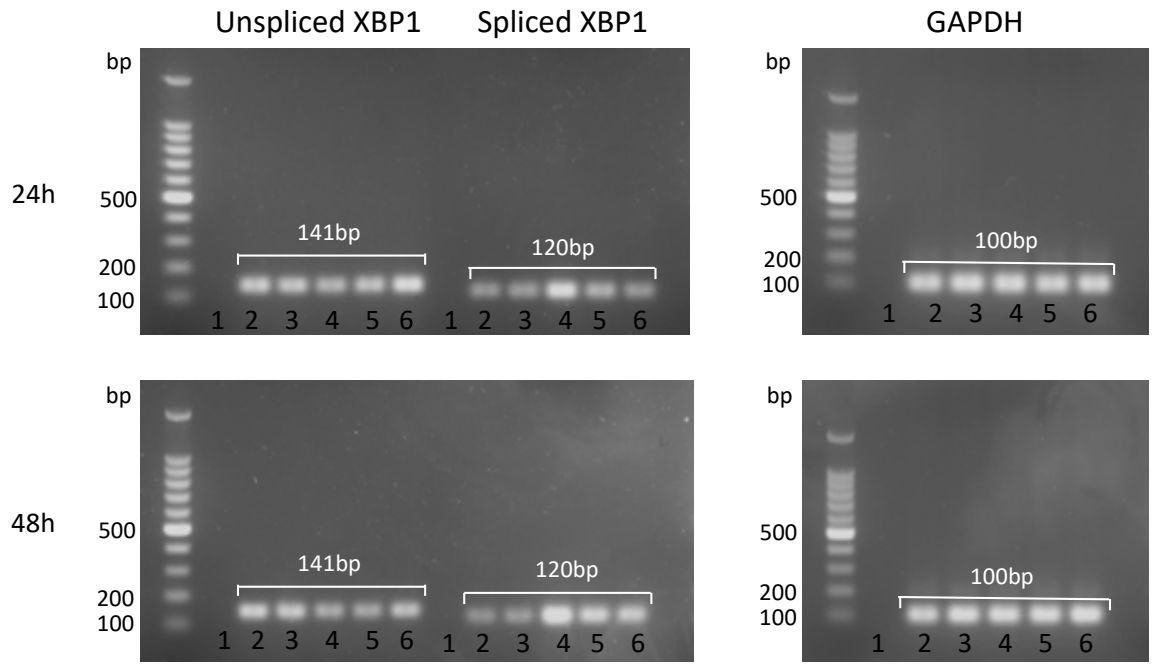

Figure 4.7 Comparison of spliced and unspliced XBP1 with EGFP and GagPol-EGFP vector. HEK293T cells were transduced with either EGFP or GagPol-EGFP vector at MOI 25 (Section 2.2.5). Cell samples were collected at 24 hours and 48 hours post-transduction (Section 2.2.2.5), RNA was extracted (Section 2.2.7.1) and cDNA was synthesised (Section 2.2.7.4). Spliced and unspliced mRNA expression was assessed by PCR (Section 2.2.1.1), and analysed by agarose gel electrophoresis (Section 2.2.1.2). DNA Ladder: 100bp DNA ladder. 1: No template control, 2: Untransduced HEK293T, 3: Empty transduction Polybrene 10 µg/mL), 4: Positive control cells treated with Tunicamycin 10 µg/mL, 5: GagPol-EGFP MOI 25, 6: EGFP MOI 25. Product sizes: Unspliced XBP1 141bp, Spliced XBP1 120bp, GAPDH 100bp.

A

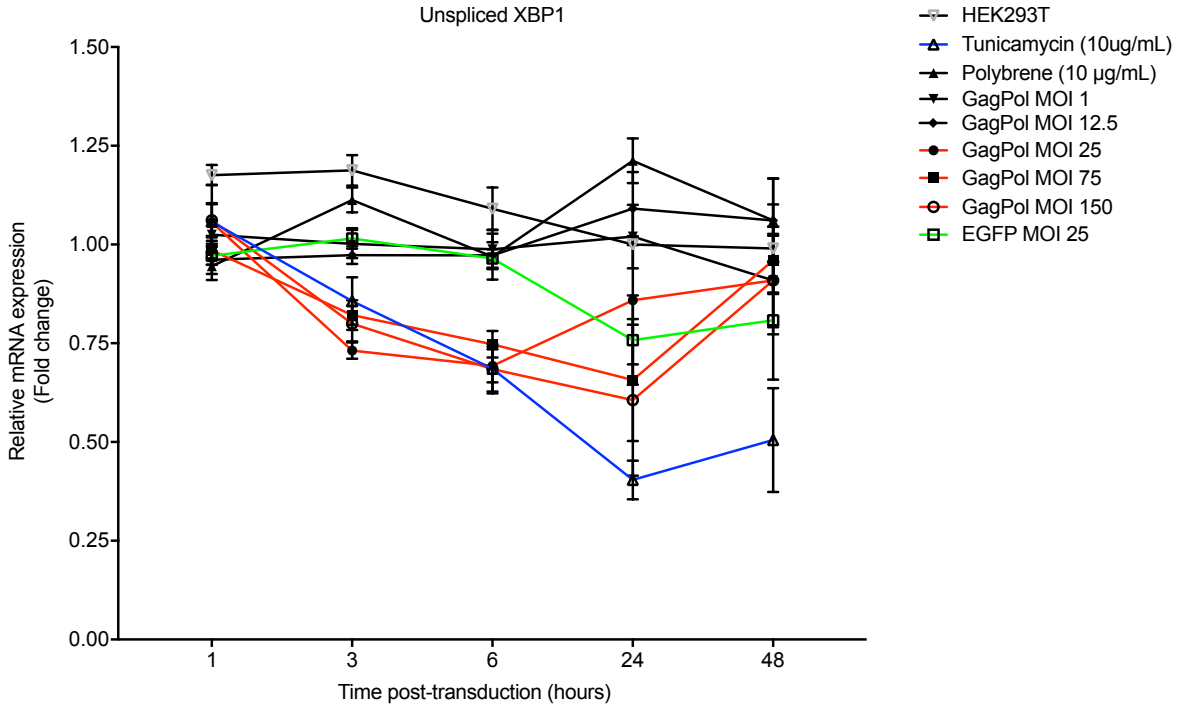

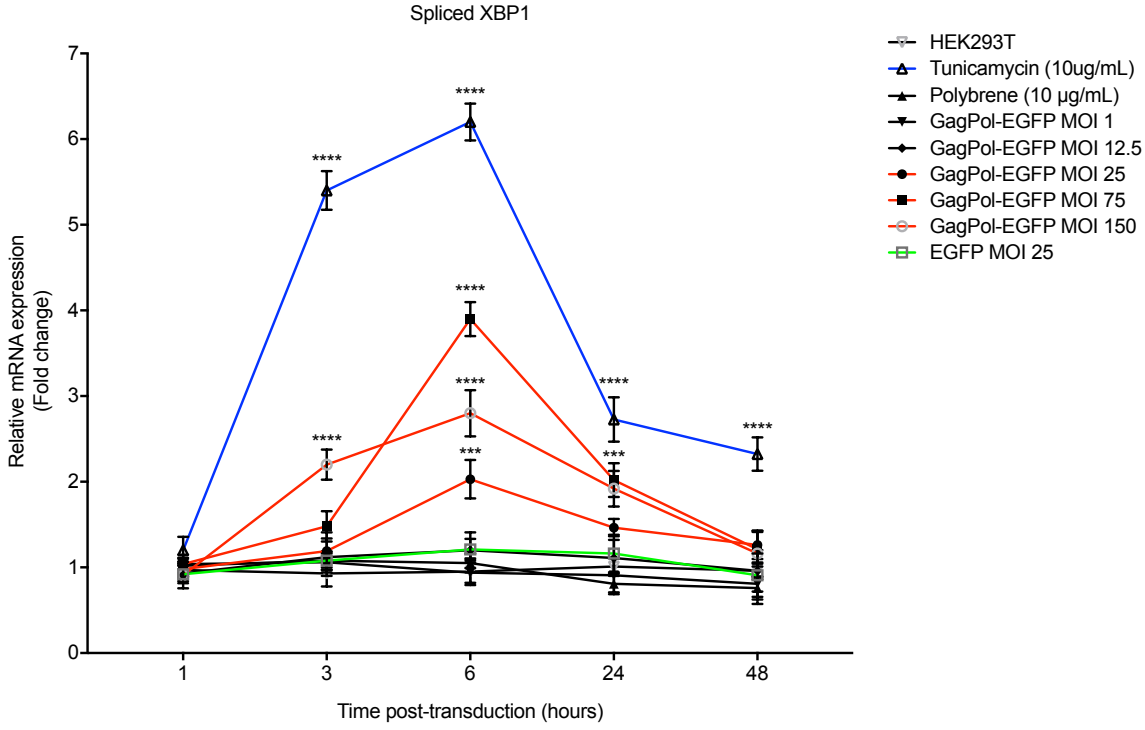

B

Figure 4.8 Quantification of spliced and unspliced XBP1 mRNA by qRT-PCR. HEK293T cells were transduced with EGFP or GagPol-EGFP vector at several MOIs (Section 2.2.5). Cell samples were collected at several time points post-transduction (Section 2.2.2.5), RNA was extracted (Section 2.2.7.1) and cDNA was synthesised

(Section 2.2.7.4). Spliced and unspliced mRNA expression was quantified by qRT-PCR (Section 2.2.7.5). (A) Unspliced XBP1 mRNA expression. (B) Spliced XBP1 mRNA expression. qRT-PCR data was analysed by the Delta Delta Ct method to calculate the relative fold gene expression of samples using GAPDH as the internal control housekeeping gene and Untransduced HEK293T cells at 24 hours as the calibrator (Described in Livak and Schmittgen, 2001). Values are mean +/- SEM of 3 biological repeats with 2 technical repeats each. Statistical analysis was carried out using Two-way ANOVA comparing samples to HEK293T control. *=$p<0.05$, **=$p<0.01$, ***=$p<0.001$, ****=$p<0.0001$.

4.3.2 ATF6, BIP, CHOP

As discussed in Section 4.3.1, a major bottleneck in recombinant protein production is the activation of the UPR and ER stress. Cell line engineering strategies have previously been developed to improve the capacity of recombinant protein production, focusing particularly on ER stress (Yu et al., 2008). It is not known how GagPol production influences HEK293T cells in terms of ER stress and UPR activation. To explore this further, targets including Activating Transcription Factor 6 (ATF6), Binding immunoglobulin protein (BIP), and CCAAT-enhancer-binding protein (C/EBP) homologous protein (CHOP) were analysed. These have key involvement in signalling cascades implicated in ER stress resulting in activation of the UPR (with linkage to XBP-1) and key facts about each are summarised below (Figure 4.9).

ATF6 is a mammalian UPR sensor and an ER stress-regulated transcription factor. It is embedded in the ER as a transmembrane protein and activates genes associated with the UPR during periods of ER stress. When protein synthesis becomes a burden, ATF6 slows the pace of protein translation. Homeostatic readjustment within mammalian cells during periods of ER stress relies heavily on ATF6 proteins (Yamamoto et al., 2006, Wu et al., 2007).

BIP is a major ER chaperone that acts as a primary sensor for UPR activation (Bertolotti et al., 2000). UPR activation is dampened by the overexpression of BIP, and the activation of various other ER stress transducers, including ATF6 and XBP1, are regulated by BIP.

CHOP is a key target when looking at ER stress and UPR activation. CHOP is expressed at low levels in the cytosol in healthy cells, however is robustly expressed upon cellular stress and accumulates in the nucleus (Nishitoh et al., 2012). CHOP is induced by several stimuli such as ER stress, oxidative stress, and nutrient starvation. The activation of CHOP has also been demonstrated to result in apoptosis.

ATF6, BIP, and CHOP were analysed by qRT-PCR to determine how the overexpression of GagPol influenced the expression of these targets. There was a

clear stimulation of ATF6 following transductions greater than MOI 25, with a higher response at samples taken at 24 hours post-transduction compared with 48 hours post-transduction (Figure 4.10 A). There was also a high response in the relative expression of BIP mRNA at MOI 12.5 and MOI 25 at 24 hours, and a high response at MOIs 25, 75, and 150 at 48 hours, where titres of over approximately 4000 nU RT/mL and over 1250 ng p24/mL were achieved (Figure 4.10 B). At least a 6-fold increase in the relative expression of CHOP mRNA was seen at 24 hours with MOIs 25, 75 and 150 (Figure 4.10 C). CHOP expression levels remained persistently high at 48 hours, with a greater than 8-fold increase in its expression relative to basal HEK293T cells. This cut-off seen in p24 productivity after an MOI of approximately 25 could reflect some sort of cellular switch whereby activation of this cellular stress response is preventing further production of p24 in a HEK293T cell.

These targets have various interactions with each other. For example, transcription of CHOP can be induced by ATF6 (Yang et al., 2020). CHOP, also often referred to as DNA-inducible transcript 3 (DDIT3), can also be induced by DNA damage (Yang et al., 2017). The high response seen during GagPol over-expression, but not with empty transduction or transduction with EGFP at MOI 25, may potentially indicate that GagPol production is causing DNA damage. It is fair to assume that the transduction process itself is not damaging to HEK293T cells, as observations from empty transductions just with polybrene in cell culture medium did not lead to a significant increase in the mRNA expression of ATF6, BIP, or CHOP (Figure 4.10). Additionally, transductions with EGFP vector at an MOI of did not cause a significant increase in mRNA expression of ATF6, BIP, or CHOP, which indicates that the introduction of foreign DNA into HEK293T cells does not cause stimulation of genes relating to ER stress and activation of the UPR.

The targets discussed in Section 4.3 generally tend to be activated to slow down translation and slow cell growth, in an attempt to ‘heal’ the cell during periods of high protein burden. GagPol may place protein assembly machinery under pressure which in turn could hinder the production of other cellular proteins, causing HEK293T cells to decrease in fitness. It is clear from data shown in this section that GagPol over-expression does disrupt key targets involved in UPR, which in turn may cause ER stress and associated cellular consequences such as apoptosis and autophagy.

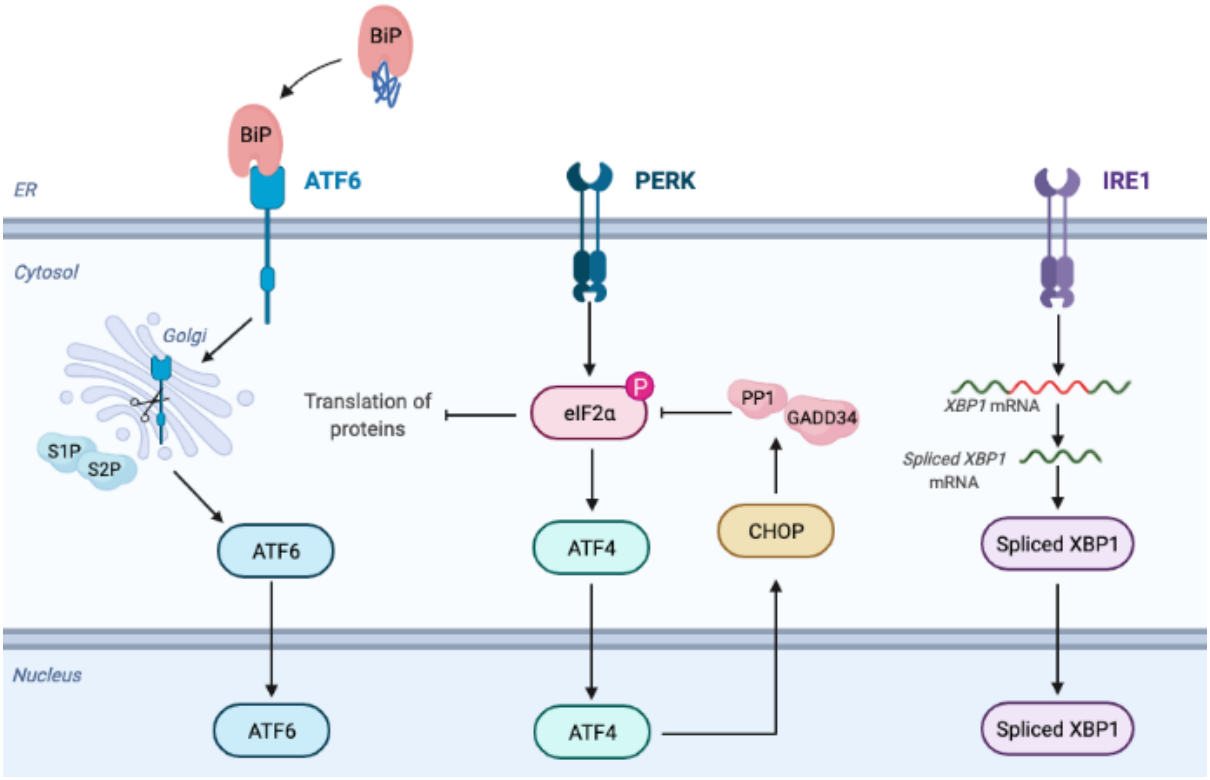

Figure 4.9 Signalling cascades involved in ER Stress and the UPR. BiP preferentially binds to ATF6, PERK, and IRE1 upon disturbance of homeostatic conditions due to accumulation of unfolded proteins. Three branches of the UPR are then activated. (1) ATF6 is cleaved by S1P and S2P proteases following translocation to the Golgi. The transcription factor ATF6(f) is then generated which modules the expression of enzymes and chaperones required for normal ER function (Yamamoto et al, 2006, Wu et al., 2007). (2) Autophosphorylation of PERK results in the phosphorylation of eIF2α, which becomes inactivated. This decreases the ER load by inhibiting protein translation, and also upregulates ATF4. ATF4 induces CHOP, which upregulates GADD34. GADD34 activates PP1 which dephosphorylates eIF2α, which allows protein synthesis to recommence as part of a negative feedback loop (Iwasaki et al., 2015). (3) IRE1 is autophosphorylated and activated, which splices the transcription factor XBP1. Genes for protein folding, maturation, and degradation of misfolded proteins are then transcribed (Yoshida et al., 2001). Created in BioRender.

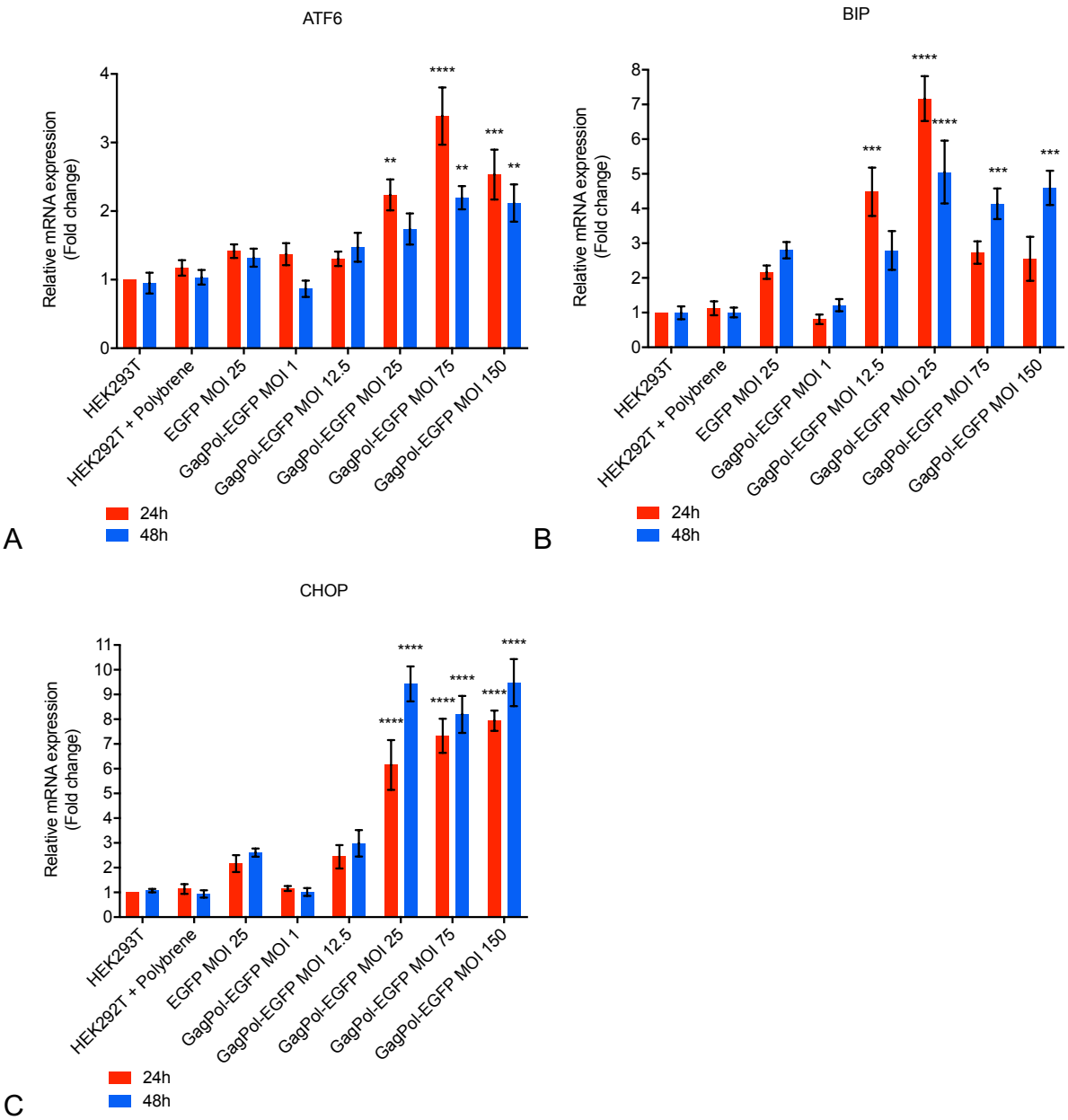

Figure 4.10 Quantification of ATF6, BIP, and CHOP expression by qRT-PCR. HEK293T cells were transduced with EGFP or GagPol-EGFP vector at several MOIs (Section 2.2.5). Cell samples were collected at several time points post-transduction (Section 2.2.2.5), RNA was extracted (Section 2.2.7.1) and cDNA was synthesised (Section 2.2.7.4). (A) ATF6, (B) BIP, and (C) CHOP expression was quantified by qRT-PCR (Section 2.2.7.5). qRT-PCR data was analysed by the Delta Delta Ct method to calculate the relative fold gene expression of samples using GAPDH as the internal control housekeeping gene and Untransduced HEK293T cells at 24 hours as the calibrator (described in Livak and Schmittgen, 2001). Values are mean +/- SEM of 3 biological repeats with 3 technical repeats each. Statistical analysis

was carried out using one-way ANOVA comparing samples to HEK293T control. *= $p<0.05$, **= $p<0.01$, ***=$p<0.001$, **** = $p<0.0001$

4.4 Apoptosis

Apoptosis is a distinctive method of programmed cell death, as discussed in Section 1.4.3, and illustrated in greater detail in Figure 5.3. Following observations of a decrease in HEK293T cell viability (Figure 4.1), an apoptosis assay was performed to determine the contribution to the loss of cell viability. This assay involved staining cells with Annexin V and PI. The rationale behind this assay is summarised in Figure 4.10.

Following transduction of HEK293T cells with GagPol-EGFP vector, there was an increase in the percentage of cells positive for Annexin V, a marker of apoptosis (Figure 4.11). Annexin V has a high affinity for both early and late apoptotic cells. Transducing cells with high MOIs of GagPol-EGFP had a similar affect to a potent stimulator of apoptosis, Actinomycin D. The transduction process itself using polybrene, a cationic polymer that enhances LV transduction, seems to slightly induce apoptosis (Chuck et al., 1996).

The increase in cell death may potentially lead to a decrease in protein production but could also have an effect on the quality of the protein produced. Considering work described in Section 4.3, examining ER stress and the UPR, it is interesting to note that stress on the ER is able to initiate signals that trigger apoptosis (Saura-Esteller). This could offer a potential reason for the high percentage of apoptotic cells observed at high MOIs. The apoptosis pathway will be looked at in greater detail in Chapter 5.2 to determine whether the observed consequences of GagPol production on apoptosis can be mitigated through use of chemical inhibitors.

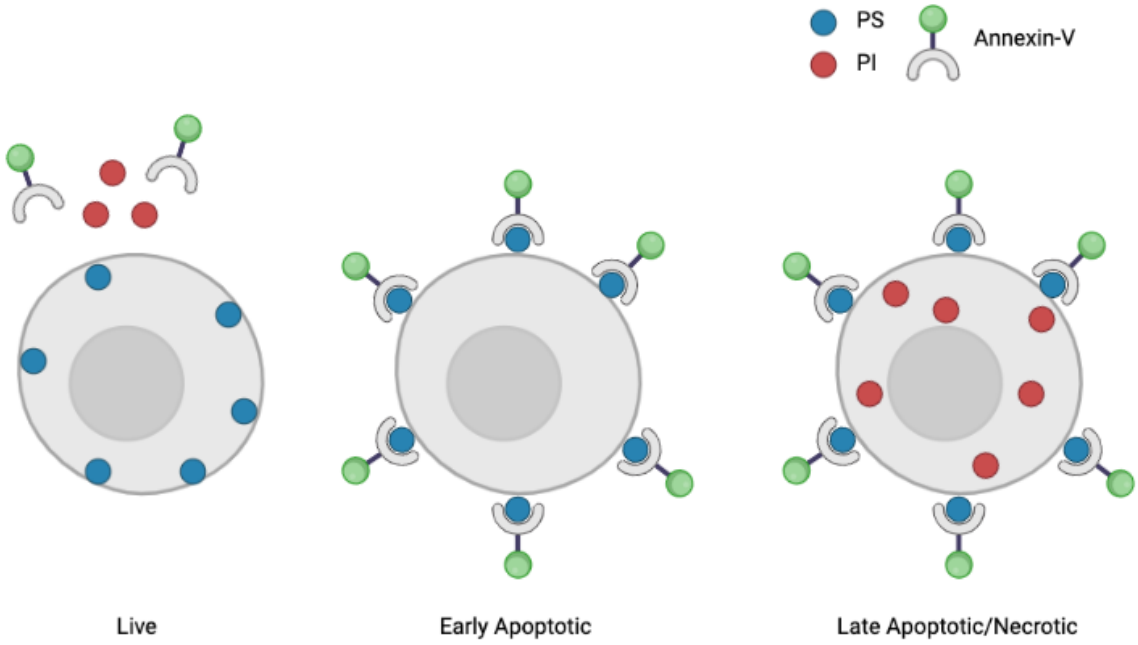

Figure 4.11 Rationale for apoptosis detection by flow cytometry using Annexin V and Propidium Iodide (PI). The membrane-associated phospholipid Phosphatidylserine (PS) translocates to the outer leaflet of the plasma membrane in apoptotic cells. Annexin-V has a high affinity for and binds to PS when on the outer leaflet of the plasma membrane. When conjugated with a fluorophore, such as FITC, binding can be quantified by flow cytometry. Early apoptotic cells exclude PI, whereas cells in the later stages of apoptosis/necrosis will take up PI as cell membranes being compromised. Created in BioRender.

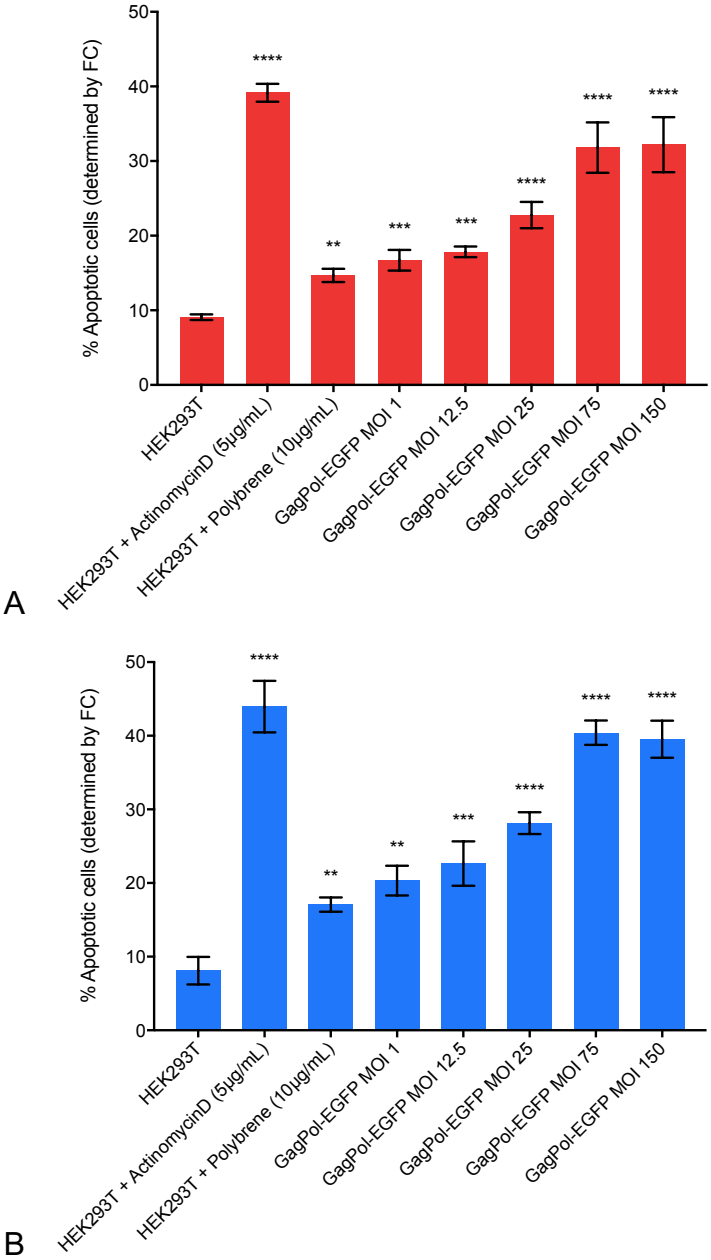

Figure 4.12 Apoptosis detection by flow cytometry in HEK293T cells transduced with GagPol-EGFP. HEK293T cells were transduced with GagPol-EGFP vector at several MOIs (Section 2.2.5). Cell samples were collected at (A) 24 hours and (B) 48 hours post-transduction (Section 2.2.2.3). Cells were stained with Annexin V and PI and were analysed by flow cytometry (Section 2.2.6.3). Values are mean +/- SEM of 3 biological repeats with 3 technical repeats each. Statistical analysis was carried out using one-way ANOVA comparing samples to HEK293T control. *= $p<0.05$, **= $p<0.01$, ***=$p<0.001$, **** = $p<0.0001$

4.5 Autophagy

Autophagy is a highly conserved self-degradative survival mechanism involving delivery of cargo to the lysosome for degradation and recycling (Figure 4.12). It is a key housekeeping process responsible for balancing energy sources during development and is a critical response to nutrient stress (Glick et al., 2010).

There were several reasons for investigating autophagy during GagPol production. Autophagy has been shown to act in both a pro-viral and anti-viral manner (Choi et al., 2018). LVVs were initially developed based on an understanding of HIV-1, which has been shown to utilise autophagic membranes as a platform for HIV-1 assembly and packaging (Kyei et al., 2009). Gag-derived proteins have been shown to co-localise with LC3 on autophagosomal membranes (Kyei et al., 2009). In addition to this, HIV-1 has been shown to hijack the earlier stages of autophagy leading to improved viral yields, in addition to inhibiting the later stages of autophagy as a means to prevent its own degradation (Kyei et al., 2009).

It is not known whether SYNGP, the synthetic HIV-1-based GagPol sequence used in LVV production, behaves in the same manner as wild-type HIV-1. Aside from the interactions with HIV-1, autophagy itself is a key response to cellular stress. Given the decrease in HEK293T cell viability with GagPol overexpression (Section 4.2), it was important to consider what impact this had on autophagy. The autophagy pathway will also be looked at in greater deal in Chapter 5.3 with a particular focus on how chemical inhibitors of autophagy influence GagPol production, in order to determine whether autophagy has a beneficial or detrimental role during the production of this viral protein.

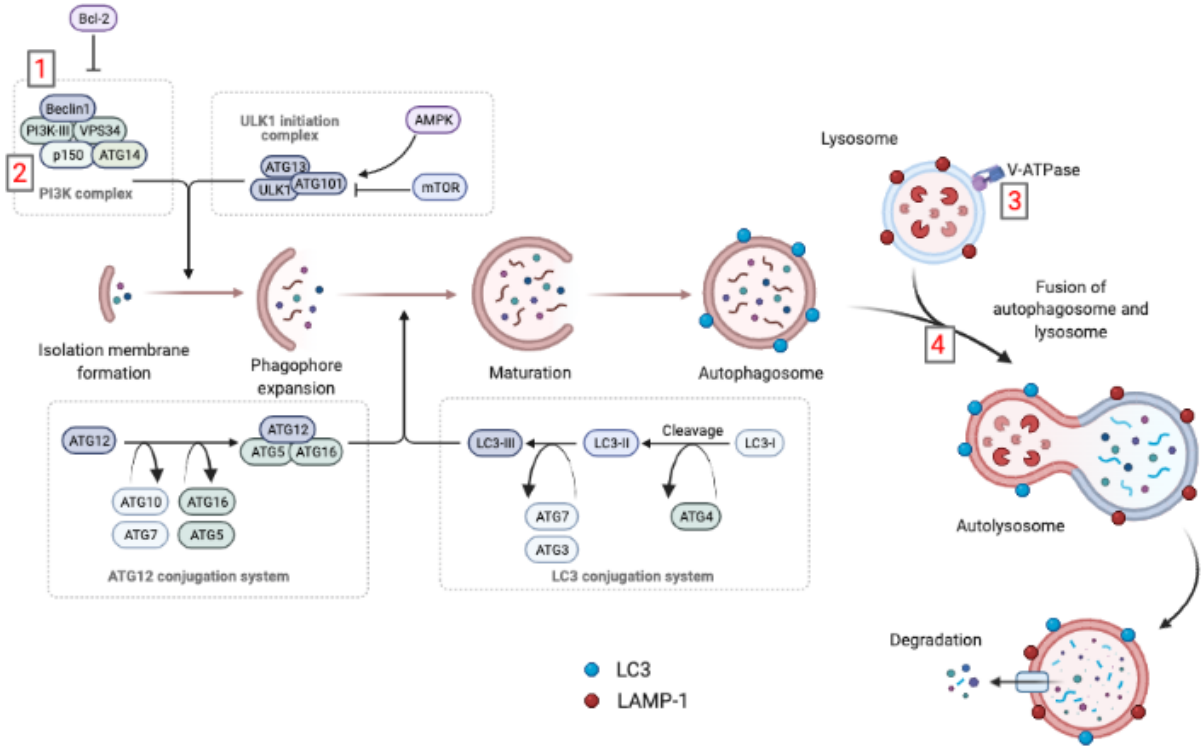

Figure 4.13 Macro-autophagy pathway and targets for inhibition of autophagy. Upon initiation of autophagy, material within the cytoplasm is engulfed by the phagophore, a double-membraned structure. The phagophore then elongates and seals around cytosolic cargo, forming an autophagosome. The autophagosome then fuses with a lysosome, where the contents are then degraded and recycled due to the highly acidic interior of the lysosome. This process involves multiple steps which are regulated by several proteins, however the mammalian target of rapamycin (mTOR) and AMP-activated kinase (AMPK) are the key autophagy regulators. Autophagy-related proteins assemble into various complexes to initiate autophagy. The Unc-51-like kinase 1 (ULK1) and the Phosphatidylinositol-3-phosphate (PI3P)-binding complex both direct autophagosome formation. ATG5, ATG12, and ATG16 form the ATG12 conjugation system which promotes LC3 conjugation. LC3-I is formed through cleavage of LC3 by ATG4. Phosphatidylethanolamine (PE) is conjugated to LC3-I to form LC3-III. LC3-III is then incorporated into autophagosomal membranes. Autophagy can be inhibited through use of various chemicals. (1) Spautin-1 inhibits autophagy initiation by enhancing Beclin-1 degradation. (2) Wortmannin inhibits the Class III PI3K pathways and subsequently blocks the formation of autophagosomes. (3) Bafilomycin A1 inhibits V-ATPase activity resulting in lysosomes and autophagosomes not being able to fuse. (4) Chloroquine increases

the pH within the lysosomes and hence blocks autophagosomes and lysosomes from binding (Parzych and Klionsk 2014). Created in BioRender.

Multispectral imaging flow cytometry was used to investigate autophagy in HEK293T cells. This technology was chosen due to its quantitative power, multiplexing potential, high-throughput capacity, as well as providing morphological details by capturing images of every cell.

During autophagy, LC3 in the cytoplasm is recruited to autophagosomal membranes (Figure 4.13). HEK293T cells undergoing autophagy were identified by quantifying fluorescently-labelled GFP-positive LC3 puncta, which represent either autophagosomes or autolysosomes (Figure 4.14). The 'Spot Count' feature in IDEAS® enables creation of a mask that recognises bright regions within an image, and the software then creates an algorithm to calculate LC3 spots. HEK293T cells transduced with GagPol-EGFP vector at an MOI of 25 were found to have a mean LC3 spot count of 2.3. Similarly, cells transduced with EGFP vector at an MOI of 25 also had a mean LC3 spot count of 2.3, meaning this response may be due to transfection rather than a response to GagPol specifically. These values are significantly higher than basal HEK293T cells which had a mean spot count of 1.3, suggesting that the expression of GagPol triggers autophagy. However, these values are lower than the mean LC3 spot count in HEK293T cells that have undergone nutrient starvation (spot count: 3.4), a potent stimulator of autophagy.

In addition to autophagosome formation, an increase in lysosomal content is a typical feature of autophagy. The Bright Detail Similarity R3 (BDS) feature in IDEAS® is able to examine the co-localisation of autophagosomes and lysosomes using LC3 and LAMP-1, a marker present on lysosomal membranes. This represents LC3 delivery to the lysosome. As discussed in Section 2.2.6.8, BDS is able to calculate the correlation of two markers that have overlapping bright spots of 3 pixels or less in radius. The BDS score between LC3 and LAMP-1 was slightly higher 24 hours-post transduction with HEK293T cells transduced with GagPol-EGFP at MOI 25. BDS was not found to be different to basal HEK293T cells 48 hours post-transduction (Figure 4.15). Interestingly, transducing HEK293T cells with EGFP at an MOI of 25 did not lead to an increase in BDS, indicating that production of EGFP is not as stressful to cells as GagPol. It is important to note that BDS does not consider the number of autophagosomes in a cell, so taken together with spot count this data gives a more representative picture of autophagy.

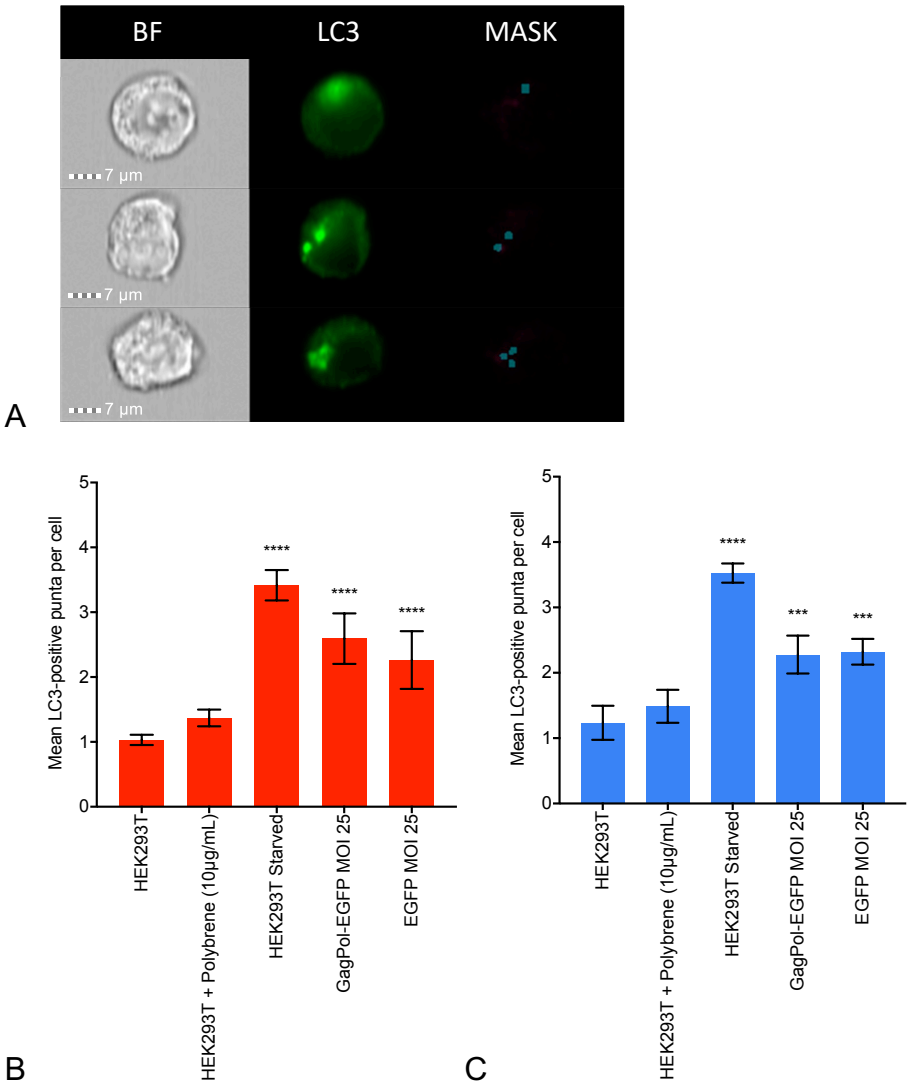

Figure 4.14 LC3-AF647 labelled HEK293T cells analysed using Spot Count feature. HEK293T cells were transduced with vector encoding EGFP or GagPol-EGFP at MOI 25 (Section 2.2.5). Cells were collected and labelled with LC3-AF647 and LAMP-1-PE (Section 2.2.6.2.1). Samples were acquired on the ImageStreamX® (Section 2.2.6.2.2). Samples were analysed to determine mean LC3-AF647 spot count per cell (Section 2.2.6.2.3). (A) Example of acquired images. BF: Bright Field image, LC3: LC3-AF647 detection (Channel 11) using 60X magnification. Mask: LC3-AF647 spot mask. Mean LC3-AF647 spot count of HEK293T cells collected at (A) 24 hours and (B) 48 hours. Values are mean +/- SEM of 3 biological repeats with 3 technical repeats each. Statistical analysis was carried out using one-way ANOVA comparing samples to HEK293T control. ***= $p<0.001$, **** = $p<0.0001$

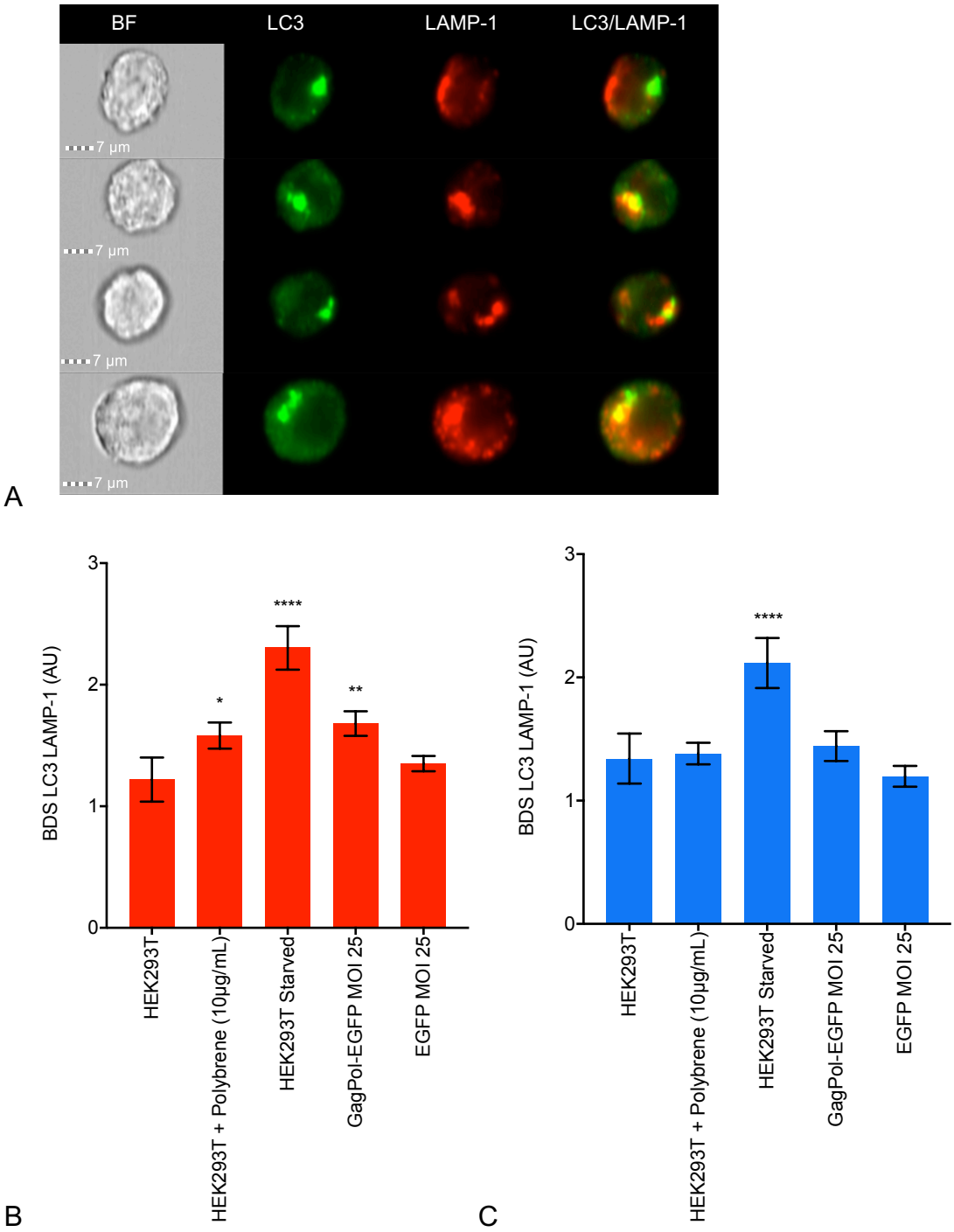

Figure 4.15 Bright Detail Similarity Score between LC3-AF647 and LAMP-1-PE in HEK293T cells. HEK293T cells were transduced with vector encoding EGFP or GagPol-EGFP at MOI 25 (Section 2.2.5). Cells were collected and labelled with LC3-AF647 and LAMP-1-PE (Section 2.2.6.2.1). Samples were acquired on the ImageStreamX® (Section 2.2.6.2.2). Samples were analysed in the IDEAS software to determine the Bright Detail Similarity (BDS) Score between two probes, LC3-AF647 and LAMP-1-PE (Section 2.2.6.2.3). (A) Example of acquired images of

Bright Field (BF, CH-1), LC3-AF647 (CH-11), LAMP-1-PE (CH-3), and a composite of LC3-AF647 and LAMP-1-PE images using 60X magnification. BDS of HEK293T cells collected at (A) 24 hours and (B) 48 hours. Values are mean +/- SEM of 3 biological repeats with 3 technical repeats each. Statistical analysis was carried out using one-way ANOVA. *=$p<0.05$, **= $p<0.01$, **** = $p<0.0001$.

4.6 Concluding remarks

This Chapter demonstrated that the over-expression of GagPol is toxic to HEK293T cells, with a decrease in cell viability seen in response to high p24 production. It was also observed that this decrease in viability was much greater upon GagPol over-expression compared with the over expression of EGFP, suggesting that specific properties of GagPol are toxic to HEK293T cells.

A marked stimulation of markers associated with ER stress and the UPR pathway were observed during high level GagPol production, specifically at the point where no further GagPol was being produced. Of particular note was the increase in spliced XBP1 in comparison to unspliced XBP1, where GagPol had a very similar affect to the potent stimulator of XBP1 splicing, Tunicamycin. Data shown in this Chapter also highlighted that the over-expression of GagPol does disrupt the activity of components of the UPR and in turn may cause further effects detrimental to cell growth, survival and synthetic functions.

This Chapter also highlighted the role of apoptosis in cell death during GagPol production, in addition to an increase in autophagy which tends to be induced during period of cell stress, which further supports the idea that GagPol production places a stress burden on HEK293T cells. The inhibition of these cellular stress pathways has the ability to enhance mAb production in CHO cells, and as such it could be considered that inhibiting these types of cellular stresses may potentially alleviate the burden of viral protein production on HEK293T cells, as discussed in detail in Section 1.4.3.

It must be noted that the effect that GagPol production has on HEK293T cellular physiology cannot be applied to a complete LVV production system (transfection with transfer and envelope plasmids). The combined expression of these vector components may potentially be further detrimental to the HEK293T cell and must be investigated further. Given that VSV-G is initially synthesised in the ER, transported to the Golgi, then transported to the plasma membrane, having additional vector components present during transduction may cause further stress on these parts of

the cell (Korant et al., 1998; Nie et al., 2002; Rumlova et al., 2014). It is widely accepted that VSV-G is harmful to cells, with its expression having cytotoxic and cytostatic effects. However, it is not known at which exact point of production VSV-G (or any other envelope protein) is harmful to a cell. This must be further elucidated, potentially by mimicking the studies undertaken in Chapter 5 by transducing HEK293T cells with high MOI's of a VSV-G expression cassette. Having observed the activation of various types of cellular stress during the production of GagPol, Chapter 5 aimed to determine whether certain types of cellular stress can be inhibited through use of various chemicals, with the aim of both increasing GagPol production and preventing cell death.

5 Consequence of inhibitors on GagPol production and HEK293T cell survival

5.1 Effect of a Protease inhibitor on cell viability and GagPol expression

As discussed in Chapter 1, components of LVVs can be cytotoxic to HEK293T cells. Of particular interest is the Protease (PR) domain within GagPol. Typically, PR is responsible for the proteolytic cleavage of *gag* and *GagPol* polyprotein precursors, leading to the generation of mature proteins that make up a virion (Blanco et al., 2003). Initially, PR is synthesised in an inactive form within *GagPol*, and only becomes active towards the later stages of the virus life cycle. Activation of PR leads to generation of the mature enzymes RT and IN, as well as structural proteins MA, CA, NC, and p6, all of which are required for maturation of the virion (Figure 1.7). Interestingly, there is evidence that the PR precursor and mature active PR have different enzymatic abilities in terms of their catalytic properties. All GagPol cleavage sites can be recognised and processed by mature PR, however precursor PR is limited in the number of sites it can cleave (Pettit et al., 2005; Ludwig et al., 2008).

Aside from cleaving viral protein precursors, HIV-1 PR has also been reported to cleave cellular proteins within the host (Riviere et al., 1991; Shoeman et al., 2001; Blanco et al., 2003). This represents part of the strategy by which HIV-1 appears to counter defence mechanisms within the host cell. Due to its ability to cleave host cell proteins when expressed in mammalian cells, HIV-1 PR has various cytotoxic effects. For example, one of the reported HIV-1 PR host cell substrates is Bcl-2, an anti-apoptotic protein, whose cleavage may induce apoptosis (Baum et al., 1990, Strack et al., 1996). This could also reflect why an increase in apoptosis was observed following GagPol production in Section 4.4 (Figure 4.12). Strack et al., demonstrated that prior to apoptosis, levels of Bcl-2 were unusually high and intact Bcl-2 could not be detected in cells that expressed HIV-1 PR. Additional investigations here shows that when Bcl-2 was ectopically expressed, this offered some protection from apoptosis, which suggested that the depletion of Bcl-2 is necessary for PR-induced apoptosis to occur. It is thought that Bcl-2 loses its protective function due to cleavage occurring between residues 112 and 113 (Korant et al., 1998; Elmore et al., 2007; Vlahakis et al., 2006).

Cytoskeletal proteins including actin, desmin, myosin, and vimentin can also be cleaved by HIV-1 PR, which has been linked to apoptotic or necrotic cell death (Shoeman et al., 1990, Adams et al., 1992). An investigation by Honer et al. showed that upon injection of HIV-PR into human fibroblast cells, stress fibres were disrupted, cytoplasmic vimentin intermediate filaments collapsed, and chromatin organisation and nuclear morphology was disrupted (Honer et al., 1999). However, the mechanisms by which this occurs are still presently unclear. Additionally, active HIV-1 PR has been demonstrated to stimulate the mitochondrial apoptotic pathway in HEK293T cells and induce cell death, however the precise mechanism of this is still not known (Rumlova et al., 2014).

To determine whether PR in the SYNGP cassette within GagPol contributed towards the decrease in viability seen in response to expression (Section 4.2, Figure 4.1), transductions with GagPol were performed in the presence and absence of the potent PR inhibitor, Saquinavir (Section 2.2.2.7). Clinically, Saquinavir is used as an antiviral agent in the treatment of HIV-1 infection. Saquinavir (which has a hydroxethylene scaffold that mimics the peptide cleavage site for the PR but which cannot be cleaved) acts as a competitive inhibitor of the active site within HIV-1 PR. By this prevention of viral polyprotein cleavage, Saquinavir has been found to be capable of completely inhibiting the processing of $Pr55^{gag}$ and $Pr160^{gag/pol}$ (Sparacio et al., 2001, Bosch et al., 2001).

Transductions in the presence of Saquinavir led to significantly higher cell viabilities during GagPol-EGFP expression above an MOI of 25, at 24-48 hours (Figure 5.1), where titres of approximately 4000 nU RT/mL and 1250 ng p24/mL were achieved (Figures 3.13 and 3.14). Again, this represents a distinct cut-off at approximately MOI 25, which is reflected in other investigations throughout this thesis. As GagPol-EGFP is over-expressed, there is an increase in the amount of Pol in the cell (measured by PERT assay, Figure 3.13). As viral PR is a domain within Pol, it can be assumed that the amount of PR increases as RT does. This increased level of viral PR could potentially have a detrimental effect to HEK293T cells given that viral PR is able to cleave host cell substrates. When Saquinavir is present in cell culture medium, the activity of viral PR is expected to be inhibited, thereby rescuing HEK293T cells, even though high quantities of GagPol-EGFP are still present in the

cell. This may be a potential reason for the significant increase in cell viabilities observed here, which could be tested by direct measurement of PR through looking at the cleavage of targets within the host cell, for example Bcl-2.

Of particular note is that viral PR has been linked to the cleavage of pro-apoptotic proteins, so by inhibiting viral PR in this instance, a lower level of cell death specifically by apoptosis might occur (Perry et al., 2021). HIV-1 PR has previously been reported to cleave and activate Procaspase 8 between residues 355 and 356 in CD4+ T-cell lines, leading to the formation of Casp8p41, along with characteristic signs of apoptosis such as nuclear condensation, DNA fragmentation, release of cytochrome C from mitochondria, and as a result, caspase 9 and 3 activation (Nie et al., 2002; Nie et al., 2007; Nie et al., 2008). The executioner caspase, Caspase 3, is involved in both the extrinsic and intrinsic apoptotic pathways (Figure 5.3). The inhibition of PR may lead to reduced caspase 3 activation and this may play a role in HEK293T cell viability being significantly higher in the presence of Saquinavir observed in this investigation, an observation which reflects what has been reported in literature (Figure 5.1) (Nie et al., 2002). Inhibition of the cleavage of Procaspase 8 by HIV-1 PR has been shown to lead to a reduction in cell death when cells were transfected with PR (Nie et al., 2008).

During transduction with GagPol at low MOIs, there will be less viral PR being produced. This could be a reason that there is not a drastic increase in cell viability when Saquinavir is present, when compared to higher MOIs (and therefore more GagPol present in the cell). Perhaps there is a threshold of the amount of viral PR that a host cell can handle before viability is affected due to host cell proteins being cleaved.

A p24 ELISA was also performed to determine how Saquinavir affected GagPol production. Despite an increase in cell viability with Saquinavir present, there was no significant change in p24 protein produced at all MOIs tested (Figure 5.2). This suggest that GagPol production itself is not sensitive to the presence of Saquinavir in cell culture medium, and that the primary effect of Saquinavir is actually on cell viability, which is linked to the cleavage of host cell proteins and not linked to the cleavage of viral proteins. Observations in Figure 5.1 showed that cell viability was

rescued, however this does not necessarily mean that the viable cells are capable of producing more protein in the case of GagPol. These results suggest that use of a viral PR inhibitor may be of use during LVV in terms of enhancing cell viabilities, but the PR inhibitor Saquinavir did not lead to increased production of GagPol at this scale of transduction. The cellular substrates cleaved by the viral PR may not play any role in GagPol production past a certain limit, however this must further be elucidated.

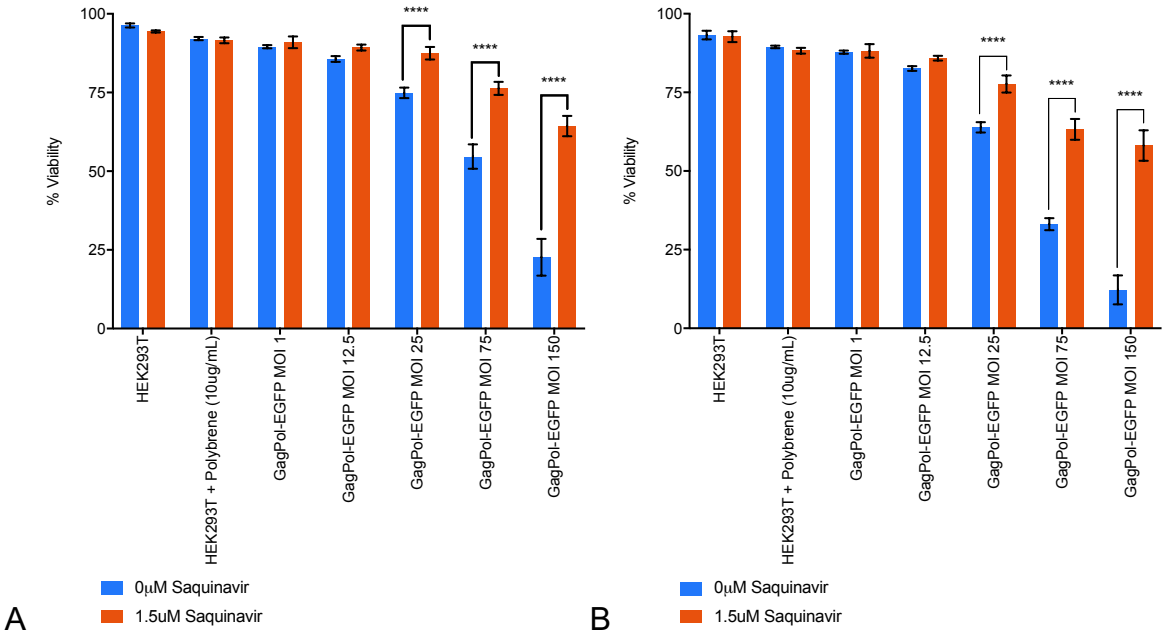

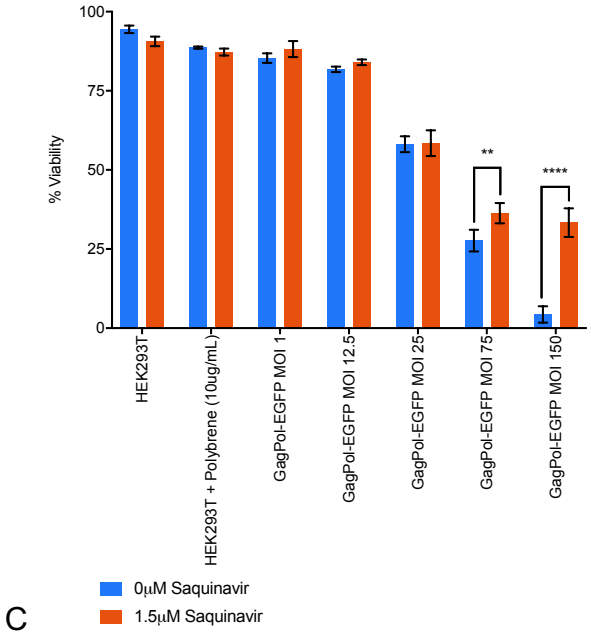

Figure 5.1 HEK293T cell viability following transductions with the Protease inhibitor Saquinavir. HEK293T cells were transduced at a range of MOIs with GagPol-EGFP vector (Section 2.2.5), with and without 1.5μM Saquinavir in cell culture medium (Section 2.2.2.7). Cell viabilities were measured at (A) 24 hours, (B) 48 hours, and (C) 72 hours post-transduction (Section 2.2.2.3). Values are mean +/- SEM of 3 biological repeats with 3 technical repeats each. Statistical analysis was carried out using one-way ANOVA. **= $p<0.01$, **** = $p<0.0001$.

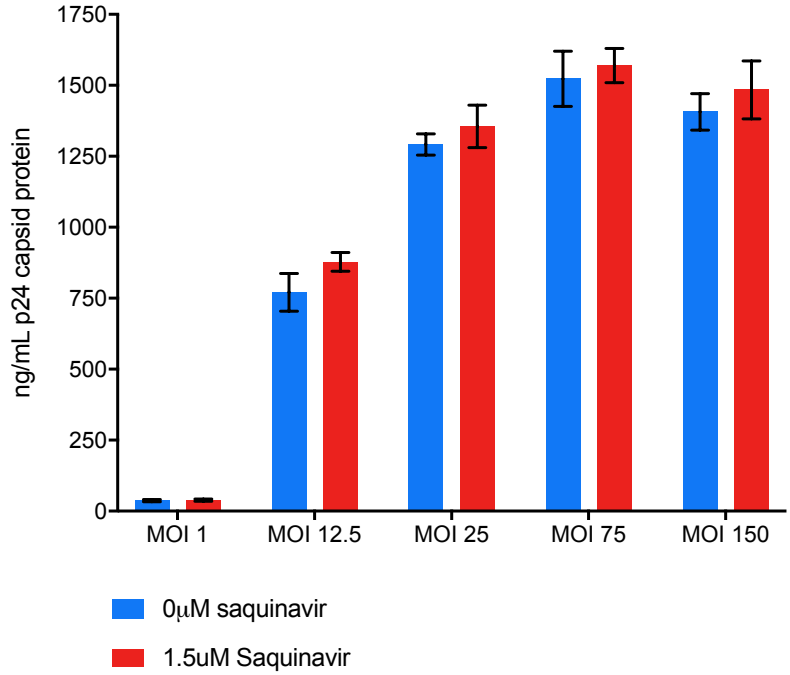

Figure 5.2 Titration of GagPol-EGFP vector by p24 ELISA. HEK293T cells were transduced at a range of MOIs with GagPol-EGFP vector (Section 2.2.5) with and without 1.5μM Saquinavir in cell culture medium (Section 2.2.2.7). Cell lysate samples were collected 48 hours post-transduction (Section 2.2.2.5) and titrated by p24 ELISA (Section 2.2.4.2). Values are mean +/- SEM of 3 biological repeats with 3 technical repeats each. Statistical analysis was carried out using one-way ANOVA.

5.2 Effect of apoptosis inhibitors on GagPol expression and cell viability

Apoptosis is a key limiting factor that determines mammalian cell culture productivity. It was observed in Chapter 4 that GagPol production led to an increase in the percentage of cells that were positive for Annexin-V (apoptosis marker) (Figure 4.11, Section 4.4). Cell line engineering strategies such as apoptosis inhibition have enabled an increase in the production of monoclonal antibodies in mammalian cells (reviewed in Krampe and Al-Rubeai, 2010). For example, engineered HEK293 cell lines with double knock-out of pro-apoptotic genes, Bak and Bax, have been developed using zinc-finger nuclease technologies (Arena et al., 2019). This cell line was shown to be much more resistant to shear stresses and apoptosis, in addition to producing higher titres of antibody at transfection scales of up to 10L. From a bioprocessing perspective, high levels of apoptosis in producer cell lines is an undesirable trait, as this decreases the efficiency of production of cellular and viral proteins (Zhang et al., 2017).

Inhibiting events that occur as part of apoptosis, such as caspase activation and mitochondrial dysfunction, are able to delay the onset of apoptosis and hence prevent destruction of a cell (Zhang et al., 2017; Arena et al., 2019). The caspase cascade has been of particular focus in recent years as a strategy of delaying apoptosis, and in turn, to improve cellular productivity and increase protein production (Betenbaugh, 2006). Upstream initiator caspases such as Caspase-8 and Caspase-9, as well as downstream effector caspases Caspase-3, Caspase-6, and Caspase-7 are actively involved in the caspase cascade (Figure 5.3).

Apoptosis can be regulated by both genetic and chemical intervention. During this investigation, several apoptosis inhibitors were utilised, including Caspase-8 inhibitor (Z-IETD-FMK, a mediator of the extrinsic apoptosis pathway), Caspase-9 inhibitor (Z-LEHD-FMK, a mediator of the intrinsic apoptosis pathway), and a broad-based Pan-Caspase inhibitor (Z-VAD-FMK) (Section 2.2.2.7). Adding these chemicals to cell culture has previously been demonstrated to be a simple but effective method for delaying apoptosis through caspase inhibition in both CHO and HEK293 cells

(Betenbaugh et al., 2002). Despite this success using chemicals, it would still be of advantage to employ cell line engineering for these targets as the chemicals themselves are expensive.

Cell viability was recorded following transduction with GagPol-EGFP and EGFP vectors at an MOI of 25 with apoptosis inhibitors in cell culture medium (Section 2.2.2.7) (Figure 5.4). All apoptosis inhibitors used led to significantly higher cell viabilities in cells transduced with GagPol-EGFP at MOI 25, where titres of over 4000 nU RT/mL and 1250 ng p24/mL from cell culture medium samples were achieved. These observations suggest that the decrease in viability seen during the production of GagPol is, only in part, caused by apoptotic cell death (Figure 4.1). The increase in cell viability during GagPol production was higher at 24 hours compared with 48 hours, suggesting that even though cells are still dying, they are dying at a later time point. This is beneficial in terms of LVV production as cells tend to be highly productive in the first 48 hours (Figures 3.13 and 3.14). Using a Caspase-9 inhibitor led to significantly higher cell viabilities in transductions with EGFP vector at MOI 25, suggesting that the Caspase-9 inhibitor is effective in preventing apoptotic cell death during production of EGFP as well as GagPol-EGFP.

A p24 assay was performed to determine whether the presence of apoptosis inhibitors had any effect on GagPol production (Figure 5.5). The presence of a Caspase-8 inhibitor in cell culture medium did not significantly affect p24 titres, despite an observed increase in cell viability during GagPol-EGFP production (Figure 5.4). This suggests that extrinsic apoptosis, involving Caspase-8, is not a key mechanism of cell death during GagPol production.

Having a Pan-caspase inhibitor present in cell culture medium during GagPol-EGFP production led to significantly higher titres of p24 protein in cell culture medium at both 24 and 48 hours (Figure 5.5). This was an encouraging result as it supported the concept that apoptosis does have a detrimental impact on GagPol production, however in terms of defining a target for cell engineering to improve protein production, this chemical inhibitor gives no specific cellular target.

The presence of a Caspase-9 inhibitor in cell culture medium led to a significant increase in GagPol production, more so at 24 hours post-transduction compared with 48 hours, however despite this being statistically significant it is still not very large in the scheme of LVV production (Figure 5.5). Since the highest LVV production is between 24 hours and 48 hours post-transduction (GSK, in-house observations), it would potentially be of great advantage to delay the onset of apoptosis until after the most productive time points. Caspase-9 is involved in the intrinsic pathway of apoptosis, which is stimulated by internal stimuli such as ER stress, metabolic stress, and nutrient stress (Figure 5.3) (Fulda and Debatin 2006). It is also important to consider that the intrinsic pathway in other mammalian cells tends to be the driver of apoptosis, particularly in CHO cell culture (Wei et al., 2011). As such, inhibition of the intrinsic pathway of apoptosis, and in particular by targeting Caspase-9, may be a potential way to prevent cell death during high levels of GagPol production. These results together with an observed increase in cell viability suggest that future work targeting apoptosis inhibitors, specifically Caspase-9, for genetic engineering in HEK293T cells could be an encouraging prospect for defining cell engineering targets and could be a feasible way of increasing LVV production.

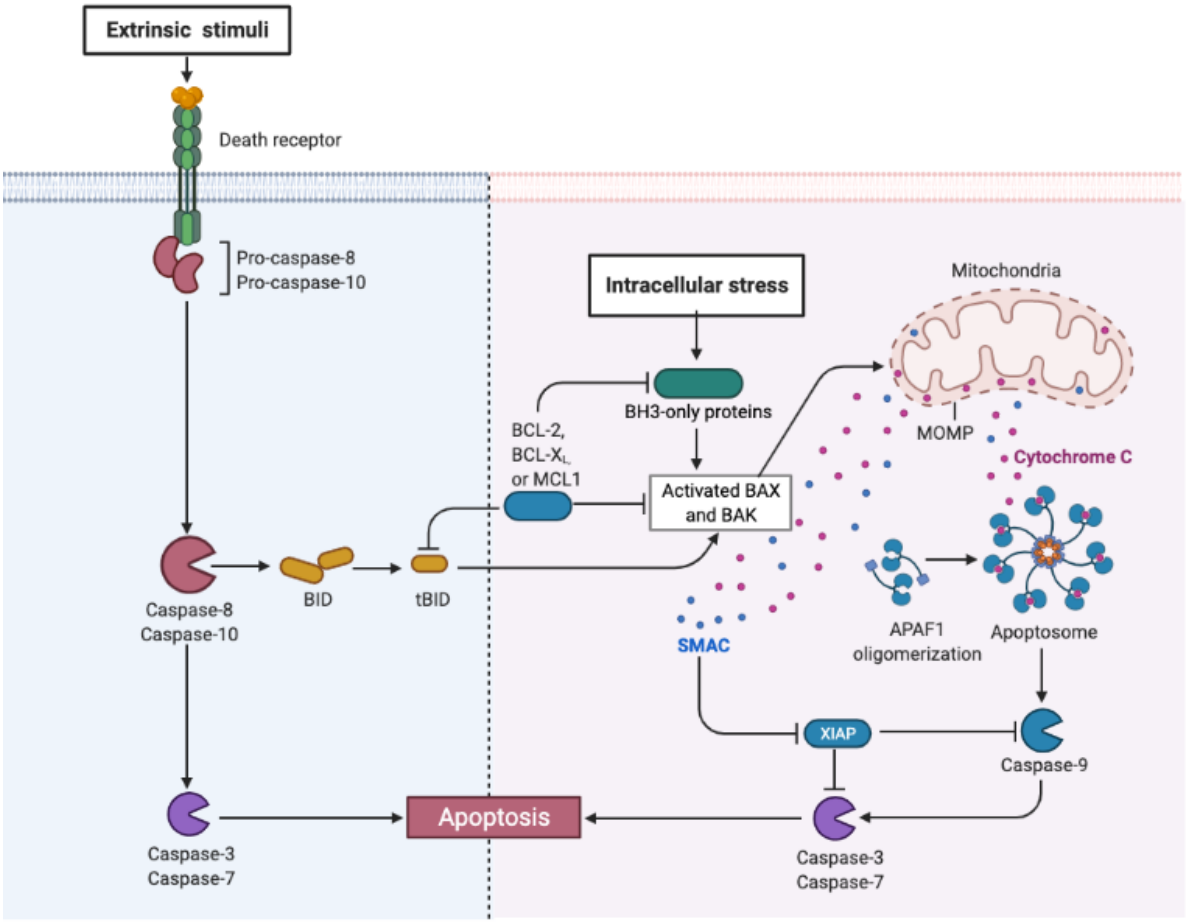

Figure 5.3 Extrinsic and Intrinsic pathways of apoptosis and targets for the inhibition of apoptosis. Extrinsic pathway: This pathway is triggered by binding of a death ligand to a death receptor such as TNFR1 or TNF-a. This transmits a death signal to intracellular signalling pathways from the cell surface. Several death domains are recruited leading to activation of Caspase-8 and Caspase-10. Here, active Caspase-8 and Caspase-10 cleave and activate executioner caspases (-3, -6, and -7), or cleave BH3-interacting domain death agonist (BID) to induce cell death. Intrinsic pathway: This pathway can be induced by cleaving BID which leads to mitochondrial dysfunction. Cytochrome C is released and activates Caspase-9 and Caspase-3. Activation of Caspase-3 leads to cell death and DNA fragmentation. A further controller of this pathways is the Bcl-2 protein family; BAX and BAK are pro-apoptotic, whereas BCL-2, BCL-XL, and MCL1 are anti-apoptotic. Additionally, pro-apoptotic molecules can cause permeabililstion of the mitochondria's outer membrane, which leads to Cytochrome C release. This binds Apaf-1 and Caspase-9 to form the Apoptosome, stimulating the activation of Caspase-3 and Caspase-7.

SMAC is also released from mitochondria into the cytosol, blocking Inhibitor of Apoptosis (IAP) proteins, hence indirectly promoting apoptosis (Reviewed by Fulda and Debatin, 2006). Apoptosis can be inhibited at several stages using chemical inhibitors of Caspase-8 (Z-IETD-FMK), Caspase-9 (Z-LEHD-FMK), in addition to using a broad-based Pan-Caspase inhibitor (Z-VAD-FMK) (Betenbaugh et al., 2002). Created in BioRender.

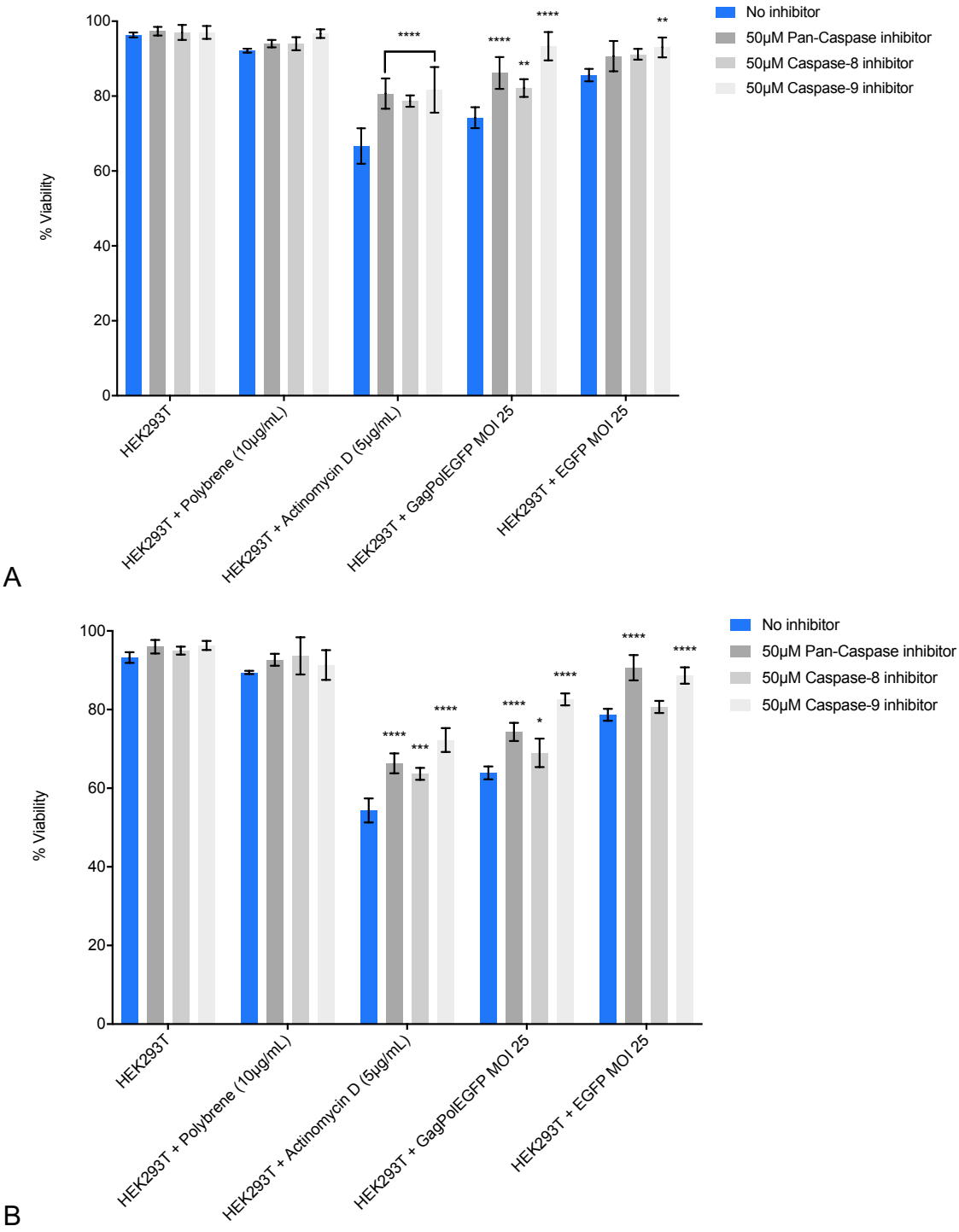

Figure 5.4 HEK293T cell viability following transduction with inhibitors of apoptosis. HEK293T cells were transduced at MOI 25 with EGFP or GagPol-EGFP vector (Section 2.2.5) with and without apoptosis inhibitors in cell culture medium (Section 2.2.2.7). Cell viabilities were measured at (A) 24 hours and (B) 48 hours post-transduction (Section 2.2.2.3). Values are mean +/- SEM of 3 biological repeats with 3 technical repeats each. Statistical analysis was carried out using one-way

ANOVA comparing inhibitors with non-inhibitor conditions for each sample.
*=p<0.05, **= p<0.01, ***=p<0.001, **** = p<0.0001

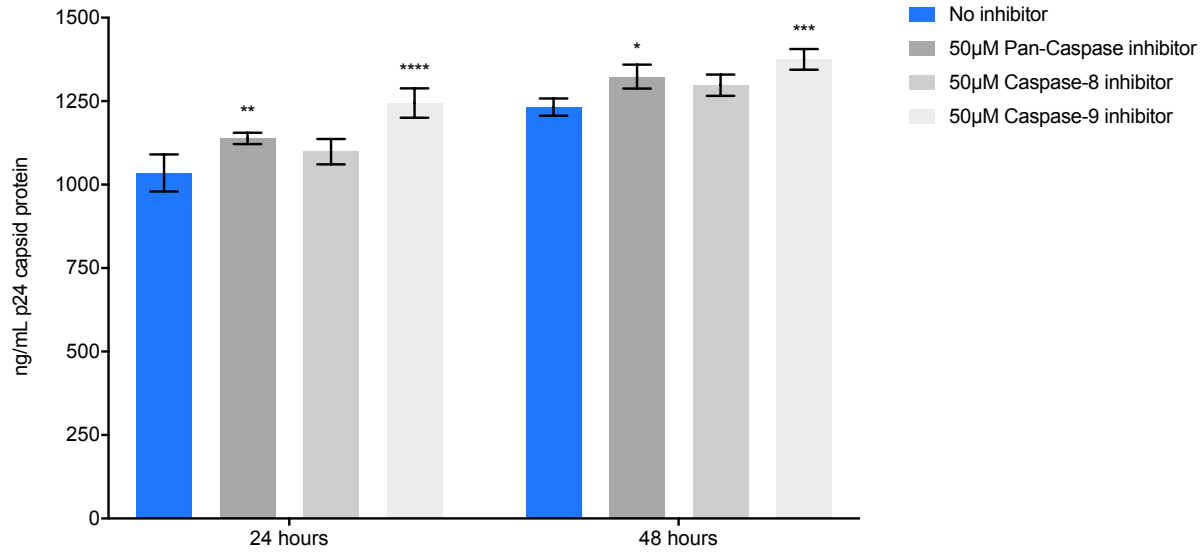

Figure 5.5 Effect of apoptosis inhibitors on p24 expression. HEK293T cells were transduced at MOI 25 with GagPol-EGFP vector (Section 2.2.5) with and without apoptosis inhibitors in cell culture medium (Section 2.2.2.7). Cell lysate samples were collected at 24 hours and 48 hours post-transduction (Section 2.2.2.5) and titrated by p24 ELISA (Section 2.2.4.2). Values are mean +/- SEM of 3 biological repeats with 3 technical repeats each. Statistical analysis was carried out using one-way ANOVA comparing inhibitors with non-inhibitor conditions for each sample. *= $p<0.05$, **= $p<0.01$, ***=$p<0.001$, **** = $p<0.0001$

5.3 Effect of autophagy inhibitors on GagPol expression and cell viability

Targeted cell engineering specific to the genetic manipulation of the autophagy pathway is of particular interest when looking to improve recombinant protein production, as this pathway has an influence on protein quality and viable cell concentration. Aside from being an important survival mechanism, autophagy is implicated in control of cell death due to stressful conditions within the cell environment (Hawng and Lee 2008). When cells are exposed to stressful conditions, protein synthesis is decreased in a co-ordinated manner with an increased rate of protein degradation (Mortimore and Poso 1988). This could be detrimental for GagPol production. As such, Section 5.3 aimed to determine the effects of inhibiting autophagy through use of various chemicals.

Autophagy is regulated by various signalling pathways (Figure 5.6). The autophagy inhibitors chosen in this investigation targeted either the onset of autophagy, namely the nucleation and double-membrane formation that is characteristic of autophagy, or inhibitors targeting the later stages of autophagy, specifically the fusion of the autophagosome and the lysosome, and subsequent degradation and recycling of cargo. To confirm the extent of autophagy observed under various conditions and the effects of inhibitors, cells were analysed using imaging flow cytometry (Section 2.2.6.5).

Focussing on inhibitors of the earlier stages of autophagy, Spautin-1 and Wortmannin were selected (Figure 5.6). Spautin-1 is a specific and potent inhibitor of autophagy that enhances Beclin-1 degradation, and subsequently inhibits the initiation of autophagy (Shao et al., 2014). Wortmannin, a PI3K inhibitor, is able to inhibit autophagy via persistent class III PI3K inhibition (Takatsuka et al., 2004). Wortmannin and Spautin-1 both displayed an ability to decrease the number of LC3-positive puncta when analysing cells by imaging flow cytometry, which represents the number of autophagosomes within a cell (Figure 5.8). This was expected as the initial stages of autophagy were inhibited with these chemicals, hence not allowing autophagosome formation. Co-localisation (BDS Score) between LC3 and LAMP-1

did not significantly change with use of these inhibitors, suggesting that the delivery of autophagosomes to lysosomes did not change in the presence of these autophagy inhibitors (Figure 5.9). Despite not seeing a change in BDS score, the fact that Wortmannin and Spautin-1 were able to decrease the number of LC3-positive puncta (autophagosomes) in HEK293T cells indicated that these were sufficient in inhibiting autophagy, and therefore were used for the remainder of this experiment.

Bafilomycin A1 and Chloroquine were selected as inhibitors of the later stages of autophagy, namely inhibiting the fusion of autophagosomes and lysosomes, meaning that the contents of the autophagosome will not get degraded by acid hydrolases in the lysosome (Figure 5.6) (Redmann et al., 2018). Specifically, Bafilomycin A1 is a V-ATPase inhibitor whose presence leads to the inability of autophagosomes and lysosomes to fuse, meaning cargo cannot be degraded and recycled (Mauvezin et al., 2015). Chloroquine works in a similar manner by preventing the fusion of autophagosomes and lysosomes by increasing lysosomal pH (Mauthe et al., 2018). No significant difference in LC3 spot count was observed with these inhibitors (Figure 5.8). It would be expected that there would be an increase in LC3 spot count due to a build-up of autophagosomes, as these structures will not fuse with lysosomes and hence would not be degraded. There was a decrease in co-localisation of LC3 and LAMP-1 with Bafilomycin A1 and Chloroquine as expected, as both of these chemicals act by inhibiting the fusion of autophagosomes with autolysosomes (Figure 5.9). The use of these chemicals enabled the inhibition of the late events of autophagy, meaning that cargo in HEK293T cells would not be degraded and recycled.

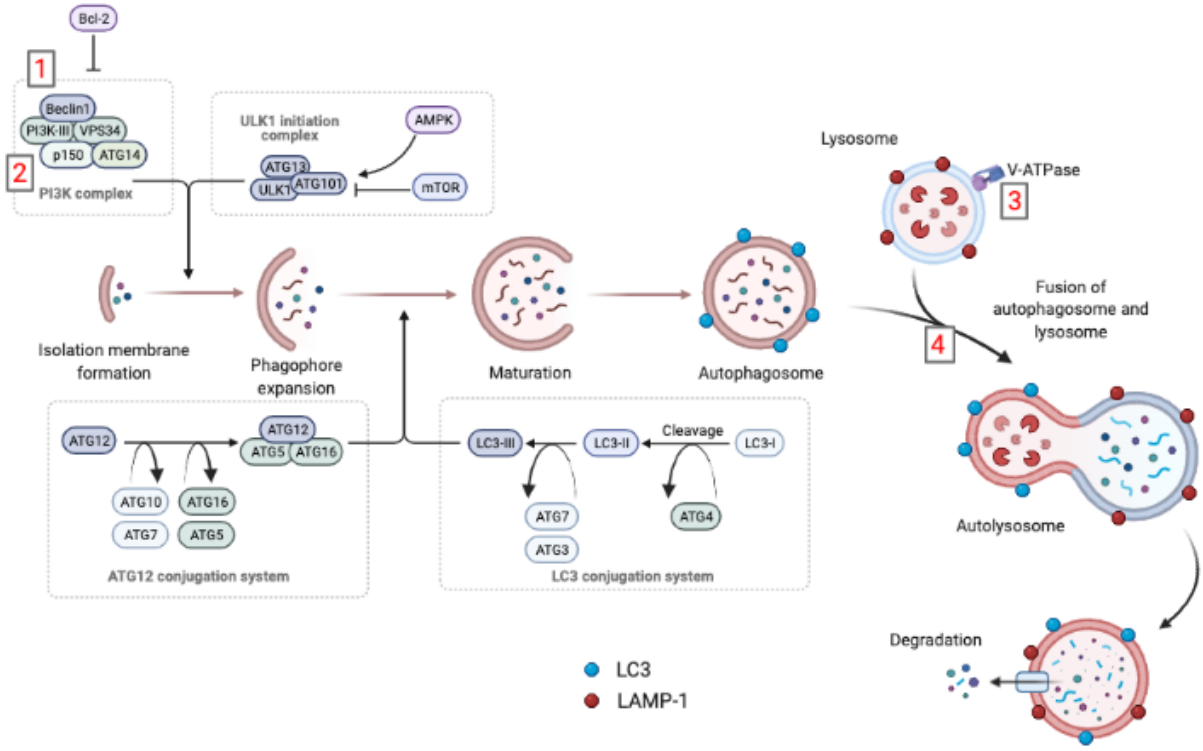

Figure 5.6 Macro-autophagy pathway and targets for inhibition of autophagy. Upon initiation of autophagy, material within the cytoplasm is engulfed by the phagophore, a double-membraned structure. The phagophore then elongates and seals around cytosolic cargo, forming an autophagosome. The autophagosome then fuses with a lysosome, where the contents are then degraded and recycled due to the highly acidic interior of the lysosome. This process involves multiple steps which are regulated by several proteins, however the mammalian target of rapamycin (mTOR) and AMP-activated kinase (AMPK) are the key autophagy regulators. Autophagy-related proteins assemble into various complexes to initiate autophagy. The Unc-51-like kinase 1 (ULK1) and the Phosphatidylinositol-3-phosphate (PI3P)-binding complex both direct autophagosome formation. ATG5, ATG12, and ATG16 form the ATG12 conjugation system which promotes LC3 conjugation. LC3-I is formed through cleavage of LC3 by ATG4. Phosphatidylethanolamine (PE) is conjugated to LC3-I to form LC3-III. LC3-III is then incorporated into autophagosomal membranes. Autophagy can be inhibited through use of various chemicals. (1) Spautin-1 inhibits autophagy initiation by enhancing Beclin-1 degradation. (2) Wortmannin inhibits the Class III PI3K pathways and subsequently blocks the formation of autophagosomes. (3) Bafilomycin A1 inhibits V-ATPase activity resulting

in lysosomes and autophagosomes not being able to fuse. (4) Chloroquine increases the pH within the lysosomes and hence blocks autophagosomes and lysosomes from binding (Parzych and Klionsk 2014). Created in BioRender.

Cell viability was recorded with autophagy inhibitors present in cell culture medium during transductions with GagPol-EGFP (Figure 5.7). Spautin-1 significantly decreased cell viability compared with no inhibitor, specifically in basal HEK293T cells, empty transduction with polybrene, and with starved HEK293T cells at both 24 hours and 48 hours. The presence of Spautin-1 during transductions both with and without GagPol-EGFP led to a significant decrease in the number of LC3-positive puncta, representing autophagosomes (Figure 5.8). Considering that autophagy itself is a cell survival mechanism during periods of cellular stress, inhibiting autophagy may lead to a disruption of the normal homeostasis of HEK293T cells, and hence this could be a reason for seeing the decrease in viability as the cell is not able to properly respond to cellular stress. This could also explain the significant decrease in p24 titres observed in both cell lysate and cell culture medium with Spautin-1 – cells are not able to respond to cellular stress by activating the autophagy pathway, which could have a detrimental impact on GagPol protein production (Figure 5.10). It must be noted here that Spautin-1 has been reported to enhance apoptosis, which may explain the observed decrease in viability (Shao et al., 2014). However, this does not explain why at 48 hours post-transduction there was no decrease in viability in cells producing GagPol-EGFP or EGFP.

The presence of Wortmannin in cell culture medium significantly increased HEK293T cell viability at 24 hours post-transduction with GagPol-EGFP, which suggests that the inhibition of Class III PI3K autophagy pathway is a potential way to increase HEK293T cell viability in this case (Figure 5.7). However, Class III PI3K has other roles aside from that in autophagy, it is also required for vesicular trafficking (Iershov et al., 2019). This is interesting when considering that Wortmannin also led to a significant decrease in GagPol production (Figure 5.10) – vesicular trafficking may play a key role in GagPol trafficking and release from the cell, and inhibiting vesicular trafficking could be detrimental to overall titres. It must be noted that this vesicular trafficking may not be relating to autophagic vesicles, as the presence of Wortmannin during transductions led to a significant decrease in autophagosome formation (Figure 5.8).

The presence of late-stage autophagy inhibitors Bafilomycin A1 and Chloroquine in cell culture medium during GagPol production had no impact on cell viability in this

investigation (Figure 5.7). Bafilomycin A1 in particular acts to inhibit autophagy by inhibiting the activity of V-ATPase which has an influence on the mTORC1 signalling pathways (Wang et al., 2021). However, the exact mechanism by which V-ATPase is inhibited is not known, and therefore it is difficult to say how this has an impact on cell viability. The presence of Bafilomycin A1 and Chloroquine both led to a significant decrease in the co-localisation of LC3 and LAMP-1 (Figure 5.9), in both basal HEK293T cells and HEK293T cells producing GagPol-EGFP, whilst not changing the number of autophagosomes within the cell (Figure 5.8). This change in the behaviour of autophagosomes compared with basal HEK293T cells is intriguing as it would be expected that the number of autophagosomes would build up as their degradation is blocked. Use of Bafilomycin A1 and Chloroquine led to significantly lower p24 titres in cell culture medium samples, however there was no change in p24 titres in cell lysate samples (Figure 5.10). Interestingly, this suggests that late-stage autophagy inhibitors have some sort of detrimental role in virus particle release. This makes sense when considering HIV-1, which has previously been reported to utilise the earlier stages of autophagy for assembly whilst inhibiting the later stages of autophagy for its own propagation, ensuring that it does not get degraded along with autophagosomal cargo (Kyei et al., 2009). As such, it is logical to suggest that the synthetic GagPol encoded in the SYNGP expression cassette would behave in a similar manner to HIV-1 GagPol and may have some sort of interaction with autophagosomal membranes (Kotsopoulou et al., 2000).

Disappointingly the use of autophagy inhibitors in this investigation did not yield higher p24 titres, however the interaction between autophagy and GagPol production must not be overlooked in future studies. Future work into exactly how the autophagy pathway intersects with this viral structural protein could illuminate targets for cell engineering with the potential to increase GagPol production.

In terms of selecting potential targets for genetic manipulation to improve HEK293T cell factories for LVV production, this Chapter highlighted the influence of manipulating autophagy on cell viability. An important consideration for choosing genetic targets for autophagy manipulation is that these targets may have effects on other homeostatic pathways. A strategy that may be of value to investigate in future would be to look at a combination of autophagy inhibitors and inducers, particularly

inducing the earlier stages of autophagy and inhibiting the later stages of autophagy, as HIV-1 does (Killian 2012).

There are several other targets in the early stages of autophagy that could be considered as inducers for autophagy, however it would be key to use chemical inducers first to see the scope of this in terms of improving GagPol induction and increasing HEK293T cell growth. As an example, previous studies have demonstrated that the knockout of Mitogen-activated protein kinase kinase kinase kinase 3 (MAP4K3) is able to promote the induction of autophagy (Dubinsky et al., 2014; Hsu et al., 2018). Combining the induction of autophagy as mentioned above with an inhibitor of late-stage autophagy (such as Bafilomycin A1 and Chloroquine) may therefore have potential in increasing GagPol production, if SYNGP behaves in a similar way to HIV-1 (Cabrera-Rodriguez et al., 2021). It would be of great value to mimic the behaviour of HIV-1 in this sense, as HIV-1 is remarkably good at propagating itself and will be using autophagosomal membranes to its own advantage.

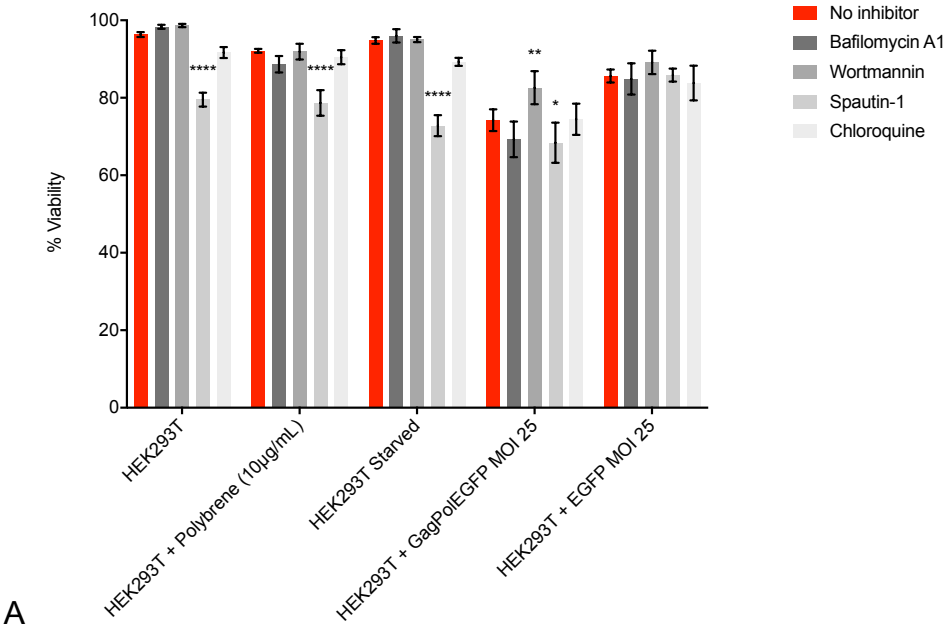

A

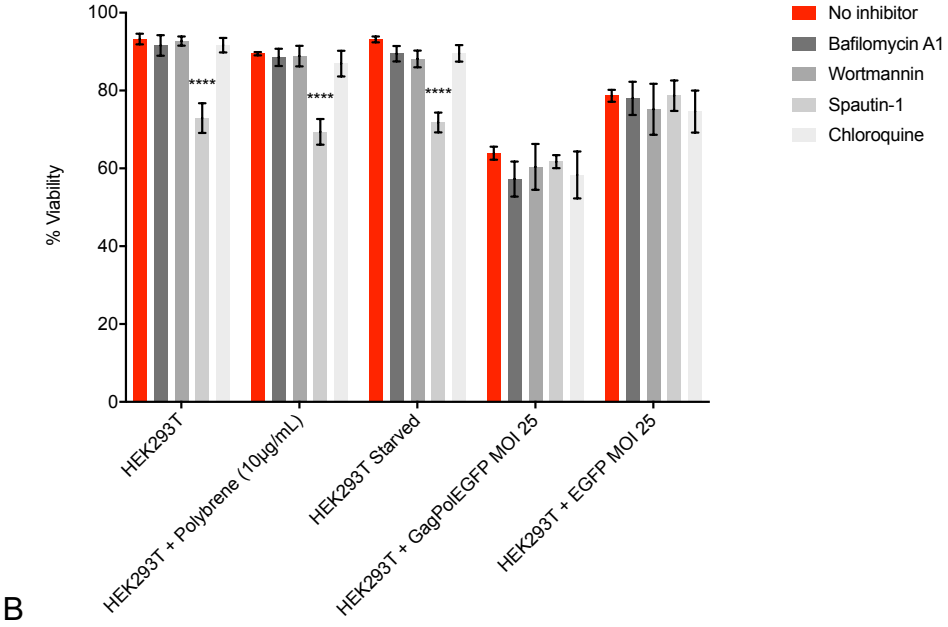

B

Figure 5.7 HEK293T cell viability following transduction with inhibitors of autophagy. HEK293T cells were transduced at MOI 25 with GagPol-EGFP vector (Section 2.2.5) with and without autophagy inhibitors in cell culture medium (Section 2.2.2.7). Cell viabilities were measured at (A) 24 hours and (B) 48 hours post-transduction (Section 2.2.2.3). Values are mean +/- SEM of 3 biological repeats with 3 technical repeats each. Statistical analysis was carried out using one-way ANOVA comparing inhibitors with non-inhibitor conditions for each sample. *= $p<0.05$, **= $p<0.01$, ***=$p<0.001$, **** = $p<0.0001$.

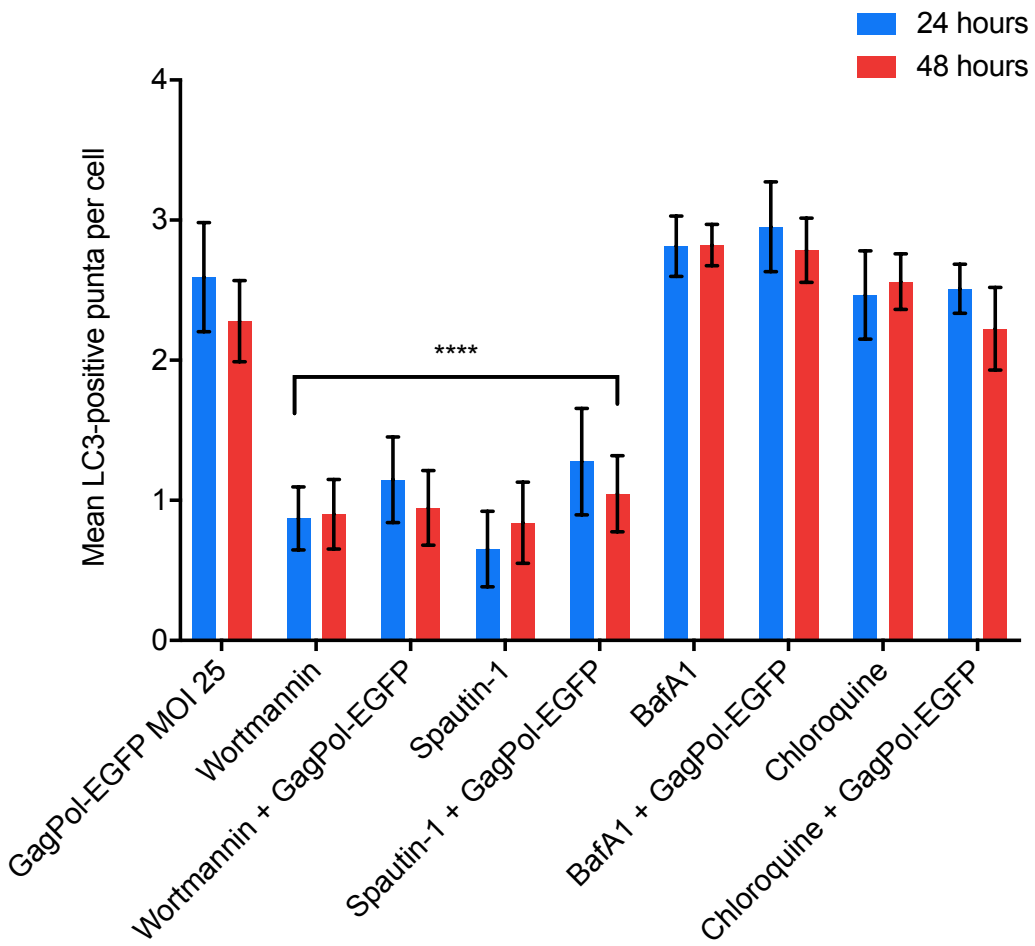

Figure 5.8 LC3-AF647 labelled HEK293T cells analysed using Spot Count feature following transductions with inhibitors of autophagy. HEK293T cells were transduced at MOI 25 with GagPol-EGFP vector (Section 2.2.5) with and without autophagy inhibitors in cell culture medium (Section 2.2.2.7). Cells were collected and labelled with LC3-AF647 and LAMP-1-PE (Section 2.2.6.6). Samples were acquired on the ImageStreamX® (Section 2.2.6.7). Samples were analysed to determine mean LC3-AF647 spot count per cell (Section 2.2.6.8). Values are mean +/- SEM of 3 biological repeats with 3 technical repeats each. Statistical analysis was carried out using one-way ANOVA comparing inhibitors with non-inhibitor conditions for each time point. **** = $p<0.0001$.

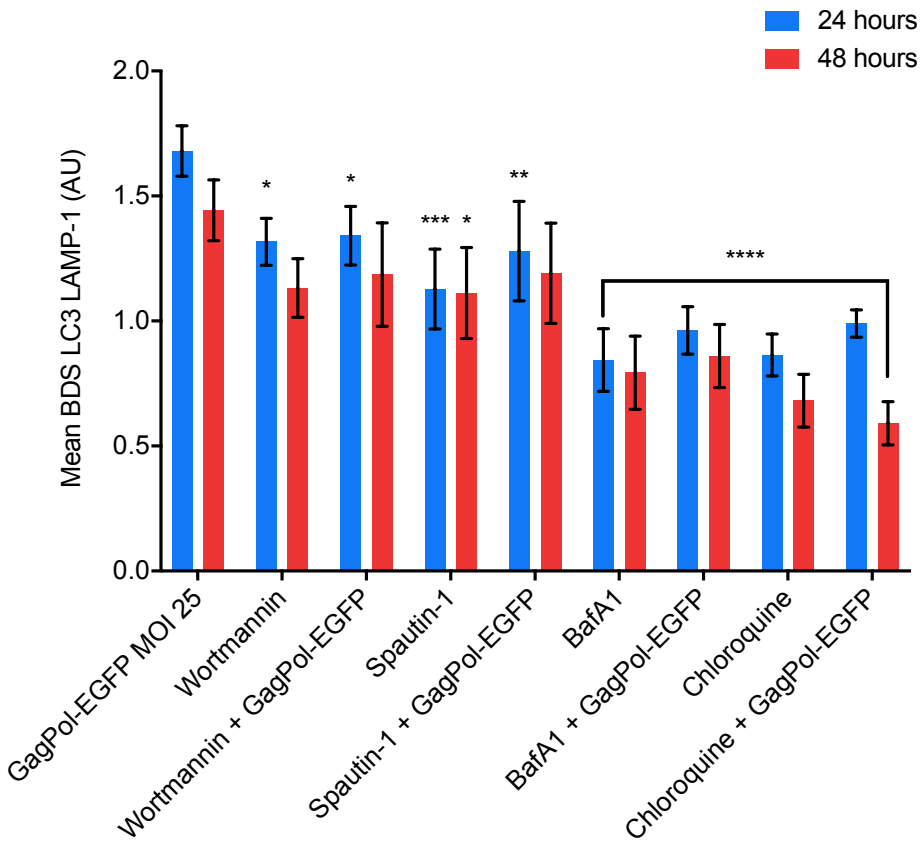

Figure 5.9 Bright Detail Similarity Score between LC3-AF647 and LAMP-1-PE in HEK293T cells following transduction with inhibitors of autophagy. HEK293T cells were transduced at MOI 25 with GagPol-EGFP vector (Section 2.2.5) with and without autophagy inhibitors in cell culture medium (Section 2.2.2.7). Cells were collected and labelled with LC3-AF647 and LAMP-1-PE (Section 2.2.6.6). Samples were acquired on the ImageStreamX® (Section 2.2.6.7). Samples were analysed in the IDEAS software to determine the Bright Detail Similarity (BDS) Score between two probes, LC3-AF647 and LAMP-1-PE (Section 2.2.6.8). Values are mean +/- SEM of 3 biological repeats with 3 technical repeats each. Statistical analysis was carried out using one-way ANOVA comparing inhibitors with non-inhibitor conditions for each time point. *= $p<0.05$, **= $p<0.01$, ***=$p<0.001$, **** = $p<0.0001$.

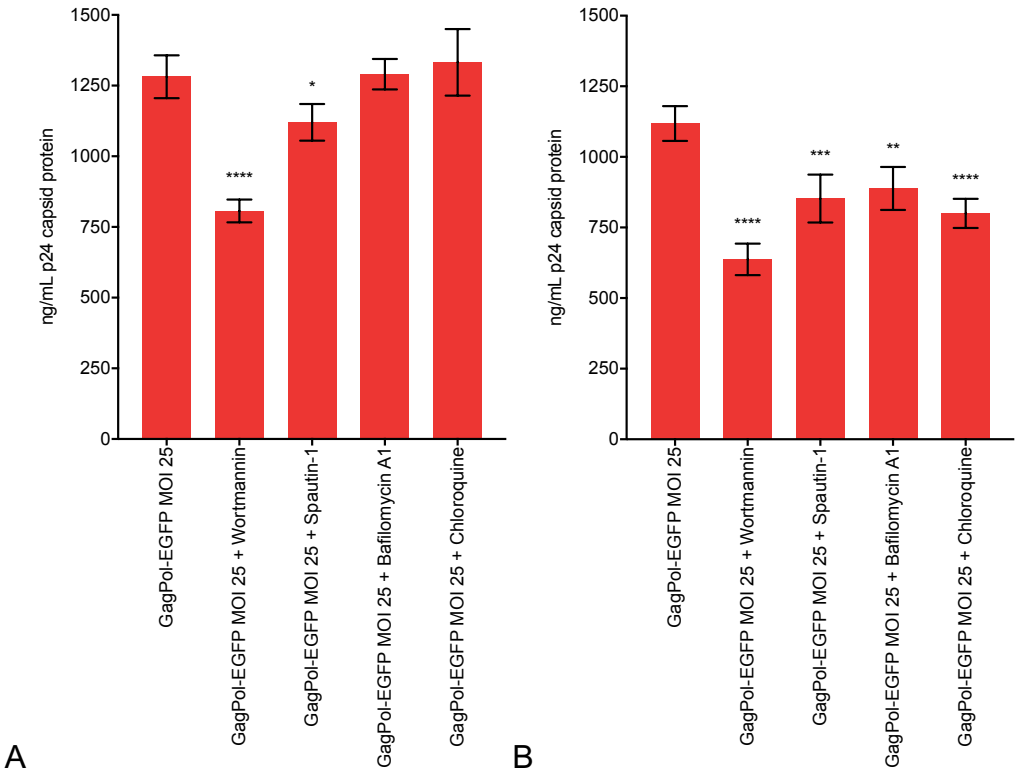

Figure 5.10 Titration of GagPol-EGFP vector by p24 ELISA with inhibitors of autophagy. HEK293T cells were transduced at MOI 25 with GagPol-EGFP vector (Section 2.2.5) with and without autophagy inhibitors in cell culture medium (Section 2.2.2.7). (A) Cell lysate and (B) cell culture medium samples were collected 48 hours post-transduction (Section 2.2.2.5 and 2.2.2.6 respectively) and titrated by p24 ELISA (Section 2.2.4.2). Values are mean +/- SEM of 3 biological repeats with 3 technical repeats each. Statistical analysis was carried out using one-way ANOVA comparing inhibitors with non-inhibitor conditions. *= $p<0.05$, **= $p<0.01$, ***=$p<0.001$, **** = $p<0.0001$.

5.4 Concluding remarks

Following observations in Chapter 4 of GagPol production causing various types of cellular stress, Chapter 5 aimed to analyse the effects of various chemical inhibitors of cellular stresses, with a particular focus on the production of GagPol and also HEK293T cell viability.

The presence of the viral PR inhibitor, Saquinavir, in cell culture medium during transductions was observed to increase HEK293T cell viability, but this did not lead to any further GagPol production (Figures 5.1 and 5.2). It would be of interest to further investigate viral PR and its interactions with host cellular substrates, specifically looking at cell viability in parallel to directly measuring the cleavage of Bcl-2, to determine whether viral PR inhibition leads to less Bcl-2 being cleaved. This would also provide further information of how apoptosis is involved in GagPol production. Measurement of Caspase 3 activation during the production of GagPol could also be looked at as this is of particular interest when using Saquinavir. Additional future work would involve using other HIV-1 PR inhibitors to assess whether these chemicals are more effective at inhibiting PR than Saquinavir. For example, Ritonavir, Tipranavir, and Indinavir have also been demonstrated to inhibit HIV-1 PR (Wang et al., 2015). Altogether Section 5.1 demonstrated that viral PR is potentially damaging to HEK293T cells, but mitigating the toxic effect of viral PR does not necessarily have an impact on GagPol production.

Sections 5.1 and 5.2 of this Chapter are very much interconnected as there are several viral PR substrates whose cleavage may lead to apoptosis, as discussed in Section 5.1. This series of experiments demonstrated that the chemical inhibitor of Caspase-9 enabled a significant increase in the production of GagPol compared with having no apoptosis inhibitors present in cell culture medium (Figure 5.5). However, this effect must be looked into further as it was only a modest increase, but it cannot be ruled out that this effect may be further improved with genetic manipulation of Caspase-9.

Recent literature has demonstrated that modifying genes involved in apoptosis can have positive effects on both cell viability, growth rates, and protein production. For example, the over-expression of Nuclear Factor Erythroid 2-Related Factor 2 (NRF2), a transcription factor that has been shown to upregulate expression of cytoprotective proteins and antioxidant enzymes, has been reported to result in higher HEK293 growth rates due to protection from oxidative stress, and up to 1.7-fold increases in recombinant protein expression (specifically Recombinant coagulation factor VII) (Abbasi-Malati et al., 2019). In addition to this, a double knock-out of BCL2 Antagonist Killer 1 (BAK) and Bcl-2-associated X protein (BAX), both of which are involved in caspase activation, has been shown to improve Human IgG1 antibody titres by 40% by enabling HEK293 cells to be resistant to apoptosis and sheer stress (Arena et al., 2019).

Inhibiting autophagy with the chemical inhibitors used in this investigation did not have a desirable effect on GagPol production (Figure 5.10). However, despite this, it is still worth examining the interplay between GagPol and autophagy further (discussed in Section 5.3), as the interactions reported between autophagosomal membranes and HIV-1 are hard to ignore in terms of what the consequences might be for LVV production. If HIV-1 does in fact assemble on autophagic membranes, it may be of value for LVV production to increase the amount of autophagy-related membranes in a HEK293T cell. However, the converse must also be considered, as perhaps Gag localises to autophagic membranes due to mis-targeting, and is in fact on a path to degradation via the lysosome. Future experiments of value include investigating the interaction between GagPol and other vesicles, such as multi-vesicular bodies and exosomes.

6 Discussion and Future Work

This thesis aimed to understand and elucidate interactions between synthetic GagPol and HEK293T cellular physiology, with a particular focus on identifying and intervening in molecular bottlenecks associated with LVV production. To achieve this aim, it was first necessary to develop plasmid constructs enabling the expression of synthetic GagPol, in addition to fluorescently-tagging GagPol to allow detection of this viral protein by use of various methods including flow cytometry (Chapter 3).

Vector production by transient transfection of HEK293T cells enabled high-level expression of GagPol and GagPol-EGFP, confirmed through various titration methods including p24 ELISA, PERT assay, and ddPCR (Chapter 3). Despite increasing the quantity of vector during transductions with high MOIs, an increase in GagPol production past approximately 1250 ng p24/mL was not observed.
The fact that GagPol copy number continues to increase when using higher MOIs of GagPol vector, but there is not a continued increase of GagPol production, was of particular interest during these investigations. It suggests that there is not an issue with the integration of genetic information into the HEK293T cell, and that the cause of the observed ceiling in GagPol production is occurring after integration.

A further key objective throughout this thesis was to characterise HEK293T cellular physiology and function following the expression of GagPol, with a specific focus on various cellular stress responses that may be activated by high levels of expression of GagPol (Chapter 4). It is still not known exactly what caused this ceiling in GagPol production as observed in Chapter 3, however work conducted in Chapter 4 made it clear that various cellular stress pathways are activated during GagPol production, including the UPR, ER Stress, apoptosis, and autophagy.

It would be very helpful to determine the exact stage(s) of LVV production that cause stress. There are a number of potential sites including several in GagPol trafficking through intracellular vesicular sites to the plasma membrane (or even between other sites of assembly within a HEK293T cell). It can be deduced from these studies that cellular stress is happening after translation, as GagPol is being detected prior to the

onset of ER stress, UPR, apoptosis and autophagy. It must be considered that additional burden may be placed on HEK293T cells when introducing the other components of a LVV.

It was clear from this investigation that a burden is placed on host cellular machinery when producing GagPol. This is consistent with the idea that in a mammalian cell, the biosynthesis of proteins consumes a substantial amount of energy. It has been reported that in an IgG-producing CHO cell line, up to approximately 90% of the occupancy of ribosomes is spent on producing proteins other than the desired recombinant protein (Kallehauge et al., 2017). It was suggested that by eliminating genes that are competing for resources for protein production, the specific productivity of a cell may be improved substantially. It is therefore of key importance to understand how over-expression of GagPol affects a HEK293T cell in order to overcome molecular bottlenecks (perhaps eliminating genes competing for essential resources) and enable increased levels of protein production whilst ensuring optimal cell growth and health.

As demonstrated in this thesis, activation of the UPR in addition to the onset of ER stress was observed when GagPol was generated with MOI's greater than 25. Production of GagPol may be competing for resources for protein production and this could place HEK293T cells under stress when producing the 'normal' proteins for maintaining homeostasis. Assuming that, following a period of 48 hours of virion production with 2 x 10^6 cells/mL, the physical titre achieved is approximately 10^3 ng p24/mL. If all of this p24 is associated with a virion, and given that there are approximately 4000 molecules of p24 (with a mass of 24 kDa), this means that cells are producing approximately 1.1 pg/cell/day by dry mass (1500 virions/cell/day). This is a lot lower than the production of recombinant protein observed in CHO cells. The folding machinery associated with producer cell lines is often challenged by unnaturally high amounts of ectopic recombinant proteins. Manipulation of genes relating to ER protein processing, including XBP1, have previously been explored during antibody production, where the over-expression of XBP1 was found to display improved characteristics relating to cell growth and viability (Mohan et al., 2010; Tigges et al., 2006). Interestingly, the beneficial functional effects of XBP1 over-expression in this instance of monoclonal antibody production were observed to be

greatest when cells were producing a maximum protein load, by a mechanism that has not yet been defined. It has also been suggested that that high DNA concentrations during transient transfection may hinder disulphide bond formation (Cain et al., 2013). Given the improvements to monoclonal antibody production, it would be of value to study how XBP1 overexpression could be beneficial for LVV production.

Oxidative stress must also be considered when looking at potential cellular stress, as there is increasing evidence that redox signalling pathways and the presence of reactive oxygen species are involved in determining cell fate (Cao and Kaufman, 2014). As previously mentioned, upon disturbance of ER homeostasis, the UPR is activated. It is not known if GagPol production in cytosolic ribosomes has an influence on cellular or ER redox state, however the proper functioning and protein homeostasis of the ER is closely linked to ER redox state, so must be examined in future. Techniques for monitoring ER redox state include assaying the redox state of genetically encoded fluorescent proteins that are redox-sensitive (by western blot, fluorescence, flow cytometry or microscopy) (Dooley et al., 2004; Hanson et al., 2004; Merksamer et al., 2008; Ponsero et al., 2017). Recent literature has made clear the interplay between the UPR, ER stress, and reactive oxygen species (Gu et al., 2016, Liang et al., 2014, Uzilday et al., 2018). Reactive oxygen species are able to act as signal molecules when at low concentrations within a cell, however upon accumulation of reactive oxygen species, DNA damage, membrane instability, and protein instability can result from oxidative stress (Mittler et al., 2012).

In the context of GagPol production, HIV-1 has been reported to induce oxidative stress, leading to increased reactive oxygen species production and induction of mitochondrial dysfunction (Banki et al., 1999; Deshmane et al., 2009). In particular, Reverse Transcriptase (RT) has been shown to mediate enhanced reactive oxygen species production (Isaguliants et al., 2013). Further work must be undertaken to understand the interactions between GagPol, oxidative stress, and an increase in reactive oxygen species. Techniques including chemiluminescence are able to directly identify various types of oxygen radicals, and would be of use when looking at the consequences of varying levels of GagPol production in HEK293T cells (Dikalov and Harrison, 2010).

An additional aspect of HEK293T cells where further investigations likely to be valuable is examination of the effect of GagPol production on cell cycle, and whether GagPol expression is able to alter cell growth. Looking further into the cell cycle is key in this investigation, as the cell cycle is connected with the expression of genes that are involved in ER stress and UPR activation, particularly ATF6 and CHOP which were observed to increase in expression as a response to the production of GagPol. It would be particularly interesting to examine which stages of the cell cycle are more productive in the context of LVV production. Looking at the cell cycle would also further illuminate details about cell growth, which is an important consideration given that the relationship between cell growth and cell size (and therefore protein content) is one with conditions that are evolutionarily optimised (Metzl-Raz et al., 2020). A decreased cell growth rate may increase cell size, which has previously been shown to be a result of cell cycle arrest (Zhurinsky et al., 2010; Neurohr et al., 2019). This could perturb transcription rates as a result, which will inevitably be detrimental for the production of GagPol. It has also previously been reported that temperature shift is capable of disturbing the cell cycle and as a result alters the properties of cellular factories (Torres et al., 2021).

It is also important to consider that protein production is highly variable across different stages of the cell cycle. Methods for increasing recombinant protein production in CHO cells by inhibiting progression through the cell cycle have led to an improvement in the specific productivity of cells by increasing the percentage of cells in G1 phase (Sunley and Butler, 2010). However, increasing protein production via controlled proliferation strategies is done so at the cost of cell growth, which could impact on GagPol production.

Following on from this, a further characteristic of interest to examine would be cell size during GagPol production. It has previously been reported that over-expression of mCherry leads to an increase in cell size, in addition to an increase in the capacity for transcription (Metzl-Raz et al., 2020). It was suggested that wild-type *S. cerevisiae* cells already transcribe highly-expressed genes at almost the maximum rates possible, and are therefore not capable of increasing the rate of transcription further. Whether this is the case for the production of GagPol must be further elucidated as this is an ectopic protein, and its limit of expression in HEK293T cells

is not known. It is still not fully known which processes limit the synthesis of GagPol protein in HEK293T cells.

Following observations that GagPol expression activated various cellular stresses in HEK293T cells (Chapter 4), further investigations were carried out to determine whether chemical inhibitors of cellular stresses were able to mitigate the toxic effects of GagPol production. In terms of potential targets for HEK293T cell manipulation that may enable increased expression of GagPol, work presented in Chapter 5.2 demonstrated that GagPol production can be improved by the chemical inhibition of apoptosis. Looking specifically at genetic targets that are of interest, Bcl-2 is an attractive target for the inhibition of apoptosis. Recent studies looking into the over-expression of Bcl-2 in the context of LVV production have enabled the stationary phase of the cell cycle to be extended by 48 hours (Sandhu and Al-Rubeai, 2009), with additional studies claiming an increase in the volumetric production of HEK293 cells of 53% (Formas-Oliveira et al., 2020). Further targets may include knocking-out pro-apoptotic factors such as Bax and Bak, an approach that has previously shown to enable resistance to shear stress and apoptosis in a HEK293 double knock-out cell line which supports recombinant protein production at large-scale (Arena et al., 2019).

Targets within the autophagy pathway that induce early stages of autophagy and inhibit the later stages of autophagy would be of value to examine further, as discussed in Section 5.4, especially considering the interactions between HIV-1 and autophagy during infection (Killian, 2012). Specific examples in inducing the earlier stages of autophagy might include over-expression of PI3K Vps34, which is required for phagophore formation (Weidberg et al., 2011). Given that HIV-1 Gag has been observed to localise on autophagosomal membranes as potential sites of assembly, increasing the production of these membranes by increasing autophagic flux could present an opportunity for increasing VLP production. However, synthesising specific membranes remains a challenge as biosynthesis of membrane proteins in the host is limited by the availability of lipids.

Various other studies have illustrated that over-expression of genes related to lipid biosynthesis as capable of improving HIV-Gag VLP production specifically, including

the targets NEDD8 (1.5-fold increase in VLPs), NEDD4L (3.3-fold increase in VLPs), UGCG (2.9-fold increase in VLPs), and CIT (2.4-fold increase in VLP production) (Lavado-Garcia et al., 2020; Lavado-Garcia et al., 2021). Through those studies, endocytosis, late endosomal pathways, and some members of the ESCRT were confirmed as bottlenecks in the production of VLPs. Further targets that have not yet been examined include increasing the availability of lipid rafts in HEK293T cells as GagPol has been found to assembly on lipid-raft-rich domains of the PM (Holm et al., 2003; Nguyen et al., 2000; Ono et al., 2005). In addition, making some cell-membrane associated proteins more abundant may have the potential to increase GagPol production, such as phosphatidylinositol-4,5-bisphosphate which is present on inner leaflet of plasma membrane, as the MA domain in GagPol associates specifically with this. Additionally, however quite laborious, designing a synthetic viral PR within GagPol in order to ensure it does not cleave host cell substrates may be of value too.

The limitations of this project include that this vector production system is focussed on synthetic GagPol (SYNGP), and these findings cannot necessarily be applied directly to HIV-1 GagPol. Similarly, the interactions that HIV-1 Gag and GagPol have with other cell types cannot be applied to the interactions between synthetic Gag and GagPol in HEK293T cells. The codon optimisation of SYNGP may mean that the Gag and GagPol polyproteins produced behave differently within a cell. There has been relatively little work undertaken on investigating how HIV-1 Gag and GagPol interact with HEK293T cells, likely due to the fact that HIV-1 normally targets CD4+ T-cells, microglial cells, and macrophages primarily (Naif 2013). It would be valuable to determine how HIV-1 GagPol alone interacts with a HEK293T cell, as this could then be applied to how LVVs interact with a HEK293T. This could help to determine whether removal of viral accessory genes in third generation LVVs (Figure 1.4) has an impact on how HEK293T cells tolerate viral vector production.

Future work looking at how other components of LVVs interact with HEK293T cellular biology would also be of importance, such as a system where the only viral protein produced is VSV-G. It is already known that VSV-G traffics to the PM for assembly via the ER and Golgi secretory pathway, however it has still not been defined how cellular stress due to production of this component can be relieved. This

would give a better picture of how LVV production in a cell occurs and the exact points of interaction with a HEK293T cell.

7 References

Abbasi-Malati, Z., Amiri, F., Mohammadipour, M., Roudkenar, M.H. (2019) HEK293 Cells Overexpressing Nuclear Factor E2-Related Factor-2 Improve Expression of Recombinant Coagulation Factor VII. Mol. Biotechnol., 61, 317–324

Adams CJ, Kopp MC, Larburu N, Nowak PR, Ali MMU. (2019) Structure and Molecular Mechanism of ER Stress Signalling by the Unfolded Protein Response Signal Activator IRE1. Front Mol Biosci. 2019 Mar 12;6:11. doi: 10.3389/fmolb.2019.00011. PMID: 30931312; PMCID: PMC6423427.

Adams LD, Tomasselli AG, Robbins P, Moss B, Heinrikson RL. (1992) HIV-1 protease cleaves actin during acute infection of human T-lymphocytes. AIDS Res Hum Retroviruses. 1992;8:291–295. doi: 10.1089/aid.1992.8.291

Aiuti, L. Biasco, S. Scaramuzza, F. Ferrua, M.P. Cicalese, C. Baricordi, F. Dionisio, A. Calabria, S. Giannelli, M.C. Castiello, (2013) Lentiviral hematopoietic stem cell gene therapy in patients with Wiskott-Aldrich syndrome. Science, 341 (2013), p. 1233151

Albertini, A. A. V., Baquero, E., Ferlin, A. & Gaudin, Y. (2012) Molecular and cellular aspects of rhabdovirus entry. Viruses 4, 117–139.

Alton E. W. F. W., Beekman J.M. , Boyd A.C., Brand J., Carlon M.S., Connolly M.M., Chan M., Conlon S., Davidson H.E., Davies J.C., (2017) Preparation for a first-in-man lentivirus trial in patients with cystic fibrosis. Thorax, 72 (2017), pp. 137

Arena, A.T.; Chou, B.; Harms, P.D.; Wong, A.W. (2019) An anti-apoptotic HEK293 cell line provides a robust and high titer platform for transient protein expression in bioreactors. mAbs, 11, 977–986

ASCGT (2021) Gene, Cell, & RNA Therapy Landscape, Q2 2021 Quarterly Data Report, available at; https://asgct.org/global/documents/asgct-pharma-intelligence-quarterly-report-july-20.aspx?_zs=sisac&_zl=Uu4h2

Atkins JF, Weiss RB, Gesteland RF. (1990) Ribosome gymnastics - degree of difficulty 9.5, style 10.0. Cell 62:413-423

Bacharach, E.; Gonsky, J.; Alin, K.; Orlova, M.; Goff, S.P. (2000) The Carboxy-Terminal Fragment of Nucleolin Interacts with the Nucleocapsid Domain of Retroviral Gag Proteins and Inhibits Virion Assembly. J. Virol. 2000, 74, 11027–11039

Backliwal, G.; Hildinger, M.; Chenuet, S.; Wulhfard, S.; De Jesus, M.; Wurm, F.M. (2008) Rational vector design and multi-pathway modulation of HEK 293E cells yield recombinant antibody titers exceeding 1 g/l by transient transfection under serum-free conditions. Nucleic Acids Res., 36, e96.

Baek, E., Kim, C. L., Kim, M. G., Lee, J. S., & Lee, G. M. (2016). Chemical inhibition of autophagy: examining its potential to increase the specific productivity of recombinant CHO cell lines. Biotechnology and Bioengineering, 113(9), 1953– 1961. https://doi.org/10.1002/bit.25962

Ballas, C, Johnson, TT and Cornetta, K (2005). Harvest Timing and Media Composition Effects on Lentiviral Vector Production. Presented at the 8th Annual Meeting of the ASGT, 1 June–5 June 2005, St. Louis, MO.

Banki K., Hutter E., Gonchoroff N. J., Perl A (1998) Molecular ordering in HIV-induced apoptosis. Oxidative stress, activation of caspases, and cell survival are regulated by transaldolase. The Journal of Biological Chemistry. 1998;273(19):11944–11953. doi: 10.1074/jbc.273.19.11944

Barrett, P. N., Mundt, W., Kistner, O. & Howard, M. K. (2009) Vero cell platform in vaccine production: moving towards cell culture-based viral vaccines. Expert Rev Vaccines 8, 607-618

Barry SC, Harder B, Brzezinski M, Flint LY, Seppen J, Osborne WR. (2001) Lentivirus vectors encoding both central polypurine tract and posttranscriptional regulatory element provide enhanced transduction and transgene expression. Hum Gene Ther. 2001 Jun 10;12(9):1103-8. doi: 10.1089/104303401750214311. PMID: 11399231.

Batonick, M.; Favre, M.; Boge, M.; Spearman, P.; Höning, S.; Thali, M. (2005) Interaction of HIV-1 Gag with the clathrin-associated adaptor AP-2. Virology 2005, 342, 190–200

Bauler, M., Roberts, J. K., Wu, C. C., Fan, B., Ferrara, F., Yip, B. H., Diao, S., Kim, Y. I., Moore, J., Zhou, S., Wielgosz, M. M., Ryu, B., & Throm, R. E. (2019) Production of Lentiviral Vectors Using Suspension Cells Grown in Serum-free Media. Molecular therapy. Methods & clinical development, 17, 58–68.

Baum, E. Z., Bebernitz, G. A., and Gluzman, Y. (1990) Isolation of mutants of human immunodeficiency virus protease based on the toxicity of the enzyme in Escherichia coli. Proc. Natl. Acad. Sci.U. S. A.87,5573–557717.

Beauséjour, Y.; Tremblay, M.J. (2004) Interaction between the cytoplasmic domain of ICAM-1 and Pr55Gag leads to acquisition of host ICAM-1 by human immunodeficiency virus type 1. J. Virol. 2004, 78, 11916–11925.

Belardinelli, J. M., & Jackson, M. (2017). Green Fluorescent Protein as a protein localization and topological reporter in mycobacteria. Tuberculosis (Edinburgh, Scotland), 105, 13–17. https://doi.org/10.1016/j.tube.2017.04.001

Bendjennat, M.; Saffarian, S. (2016) The Race against Protease Activation Defines the Role of ESCRTs in HIV Budding. PLoS Pathog. 2016, 12, e1005657

Bernales, S., McDonald, K. L., and Walter, P. (2006). Autophagy counterbalances endoplasmic reticulum expansion during the unfolded protein response. PLoS Biol. 4:e423. doi: 10.1371/journal.pbio.0040423

Bertolotti A, Zhang Y, Hendershot LM, Harding HP, Ron D. (2000) Dynamic interaction of BiP and ER stress transducers in the unfolded-protein response. Nat Cell Biol. 2000 Jun;2(6):326-32. doi: 10.1038/35014014. PMID: 10854322.

Biffi A, Bartolomae CC, Cesana D, Cartier N, Aubourg P, Ranzani M, Cesani M, Benedicenti F, Plati T, Rubagotti E, Merella S, Capotondo A, Sgualdino J, Zanetti G, von Kalle C, Schmidt M, Naldini L, Montini E. (2011) Lentiviral vector common integration sites in preclinical models and a clinical trial reflect a benign integration bias and not oncogenic selection. Blood. May 19;117(20):5332-9

Biffi, E. Montini, L. Lorioli, M. Cesani, F. Fumagalli, T. Plati, C. Baldoli, S. Martino, A. Calabria, S. Canale, (2013) Lentiviral hematopoietic stem cell gene therapy benefits metachromatic leukodystrophy. Science, 341 (2013), p. 1233158

Blondeel EJM, Ho R, Schulze S, (2016) An omics approach to rational feed: enhancing growth in CHO cultures with NMR metabolomics and 2D-DIGE proteomics. J Biotechnol. 2016;234:127–138.

Blot G, Janvier K, Le Panse S, Benarous R, Berlioz-Torrent C. (2003) Targeting of the human immunodeficiency virus type 1 envelope to the trans-Golgi network through binding to TIP47 is required for env incorporation into virions and infectivity. J Virol. 2003 Jun;77(12):6931-45. doi: 10.1128/jvi.77.12.6931-6945.2003. PMID: 12768012; PMCID: PMC156179.

Bordignon C, Notarangelo LD, Nobili N, Ferrari G, Casorati G, Panina P, Mazzolari E, Maggioni D, Rossi C, Servida P, Ugazio AG, Mavilio F. (1995) Gene therapy in peripheral blood lymphocytes and bone marrow for ADA- immunodeficient patients. Science. Oct 20;270(5235):470-5. doi: 10.1126/science.270.5235.470

Bouamr F, Scarlata S, Carter CA, (2003) Role of myristylation in HIV-1 Gag assembly. Biochemistry 42(21):6408–6417

Braasch K, Kryworuchko M, Piret JM. (2021) Autophagy-inducing peptide increases CHO cell monoclonal antibody production in batch and fed-batch cultures. Biotechnol

Bioeng. May;118(5):1876-1883. doi: 10.1002/bit.27703. Epub 2021 Feb 19. PMID: 33543765

Braaten, D., & Luban, J. (2001). Cyclophilin A regulates HIV-1 infectivity, as demonstrated by gene targeting in human T cells. The EMBO journal, 20(6), 1300–1309. https://doi.org/10.1093/emboj/20.6.1300

Brejc K, Sixma TK, Kitts PA, Kain SR, Tsien RY, Ormo M, Remington SJ. (1997) Structural basis for dual excitation and photoisomerization of the Aequorea victoria green fluorescent protein. Proc Natl Acad Sci U S A. 1997;94:2306–2311.

Briggs, J. A. & Krausslich, H. G. (2011). The molecular architecture of HIV. Journal of Molecular Biology, 410, 491-500.

Broussau S, Jabbour N, Lachapelle G, Durocher Y, Tom R, Transfiguracion J, Gilbert R, Massie B. (2008) Inducible packaging cells for large-scale production of lentiviral vectors in serum-free suspension culture. Mol Ther. 2008 Mar;16(3):500-7. doi: 10.1038/sj.mt.6300383. Epub 2008 Jan 8. PMID: 18180776.

Bukrinskaya, A. (2007) HIV-1 matrix protein: A mysterious regulator of the viral life cycle. Virus Res. 2007, 124, 1–11.

Bulcha, J.T., Wang, Y., Ma, H. (2021) Viral vector platforms within the gene therapy landscape. Sig Transduct Target Ther 6, 53 https://doi.org/10.1038/s41392-021-00487-6

Burns JC, Friedmann T, Driever W, Burrascano M, Yee JK. (1993) Vesicular stomatitis virus G glycoprotein pseudotyped retroviral vectors: concentration to very high titer and efficient gene transfer into mammalian and nonmammalian cells. Proc Natl Acad Sci USA 1993; 90: 8033–8037.

Burns, J. C., Friedmann, T., Driever, W., Burrascano, M., & Yee, J.-K. (1993). Vesicular Stomatitis Virus G Glycoprotein Pseudotyped Retroviral Vectors: Concentration to Very High Titer and Efficient Gene Transfer into Mammalian and

Nonmammalian Cells. Proceedings of the National Academy of Sciences of the United States of America, 90(17), 8033–8037

Bushman FD. (2020) Retroviral Insertional Mutagenesis in Humans: Evidence for Four Genetic Mechanisms Promoting Expansion of Cell Clones. Mol Ther. 2020 Feb 5;28(2):352-356. doi: 10.1016/j.ymthe.2019.12.009. Epub 2020 Jan 7. PMID: 31951833; PMCID: PMC7001082.

Bussienne, C., Marquet, R., Paillart, J. C., & Bernacchi, S. (2021). Post-Translational Modifications of Retroviral HIV-1 Gag Precursors: An Overview of Their Biological Role. International journal of molecular sciences, 22(6), 2871. https://doi.org/10.3390/ijms22062871

Buttgereit F., Brand M. D., (1995) A hierarchy of ATP-consuming processes in mammalian cells. Biochem. J., 312, pp. 163

Cabrera-Rodríguez R, Pérez-Yanes S, Estévez-Herrera J, Márquez-Arce D, Cabrera C, Espert L, Blanco J, Valenzuela-Fernández A. (2021) The Interplay of HIV and Autophagy in Early Infection. Front Microbiol. Apr 28;12:661446. doi: 10.3389/fmicb.2021.661446. PMID: 33995324; PMCID: PMC8113651.

Cain K, Peters S, Hailu H, Sweeney B, Stephens P, Heads J, Sarkar K, Ventom A, Page C, Dickson A. (2013) A CHO cell line engineered to express XBP1 and ERO1-Lα has increased levels of transient protein expression. Biotechnol Prog. 2013 May-Jun;29(3):697-706. doi: 10.1002/btpr.1693. Epub 2013 Mar 20. PMID: 23335490.

Campbell SM, Crowe SM, Mak J. (2001) Lipid rafts and HIV-1: from viral entry to assembly of progeny virions. J Clin Virol. 2001 Oct;22(3):217-27. doi: 10.1016/s1386-6532(01)00193-7. PMID: 11564586.

Camus, G.; Segura-Morales, C.; Molle, D.; Lopez-Verges, S.; Begon-Pescia, C.; Cazevieille, C.; Schu, P.; Bertrand, E.; Berlioz-Torrent, C.; Basyuk, E. (2007) The Clathrin Adaptor Complex AP-1 Binds HIV-1 and MLV Gag and Facilitates Their BuddingD. Mol. Biol. Cell 2007, 18, 11.

Cao SS, Kaufman RJ. (2014) Endoplasmic reticulum stress and oxidative stress in cell fate decision and human disease. Antioxid Redox Signal. 2014 Jul 20;21(3):396-413. doi: 10.1089/ars.2014.5851. Epub 2014 Jun 12. PMID: 24702237; PMCID: PMC4076992.

Caron AL, Biaggio RT, Swiech K. (2018) Strategies to Suspension Serum-Free Adaptation of Mammalian Cell Lines for Recombinant Glycoprotein Production. Methods Mol Biol. 2018;1674:75-85. doi: 10.1007/978-1-4939-7312-5_6. PMID: 28921429.

Cesana, D.; Ranzani, M.; Volpin, M.; Bartholomae, C.; Duros, C.; Artus, A.; Merella, S.; Benedicenti, F.; Sergi Sergi, L.; Sanvito, F.; (2014) Uncovering and dissecting the genotoxicity of self-inactivating lentiviral vectors in vivo. Mol. Ther 2014, 22, 774–785

Chatel-Chaix, L., Clément, J. F., Martel, C., Bériault, V., Gatignol, A., DesGroseillers, L., & Mouland, A. J. (2004). Identification of Staufen in the human immunodeficiency virus type 1 Gag ribonucleoprotein complex and a role in generating infectious viral particles. Molecular and cellular biology, 24(7), 2637–2648.

Checkley, M. A., Luttge, B. G., & Freed, E. O. (2011). HIV-1 envelope glycoprotein biosynthesis, trafficking, and incorporation. Journal of molecular biology, 410(4), 582–608. https://doi.org/10.1016/j.jmb.2011.04.042

Chen YH, Pallant C, Sampson CJ, Boiti A, Johnson S, Brazauskas P, Hardwicke P, Marongiu M, Marinova VM, Carmo M, Sweeney NP, Richard A, Shillings A, Archibald P, Puschmann E, Mouzon B, Grose D, Mendez-Tavio M, Chen MX, Warr SRC, Senussi T, Carter PS, Baker S, Jung C, Brugman MH, Howe SJ, Vink CA. (2020) Rapid Lentiviral Vector Producer Cell Line Generation Using a Single DNA Construct. Mol Ther Methods Clin Dev. Aug 14;19:47-57. doi: 10.1016/j.omtm.2020.08.011

Chin CL, Goh JB, Srinivasan H, Liu KI, Gowher A, Shanmugam R, Lim HL, Choo M, Tang WQ, Tan AH, Nguyen-Khuong T, Tan MH, Ng SK. (2019) A human expression

system based on HEK293 for the stable production of recombinant erythropoietin. Sci Rep. Nov 14;9(1):16768. doi: 10.1038/s41598-019-53391-z

Choi, Y., Bowman, J.W. & Jung, J.U. (2018) Autophagy during viral infection — a double-edged sword. Nat Rev Microbiol 16, 341–354 https://doi.org/10.1038/s41579-018-0003-6

Chuck AS, Clarke MF, Palsson BO., (1996) Retroviral infection is limited by Brownian motion. Hum GENE Ther Y. 1996;7(13):1527–34. https://doi.org/10.1089/hum.1996.7.13-1527.

Chukkapalli V, Hogue IB, Boyko V, Hu W-S, Ono A (2008) Interaction between HIV-1 Gag matrix domain and phosphatidylinositol-(4,5)-bisphosphate is essential for efficient Gag-membrane binding. J Virol 82:2405–2417.

Chun T. W., L. Carruth, D. Finzi, X. Shen, J.A. DiGiuseppe, H. Taylor, M. Hermankova, K. Chadwick, J. Margolick, T.C. Quinn, Y.H. Kuo, R. Brookmeyer, M.A. Zeiger, P. Barditch-Crovo, R.F. Siliciano (1997) Quantification of latent tissue reservoirs and total body viral load in HIV-1 infection. Nature, 387 (1997), pp. 183-188

Chun, TW., Carruth, L., Finzi, D. (1997) Quantification of latent tissue reservoirs and total body viral load in HIV-1 infection. Nature 387, 183–188. https://doi.org/10.1038/387183a0

Ci Y, Yang Y, Xu C, Shi L. (2018) Vesicular stomatitis virus G protein transmembrane region is crucial for the hemi-fusion to full fusion transition. Sci Rep. Jul 13;8(1):10669. doi: 10.1038/s41598-018-28868-y

Cimarelli, A.; Luban, J. (1999) Translation elongation factor 1-alpha interacts specifically with the human immunodeficiency virus type 1 Gag polyprotein. J. Virol. 1999, 73, 5388–5401.

Cimarelli, A.; Sandin, S.; Höglund, S.; Luban, J. (2000) Basic Residues in Human Immunodeficiency Virus Type 1 Nucleocapsid Promote Virion Assembly via Interaction with RNA. J. Virol., 74, 3046–3057

Ciuffi A. (2008) Mechanisms governing lentivirus integration site selection. Curr. Gene Ther. 2008;8(6):419–429

Clavel, François, Mammano, Fabrizio. (2010). Role of Gag in HIV Resistance to Protease Inhibitors. Viruses. 2. 1411-26. 10.3390/v2071411.

Cooper, J.; Liu, L.; Woodruff, E.A.; Taylor, H.E.; Goodwin, J.S.; D'Aquila, R.T.; Spearman, P.; Hildreth, J.E.K.; Dong, X., (2011) Filamin A protein interacts with human immunodeficiency virus type 1 Gag protein and contributes to productive particle assembly. J. Biol. Chem. 2011, 286, 28498–28510.

Coroadinha AS, Schucht R, Gama-Norton L, Wirth D, Hauser H, Carrondo MJ. (2006) The use of recombinase mediated cassette exchange in retroviral vector producer cell lines: predictability and efficiency by transgene exchange. J Biotechnol. Jul 13;124(2):457-68. doi: 10.1016/j.jbiotec.2006.01.037

Cosset, F.-L., Takeuchi, Y., Battini, J.-L., Weiss, R.A. & Collins, M.K. (1995) High-titer packaging cells producing recombinant retroviruses resistant to human serum. J. Virol. 69, 7430–7436

Cronin, J., Zhang, X. Y. & Reiser, J. (2005) Altering the tropism of lentiviral vectors through pseudotyping. Curr. Gene Ther. 5, 387–398

Cureton, D. K., Massol, R. H., Saffarian, S., Kirchhausen, T. L. & Whelan, S. P. (2009) Vesicular stomatitis virus enters cells through vesicles incompletely coated with clathrin that depend upon actin for internalization. PLoS Pathog. 5, e1000394

Dannull, J.; Surovoy, A.; Jung, G.; Moelling, K. (1994) Specific binding of HIV-1 nucleocapsid protein to PSI RNA in vitro requires N-terminal zinc finger and flanking basic amino acid residues. EMBO J., 13, 1525–1533.

Daussy CF, Galais M, Pradel B, Robert-Hebmann V, Sagnier S, Pattingre S, Biard-Piechaczyk M, Espert L. (2020) HIV-1 Env induces pexophagy and an oxidative stress leading to uninfected CD4+ T cell death. Autophagy. 17(9):2465-2474. doi: 10.1080/15548627.2020.1831814. Epub 2020 Oct 19. PMID: 33073673; PMCID: PMC8496731.

Davie JR. (2003) Inhibition of histone deacetylase activity by butyrate. J Nutr. 2003 Jul;133(7 Suppl):2485S-2493S. doi: 10.1093/jn/133.7.2485S. PMID: 12840228.

Davis, A.J., Carr, J.M., Bagley, C.J. (2008). Human Immunodeficiency Virus type-1 reverse transcriptase exists as post-translationally modified forms in virions and cells. Retrovirology 5, 115 https://doi.org/10.1186/1742-4690-5-115

Dean, R., Jensen, I., Cyr, P., Miller, B., Maru, B., Sproule, D. M., Feltner, D. E., Wiesner, T., Malone, D. C., Bischof, M., Toro, W., & Dabbous, O. (2021). An updated cost-utility model for onasemnogene abeparvovec (Zolgensma®) in spinal muscular atrophy type 1 patients and comparison with evaluation by the Institute for Clinical and Effectiveness Review (ICER). Journal of market access & health policy, 9(1), 1889841. https://doi.org/10.1080/20016689.2021.1889841

DeBoer, J.; Madson, C.J.; Belshan, M. (2016) Cyclophilin B enhances HIV-1 infection. Virology 2016, 489, 282–291.

Demaison, C. (2002) High-level transduction and gene expression in hematopoietic repopulation cells using a human immunodeficiency virus type 1–based lentiviral vector containing an internal spleen focus forming virus promoter. Hum. Gene Ther. 13, 803–813

DePolo NJ, Reed JD, Sheridan PL, Townsend K, Sauter SL, Jolly DJ, Dubensky TW Jr. (2000) VSV-G pseudotyped lentiviral vector particles produced in human cells are inactivated by human serum. Mol Ther. Sep;2(3):218-22. doi: 10.1006/mthe.2000.0116

Deshmane S. L., Mukerjee R., Fan S., (2009) Activation of the oxidative stress pathway by HIV-1 Vpr leads to induction of hypoxia-inducible factor 1α expression. The Journal of Biological Chemistry. 2009;284(17):11364–11373. doi: 10.1074/jbc.m809266200.

Dharan, A., Talley, S., Tripathi, A., Mamede, J. I., Majetschak, M., Hope, T. J., & Campbell, E. M. (2016). KIF5B and Nup358 Cooperatively Mediate the Nuclear Import of HIV-1 during Infection. PLoS pathogens, 12(6), e1005700. https://doi.org/10.1371/journal.ppat.1005700

Dikalov, S. I., & Harrison, D. G. (2014). Methods for detection of mitochondrial and cellular reactive oxygen species. Antioxidants & redox signaling, 20(2), 372–382. https://doi.org/10.1089/ars.2012.4886

Ding P, Kharytonchyk S, Waller A, Mbaekwe U, Basappa S, Kuo N, Frank HM, Quasney C, Kidane A, Swanson C, Van V, Sarkar M, Cannistraci E, Chaudhary R, Flores H, Telesnitsky A, Summers MF. (2020) Identification of the initial nucleocapsid recognition element in the HIV-1 RNA packaging signal. Proc Natl Acad Sci U S A. 2020 Jul 28;117(30):17737-17746. doi: 10.1073/pnas.2008519117. Epub 2020 Jul 9. PMID: 32647061; PMCID: PMC7395439.

Dochi T, Nakano T, Inoue M, Takamune N, Shoji S, Sano K, Misumi S. (2014) Phosphorylation of human immunodeficiency virus type 1 capsid protein at serine 16, required for peptidyl-prolyl isomerase-dependent uncoating, is mediated by virion-incorporated extracellular signal-regulated kinase 2. J Gen Virol. May;95(Pt 5):1156-1166. doi: 10.1099/vir.0.060053-0

Dong, X.; Li, H.; Derdowski, A.; Ding, L.; Burnett, A.; Chen, X.; Peters, T.R.; Dermody, T.S.; Woodruff, E.; Wang, J.-J.; (2005) AP-3 directs the intracellular trafficking of HIV-1 Gag and plays a key role in particle assembly. Cell 2005, 120, 663–674.

Dooley CT, Dore TM, Hanson GT, Jackson WC, Remington SJ & Tsien RY (2004) Imaging dynamic redox changes in mammalian cells with green fluorescent protein indicators. J Biol Chem 279, 22284–22293.

Dubinsky AN, (2014) Let-7 coordinately suppresses components of the amino acid sensing pathway to repress mTORC1 and induce autophagy. Cell Metab. 2014;20:626–638. doi: 10.1016/j.cmet.2014.09.001

Dubois, N.; Khoo, K.K.; Ghossein, S.; Seissler, T.; Wolff, P.; McKinstry, W.J.; Mak, J.; Paillart, J.-C.; Marquet, R.; Bernacchi, S. (2018) The C-terminal p6 domain of the HIV-1 Pr55Gag precursor is required for specific binding to the genomic RNA. RNA Biol., 15, 923–936.

Dumont, J., Euwart, D., Mei, B., Estes, S., & Kshirsagar, R. (2016). Human cell lines for biopharmaceutical manufacturing: history, status, and future perspectives. Critical reviews in biotechnology, 36(6), 1110–1122

Dussupt, V.; Javid, M.P.; Abou-Jaoudé, G.; Jadwin, J.A.; de La Cruz, J.; Nagashima, K.; Bouamr, F., (2009) The nucleocapsid region of HIV-1 Gag cooperates with the PTAP and LYPXnL late domains to recruit the cellular machinery necessary for viral budding. PLoS Pathog. 2009, 5, e1000339

Dussupt, V.; Sette, P.; Bello, N.F.; Javid, M.P.; Nagashima, K.; Bouamr, F. (2011) Basic residues in the nucleocapsid domain of Gag are critical for late events of HIV-1 budding. J. Virol. 2011, 85, 2304–2315.

El Meshri, S.E.; Boutant, E.; Mouhand, A.; Thomas, A.; Larue, V.; Richert, L.; Vivet-Boudou, V.; Mély, Y.; Tisné, C.; Muriaux, D.; (2018) The NC domain of HIV-1 Gag contributes to the interaction of Gag with TSG101. Biochim. Biophys. Acta BBA-Gen. Subj. 2018, 1862, 1421–1431.

El Meshri, S.E.; Dujardin, D.; Godet, J.; Richert, L.; Boudier, C.; Darlix, J.L.; Didier, P.; Mély, Y.; De Rocquigny, H. (2015) Role of the Nucleocapsid Domain in HIV-1

Gag Oligomerization and Trafficking to the Plasma Membrane: A Fluorescence Lifetime Imaging Microscopy Investigation. J. Mol. Biol., 427, 1480–1494.

Elegheert, J., Behiels, E., Bishop, B., (2018) Lentiviral transduction of mammalian cells for fast, scalable and high-level production of soluble and membrane proteins. Nat Protoc 13, 2991–3017 https://doi.org/10.1038/s41596-018-0075-9

Elias, C.B.; Carpentier, E.; Durocher, Y.; Bisson, L.; Wagner, R.; Kamen, A. (2003) Improving Glucose and Glutamine Metabolism of Human HEK 293 and Trichoplusiani Insect Cells Engineered To Express a Cytosolic Pyruvate Carboxylase Enzyme. Biotechnol. Prog., 19, 90–97

Elmore S. (2007) Apoptosis: a review of programmed cell death. Toxicol Pathol. 2007;35:495–516. doi: 10.1080/01926230701320337

Engedal N., Mari M., Reggiori F., (2018) Chloroquine inhibits autophagic flux by decreasing autophagosome-lysosome fusion, Autophagy, 14:8, 1435-1455, DOI: 10.1080/15548627.2018.1474314

Fan Y, Ley D, Andersen MR. (2018) Fed-Batch CHO Cell Culture for Lab-Scale Antibody Production. Methods Mol Biol. 2018;1674:147-161. doi: 10.1007/978-1-4939-7312-5_12. PMID: 28921435.

Feldman SA, Farrell KB, Murthy RK, Russ JL, Eiden MV. (2004) Identification of an extracellular domain within the human PiT2 receptor that is required for amphotropic murine leukemia virus binding. J Virol. 2004 Jan;78(2):595-602. doi: 10.1128/jvi.78.2.595-602.2004. PMID: 14694091; PMCID: PMC368782.

Fernandes, J., Jayaraman, B., & Frankel, A. (2012). The HIV-1 Rev response element: an RNA scaffold that directs the cooperative assembly of a homo-oligomeric ribonucleoprotein complex. RNA biology, 9(1), 6–11. https://doi.org/10.4161/rna.9.1.18178

Fernandez, J.; Portilho, D.M.; Danckaert, A.; Munier, S.; Becker, A.; Roux, P.; Zambo, A.; Shorte, S.; Jacob, Y.; Vidalain, P.-O.; (2015) Microtubule-associated proteins 1 (MAP1) promote human immunodeficiency virus type I (HIV-1) intracytoplasmic routing to the nucleus. J. Biol. Chem. 2015, 290, 4631–4646.

Figueroa Jr., B., Ailor, E., Osborne, D., Hardwick, J. M., Reff, M., & Betenbaugh, M. J. (2007). Enhanced cell culture performance using inducible anti-apoptotic genes E1B-19K and Aven in the production of a monoclonal antibody with Chinese Hamster Ovary cells. Biotechnology and Bioengineering, 97, 877–892. https://doi.org/10.1002/bit.21222

Finkelshtein D, Werman A, Novick D, Barak S, Rubinstein M. (2013) LDL receptor and its family members serve as the cellular receptors for vesicular stomatitis virus., Proc Natl Acad Sci U S A, 2013, vol. 110 18 (pg. 7306-7311)

Fischer S., Handrick R., Otte K., (2015) The art of CHO cell engineering: a comprehensive retrospect and future perspectives Biotechnol Adv, 33 (8) (2015), pp. 1878-1896

Floderer, C., Masson, JB., Boilley, E., Georgeault S., Merida P., El Beheiry M., Dahan M., Roingeard P., Sibarita J.-B., Favard C., Muriaux D. (2018) Single molecule localisation microscopy reveals how HIV-1 Gag proteins sense membrane virus assembly sites in living host CD4 T cells. Sci Rep 8, 16283 https://doi.org/10.1038/s41598-018-34536-y

Follenzi, A., Ailles, L. E., Bakovic, S., Geuna, M. & Naldini, L. (2000) Gene transfer by lentiviral vectors is limited by nuclear translocation and rescued by HIV-1 pol sequences. Nature Genetics, 25, 217-22

Formas-Oliveira, A.S.; Basílio, J.S.; Rodrigues, A.F.; Coroadinha, A.S. (2020) Overexpression of ER Protein Processing and Apoptosis Regulator Genes in Human Embryonic Kidney 293 Cells Improves Gene Therapy Vectors Production. Biotechnol. J., 15, e1900562.

Freed EO. (1998) HIV-1 gag proteins: diverse functions in the virus life cycle. Virology 1998, 251:1-15.

Frenzel, A.; Hust, M.; Schirrmann, T. (2013) Expression of Recombinant Antibodies. Front. Immunol., 4, 217

Fulda, S., Debatin, KM. (2006) Extrinsic versus intrinsic apoptosis pathways in anticancer chemotherapy. Oncogene 25, 4798–4811. https://doi.org/10.1038/sj.onc.1209608

Full, T., Zufferey, R., Kelly, M., Mandel, R. J., Nguyen, M., Trono, D. & Naldini, L. (1998) A Third-Generation Lentivirus Vector with a Conditional Packaging System. Journal of Virology, 72, 8463-8471.

Gaines, C.R., Tkacik, E., Rivera-Oven, A., Somani, P., Achimovich, A., Alabi, T., Zhu, A., Getachew, N., Yang, A.L., McDonough, M., (2018) HIV-1 Matrix Protein Interactions with tRNA: Implications for Membrane Targeting. J. Mol. Biol., 430, 2113–2127.

Gantenbein B, Tang S, Guerrero J, Higuita-Castro N, Salazar-Puerta AI, Croft AS, Gazdhar A and Purmessur D (2020) Non-viral Gene Delivery Methods for Bone and Joints. Front. Bioeng. Biotechnol. 8:598466. doi: 10.3389/fbioe.2020.598466

Gao, W.; Li, M.; Zhang, J. (2014) Tandem immunoprecipitation approach to identify HIV-1 Gag associated host factors. J. Virol. Methods 2014, 203, 116–119

Garnier L, Bowzard JB, Wills JW. (1998) Recent advances and remaining problems in HIV assembly.AIDS 1998, 12:S5-S16.

Garrus, J.E.; von Schwedler, U.K.; Pornillos, O.W.; Morham, S.G.; Zavitz, K.H.; Wang, H.E.; Wettstein, D.A.; Stray, K.M.; Côté, M.; Rich, R.L.; (2001) Tsg101 and the vacuolar protein sorting pathway are essential for HIV-1 budding. Cell 2001, 107, 55–65

Gawlitzek, M.; Valley, U.; Wagner, R. (1998) Ammonium ion and glucosamine dependent increases of oligosaccharide complexity in recombinant glycoproteins secreted from cultivated BHK-21 cells. Biotechnol. Bioeng.57, 518–528.

Gesteland RF, Weiss RB, Atkins JF, (1992) Recoding: Reprogrammed genetic decoding. Science 257:1640-1643

Ghanam, R.H.; Fernandez, T.F.; Fledderman, E.L.; Saad, J.S. (2010) Binding of calmodulin to the HIV-1 matrix protein triggers myristate exposure. J. Biol. Chem. 2010, 285, 41911–41920. [CrossRef] [PubMed]

Ghoujal B, Milev MP, Ajamian L, Abel K, Mouland AJ. (2012) ESCRT-II's involvement in HIV-1 genomic RNA trafficking and assembly. Biol Cell. Dec;104(12):706-21. doi: 10.1111/boc.201200021

Ghoujal, B.; Milev, M.P.; Ajamian, L.; Abel, K.; Mouland, A.J. (2012) ESCRT-II's involvement in HIV-1 genomic RNA trafficking and assembly. Biol. Cell 2012, 104, 706–721

Glick, D., Barth, S., & Macleod, K. F. (2010) Autophagy: cellular and molecular mechanisms. The Journal of pathology, 221(1), 3–12. https://doi.org/10.1002/path.2697

Goergen, J.L.; Marc, A.; Engasser, J.M. (1994) Influence of lactate and ammonia on the death rate of hybridoma. In Animal Cell Technology; Spier, R.E., Griffiths, J.B., Berthold, W., Eds.; Butterworth-Heinemann: Oxford, UK,; pp. 161–163.

Goochee, C.F.; Gramer, M.J.; Andersen, D.C.; Bahr, J.B.; Rasmussen, J.R. (1991) The Oligosaccharides of Glycoproteins: Bioprocess Factors Affecting Oligosaccharide Structure and their Effect on Glycoprotein Properties. Bio/Technology, 9, 1347–1355.

Gossen M, Bujard H. (1992) Tight control of gene expression in mammalian cells by tetracycline-responsive promoters. Proc Natl Acad Sci U S A. Jun 15;89(12):5547-51. doi: 10.1073/pnas.89.12.5547

Gossen M, Freundlieb S, Bender G, Müller G, Hillen W, Bujard H. (1995) Transcriptional activation by tetracyclines in mammalian cells. Science. Jun 23;268(5218):1766-9. doi: 10.1126/science.7792603

Grammatikos, S.I.; Valley, U.; Nimtz, M.; Conradt, H.S.; Wagner, R. (1998) Intracellular UDP-N-Acetylhexosamine Pool Affects N-Glycan Complexity: A Mechanism of Ammonium Action on Protein Glycosylation. Biotechnol. Prog., 14, 410–419.

Grandchamp, N., Henriot, D., Philippe, S., Amar, L., Ursulet, S., Serguera, C., Mallet, J., & Sarkis, C. (2011). Influence of insulators on transgene expression from integrating and non-integrating lentiviral vectors. Genetic vaccines and therapy, 9(1), 1. https://doi.org/10.1186/1479-0556-9-1

Groppelli E, Len AC, Granger LA, Jolly C (2014) Retromer Regulates HIV-1 Envelope Glycoprotein Trafficking and Incorporation into Virions. PLOS Pathogens 10(11): e1004518. https://doi.org/10.1371/journal.ppat.1004518

Gu S, Chen C, Jiang X, Zhang Z. (2016). ROS-mediated endoplasmic reticulum stress and mitochondrial dysfunction underlie apoptosis induced by resveratrol and arsenic trioxide in A549 cells. Chemico-Biological Interactions 245, 100–109.

Guo FJ, Liu Y, Zhou J, Luo S, Zhao W, Li X, Liu C. (2012) XBP1S protects cells from ER stress-induced apoptosis through Erk1/2 signaling pathway involving CHOP. Histochem Cell Biol. 2012 Sep;138(3):447-60. PMID: 22669460.

Gupta, K.; Ott, D.; Hope, T.J.; Siliciano, R.F.; Boeke, J.D. (2000) A Human Nuclear Shuttling Protein That Interacts with Human Immunodeficiency Virus Type 1 Matrix Is Packaged into Virions. J. Virol. 2000, 74, 11811–11824.

Gupta, P.; Singhal, P.K.; Rajendrakumar, P.; Padwad, Y.; Tendulkar, A.V.; Kalyanaraman, V.S.; Schmidt, R.E.; Srinivasan, A.; Mahalingam, S. (2011) Mechanism of Host Cell MAPK/ERK-2 Incorporation into Lentivirus Particles: Characterization of the Interaction between MAPK/ERK-2 and Proline-Rich-Domain Containing Capsid Region of Structural Protein Gag. J. Mol. Biol. 2011, 410, 681–697

Hanson GT, Aggeler R, Oglesbee D, Cannon M, Capaldi RA, Tsien RY & Remington SJ (2004) Investigating mitochondrial redox potential with redox-sensitive green fluorescent protein indicators.

He, Y., Sun, S., Sha, H., Liu, Z., Yang, L., Xue, Z., Chen, H., & Qi, L. (2010). Emerging roles for XBP1, a sUPeR transcription factor. Gene expression, 15(1), 13–25. https://doi.org/10.3727/105221610x12819686555051

Heim R, Tsien RY. (1996) Engineering green fluorescent protein for improved brightness, longer wavelengths and fluorescence resonance energy transfer. Curr Biol. 1996;6:178–182.

Henry, O.; Durocher, Y. (2011) Enhanced glycoprotein production in HEK-293 cells expressing pyruvate carboxylase. Metab. Eng., 13, 499–507

Heo, W. D., Inoue, T., Park, W. S., Kim, M. L., Park, B. O., Wandless, T. J., & Meyer, T. (2006). PI(3,4,5)P3 and PI(4,5)P2 lipids target proteins with polybasic clusters to the plasma membrane. Science (New York, N.Y.), 314(5804), 1458–1461

Hermida-Matsumoto, L., & Resh, M. D. (2000). Localization of human immunodeficiency virus type 1 Gag and Env at the plasma membrane by confocal imaging. Journal of virology, 74(18), 8670–8679

Higashimoto, T., Urbinati, F., Perumbeti, A. (2007). The woodchuck hepatitis virus post-transcriptional regulatory element reduces readthrough transcription from retroviral vectors. Gene Ther 14, 1298–1304. https://doi.org/10.1038/sj.gt.3302979

Hirota M, Kitagaki M, Itagaki H, Aiba S. (2006) Quantitative measurement of spliced XBP1 mRNA as an indicator of endoplasmic reticulum stress. J Toxicol Sci. May;31(2):149-56. doi: 10.2131/jts.31.149. PMID: 16772704.
Hollien, J., and Weissman, J. S. (2006) Decay of endoplasmic reticulum-localized mRNAs during the unfolded protein response. Science 313, 104–107. doi: 10.1126/science.1129631

Holm K., Weclewicz K., Hewson R., Suomalainen M. (2003) Human immunodeficiency virus type 1 assembly and lipid rafts: Pr55(gag) associates with membrane domains that are largely resistant to Brij98 but sensitive to Triton X-100. J. Virol. 77:4805–4817

Honer B, Shoeman RL, Traub P., (1991) Human immunodeficiency virus type 1 protease microinjected into cultured human skin fibroblasts cleaves vimentin and affects cytoskeletal and nuclear architecture. J Cell Sci. 1991, 100 (Pt 4): 799-807.

Hsu, C. L., Lee, E. X., Gordon, K. L., Paz, E. A., Shen, W. C., Ohnishi, K., Meisenhelder, J., Hunter, T., & La Spada, A. R. (2018). MAP4K3 mediates amino acid-dependent regulation of autophagy via phosphorylation of TFEB. Nature communications, 9(1), 942. https://doi.org/10.1038/s41467-018-03340-7

Hu, P., Li, Y., Sands, M. S., McCown, T. & Kafri, T. (2015) Generation of a stable packaging cell line producing high-titer PPT-deleted integration-deficient lentiviral vectors. Mol. Ther. — Methods Clin. Dev. 2, 15025

Huang, L., & Chen, C. (2013). Understanding HIV-1 protease autoprocessing for novel therapeutic development. Future medicinal chemistry, 5(11), 1215–1229. https://doi.org/10.4155/fmc.13.89

Huang YM, Hu W, Rustandi E, Chang K, Yusuf-Makagiansar H, Ryll T. (2010) Maximizing productivity of CHO cell-based fed-batch culture using chemically defined media conditions and typical manufacturing equipment. Biotechnol Prog. 2010 Sep-Oct;26(5):1400-10. doi: 10.1002/btpr.436. PMID: 20945494.

Hunter E. (1994) Macromolecular interactions in the assembly of HIV and other retroviruses.Semin Virol 1994, 5:71-83.

Hwang SO, Lee GM (2008) Nutrient deprivation induces autophagy as well as apoptosis in Chinese hamster ovary cell culture. Biotechnol Bioeng 99:678–685

Iershov, A., Nemazanyy, I., Alkhoury, C. (2019) The class 3 PI3K coordinates autophagy and mitochondrial lipid catabolism by controlling nuclear receptor PPARα. Nat Commun 10, 1566 https://doi.org/10.1038/s41467-019-09598-9

Ikeda Y, Takeuchi Y, Martin F, Cosset FL, Mitrophanous K, Collins M. (2003) Continuous high-titer HIV-1 vector production. Nat Biotechnol. May;21(5):569-72. doi: 10.1038/nbt815

Isaguliants M., Smirnova O., Ivanov A. V., (2013) Oxidative stress induced by HIV-1 reverse transcriptase modulates the enzyme's performance in gene immunization. Human Vaccines and Immunotherapeutics. 2013;9(10):2111–2119. doi: 10.4161/hv.25813

Iwasaki N, Sugiyama Y, Miyazaki S, Nakagawa H, Nishimura K, Matsuo S. (2015) An ATF4-Signal-Modulating Machine Other Than GADD34 Acts in ATF4-to-CHOP Signaling to Block CHOP Expression in ER-Stress-Related Autophagy. J Cell Biochem. 2015 Jul;116(7):1300-9. doi: 10.1002/jcb.25085. PMID: 25737469.

Jaalouk, DE, Crosato, M, Brodt, P and Galipeau, J (2006). Inhibition of histone deacetylation in 293GPG packaging cell line improves the production of self-inactivating MLV-derived retroviral vectors. Virol J 3: 27.

Jacks T, Power MD, Masiarz FR, Luciw PA, Barr PJ, Varmus HE (1988) Characterization of ribosomal frameshifting in HIV-1 gag-pol expression. Nature. Jan 21; 331(6153):280-3.

Jalaguier, P.; Cantin, R.; Maaroufi, H.; Tremblay, M.J. (2015) Selective acquisition of host-derived ICAM-1 by HIV-1 is a matrix-dependent process. J. Virol. 2015, 89, 323–336

Jaluria, P.; Betenbaugh, M.; Konstantopoulos, K.; Shiloach, J. (2007) Enhancement of cell proliferation in various mammalian cell lines by gene insertion of a cyclin-dependent kinase homolog. BMC Biotechnol., 7, 71

Jardon MA, Sattha B, Braasch K, Leung AO, Cote HCF, Butler M, Gorski S, Piret JM. (2012). Inhibition of glutamine-dependent autophagy increases t-PA production in CHO cell fed-batch process. Biotechnol Bioeng 109(5):1228–1238

Javanbakht, H.; Halwani, R.; Cen, S.; Saadatmand, J.; Musier-Forsyth, K.; Gottlinger, H.; Kleiman, L. (2003) The Interaction between HIV-1 Gag and Human Lysyl-tRNA Synthetase during Viral Assembly. J. Biol. Chem. 2003, 278, 27644–27651.

Johannsdottir, H. K., Mancini, R., Kartenbeck, J., Amato, L. & Helenius, A. (2009) Host cell factors and functions involved in vesicular stomatitis virus entry. J. Virol. 83, 440–453

Joshi, A.; Garg, H.; Ablan, S.D.; Freed, E.O. (2011) Evidence of a role for soluble N-ethylmaleimide-sensitive factor attachment protein receptor (SNARE) machinery in HIV-1 assembly and release. J. Biol. Chem. 2011, 286, 29861–29871

Jowett J B, Planelles V, Poon B, Shah N P, Chen M-L, Chen I S Y. (1995) The human immunodeficiency virus type 1 vpr gene arrests infected T cells in the G2 + M phase of the cell cycle. J Virol. 1995;69:6304–6313

Jun Lin, Zhihai Huang, Hao Wu, Wei Zhou, Peipei Jin, Pengfei Wei, Yunjiao Zhang, Fang Zheng, Jiqian Zhang, Jing Xu, Yi Hu, Yanhong Wang, Yajuan Li, Ning Gu & Longping Wen (2014) Inhibition of autophagy enhances the anticancer activity of silver nanoparticles, Autophagy, 10:11, 2006-2020, DOI: 10.4161/auto.36293

Kallehauge, T., Li, S., Pedersen, L. (2017). Ribosome profiling-guided depletion of an mRNA increases cell growth rate and protein secretion. Sci Rep 7, 40388. https://doi.org/10.1038/srep40388

Kamimoto, T., Shoji, S., Hidvegi, T., Mizushima, N., Umebayashi, K., Perlmutter, D. H., (2006). Intracellular inclusions containing mutant alpha1-antitrypsin Z are propagated in the absence of autophagic activity. J. Biol. Chem. 281, 4467–4476. doi: 10.1074/jbc.M509409200

Kamiyama, H., Yoshii, H., Tanaka, Y., Sato, H., Yamamoto, N., and Kubo, Y. (2009). Raft localization of CXCR4 is primarily required for X4-tropic human immunodeficiency virus type 1 infection. Virology 386, 23–31. doi: 10.1016/j.virol.2008.12.033

Karengera, E.; Robotham, A.; Kelly, J.; Durocher, Y.; De Crescenzo, G.; Henry, O. (2017) Altering the central carbon metabolism of HEK293 cells: Impact on recombinant glycoprotein quality. J. Biotechnol., 242, 73–82.

Kavanaugh M. P., D.G. Miller, W. Zhang, W. Law, S.L. Kozak, D. Kabat, A.D. Miller (1994) Cell-surface receptors for gibbon ape leukemia virus and amphotropic murine retrovirus are inducible sodium-dependent phosphate symporters Proc. Natl. Acad. Sci. USA, 91, pp. 7071-

Keeler AM, ElMallah MK, Flotte TR. (2017) Gene therapy 2017: progress and future directions. Clin Transl Sci. 10(4):242-248.

Killian M. S. (2012). Dual role of autophagy in HIV-1 replication and pathogenesis. AIDS research and therapy, 9(1), 16. https://doi.org/10.1186/1742-6405-9-16

Kim HJ, Gatz C, Hillen W, Jones TR. (1995) Tetracycline repressor-regulated gene repression in recombinant human cytomegalovirus. J Virol. Apr;69(4):2565-73. doi: 10.1128/JVI.69.4.2565-2573.1995

Kim VN, Mitrophanous K, Kingsman SM, Kingsman AJ. (1998) Minimal requirement for a lentivirus vector based on human immunodeficiency virus type 1. J Virol.; 72:811–816.

Kim J. Y, Y.G. Kim, G.M. Lee (2012) CHO cells in biotechnology for production of recombinant proteins: current state and further potential. Appl Microbiol Biotechnol, 93 (3), pp. 917-930, 10.1007/s00253-011-3758-5

Kim, K.; Dauphin, A.; Komurlu, S.; McCauley, S.M.; Yurkovetskiy, L.; Carbone, C.; Diehl, W.E.; Strambio-De-Castillia, C.; Campbell, E.M.; Luban, J. (2019) Cyclophilin A protects HIV-1 from restriction by human TRIM5α. Nat. Microbiol., 4, 2044–2051

Kim, N. S., & Lee, G. M. (2002). Response of recombinant Chinese Hamster Ovary cells to hyperosmotic pressure: Effect of Bcl-2 overexpression. Journal of Biotechnology, 95(3), 237–248. https://doi.org/10.1016/s0168-1656(02)00011-1

Kleeff J, Kornmann M, Sawhney H, Korc M. (2000) Actinomycin D induces apoptosis and inhibits growth of pancreatic cancer cells. Int J Cancer. 2000 May 1;86(3):399-407. PMID: 10760829

Klein, K. C., Reed, J. C., Tanaka, M., Nguyen, V. T., Giri, S., & Lingappa, J. R. (2011). HIV Gag-leucine zipper chimeras form ABCE1-containing intermediates and RNase-resistant immature capsids similar to those formed by wild-type HIV-1 Gag. Journal of virology, 85(14), 7419–7435. https://doi.org/10.1128/JVI.00288-11

Kobayashi Y, Zhuang J, Peltz S, Dougherty J (2010). Identification of a cellular factor that modulates HIV-1 programmed ribosomal frameshifting. The Journal of Biological Chemistry. 285 (26): 19776–19784. doi:10.1074/jbc.M109.085621. PMC 2888388. PMID 20418372.

Korant BD, Strack P, Frey MW, Rizzo CJ., (1998) A cellular anti-apoptosis protein is cleaved by the HIV-1 protease. Adv Exp Med Biol. 1998;436:27–29. doi: 10.1007/978-1-4615-5373-1_3

Kotsopoulou, E., Kim, V. N., Kingsman, A. J., Kingsman, S. M., & Mitrophanous, K. A. (2000). A Rev-independent human immunodeficiency virus type 1 (HIV-1)-based vector that exploits a codon-optimized HIV-1 gag-pol gene. Journal of virology, 74(10), 4839–4852

Kouroku, Y., Fujita, E., Tanida, I., Ueno, T., Isoai, A., Kumagai, H., (2007). ER stress (PERK/eIF2alpha phosphorylation) mediates the polyglutamine-induced LC3 conversion, an essential step for autophagy formation. Cell Death Differ. 14, 230–239. doi: 10.1038/sj.cdd.4401984

Ku SC, Ng DT, Yap MG, Chao SH. (2008) Effects of overexpression of X-box binding protein 1 on recombinant protein production in Chinese hamster ovary and NS0 myeloma cells. Biotechnol Bioeng. 2008 Jan 1;99(1):155-64. doi: 10.1002/bit.21562. PMID: 17614336.

Kuriakose, N. Chirmule, P. Nair (2016) Immunogenicity of biotherapeutics: causes and association with posttranslational modifications. J Immunol Res, 2016 (2016), Article 1298473, 10.1155/2016/1298473

Kutner, R. H., Puthli, S., Marino, M. P. & Reiser, J. (2009) Simplified production and concentration of HIV-1-based lentiviral vectors using HYPERFlask vessels and anion exchange membrane chromatography. BMC Biotechnol 9, 10

Kyei GB, Dinkins C, Davis AS, Roberts E, Singh SB, Dong C, Wu L, Kominami E, Ueno T, Yamamoto A, Federico M, Panganiban A, Vergne I, Deretic V. (2009) Autophagy pathway intersects with HIV-1 biosynthesis and regulates viral yields in macrophages. J Cell Biol. Jul 27;186(2):255-68. doi: 10.1083/jcb.200903070. PMID: 19635843; PMCID: PMC2717652.

Lai T., Y. Yang, S.K. Ng (2013) Advances in Mammalian cell line development technologies for recombinant protein production. Pharmaceuticals (Basel), 6 (5), pp. 579-603,

LaGory E. L., Wu C., Taniguchi C. M., Ding C. K., Chi J. T., von Eyben R., Scott D. A., Richardson A. D. and Giaccia A. J.(2015). Suppression of PGC-1α is critical for reprogramming oxidative metabolism in renal cell carcinoma. Cell Rep 12:116-127.

Lama, J.; Trono, D. (1998) Human immunodeficiency virus type 1 matrix protein interacts with cellular protein HO3. J. Virol. 1998, 72, 1671–1676.

Le Sage, V.; Cinti, A.; Mouland, A.J. (2015) No-Go'ing Back: Co-opting RVB-2 to Control HIV-1 Gene Expression and Immune Response. Trends Microbiol. 2015, 23, 593–595.

Le, T.T., Andreadakis, Z., Kumar, A., Román, R.G., Tollefsen, S., Saville, M. Mayhew, S., (2020). The COVID-19 vaccine development landscape. Nat Rev Drug Discov, 19(5), pp.305-306.

Lee JS, Ha TK, Park JH, Lee GM. (2013). Anti-cell death engineering of CHO cells: Co-overexpression of Bcl-2 for apoptosis inhibition, Beclin-1 for autophagy induction. Biotechnol Bioeng 110(8):2195–2207

Leiherer, A., Ludwig, C., & Wagner, R. (2009). Uncoupling human immunodeficiency virus type 1 Gag and Pol reading frames: role of the transframe protein p6* in viral replication. Journal of virology, 83(14), 7210–7220. https://doi.org/10.1128/JVI.02603-08

Lennaertz, A., Knowles, S., Drugmand, J. C., & Castillo, J. (2013). Viral vector production in the integrity® iCELLis® single-use fixed-bed bioreactor, from bench-scale to industrial scale. BMC Proceedings, 7(Suppl 6), P59. https://doi.org/10.1186/1753-6561-7-S6-P59

Lesch, H., Laitinen, A., Peixoto, C., (2011) Production and purification of lentiviral vectors generated in 293T suspension cells with baculoviral vectors. Gene Ther 18, 531–538 https://doi.org/10.1038/gt.2010.162

Levin, J. G., Mitra, M., Mascarenhas, A., & Musier-Forsyth, K. (2010). Role of HIV-1 nucleocapsid protein in HIV-1 reverse transcription. RNA biology, 7(6), 754–774. https://doi.org/10.4161/rna.7.6.14115

Lewinski MK, Yamashita M, Emerman M, Ciuffi A, Marshall H, Crawford G, Collins F, Shinn P, Leipzig J, Hannenhalli S, Berry CC, Ecker JR, Bushman FD. (2006) Retroviral DNA integration: viral and cellular determinants of target-site selection. PLoS Pathog. Jun;2(6):e60. doi: 10.1371/journal.ppat.0020060

Li M, Husic N, Lin Y, Christensen H, Malik I, McIver S, LaPash Daniels CM, Harris DA, Kotzbauer PT, Goldberg MP, Snider BJ. (2010) Optimal promoter usage for lentiviral vector-mediated transduction of cultured central nervous system cells. J Neurosci Methods. May 30;189(1):56-64. doi: 10.1016/j.jneumeth.2010.03.019

Li, B., Wang, X., Wang, Y., Gou, W., Yuan, X., Peng, J., Guo, Q., & Lu, S. (2015). Past, present, and future of microcarrier-based tissue engineering. Journal of orthopaedic translation, 3(2), 51-57

Li, D.; Wei, T.; Rawle, D.J.; Qin, F.; Wang, R.; Soares, D.C.; Jin, H.; Sivakumaran, H.; Lin, M.-H.; Spann, K.; (2015) Specific Interaction between eEF1A and HIV RT Is Critical for HIV-1 Reverse Transcription and a Potential Anti-HIV Target. PLoS Pathog. 2015, 11, e1005289

Liang X, Dickman MB, Becker DF. (2014). Proline biosynthesis is required for endoplasmic reticulum stress tolerance in Saccharomyces cerevisiae. Journal of Biological Chemistry 289, 27794–27806.

Lin, J. H., Li, H., Yasumura, D., Cohen, H. R., Zhang, C., Panning, B., Shokat, K. M., Lavail, M. M., & Walter, P. (2007). IRE1 signaling affects cell fate during the unfolded protein response. Science (New York, N.Y.), 318(5852), 944–949

Lingappa JR, Reed JC, Tanaka M, Chutiraka K, Robinson BA. (2014) How HIV-1 Gag assembles in cells: Putting together pieces of the puzzle. Virus Res. 2014 Nov

26;193:89-107. doi: 10.1016/j.virusres.2014.07.001. Epub 2014 Jul 24. PMID: 25066606; PMCID: PMC4351045

Liste-Calleja L, Lecina M, Cairó JJ. (2014) HEK293 cell culture media study towards bioprocess optimization: Animal derived component free and animal derived component containing platforms. J Biosci Bioeng. 2014 Apr;117(4):471-7. doi: 10.1016/j.jbiosc.2013.09.014. Epub 2013 Oct 30. PMID: 24183458.

Livak KJ, Schmittgen TD. (2001) Analysis of relative gene expression data using real-time quantitative PCR and the 2(-Delta Delta C(T)) Method. Methods. 2001 Dec;25(4):402-8. doi: 10.1006/meth.2001.1262. PMID: 11846609.

Lorenzo Galluzzi & Peter Martin (2017) CARs on a highway with roadblocks, OncoImmunology, 6:12, DOI: 10.1080/2162402X.2017.1388486

Luban, J. (2012) TRIM5 and the Regulation of HIV-1 Infectivity. Mol. Biol. Int. 2012, 2012, 426840

Ludwig C, Leiherer A, Wagner R. (2008) Importance of protease cleavage sites within and flanking human immunodeficiency virus type 1 transframe protein p6* for spatiotemporal regulation of protease activation. J Virol. 2008;82(9):4573–4584.

Lv, Z., Chu, Y., & Wang, Y. (2015). HIV protease inhibitors: a review of molecular selectivity and toxicity. HIV/AIDS (Auckland, N.Z.), 7, 95–104

Marandin, A. (1998) Retrovirus-mediated gene transfer into human CD34+38low primitive cells capable of reconstituting long-term cultures in vitro and nonobese diabetic-severe combined immunodeficiency mice in vivo. Hum. Gene Ther. 9, 1497–1511

Marceau, N and Gasmi, M, (2013) Scalable lentiviral vector production system compatible with industrial pharmaceutical applications, WO 2013076309 A1

Martinez, N.W.; Xue, X.; Berro, R.G.; Kreitzer, G.; Resh, M.D. (2008) Kinesin KIF4 regulates intracellular trafficking and stability of the human immunodeficiency virus type 1 Gag polyprotein. J. Virol. 2008, 82, 9937–9950.

Maruggi, G.; Porcellini, S.; Facchini, G.; Perna, S.K.; Cattoglio, C.; Sartori, D.; Ambrosi, A.; Schambach, A.; Baum, C.; Bonini, C., (2009) Transcriptional Enhancers Induce Insertional Gene Deregulation Independently From the Vector Type and Design. Mol. Ther. 2009, 17, 851–856

Mastrangelo, A. J., Hardwick, J. M., Zou, S., & Betenbaugh, M. J. (2000). Part II. Overexpression of bcl-2 family members enhances survival of mammalian cells in response to various culture insults. Biotechnology and Bioengineering, 67(5), 555–564

Mauthe M., Orhon I., Rocchi C., Zhou X., Luhr M., Hijlkema K. J., Coppes R. P., Mauvezin, C., Nagy, P., Juhász, G. (2015) Autophagosome–lysosome fusion is independent of V-ATPase-mediated acidification. Nat Commun 6, 7007 (2015). https://doi.org/10.1038/ncomms8007

McCarron A., Donnelley M., McIntyre C., Parsons D. (2016) Challenges of up-scaling lentivirus production and processing. J. Biotechnol. 2016;240:23–30

Mekkaoui L, Parekh F, Kotsopoulou E, Darling D, Dickson G, Cheung GW, Chan L, MacLellan-Gibson K, Mattiuzzo G, Farzaneh F, Takeuchi Y, Pule M. (2018) Lentiviral Vector Purification Using Genetically Encoded Biotin Mimic in Packaging Cell. Mol Ther Methods Clin Dev. Oct 23;11:155-165. doi: 10.1016/j.omtm.2018.10.008

Meng X, Zhao G, Yufenyuy E, Ke D, Ning J, Delucia M, Ahn J, Gronenborn AM, Aiken C, Zhang P. (2012). Protease cleavage leads to formation of mature trimer interface in HIV-1 capsid. PLoS Pathog 8:e1002886

Merten, O. W. (2011) Large-scale manufacture and characterization of a lentiviral vector produced for clinical ex vivo gene therapy application. Hum Gene Ther 22, 343-356

Merten, O. W., Hebben, M., & Bovolenta, C. (2016). Production of lentiviral vectors. Molecular therapy. Methods & clinical development, 3, 16017. https://doi.org/10.1038/mtm.2016.17

Merten, O.-W.; Charrier, S.; Laroudie, N.; Fauchille, S.; Dugué, C.; Jenny, C.; Audit, M.; Zanta-Boussif, M.-A.; Chautard, H.; Radrizzani, M.; (2011) Large-Scale Manufacture and Characterization of a Lentiviral Vector Produced for Clinical Ex Vivo Gene Therapy Application. Hum. Gene Ther. 2011, 22, 343–356. [CrossRef]

Metzl-Raz, E., Kafri, M., Yaakov, G., & Barkai, N. (2020) Gene Transcription as a Limiting Factor in Protein Production and Cell Growth. G3 (Bethesda, Md.), 10(9), 3229–3242. https://doi.org/10.1534/g3.120.401303

Milani M., Annoni A., Bartolaccini S., Biffi M., Russo F., Di Tomaso T., Raimondi A., Lengler J., Holmes M.C., Scheiflinger F. (2017) Genome editing for scalable production of alloantigen-free lentiviral vectors for in vivo gene therapy. EMBO Mol. Med. 2017;9:1558–1573.

Miller D G, Edwards RH, Miller AD (1994) Cloning of the cellular receptor for amphotropic murine retroviruses reveals homology to that for gibbon ape leukemia virus. Proc NatlAcad Sci USA 91:78—82

Miller, D. G., & Miller, A. D. (1994). A family of retroviruses that utilize related phosphate transporters for cell entry. Journal of virology, 68(12), 8270–8276. https://doi.org/10.1128/JVI.68.12.8270-8276.1994

Mittler R, Finka A, Goloubinoff P. (2012) How do plants feel the heat? Trends in Biochemical Sciences 37, 118–125.
Miyakawa, K.; Nishi, M.; Matsunaga, S.; Okayama, A.; Anraku, M.; Kudoh, A.;

Hirano, H.; Kimura, H.; Morikawa, Y.; Yamamoto, N.; (2017) The tumour suppressor APC promotes HIV-1 assembly via interaction with Gag precursor protein. Nat. Commun. 2017, 8, 14259.

Lavado-García,J.; Díaz-Maneh, A. ; Canal-Paulí , N. ; Pérez Rubio, P. ; Gòdia,F.; Cervera,L.; (2021) Metabolic engineering of HEK293 cells to improve transient transfection and cell budding of HIV-1 virus-like particles. Biotechnol. Bioeng., 118, 1630–1644

Lavado-García, J.; Jorge, I.; Cervera, L.; Vázquez, J.; Gòdia, F. (2020) Multiplexed Quantitative Proteomic Analysis of HEK293 Pro-vides Insights into Molecular Changes Associated with the Cell Density Effect, Transient Transfection, and Virus-Like Particle Production. J. Proteome Res., 19, 1085–1099

Merksamer PI, Trusina A & Papa FR (2008) Real-time redox measurements during endoplasmic reticulum stress reveal interlinked protein folding functions. Cell 135, 933–947.

Mohan C, Lee GM.., (2010) Effect of inducible co-overexpression of protein disulfide isomerase and endoplasmic reticulum oxidoreductase on the specific antibody productivity of recombinant Chinese hamster ovary cells. Biotechnol Bioeng. 2010 Oct 1;107(2):337-46. doi: 10.1002/bit.22781. PMID: 20506311.

Mortimore GE, Pösö AR (1988) Amino acid control of intracellular protein degradation. Methods Enzymol 166:461–476

Mouland, A. J., Mercier, J., Luo, M., Bernier, L., DesGroseillers, L., & Cohen, E. A. (2000) The double-stranded RNA-binding protein Staufen is incorporated in human immunodeficiency virus type 1: evidence for a role in genomic RNA encapsidation. Journal of virology, 74(12), 5441–5451. https://doi.org/10.1128/jvi.74.12.5441-5451.2000

Mu, X.; Fu, Y.; Zhu, Y.; Wang, X.; Xuan, Y.; Shang, H.; Goff, S.P.; Gao, G. (2015) HIV-1 Exploits the Host Factor RuvB-like 2 to Balance Viral Protein Expression. Cell Host Microbe 2015, 18, 233–242.

Murphy, R. E., & Saad, J. S. (2020). The Interplay between HIV-1 Gag Binding to the Plasma Membrane and Env Incorporation. Viruses, 12(5), 548. https://doi.org/10.3390/v12050548

Musiwaro P, Smith M, Manifava M, Walker SA, Ktistakis NT. (2013) Characteristics and requirements of basal autophagy in HEK 293 cells. Autophagy. 2013 Sep;9(9):1407-17. doi: 10.4161/auto.25455. Epub 2013 Jun 20. PMID: 23800949.

Na Nakorn, P.; Treesuwan, W.; Choowongkomon, K.; Hannongbua, S.; Boonyalai, N. (2011) In vitro and in silico binding study of the peptide derived from HIV-1 CA-CTD and LysRS as a potential HIV-1 blocking site. J. Theor. Biol. 2011, 270, 88–97.

Naif H. M. (2013). Pathogenesis of HIV Infection. Infectious disease reports, e6. https://doi.org/10.4081/idr.2013.s1.e6

Nakatsukasa, K.; Brodsky, J.L. (2008) The Recognition and Retrotranslocation of Misfolded Proteins from the Endoplasmic Reticulum. Traffic, 9, 861–870.

Naldini L, Blömer U, Gallay P, Ory D, Mulligan R, Gage FH, Verma IM, Trono D. (1996) In vivo gene delivery and stable transduction of nondividing cells by a lentiviral vector. Science. Apr 12;272(5259):263-7. doi: 10.1126/science.272.5259.263

Navia MA, Fitzgerald PM, McKeever BM, Leu CT, Heimbach JC, Herber WK, Sigal IS, Darke PL, Springer JP (1989) Three-dimensional structure of aspartyl protease from human immunodeficiency virus HIV-1. Nature. 1989, 337: 615-620. 10.1038/337615a0.

Neurohr GE, Terry RL, Lengefeld J, Bonney M, Brittingham GP, Moretto F, Miettinen TP, Vaites LP, Soares LM, Paulo JA, Harper JW, Buratowski S, Manalis S, van Werven FJ, Holt LJ, Amon A (2019) Excessive Cell Growth Causes Cytoplasm Dilution And Contributes to Senescence. Cell. 2019 Feb 21; 176(5):1083-1097.e18.

Newland, M.; Greenfield, P.F.; Reid, S. (1990) Hybridoma growth limitations: The roles of energy metabolism and ammonia production. Cytotechnology, 3, 215–229

Nguyen D. H., Hildreth J. E. (2000). Evidence for budding of human immunodeficiency virus type 1 selectively from glycolipid-enriched membrane lipid rafts. J. Virol. 74:3264–3272

Nie Z, Bren GD, Rizza SA, Badley AD., (2008) HIV Protease Cleavage of Procaspase 8 is Necessary for Death of HIV-Infected Cells. Open Virol J. 2008, 2: 1-7. 10.2174/1874357900802010001

Nie Z, Bren GD, Vlahakis SR, Schimnich AA, Brenchley JM, Trushin SA, Warren S, Schnepple DJ, Kovacs CM, Loutfy MR, Douek DC, Badley AD., (2007) Human immunodeficiency virus type 1 protease cleaves procaspase 8 in vivo. J Virol. 2007, 81: 6947-6956. 10.1128/JVI.02798-06

Nie Z, Phenix BN, Lum JJ, Alam A, Lynch DH, Beckett B, Krammer PH, Sekaly RP, Badley AD., (2002) HIV-1 protease processes procaspase 8 to cause mitochondrial release of cytochrome c, caspase cleavage and nuclear fragmentation. Cell Death Differ. 2002, 9: 1172-1184. 10.1038/sj.cdd.4401094

Nishi, M.; Ryo, A.; Tsurutani, N.; Ohba, K.; Sawasaki, T.; Morishita, R.; Perrem, K.; Aoki, I.; Morikawa, Y.; Yamamoto, N. (2009) Requirement for microtubule integrity in the SOCS1-mediated intracellular dynamics of HIV-1 Gag. FEBS Lett. 2009, 583, 1243–1250

Nishitoh H. (2012) CHOP is a multifunctional transcription factor in the ER stress response. J Biochem. 2012 Mar;151(3):217-9. doi: 10.1093/jb/mvr143. Epub 2011 Dec 30. PMID: 22210905.

Humbert O., Gisch D.W., Wohlfahrt M.E., Adams A.B., Greenberg P.D., Schmitt T.M., Trobridge G.D., Kiem H.P., (2016) Development of third-generation cocal envelope producer cell lines for robust lentiviral gene transfer into hematopoietic stem cells and t-cells. Mol. Ther., 24, pp. 1237-1246

Ohsumi Y. (2001) Molecular dissection of autophagy: two ubiquitin-like systems. Nat Rev Mol Cell Biol.; 2:211–216

Oka Y., (2010) 293FT cells transduced with four transcription factors (OCT4, SOX2, NANOG, and LIN28) generate aberrant ES-like cells. J. Stem Cells Regen. Med. 2010;6:149–156.

Orellana. C.A., E. Marcellin, P.P. Gray, L.K. Nielsen (2017) Overexpression of the regulatory subunit of glutamate-cysteine ligase enhances monoclonal antibody production in CHO cells. Biotechnol Bioeng, 114 (8), pp. 1825-1836, 10.1002/bit.26316

Ono A, Ablan SD, Lockett SJ, Nagashima K, Freed EO (2004) Phosphatidylinositol (4,5) bisphosphate regulates HIV-1 Gag targeting to the plasma membrane. Proc Natl Acad Sci USA 101(41):14889–14894.

Ono, A. (2009). HIV-1 assembly at the plasma membrane: Gag trafficking and localization. Future Virol. 4, 241–257.

Ono, A. (2010). Relationships between plasma membrane microdomains and HIV-1 assembly. Biol. Cell 102, 335–350.

Ono, A., Ablan, S. D., Lockett, S. J., Nagashima, K., and Freed, E. O. (2004). Phosphatidylinositol (4,5) bisphosphate regulates HIV-1 Gag targeting to the plasma membrane. Proc. Natl. Acad. Sci. U.S.A. 101, 14889–14894.

Ono, A., and Freed, E. O. (2005). Role of lipid rafts in virus replication. Adv. Virus Res. 64, 311–358.

Ott, D. E., Coren, L. V., and Gagliardi, T. D. (2005). Redundant roles for nucleocapsid and matrix RNA-binding sequences in human immunodeficiency virus type 1 assembly. J. Virol. 79, 13839–13847.

Ott, D.E.; Coren, L.V.; Shatzer, T. (2009) The Nucleocapsid Region of Human Immunodeficiency Virus Type 1 Gag Assists in the Coordination of Assembly and Gag Processing: Role for RNA-Gag Binding in the Early Stages of Assembly. J. Virol. 2009, 83, 7718–7727

Ozturk, S.S.; Riley, M.R.; Palsson, B.O. (1992) Effects of ammonia and lactate on hybridoma growth, metabolism, and antibody production. Biotechnol. Bioeng., 39, 418–431

Pahl H. L. (1999) Signal transduction from the endoplasmic reticulum to the cell nucleus. Physiol. Rev., 79, 1999, pp. 683-701

Pall Biotech (2017) Cost modelling of upstream production process of lentiviral vectors in HEK-293 cells comparing multi-tray 10 stacks and fixed-bed bioreactor. Poster ESACT

Pan, X., Streefland, M., Dalm, C., Wijffels, R. H., & Martens, D. E. (2017). Selection of chemically defined media for CHO cell fed-batch culture processes. Cytotechnology, 69(1), 39–56. https://doi.org/10.1007/s10616-016-0036-5

Parzych, K. R., & Klionsky, D. J. (2014) An overview of autophagy: morphology, mechanism, and regulation. Antioxidants & redox signaling, 20(3), 460–473. https://doi.org/10.1089/ars.2013.5371

Patience Musiwaro, Matthew Smith, Maria Manifava, Simon A. Walker & Nicholas T. Ktistakis (2013) Characteristics and requirements of basal autophagy in HEK 293 cells, Autophagy, 9:9, 1407-1417, DOI: 10.4161/auto.25455

Pelchen-Matthews A, Kramer B, Marsh M. (2003) Infectious HIV-1 assembles in late endosomes in primary macrophages. J Cell Biol. 2003 Aug 4;162(3):443-55. doi: 10.1083/jcb.200304008. Epub 2003 Jul 28. PMID: 12885763; PMCID: PMC2172706.

Peng, R. W. ; Fussenegger, M. (2009) Molecular engineering of exocytic vesicle traffic enhances the productivity of Chinese hamster ovary cells. Biotechnol. Bioeng., 102, 1170–1181

Pérez-Rodriguez, S., Ramírez-Lira, M. J., Trujillo-Roldán, M. A., & Valdez-Cruz, N. A. (2020). Nutrient supplementation strategy improves cell concentration and longevity, monoclonal antibody production and lactate metabolism of Chinese hamster ovary cells. Bioengineered, 11(1), 463–471.

Perry C, Rayat ACME. (2021) Lentiviral Vector Bioprocessing. Viruses. Feb 9;13(2):268. doi: 10.3390/v13020268. PMID: 33572347; PMCID: PMC7916122.

Petropoulos C. (1997) Retroviral Taxonomy, Protein Structures, Sequences, and Genetic Maps. In: Coffin JM, Hughes SH, Varmus HE, editors. Retroviruses. Cold Spring Harbor (NY): Cold Spring Harbor Laboratory Press; 1997. Available from: https://www.ncbi.nlm.nih.gov/books/NBK19417/

Pettit SC, Clemente JC, Jeung JA, Dunn BM, Kaplan AH. (2005) Ordered processing of the human immunodeficiency virus type 1 GagPol precursor is influenced by the context of the embedded viral protease. J Virol. 2005;79(16):10601–10607.

Pluta K and Kacprzak MM. (2009) Use of HIV as a gene transfer vector. Acta Biochim Pol. 2009; 56(4):531-595.

Polus A, Bociaga-Jasik M, Czech U, Goralska J, Cialowicz U, Chojnacka M, Polus M, Jurowski K, Dembinska-Kiec A. (2017) The human immunodeficiency virus (HIV1) protease inhibitor sanquinavir activates autophagy and removes lipids deposited in lipid droplets. J Physiol Pharmacol. 2017 Apr;68(2):283-293. PMID: 28614778.

Ponsero AJ, Igbaria A, Darch MA, Miled S, Outten CE, Winther JR, Palais G, D'Autréaux B, Delaunay-Moisan A & Toledano MB (2017) Endoplasmic reticulum transport of glutathione by Sec61 Is regulated by Ero1 and Bip. Mol Cell 67, 962–973 e5.

Popik, W., Alce, T. M., and Au, W.-C. (2002). Human immunodeficiency virus type 1 uses lipid raft-colocalized CD4 and chemokine receptors for productive entry into CD4+ T cells. J. Virol. 76, 4709–4722. doi: 10.1128/jvi.76.10.4709-4722.2002

Popov, S.; Popova, E.; Inoue, M.; Wu, Y.; Göttlinger, H. (2018) HIV-1 gag recruits PACSIN2 to promote virus spreading. Proc. Natl. Acad. Sci. USA 2018, 115, 7093–7098

Prazeres DMF, Monteiro GA. (2014) Plasmid Biopharmaceuticals. Microbiol Spectr. 2014 Dec;2(6). doi: 10.1128/microbiolspec.PLAS-0022-2014. PMID: 26104457

Pugsley HR. (2017) Assessing Autophagic Flux by Measuring LC3, p62, and LAMP1 Co-localization Using Multispectral Imaging Flow Cytometry. J Vis Exp. Jul 21;(125):55637. doi: 10.3791/55637. PMID: 28784946; PMCID: PMC5612559.

Pugsley HR. (2017) Quantifying autophagy: Measuring LC3 puncta and autolysosome formation in cells using multispectral imaging flow cytometry. Methods. 2017 Jan 1;112:147-156. doi: 10.1016/j.ymeth.2016.05.022. PMID: 27263026.

Ragheb JA, Yu H, Hofmann T, Anderson WF. (1995) The amphotropic and ecotropic murine leukemia virus envelope TM subunits are equivalent mediators of direct membrane fusion: implications for the role of the ecotropic envelope and receptor in syncytium formation and viral entry. J Virol. 1995 Nov;69(11):7205-15. doi: 10.1128/JVI.69.11.7205-7215.1995. PMID: 7474142; PMCID: PMC189642.

Rajan R, Karbowniczek M, Pugsley HR, Sabnani MK, Astrinidis A, La-Beck NM (2015) Quantifying autophagosomes and autolysosomes in cells using imaging flow cytometry. Cytometry A. 87(5):451-8. doi: 10.1002/cyto.a.22652. Epub 2015 Feb 27. PMID: 25728685.

Rajendra, Y., Kiseljak, D., Baldi, L., Hacker, D. L., & Wurm, F. M. (2011). Influence of glutamine on transient and stable recombinant protein production in CHO and HEK-

293 cells. BMC proceedings, 5 Suppl 8(Suppl 8), P35. https://doi.org/10.1186/1753-6561-5-S8-P35

Rajendra Y, Kiseljak D, Baldi L, Hacker D. L & Wurm F. M. (2012) Reduced glutamine concentration improves protein production in growth-arrested CHO-DG44 and HEK-293E cells. Biotechnol. Lett. 2012;34:619–626

Rao, S.; Cinti, A.; Temzi, A.; Amorim, R.; You, J.C.; Mouland, A.J. (2018) HIV-1 NC-induced stress granule assembly and translation arrest are inhibited by the dsRNA binding protein Staufen1. RNA 2018, 24, 219–236

Redmann, M., Benavides, G. A., Berryhill, T. F., Wani, W. Y., Ouyang, X., Johnson, M. S., Ravi, S., Barnes, S., Darley-Usmar, V. M., & Zhang, J. (2017). Inhibition of autophagy with bafilomycin and chloroquine decreases mitochondrial quality and bioenergetic function in primary neurons. Redox biology, 11, 73–81. https://doi.org/10.1016/j.redox.2016.11.004

Reiser, J. (2000) Production and concentration of pseudotyped HIV-1-based gene transfer vectors. Gene Ther. 7, 910–913

van Riel, D., de Wit, E., (2020) Next-generation vaccine platforms for COVID-19. Nat. Mater. 19, 810–812. https://doi.org/10.1038/s41563-020-0746-0

Ritacco FV, Wu Y, Khetan A. (2018) Cell culture media for recombinant protein expression in Chinese hamster ovary (CHO) cells: history, key components, and optimization strategies. Biotechnol Prog. 2018;34(6):1407–1426.

Rivière Y, Blank V, Kourilsky P, Israël A. (1991) Processing of the precursor of NF-kappa B by the HIV-1 protease during acute infection. Nature. 1991 Apr 18;350(6319):625-6. doi: 10.1038/350625a0. PMID: 2017258.

Rodrigues, A.F.; Guerreiro, M.; Formas-Oliveira, A.S.; Fernandes, P.; Blechert, A.-K.; Genzel, Y.; Alves, P.; Hu, W.S.; Coroadinha, A.S. (2016) Increased titer and

reduced lactate accumulation in recombinant retrovirus production through the down-regulation of HIF1 and PDK. Biotechnol. Bioeng., 113, 150–162

Ron, D.; Walter, P. (2007) Signal integration in the endoplasmic reticulum unfolded protein response. Nat. Rev. Mol. Cell Biol., 8, 519–529.

Roobol, A.; Smith, M.E.; Carden, M.J.; Hershey, J.W.; Willis, A.E.; Smales, C.M. (2020) Engineered transient and stable overexpression of translation factors eIF3i and eIF3c in CHOK1 and HEK293 cells gives enhanced cell growth associated with increased c-Myc expression and increased recombinant protein synthesis. Metab. Eng., 59, 98–105

Rumlová, M., Křížová, I., Keprová, A., Hadravová, R., Doležal, M., Strohalmová, K., Pichová, I., Hájek, M., & Ruml, T. (2014). HIV-1 protease-induced apoptosis. Retrovirology, 11, 37. https://doi.org/10.1186/1742-4690-11-37

Russell J. B., Cook G. M/, (1995) Energetics of bacterial growth: balance of anabolic and catabolic reactions Microbiol. Rev., 59, pp. 48-62

Ryo, A.; Tsurutani, N.; Ohba, K.; Kimura, R.; Komano, J.; Nishi, M.; Soeda, H.; Hattori, S.; Perrem, K.; Yamamoto, M.; (2008) SOCS1 is an inducible host factor during HIV-1 infection and regulates the intracellular trafficking and stability of HIV-1 Gag. Proc. Natl. Acad. Sci. USA 2008, 105, 294–299

Sabo, Y.; de los Santos, K.; Goff, S.P. (2020) IQGAP1 Negatively Regulates HIV-1 Gag Trafficking and Virion Production. Cell Rep. 2020, 30, 4065–4081.e4

Sabo, Y.; Walsh, D.; Barry, D.S.; Tinaztepe, S.; de los Santos, K.; Goff, S.P.; Gundersen, G.G.; Naghavi, M.H. (2013) HIV-1 Induces the Formation of Stable Microtubules to Enhance Early Infection. Cell Host Microbe 2013, 14, 535–546.

Sakuma, R.; Ohmine, S.; Ikeda, Y. (2010) Determinants for the rhesus monkey TRIM5alpha-mediated block of the late phase of HIV-1 replication. J. Biol. Chem. 2010, 285, 3784–3793

Salaün C., Gyan E., Rodrigues P., Heard J. M. (2002) Pit2 assemblies at the cell surface are modulated by extracellular inorganic phosphate concentration J. Virol., 76, pp. 4304-4311

Samal, A.B.; Ghanam, R.H.; Fernandez, T.F.; Monroe, E.B.; Saad, J.S. (2011) NMR, biophysical, and biochemical studies reveal the minimal Calmodulin binding domain of the HIV-1 matrix protein. J. Biol. Chem. 2011, 286, 33533–33543.

Sanber KS, Knight SB, Stephen SL, Bailey R, Escors D, Minshull J, Santilli G, Thrasher AJ, Collins MK, Takeuchi Y. (2015) Construction of stable packaging cell lines for clinical lentiviral vector production. Sci Rep. Mar 12;5:9021. doi: 10.1038/srep09021

Sandhu, K.S.; Al-Rubeai, M. (2009) The effect of Bcl-2, YAMA, and XIAP over-expression on apoptosis and adenovirus production in HEK293 cell line. Biotechnol. Bioeng., 104, 752–765.

Sarafianos, S. G., Marchand, B., Das, K., Himmel, D. M., Parniak, M. A., Hughes, S. H., & Arnold, E. (2009). Structure and function of HIV-1 reverse transcriptase: molecular mechanisms of polymerization and inhibition. Journal of molecular biology, 385(3), 693–713. https://doi.org/10.1016/j.jmb.2008.10.071

Sauerwald TM, Oyler GA, Betenbaugh MJ. (2003) Study of caspase inhibitors for limiting death in mammalian cell culture. Biotechnol Bioeng. Feb 5;81(3):329-40. doi: 10.1002/bit.10473. PMID: 12474256.

Sauerwald, T.M.; Betenbaugh, M.J.; Oyler, G.A. (2002) Inhibiting apoptosis in mammalian cell culture using the caspase inhibitor XIAP and deletion mutants. Biotechnol. Bioeng., 77, 704–716.

Saura-Esteller J, Sánchez-Vera I, Núñez-Vázquez S, Cosialls AM, Gama-Pérez P, Bhosale G, Mendive-Tapia L, Lavilla R, Pons G, Garcia-Roves PM, Duchen MR, Iglesias-Serret D, Gil J. (2021) Activation of the Integrated Stress Response and ER Stress Protect from Fluorizoline-Induced Apoptosis in HEK293T and U2OS Cell

Lines. Int J Mol Sci. Jun 6;22(11):6117. doi: 10.3390/ijms22116117. PMID: 34204139; PMCID: PMC8201103

Schalk, J. A., Mooi, F. R., Berbers, G. A., van Aerts, L. A., Ovelgonne, H., and Kimman, T. G. (2006) Preclinical and clinical safety studies on DNA vaccines, Hum. Vaccin 2, 45–53.

Schiller, L. T. ; Diaz, N. L. ; Ferreira, R. R. ; Böker, K. O. ; Gruber, J. (2018) Enhanced Production of Exosome-Associated AAV by Overexpression of the Tetraspanin CD. Mol. Ther. Methods Clin. Dev., 9, 278–287.

Schröder AR, Shinn P, Chen H, Berry C, Ecker JR, Bushman F. (2002) HIV-1 integration in the human genome favors active genes and local hotspots. Cell. 2002;110:521–529

Segura MM, Garnier A, Durocher Y, Coelho H, Kamen A. (2007) Production of lentiviral vectors by large-scale transient transfection of suspension cultures and affinity chromatography purification. Biotechnol Bioeng.; 98: 789–799.

Segura, M. M., Mangion, M., Gaillet, B. & Garnier, A. (2013) New developments in lentiviral vector design, production and purification. Expert Opin Biol Ther 13, 987-1011

Segura, M.D.L.M.; Garnier, A.; Kamen, A. (2006) Purification and characterization of retrovirus vector particles by rate zonal ultracentrifugation. J. Virol. Methods, 133, 82–91.

Sena-Esteves M, Gao G. (2018) Production of High-Titer Retrovirus and Lentivirus Vectors. Cold Spring Harb Protoc. Apr 2;2018(4). doi: 10.1101/pdb.prot95687

Sena-Esteves, M., Tebbets, J.C., Steffens, S., Crombleholme, T. & Flake, A.W. (2004) Optimized large-scale production of high titer lentivirus vector pseudotypes. J. Virol. Methods 122, 131–139

Sertkaya H, Ficarelli M, Sweeney NP, Parker H, Vink CA, Swanson CM. (2021) HIV-1 sequences in lentiviral vector genomes can be substantially reduced without compromising transduction efficiency. Sci Rep. Jun 8;11(1):12067. doi: 10.1038/s41598-021-91309-w

Sette, P., Dussupt, V., & Bouamr, F. (2012). Identification of the HIV-1 NC binding interface in Alix Bro1 reveals a role for RNA. Journal of virology, 86(21), 11608–11615. https://doi.org/10.1128/JVI.01260-12

Sette P, Jadwin JA, Dussupt V, Bello NF, Bouamr F. (2010) The ESCRT-associated protein Alix recruits the ubiquitin ligase Nedd4-1 to facilitate HIV-1 release through the LYPXnL L domain motif. J Virol. 2010 Aug;84(16):8181-92. doi: 10.1128/JVI.00634-10. Epub 2010 Jun 2. PMID: 20519395; PMCID: PMC2916511.

Sette, P.; O'Connor, S.K.; Yerramilli, V.S.; Dussupt, V.; Nagashima, K.; Chutiraka, K.; Lingappa, J.; Scarlata, S.; Bouamr, F. (2016) HIV-1 Nucleocapsid Mimics the Membrane Adaptor Syntenin PDZ to Gain Access to ESCRTs and Promote Virus Budding. Cell Host Microbe 2016, 19, 336–348. [CrossRef]

Sevier CS, Weisz OA, Davis M, Machamer CE. (2000) Efficient export of the vesicular stomatitis virus G protein from the endoplasmic reticulum requires a signal in the cytoplasmic tail that includes both tyrosine-based and di-acidic motifs. Mol Biol Cell. 2000 Jan;11(1):13-22. doi: 10.1091/mbc.11.1.13. PMID: 10637287; PMCID: PMC14753.

Shao S, Li S, Qin Y, Wang X, Yang Y, Bai H, Zhou L, Zhao C, Wang C. (2014) Spautin-1, a novel autophagy inhibitor, enhances imatinib-induced apoptosis in chronic myeloid leukemia. Int J Oncol. 2014 May;44(5):1661-8. doi: 10.3892/ijo.2014.2313. Epub 2014 Feb 27. PMID: 24585095; PMCID: PMC6904104.

Shehu-Xhilaga, M., Crowe, S. M., & Mak, J. (2001). Maintenance of the Gag/Gag-Pol ratio is important for human immunodeficiency virus type 1 RNA dimerization and viral infectivity. Journal of virology, 75(4), 1834–1841. https://doi.org/10.1128/JVI.75.4.1834-1841.2001

Shoeman RL, Hüttermann C, Hartig R, Traub P. (2001) Amino-terminal polypeptides of vimentin are responsible for the changes in nuclear architecture associated with human immunodeficiency virus type 1 protease activity in tissue culture cells. Mol Biol Cell. 2001 Jan;12(1):143-54. doi: 10.1091/mbc.12.1.143. PMID: 11160829; PMCID: PMC30574.

Shoeman RL, Kesselmier C, Mothes E, Höner B, Traub P. Non-viral cellular substrates for human immunodeficiency virus type 1 protease. FEBS Lett. 1991 Jan 28;278(2):199-203. doi: 10.1016/0014-5793(91)80116-k. PMID: 1991513.

Sibbald B. (2001). Death but one unintended consequence of gene-therapy trial. CMAJ : Canadian Medical Association journal = journal de l'Association medicale canadienne, 164(11), 1612

Soldi M, Sergi Sergi L, Unali G, Kerzel T, Cuccovillo I, Capasso P, Annoni A, Biffi M, Rancoita PMV, Cantore A, Lombardo A, Naldini L, Squadrito ML, Kajaste-Rudnitski A. (2002) Laboratory-Scale Lentiviral Vector Production and Purification for Enhanced Ex Vivo and In Vivo Genetic Engineering. Mol Ther Methods Clin Dev. 2020 Oct 20;19:411-425. doi: 10.1016/j.omtm.2020.10.009. PMID: 33294490; PMCID: PMC7683235.

Sparacio S, Pfeiffer T, Schaal H, Bosch V. (2001) Generation of a flexible cell line with regulatable, high-level expression of HIV Gag/Pol particles capable of packaging HIV-derived vectors. Mol Ther. 2001 Apr;3(4):602-12. doi: 10.1006/mthe.2001.0296. PMID: 11319923.

Steliou, K., Boosalis, M. S., Perrine, S. P., Sangerman, J., & Faller, D. V. (2012). Butyrate histone deacetylase inhibitors. BioResearch open access, 1(4), 192–198. https://doi.org/10.1089/biores.2012.0223

Stewart, H. J., Leroux-Carlucci, M. a, Sion, C. J. M., Mitrophanous, K. a & Radcliffe, P. a. (2009) Development of inducible EIAV-based lentiviral vector packaging and producer cell lines. Gene Ther. 16, 805–814

Strack, B.; Calistri, A.; Craig, S.; Popova, E.; Göttlinger, H.G. (2003) AIP1/ALIX is a binding partner for HIV-1 p6 and EIAV p9 functioning in virus budding. Cell 2003, 114, 689–699.

Strack, P. R., West Frey, M., Rizzo, C. J., Cordova, B., George, H. J., Meade, R.,Peng Ho, S., Corman, J., Tritch, R., and Korant, B. D. (1996) Proc. Natl.Acad. Sci. U. S. A.93,9571–9576

Summers, M. F., L. E. Henderson, M. R. Chance, J. W. Bess, Jr., T. L. South, P. R. Blake, I. Sagi, G. Perez-Alvarado, R. C. Sowder III, D. R. Hare, (1992) Nucleocapsid zinc fingers detected in retroviruses: EXAFS studies of intact viruses and the solution-state structure of the nucleocapsid protein from HIV-1. Protein Sci. 1:563-574.

Sunley K, Butler M. (2010) Strategies for the enhancement of recombinant protein production from mammalian cells by growth arrest. Biotechnol Adv. 2010 May-Jun;28(3):385-94. doi: 10.1016/j.biotechadv.2010.02.003. Epub 2010 Feb 13. PMID: 20156545.

Suzuki, N., Yoshida, T., Takeuchi, H. Sakuma R., Sukegawa S., Yamaoka S., (2018) Robust Enhancement of Lentivirus Production by Promoter Activation. Sci Rep 8, 15036 https://doi.org/10.1038/s41598-018-33042-5

Swanstrom R, Wills JW. (1997) Synthesis, assembly, and processing of viral proteins. In Retroviruses. Edited by Coffin JM, Hughes SH, Varmus HE. Cold Spring Harbor, NY: Cold Spring Harbor Laboratory Press; 1997:263-334.

Takatsuka C, Inoue Y, Matsuoka K, Moriyasu Y. (2004) 3-Methyladenine inhibits autophagy in tobacco culture cells under sucrose starvation conditions. Plant Cell Physiol. 2004;45:265–74.

Tajer P, Pike-Overzet K, Arias S, Havenga M, Staal F. (2019) Ex vivo expansion of hematopoietic stem cells for therapeutic purposes: lessons from development and the niche. Cells. 8(169);1-15.

Tandon, N., Thakkar, K. N., LaGory, E. L., Liu, Y., & Giaccia, A. J. (2018). Generation of Stable Expression Mammalian Cell Lines Using Lentivirus. Bio-protocol, 8(21), e3073

Tang, Y.; Winkler, U.; Freed, E.O.; Torrey, T.A.; Kim, W.; Li, H.; Goff, S.P.; Morse, H.C. (1999) Cellular motor protein KIF-4 associates with retroviral Gag. J. Virol. 1999, 73, 10508–10513. [C

Taylor, J.E.; Chow, J.Y.H.; Jeffries, C.M.; Kwan, A.H.; Duff, A.P.; Hamilton, W.A.; Trewhella, J. (2012) Calmodulin binds a highly extended HIV-1 MA protein that refolds upon its release. Biophys. J. 2012, 103, 541–549.

Tey, B. T., Singh, R. P., Piredda, L., Piacentini, M., & Al-Rubeai, M. (2000). Influence of Bcl-2 on cell death during the cultivation of a Chinese hamster ovary cell line expressing a chimeric antibody. Biotechnology and Bioengineering, 68(1), 31–43.

Tharmalingam T, Ghebeh H, Wuerz T, Butler M. (2008) Pluronic enhances the robustness and reduces the cell attachment of mammalian cells. Mol Biotechnology Jun;39(2):167-77. doi: 10.1007/s12033-008-9045-8

Thornhill, D.; Olety, B.; Ono, A. (2019) Relationships between MA-RNA Binding in Cells and Suppression of HIV-1 Gag Mislocalization to Intracellular Membranes. J. Virol., 93, 23.

Tihanyi B., Nyitray L., (2021) Recent advances in CHO cell line development for recombinant protein production, Drug Discovery Today: Technologies, 2021, ISSN 1740-6749, https://doi.org/10.1016/j.ddtec.2021.02.003.

Tigges M, Fussenegger M. (2006) Xbp1-based engineering of secretory capacity enhances the productivity of Chinese hamster ovary cells. Metab Eng. 2006 May;8(3):264-72. doi: 10.1016/j.ymben.2006.01.006. PMID: 16635796.

Torres M, Akhtar S, McKenzie EA, Dickson AJ. (2020) Temperature Down-Shift Modifies Expression of UPR-/ERAD-Related Genes and Enhances Production of a

Chimeric Fusion Protein in CHO Cells. Biotechnol J. 2021 Feb;16(2):e2000081. doi: 10.1002/biot.202000081. Epub 2020 Apr 27. PMID: 32271992.

Uckert W., G. Willimsky, F.S. Pedersen, T. Blankenstein, L. Pedersen. (1998) RNA levels of human retrovirus receptors Pit1 and Pit2 do not correlate with infectibility by three retroviral vector pseudotypes. Hum. Gene. Ther., 9 pp. 2619-2627

Urlinger S, Baron U, Thellmann M, Hasan MT, Bujard H, Hillen W. (2000) Exploring the sequence space for tetracycline-dependent transcriptional activators: novel mutations yield expanded range and sensitivity. Proc Natl Acad Sci U S A. Jul 5;97(14):7963-8. doi: 10.1073/pnas.130192197

Usami, Y.; Popov, S.; Göttlinger, H.G. (2007) Potent rescue of human immunodeficiency virus type 1 late domain mutants by ALIX/AIP1 depends on its CHMP4 binding site. J. Virol. 2007, 81, 6614–6622

Ustek D, Sirma S, Gumus E, Arikan M, Cakiris A, Abaci N, Mathew J, Emrence Z, Azakli H, Cosan F, Cakar A, Parlak M, Kursun O. (2012) A genome-wide analysis of lentivector integration sites using targeted sequence capture and next generation sequencing technology. Infect Genet Evol. Oct;12(7):1349-54. doi: 10.1016/j.meegid.2012.05.001

Uzilday B, Ozgur R, Sekmen AH, Turkan I. (2018) Endoplasmic reticulum stress regulates glutathione metabolism and activities of glutathione related enzymes in Arabidopsis. Functional Plant Biology 45, 284–296

Valkama AJ, Leinonen HM, Lipponen EM, Turkki V, Malinen J, Heikura T, Ylä-Herttuala S, Lesch HP. (2018) Optimization of lentiviral vector production for scale-up in fixed-bed bioreactor. Gene Ther. Jan;25(1):39-46. doi: 10.1038/gt.2017.91

Valkama AJ, Oruetxebarria I, Lipponen EM, Leinonen HM, Käyhty P, Hynynen H, Turkki V, Malinen J, Miinalainen T, Heikura T, Parker NR, Ylä-Herttuala S, Lesch HP. (2020) Development of Large-Scale Downstream Processing for Lentiviral

Vectors. Mol Ther Methods Clin Dev. Mar 30;17:717-730. doi: 10.1016/j.omtm.2020.03.025. PMID: 32346549; PMCID: PMC7177191.

Vallée, C.; Durocher, Y.; Henry, O. (2014) Exploiting the metabolism of PYC expressing HEK293 cells in fed-batch cultures. J. Biotechnol., 169, 63–70.

Vermeire J, Naessens E, Vanderstraeten H, Landi A, Iannucci V., (2012) Quantification of Reverse Transcriptase Activity by Real-Time PCR as a Fast and Accurate Method for Titration of HIV, Lenti- and Retroviral Vectors. PLOS ONE 7(12): e50859. https://doi.org/10.1371/journal.pone.0050859

VerPlank, L.; Bouamr, F.; LaGrassa, T.J.; Agresta, B.; Kikonyogo, A.; Leis, J.; Carter, C.A. (2001) Tsg101, a homologue of ubiquitin-conjugating (E2) enzymes, binds the L domain in HIV type 1 Pr55Gag. Proc. Natl. Acad. Sci. USA 2001, 98, 7724–7729

Vlahakis SR., (2006) Cell Death During HIV Infection. Badley AD, editor. CRC Press, Taylor and Francis Group, Florida; 2006. Cell Death In HIV Infection: gp120; pp. 95–108

Vogt, V. M., and M. N. Simon (1999) Mass determination of Rous sarcoma virus virions by scanning transmission electron microscopy. J. Virol. 73:7050-7055.

W. Uckert, G. Willimsky, F.S. Pedersen, T. Blankenstein, L. Pedersen (1998) RNA levels of human retrovirus receptors Pit1 and Pit2 do not correlate with infectibility by three retroviral vector pseudotypes. Hum. Gene. Ther.,9, pp. 2619-2627

Wang X, Olszewska M, Qu J, Wasielewska T, Bartido S, Hermetet G, Sadelain M, Rivière I. (2015) Large-scale clinical-grade retroviral vector production in a fixed-bed bioreactor. J Immunother. Apr;38(3):127-35

Wang, M., and Kaufman, R. J. (2016) Protein misfolding in the endoplasmic reticulum as a conduit to human disease. Nature 529, 326–335. doi: 10.1038/nature17041

Wang, R., Wang, J., Hassan, A. (2021) Molecular basis of V-ATPase inhibition by bafilomycin A1. Nat Commun 12, 1782. https://doi.org/10.1038/s41467-021-22111-5

Webb, J.A.; Jones, C.P.; Parent, L.J.; Rouzina, I.; Musier-Forsyth, K. (2013) Distinct binding interactions of HIV-1 Gag to Psi and non-Psi RNAs: Implications for viral genomic RNA packaging. RNA, 19, 1078–1088

Weidberg H., E. Shvets, Z. Elazar (2011) Biogenesis and cargo selectivity of autophagosomes. Annu. Rev. Biochem., 80, pp. 125-156

Weiss, E.R.; Popova, E.; Yamanaka, H.; Kim, H.C.; Huibregtse, J.M.; Göttlinger, H. (2010) Rescue of HIV-1 Release by Targeting Widely Divergent NEDD4-Type Ubiquitin Ligases and Isolated Catalytic HECT Domains to Gag. PLoS Pathog. 2010, 6, e1001107.

Werner, N.S.; Weber, W.; Fussenegger, M.; Geisse, S. (2007) A gas-inducible expression system in HEK.EBNA cells applied to controlled proliferation studies by expression of P27kip1. Biotechnol. Bioeng., 96, 1155–1166.

Wills J W, Craven R C. (1991) Form, function, and use of retroviral Gag proteins. AIDS. 5:639–654

Wlodawer A, Miller M, Jaskolski M, Sathyanarayana BK, Baldwin E, Weber IT, Selk LM, Clawson L, Schneider J, Kent SB., (1989) Conserved folding in retroviral proteases: crystal structure of a synthetic HIV-1 protease. Science. 1989, 245: 616-621. 10.1126/science.2548279.

Wu J, Rutkowski DT, Dubois M, Swathirajan J, Saunders T, Wang J, Song B, Yau GD, Kaufman RJ. (2007) ATF6alpha optimizes long-term endoplasmic reticulum function to protect cells from chronic stress. Dev Cell. 2007 Sep;13(3):351-64. doi: 10.1016/j.devcel.2007.07.005. PMID: 17765679.

Wu, J., Chen, S., Liu, H. (2018) Tunicamycin specifically aggravates ER stress and overcomes chemoresistance in multidrug-resistant gastric cancer cells by inhibiting N-glycosylation. J Exp Clin Cancer Res 37, 272

Xu, K., Ma, H., McCown, T. J., Verma, I. M. & Kafri, T. (2001) Generation of a stable cell line producing high-titer self-inactivating lentiviral vectors. Mol. Ther. 3, 97–104

Yamamoto K, Sato T, Matsui T, Sato M, Okada T, Yoshida H, Harada A, Mori K. (2007) Transcriptional induction of mammalian ER quality control proteins is mediated by single or combined action of ATF6alpha and XBP1. Dev Cell. 2007 Sep;13(3):365-76. doi: 10.1016/j.devcel.2007.07.018. PMID: 17765680.

Yang H, Niemeijer M, van de Water B, Beltman JB. (2020) ATF6 Is a Critical Determinant of CHOP Dynamics during the Unfolded Protein Response. iScience. 2020 Feb 21;23(2):100860. doi: 10.1016/j.isci.2020.100860. Epub 2020 Jan 23. PMID: 32058971; PMCID: PMC7005498.

Yang Y, Liu L, Naik I, Braunstein Z, Zhong J, Ren B.., (2017) Transcription Factor C/EBP Homologous Protein in Health and Diseases. Front Immunol. 2017 Nov 27;8:1612. doi: 10.3389/fimmu.2017.01612. PMID: 29230213; PMCID: PMC5712004

Yao F., Svensjö T., Winkler T., Lu M., Eriksson C., Eriksson E. (1998) Tetracycline repressor, tetR, rather than the tetR-mammalian cell transcription factor fusion derivatives, regulates inducible gene expression in mammalian cells. Hum. Gene Ther.; 9: 1939-1950

Yee JK, Miyanohara A, LaPorte P, Bouic K, Burns JC, Friedmann T., (1994) A general method for the generation of high-titer, pantropic retroviral vectors: highly efficient infection of primary hepatocytes. Proc Natl Acad Sci USA 1994; 91: 9564–9568.

Yip, A., Webster, R. (2018) The market for chimeric antigen receptor T cell therapies. Nat Rev Drug Discov 17, 161–162 https://doi.org/10.1038/nrd.2017.266

Yoon SB, Park YH, Choi SA, Yang HJ, Jeong PS, Cha JJ, Lee S, Lee SH, Lee JH, Sim BW, Koo BS, Park SJ, Lee Y, Kim YH, Hong JJ, Kim JS, Jin YB, Huh JW, Lee SR, Song BS, Kim SU. (2019) Real-time PCR quantification of spliced X-box binding protein 1 (XBP1) using a universal primer method. PLoS One. Jul 22;14(7):e0219978. doi: 10.1371/journal.pone.0219978

Yorimitsu, T., Nair, U., Yang, Z., and Klionsky, D. J. (2006). Endoplasmic reticulum stress triggers autophagy. J. Biol. Chem. 281, 30299–30304. doi: 10.1074/jbc.M607007200

Yoshida H, Matsui T, Yamamoto A, Okada T, Mori K. (2001) XBP1 mRNA is induced by ATF6 and spliced by IRE1 in response to ER stress to produce a highly active transcription factor. Cell. 2001 Dec 28;107(7):881-91. doi: 10.1016/s0092-8674(01)00611-0. PMID: 11779464.

Yoshida, H., Matsui, T., Yamamoto, A., Okada, T., and Mori, K. (2001) XBP1 mRNA is induced by ATF6 and spliced by IRE1 in response to ER stress to produce a highly active transcription factor. Cell 107, 881–891. doi: 10.1016/S0092-8674(01)00611-0

Yu FH, Chou TA, Liao WH, Huang KJ, Wang CT (2015) Gag-Pol Transframe Domain p6* Is Essential for HIV-1 Protease-Mediated Virus Maturation. PLOS ONE 10(6): e0127974. https://doi.org/10.1371/journal.pone.0127974

Yu FH, Chou TA, Liao WH, Huang KJ, Wang CT. (2015) Gag-Pol Transframe Domain p6* Is Essential for HIV-1 Protease-Mediated Virus Maturation. PLoS One. 2015 Jun 1;10(6):e0127974. doi: 10.1371/journal.pone.0127974. PMID: 26030443; PMCID: PMC4451514.

Zhang, W.; Xiao, D.; Shan, L.; Zhao, J.; Mao, Q.; Xia, H. (2017) Generation of apoptosis-resistant HEK293 cells with CRISPR/Cas mediated quadruple gene knockout for improved protein and virus production. Biotechnol. Bioeng., 114, 2539–2549.

Zhao G, Perilla JR, Yufenyuy EL, Meng X, Chen B, Ning J, Ahn J, Gronenborn AM, Schulten K, Aiken C, Zhang P. (2013) Mature HIV-1 capsid structure by cryo-electron microscopy and all-atom molecular dynamics. Nature. May 30;497(7451):643-6. doi: 10.1038/nature12162

Zhou, Y.; Rong, L.; Lu, J.; Pan, Q.; Liang, C. (2008) Insulin-like growth factor II mRNA binding protein 1 associates with Gag protein of human immunodeficiency virus type 1, and its overexpression affects virus assembly. J. Virol. 2008, 82, 5683–5692

Zhurinsky J, Leonhard K, Watt S, Marguerat S, Bähler J, Nurse P (2010) A coordinated global control over cellular transcription. Curr Biol. 2010 Nov 23; 20(22):2010-5.

Zufferey R, Donello JE, Trono D, Hope TJ. (1999) Woodchuck hepatitis virus posttranscriptional regulatory element enhances expression of transgenes delivered by retroviral vectors. J Virol. Apr;73(4):2886-92. doi: 10.1128/JVI.73.4.2886-2892.1999

Zufferey R, Nagy D, Mandel RJ, Naldini L, Trono D. (1997) Multiply attenuated lentiviral vector achieves efficient gene delivery in vivo. Nat Biotechnol.; 15:871–875.

Zufferey, R., Dull, T., Mandel, R. J., Bukovsky, A., Quiroz, D., Naldini, L., & Trono, D. (1998). Self-inactivating lentivirus vector for safe and efficient in vivo gene delivery. Journal of virology, 72(12), 9873–9880.

8 Appendix

8.1 Reagents list

Reagent	Supplier	Notes
1 kb DNA ladder	New England Biolabs, UK	
Accutase	Thermo Fisher Scientific, UK	
Agarose powder	Thermo Fisher Scientific, UK	
Amphopack293 cell line	Takara Bio, USA	
Ampicillin	Sigma Aldrich, UK	
Annexin V Apoptosis Detection A13203	AbCam, UK	
Anti-HIV-1 p17 Antibody	AbCam, UK	[17-1], AbCam, ab66641, Mouse monoclonal (1:1000 dilution used)
Anti-HIV-1 p24 Antibody	AbCam, UK	[39/5.4A], AbCam, ab9071, Mouse monoclonal (1:1000 dilution used)
Bafilomycin A1	Invivogen, CA, USA	
Bovine Serum Albumin	Sigma Aldrich, UK	
Chloroform	Sigma Aldrich, UK	
Chloroquine	Sigma Aldrich, UK	
Collagen	Sigma Aldrich, UK	
Cut-Smart® Buffer	New England Biolabs, UK	
ddPCR probes	Eurofins, Germany	
Dimethyl sulfoxide	Sigma Aldrich, UK	

DNAse buffer	Thermo Fisher Scientific, UK	
DNAse I enzyme	Thermo Fisher Scientific, UK	
Dneasy Blood and Tissue kit	Qiagen Ltd., UK	
dNTP set	BioLine, UK	
Dulbecco's Modified Eagle Medium	Thermo Fisher Scientific, UK	
Ethanol	Sigma Aldrich, UK	
Fetal Bovine Serum	Sigma Aldrich, UK	
Gel loading dye, purple (6X)	Sigma Aldrich, UK	
Gibson Assembly® cloning kit	New England Biolabs, UK	
Glycerol	Sigma Aldrich, UK	
GoTaq DNA Polymerase	Promega, UK	
HEK293T cells	GlaxoSmithKline, Stevenage, UK	
HIV-1 p24 ELISA Kit ab218268	AbCam, UK	
Hydrochloric acid (HCl)	Thermo Fisher Scientific, UK	
Kanamycin	Sigma Aldrich, UK	
LAMP-1 Antibody	BD BioSciences, UK	[BV510], BD BioSciences, CD107a, Mouse Anti-Human (1:200 dilution)
LC3B Antibody	Novus Biologicals, UK	(1251D) [Alexa Fluor® 647], Novus Biologicals (1:1000 dilution used)
MS2 RNA from Bacteriophase MS2	Sigma Aldrich, UK	
NEB® 10-beta Competent E. coli	New England Biolabs, UK	

NEB® 5-alpha Competent E. coli	New England Biolabs, UK	
Nucleospin® RNA Virus	Macherey-Nagel, Germany	
Oligonucleotide primers	Eurofins, Germany	
OptiMEM ™	Thermo Fisher Scientific, UK	
Paraformaldehyde	Sigma Aldrich, UK	
pBS-CMV-GagPol	Addgene, MA, USA	Patrick Salmon (Addgene plasmid # 35614)
PCR Master Mix 2X	Thermo Fisher Scientific, UK	
PEI	Polyplus Transfection, UK	
pG3-SYNGP	GlaxoSmithKline, Stevenage, UK	
Phosphate Buffered Solution tablets	Sigma Aldrich, UK	
Plasmid mini/midi/maxi kit	Qiagen Ltd., UK	
pMD2.G	Addgene, MA, USA	Didier Trono (Addgene plasmid #12259)
Polybrene	Sigma Aldrich, UK	
Potassium Chloride (KCl)	Sigma Aldrich, UK	
PowerUp™ SYBR™ Green Master Mix	Thermo Fisher Scientific, UK	
pQCXIP-EGFP-F	Addgene, MA, USA	Michael Grusch (Addgene plasmid # 73014)
pQCXIX	Takara Bio, USA	
Q5 Hot Start High-Fidelity DNA polymerase	New England Biolabs, UK	
QIA Spin Miniprep Kit	Qiagen Ltd., UK	
QIAquick Gel Extraction Kit	Qiagen Ltd., UK	
QIAquick PCR Purification Kit	Qiagen Ltd., UK	

Quant-X™ One-Step qRT-PCR Kit	Takara Bio, USA	
Recombinant Anti-SQSTM1 p62 antibody	AbCam, UK	[EPR4844], Alexa Fluor® 647, AbCam, ab194721, Rabbit monoclonal (1:500 dilution used)
Recombinant HIV-1 p24 protein	AbCam, UK	
Retro-X qRT-PCR Titration Kit	Takara Bio, USA	
SafeView™ Nucleic acid stain	Thermo Fisher Scientific, UK	
Saquinavir	Sigma Aldrich, UK	
Sodium azide	Sigma Aldrich, UK	
Sodium Chloride (NaCl)	Sigma Aldrich, UK	
Spautin-1	Sigma Aldrich, UK	
TAE Buffer 50X	National Diagnostics, UK	
Tetro cDNA synthesis kit	Meridian Bioscience, OH, USA	
Tris Base	Sigma Aldrich, UK	
Triton X-100	Sigma Aldrich, UK	
TRIzol™	Thermo Fisher Scientific, UK	
Trypan Blue	LifeTechnologies™ UK	
Trypsin	Thermo Fisher Scientific, UK	
Tryptone	Sigma Aldrich, UK	
Tunicamycin	Sigma Aldrich, UK	
Tween® 20	Sigma Aldrich, UK	

VspI Restriction Enzyme	New England Biolabs, UK
Wortmannin	Invivogen, CA, USA
Xfect™ Transfection Reagent	Takara Bio, USA
Yeast Extract	Sigma Aldrich, UK
Z-IETD-FMK (Caspase-8 inhibitor)	Promega, UK
Z-LEHD-FMK (Caspase-9 inhibitor)	Promega, UK
Z-VAD-FMK (Pan-Caspase inhibitor)	Promega, UK

8.2 Equipment and software list

Equipment/Software	**Company**
Amnis® ImageStream®X Mk II	Liminex, USA
Automated droplet generator	Bio-Rad Laboratories Ltd., UK
Cell culture vessels	Corning Inc. Life Sciences, USA
ChemiDoc MP Imaging System	Bio-Rad Laboratories Ltd., UK
Falcon tubes	Corning Inc. Life Sciences, USA
FlowJo™ V9	BD Biosciences, UK
Haemocytometer	ThermoFisher Scientific, UK
Light Microscope (Axiovert 35)	Carl Zeiss, Germany
Mr. Frosty™ freezing container	ThermoFisher Scientific, UK
NanoDrop™ Spectrophotometer	ThermoFisher Scientific, UK
PCR Thermocycler	Bio-Rad Laboratories Ltd., UK
qPCR Machine	Bio-Rad Laboratories Ltd., UK
SH800S Cell Sorter	Sony, UK
SnapGene Viewer	SnapGene, UK
Table top centrifuge	Boeco, Germany
Vi-CELL XR Cell Viability Analyser	Beckman Coulter, USA

8.3 Primers used for plasmid generation by Gibson Assembly reaction

Table 8.1. Primers used to produce pQCXIX-SYNGP

Primer Name	Primer Sequence (5'-3')	Annealing temperature (°C)	Template plasmid
Gib_pQCXIX_F	AGACAGGATGAGGATTAGAG TGGTCCAGGCTCTAGTTT	65	pQCXIX
Gib_ampS_R	GCACGAGTGGGTTACATCGA ACT GGATCTC		pQCXIX
Gib_ampS_F	GAGATCCAGTTCGATGTAACC CA CTCGTGC	65	pQCXIX
Gib_pQCXIX_R	TCAATAATCAATGCCGACTCT AGAGGATCGATCCCCCA		pQCXIX
Gib_SYNGP_F	TCGATCCTCTAGAGTCGGCAT TGATTATTGACTAGT	65	pG3-SYNGP
Gib_SYNGP_R	AGAGCCTGGACCACTCTAATC CTCATCCTGTCTGCT		pG3-SYNGP

Table 8.2. Primers used to produce pQCXIX-SYNGP-EGFP

Primer Name	Primer Sequence (5'-3')	Annealing temperature (°C)	Template plasmid
gib_Chen07_1 egfp_F	CAGGTCAGCCAGAACTACCCC ATCGTGCAGATGGTGAGCAAG GGCGAGGA	60	Bt-mod- V2
gib_Chen07_2 egfp_R	TTCTGCACGATGGGGTAGTTCT GGCTCTTGTACAGCTCGTCCAT GCCGAG		Bt-mod- V2
gib_Chen07_2 egfp_F	ATGGACGAGCTGTACAAGAGC CAGAACTACCCCATCGTGCAG AACATCCA	60	pQCXIX-SYNGP
gib_ampS_R	GCACGAGTGGGTTACATCGAA CTGGATCTC		pQCXIX-SYNGP
gib_ampS_F	GAGATCCAGTTCGATGTAACC CACTCGTGC	60	pQCXIX-SYNGP
gib_Chen07_1 egfp_R	CCCTTGCTCACCATCTGCACG ATGGGGTAGTTCTGGCTGACC TGGTTGCT		pQCXIX-

8.4 Primers for use in qRT-PCR

Table 8.3. Primers for use in qRT-PCR

Target	Primer name	Primer sequence (5'-3')	Annealing temperature for PCR(ºC)
Unspliced XBP1	UXBP1_F	TCCGCAGCACTCAGACTACG	60
	UXBP1_R	AGTTGTCCAGAATGCCCAACA	
Spliced XBP1	SXBP1_F	CTGAGTCCGCAGCAGGTG	57
	SXBP1_R	AGTTGTCCAGAATGCCCAACA	
BIP	Human_BIP_F	GCCTGTATTTCTAGACCTGCC	60
	Human_BIP_R	TTCATCTTGCCAGCCAGTTG	
CHOP	Human_CHOP_F	ACCAAGGGAGAACCAGGAAACG	60
	Human_CHOP_R	TCACCATTCGGTCAATCAGAGC	
ATF6	Human_ATF6_F	GCTTTACATTCCTCCACCTCCTTG	55
	Human_ATF6_R	ATTTGAGCCCTGTTCCAGAGCAC	
GAPDH	GAPDH_F	ACCCACTCCTCCACCTTTGAC	57
	GAPDH_R	TGTTGCTGTAGCCAAATTCGTT	57

8.5 Plasmid maps

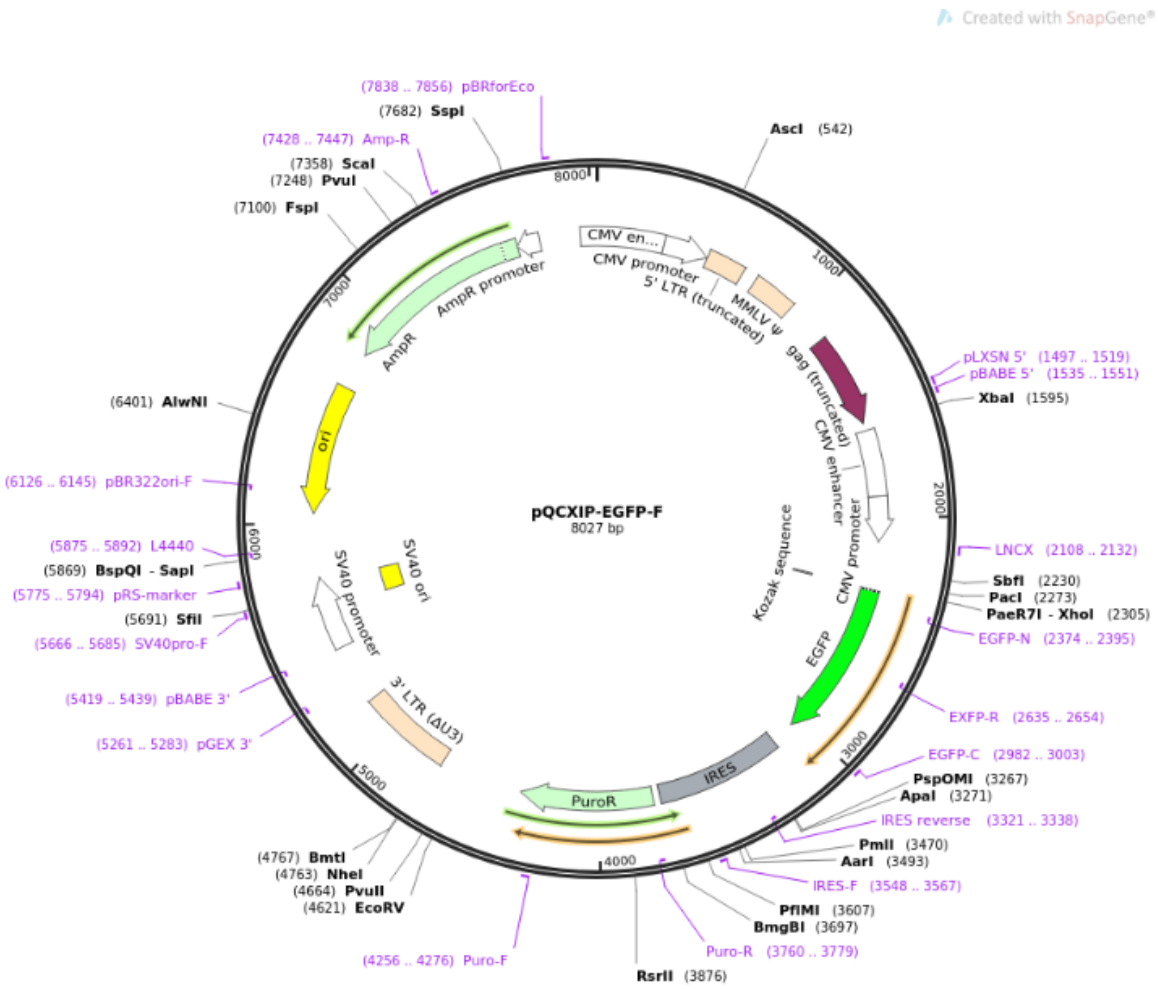

Figure A1 Plasmid map of pQCXIP-EGFP-F

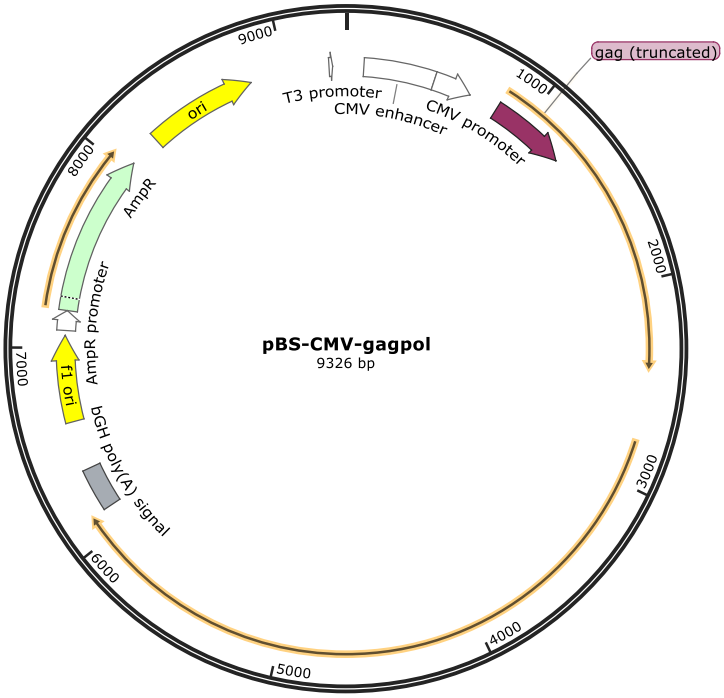

Figure A2 Plasmid map of pBS-CMV-GagPol

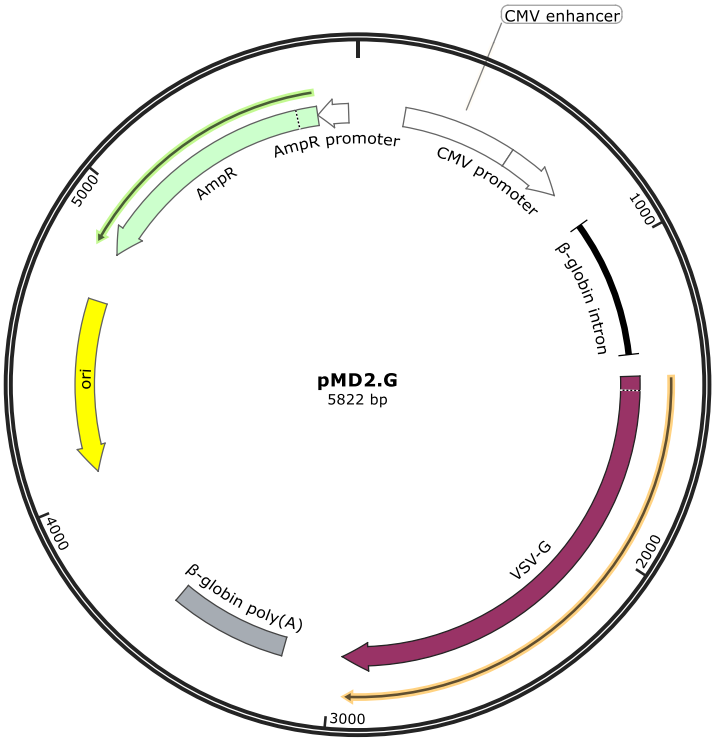

Figure A3 Plasmid map of pMD2.G

8.6 Primers for sequencing

Table 8.4 Primer sequences for sequencing plasmids

Primer name	Primer sequence (5'-3')	Plasmid
pQCXIX-SYNGP-seq_1	GCCCGACCTGAGGAAGGGAG	pQCXIX-SYNGP, pQCXIX-SYNGP-EGFP
pQCXIX-SYNGP-seq_2	CAGACTGTTACCACTCCCTT	pQCXIX-SYNGP, pQCXIX-SYNGP-EGFP
pQCXIX-SYNGP-seq_2A	CAGACTGTTACCACTCCCTT	pQCXIX-SYNGP, pQCXIX-SYNGP-EGFP
pQCXIX-SYNGP-seq_4	TTCTCTAGGCGCCGGAATTG	pQCXIX-SYNGP, pQCXIX-SYNGP-EGFP
pQCXIX-SYNGP-seq_4A	ATCACTAGAAGCTTTATTGC	pQCXIX-SYNGP, pQCXIX-SYNGP-EGFP
pQCXIX-SYNGP-seq_6	TGTGACCGTCTCCGGGAGCT	pQCXIX-SYNGP, pQCXIX-SYNGP-EGFP
pQCXIX-SYNGP-seq_6A	AGCTCCCGGAGAGACGGTCAC A	pQCXIX-SYNGP, pQCXIX-SYNGP-EGFP
pQCXIX-SYNGP-seq_7	ATGCAGAGGCCGAGGCCGCC	pQCXIX-SYNGP, pQCXIX-SYNGP-EGFP
pQCXIX-SYNGP-seq_8	AGCTATGAGAAAGCGCCACG	pQCXIX-SYNGP, pQCXIX-SYNGP-EGFP
pQCXIX-SYNGP-seq_8A	CGTGGCGCTTTCTCATAGCT	pQCXIX-SYNGP, pQCXIX-SYNGP-EGFP
pQCXIX-SYNGP-seq_9	TATGAGTAAACTTGGTCTGA	pQCXIX-SYNGP, pQCXIX-SYNGP-EGFP
pQCXIX-SYNGP-seq_12	TACCCATCGTGCAGATGGT	pQCXIX-SYNGP, pQCXIX-SYNGP-EGFP
pQCXIX-SYNGP-seq_13	TTCAGCCGCTACCCCGACCA	pQCXIX-SYNGP, pQCXIX-SYNGP-EGFP
pQCXIX-SYNGP-seq_14	AACAGCCACAACGTCTATAT	pQCXIX-SYNGP, pQCXIX-SYNGP-EGFP

pQCXIX-SYNGP-seq_15	GGAGTTCGTGACCGCCGCCG	pQCXIX-SYNGP, pQCXIX-SYNGP-EGFP
pQCXIX-SYNGP-seq_16	AAGAGCCAGAACTACCCCAT	pQCXIX-SYNGP, pQCXIX-SYNGP-EGFP
pG3-S_930	TAGAAACTGGGCTTGTCGAG	pQCXIX-SYNGP-EGFP
pG3-S_1021	CAGGTGTCCACTCCCAGTTC	pQCXIX-SYNGP-EGFP
pG3-S_1332	TGCGCAGCCTGTACAACACC	pQCXIX-SYNGP-EGFP
pG3-S_1724	AATGAGGAGGCTGCCGAATG	pQCXIX-SYNGP-EGFP
pG3-S_2127	CGGCTACCCTAGAGGAAATG	pQCXIX-SYNGP-EGFP
pG3-S_2536	GGAGCCGATAGACAAGGAAC	pQCXIX-SYNGP-EGFP
pG3-S_2940	GCCATTGACAGAGGAGAAG	pQCXIX-SYNGP-EGFP
pG3-S_3338	CCGCAATCTTCCAGAGTAGC	pQCXIX-SYNGP-EGFP
pG3-S_3720	CGGAACCAAGGCACTCACAG	pQCXIX-SYNGP-EGFP
pG3-S_4097	GGATTCCTGAGTGGCAGTTC	pQCXIX-SYNGP-EGFP
pG3-S_4539	GAAGGTGCTATTCCTGGATG	pQCXIX-SYNGP-EGFP
pG3-S_4910	TCACCAGTGCTACGGTTAAC	pQCXIX-SYNGP-EGFP
pG3-S_5321	AGGTGGTGCCCAGAAGAAAG	pQCXIX-SYNGP-EGFP
Pit2_F_1	ACGCTTACAATTTCCATTCG	Pit-2
Pit2_F_2	TCCGGTACCGAGGAGATCTG	Pit-2
Pit2_F_3	CTTTTCCATCATGTACACAG	Pit-2
Pit2_F_4	ACGACAGCTACTCGAGCTAC	Pit-2
Pit2_F_5	CTGCTGTCATGGCTCTTCTC	Pit-2
Pit2_F_6	TGGGACATTTGAGTTGCTTG	Pit-2
Pit2_F_7	CGGCTACACTAGAAGAACAG	Pit-2
Pit2_F_8	TTGGTCGGTCATTTCGAACC	Pit-2
Pit2_F_9	TGTTGTGCCCAGTCATAGCC	Pit-2
Pit2_F_10	TTCCGATTTAGTGCTTTACG	Pit-2
pMD2.G_F_1	CTCATGTCCAACATTACCGC	pMD2.G
pMD2.G_F_2	ACATCAATGGGCGTGGATAG	pMD2.G
pMD2.G_F_3	ATGATACAATGTATCATGCC	pMD2.G
pMD2.G_F_4	TGAGATCTGAATTCTGACAC	pMD2.G
pMD2.G_F_5	CGAAGCAGTGATTGTCCAGG	pMD2.G

pMD2.G_F_6	TCTCTCCAGTGGATCTCAGC	pMD2.G
pMD2.G_F_7	GAGTTGGTATCCATCTTTGC	pMD2.G
pMD2.G_F_8	CGGTTATCCACAGAATCAGG	pMD2.G
pMD2.G_F_9	GTATATATGAGTAAACTTGG	pMD2.G
pMD2.G_F_10	ATAATACCGCGCCACATAGC	pMD2.G
pBS_F_1	CTCATGTCCAACATTACCGC	pBS-CMV-GagPol
pBS_F_2	GTTGTCTCTGTCTGACTGTG	pBS-CMV-GagPol
pBS_F_3	AGCCCTCACTCCTTCTCTAG	pBS-CMV-GagPol
pBS_F_4	TCAACTGCCCAATGAAGTCG	pBS-CMV-GagPol
pBS_F_5	ACATAGAGAGATGAGCAAGC	pBS-CMV-GagPol
pBS_F_6	ATCAGGAGCTCAGGTTATGG	pBS-CMV-GagPol
pBS_F_7	GATGCCTTTTTCTGCCTGAG	pBS-CMV-GagPol
pBS_F_8	GTACCCTCTCACCAAAACGG	pBS-CMV-GagPol
pBS_F_9	CTTGATATCCTGGCCGAAGC	pBS-CMV-GagPol
pBS_F_10	CACCTCTACCCTCCTCATAG	pBS-CMV-GagPol
pBS_F_11	CAAGGTCGTAACCAAGAAGC	pBS-CMV-GagPol
pBS_F_12	CTAGAACCTCGCTGGAAAGG	pBS-CMV-GagPol
pBS_F_13	TGTCTGAGTAGGTGTCATTC	pBS-CMV-GagPol
pBS_F_14	TCCGATTTAGTGCTTTACGG	pBS-CMV-GagPol
pBS_F_15	GTTACATCGAACTGGATCTC	pBS-CMV-GagPol
pBS_F_16	GAAATAGACAGATCGCTGAG	pBS-CMV-GagPol
pBS_F_17	CGATAAGTCGTGTCTTACCG	pBS-CMV-GagPol
pBS_F_18	ATTAATGCAGCTGGCACGAC	pBS-CMV-GagPol
seq_f_1	TAAGCAGAGCTCAATAAAAG	pQCXIP-EGFP-F
seq_f_2	GAGACGTCCCAGGGACTTTG	pQCXIP-EGFP-F
seq_f_3	AGACGGCACCTTTAACCGAG	pQCXIP-EGFP-F
seq_f_4	TAAGCAGAGCTCGTTTAGTG	pQCXIP-EGFP-F
seq_f_5	TCGCCACCATGGTGAGCAAG	pQCXIP-EGFP-F
seq_f_6	CAAGGAGGACGGCAACATCC	pQCXIP-EGFP-F
seq_f_7	TCCTGAGGATCCGGAATTCC	pQCXIP-EGFP-F
seq_f_8	CGTTGTGAGTTGGATAGTTG	pQCXIP-EGFP-F
seq_f_9	GCAACCTCCCCTTCTACGAG	pQCXIP-EGFP-F

seq_f_10	TCACCAGCTGAAGCCTATAG	pQCXIP-EGFP-F
seq_f_11	TCCAATAAACCCTCTTGCAG	pQCXIP-EGFP-F
seq_f_12	GCCTAGGCTTTTGCAAAAAG	pQCXIP-EGFP-F
seq_f_13	GTAACAGGATTAGCAGAGCG	pQCXIP-EGFP-F
seq_f_14	ATACTCATACTCTTCCTTTT	pQCXIP-EGFP-F